Thermo-environomic optimisation of fuel decarbonisation alternative processes for hydrogen and power production

THÈSE N^{O} 5655 (2013)

PRÉSENTÉE LE 22 MARS 2013
À LA FACULTÉ DES SCIENCES ET TECHNIQUES DE L'INGÉNIEUR
LABORATOIRE D'ÉNERGÉTIQUE INDUSTRIELLE
PROGRAMME DOCTORAL EN ENERGIE

ÉCOLE POLYTECHNIQUE FÉDÉRALE DE LAUSANNE

POUR L'OBTENTION DU GRADE DE DOCTEUR ÈS SCIENCES

PAR

Laurence TOCK

acceptée sur proposition du jury:

Prof. D. Bonvin, président du jury
Prof. F. Maréchal, directeur de thèse
Prof. R. Agrawal, rapporteur
Prof. M. Mazzotti, rapporteur
Dr M. Wolf, rapporteur

ÉCOLE POLYTECHNIQUE
FÉDÉRALE DE LAUSANNE
Suisse
2013

Learn from yesterday,
live for today,
hope for tomorrow.
The important thing is
not to stop questioning.

Albert Einstein

Acknowledgements

First of all, I would like to thank Prof. François Maréchal, my thesis director, for having given me the opportunity to complete this thesis. His scientific passion, his multi-disciplinary expertise, his inspiration, his endless ambitions and his advice have been invaluable driving forces for the accomplishment of this thesis. The confidence he has placed in me, as well as the autonomy and the freedom he has accorded me have always motivated me and pushed me forward.

At this place I would also like to thank the members of the jury for having evaluated this thesis and for the interesting and enriching discussion. It has been a great pleasure and honour to have Prof. Rakesh Agrawal, Prof. Marco Mazzotti and Dr. Markus Wolf on my thesis jury headed by Prof. Dominique Bonvin.

I further gratefully acknowledge the financial support of the Competence Center Energy and Mobility (CCEM) and the Competence Center Environment and Sustainability (CCES) in the frame of the CARMA project, as well as the funding of swisselectric and Alstom that have enabled this research work.

I have highly appreciated the collaboration in the interdisciplinary research projects 'Carbon dioxide management in power generation (CARMA)' and 'Technologies for Gas Turbine Power Generation with CO_2 Mitigation'. I would like to thank the head of the CARMA project Marco Mazzotti, as well as Timothy Griffin and Dieter Winkler from Fachhochschule Nordwest Schweiz (FHNW) and the groups of Peter Jansohn, Ioannis Mantzaras and Stefan Hirschberg from PSI for the fruitful collaboration and the competent advice having allowed to validate some of the developed models.

The software support of the BELSIM SA team has been very valuable for the implementation of the flowsheeting models.

One of the key factors for the successful accomplishment of this work has been the professional and lively atmosphere at the Industrial Energy System Laboratory headed by Prof. Daniel Favrat, to whom I would like to express my gratitude, as well as to the secretaries for the friendly and valuable administrative support. A great thank also to all my colleagues at LENI for the scientific and motivational support and for the great time we have spent together at work, as well as after work. It has been a pleasure to work together with them and they have all contributed in various ways to my research. Especially I want to thank Nicolas Borboën for having solved many IT troubles; Martin Gassner for having passed to me his passion and knowledge for modelling processes, notably in the field of biomass conversion; Léandro Salgueiro for all his support in many different fields and his constant encouragements; Matthias Dubuis for the collaboration in the research projects and the teaching activities, but especially for his cheerfulness; Léda Gerber for the advices with regard to LCA and Emanuela Peduzzi for contributing to the study of several aspects related to this research. Zacharie, Thierry and Matthias, it has been a pleasure to share the office with you. Thanks a lot for the enjoyable but at the same time quiet atmosphere (before the beginning of the construction works...), for your support and for your patience during the eternal discussions with all my students.

Special thanks to my dear friends from Lausanne and Luxembourg for the unforgettable and joyful time we have spent together. These have been precious moments to distract myself from the never-ending programming bugs. A great thank to Ralph for all the encouragements during the Master studies and the spontaneous help at the final stage of this thesis.

Finally, many thanks go to my family, particularly my parents and my sisters Pascale and Françoise for their constant support during all these years, for sharing my happiness and sadness, and for always believing in me.

Last but not least I would like to thank Scharel for his humour, his optimism and the time we have spent together.

Lausanne, 10 February 2013 L. T.

Abstract

To meet the CO_2 reduction targets and to ensure a reliable energy supply, the development and wide scale deployment of cost-competitive innovative low-carbon energy technologies is essential. Switching to renewable resources and CO_2 capture and storage in power plants, are regarded as promising alternatives. To design and evaluate the competitiveness of such complex integrated energy conversion systems, a systematic comparison including thermodynamic, economic and environmental considerations is required. This thesis presents the development of a systematic thermo-environomic optimisation strategy for the consistent modelling, comparison and optimisation of fuel decarbonisation process options. The environmental benefit and the energetic and economic costs of carbon capture are assessed for several process options and energy systems, including H_2 and/or electricity production from natural gas or biomass resources and considering different CO_2 capture technologies. The process performance is systematically compared and the trade-offs are assessed to support decision-making and identify optimal process configurations with regard to the polygeneration of H_2, electricity, heat and captured CO_2.

The results from the systematic process design and comparison studies reveal the importance of process integration, maximising the rational energy recovery by cogeneration, in the synthesis of efficient decarbonisation processes. In addition, the influence of the economic scenario on the process competitiveness and hence on the optimal process design is pointed out. It appears that the various process options are in competition, even with conventional plants without CO_2 capture when a carbon tax is introduced. The choice of the optimal configuration is defined by the production scope and the priorities given to the different thermo-environomic criteria.

Keywords: CO_2 capture and storage, hydrogen, biomass, power plant, process design, process modelling, energy integration, multi-objective optimisation.

Résumé

Afin d'atteindre les objectifs de réduction des émissions de gaz à effet de serre et d'assurer un approvisionnement durable en énergie, le développement et la dissémination à grande échelle de technologies énergétiques innovantes à faible intensité en carbone sont essentiels. La transition vers l'utilisation de ressources renouvelables, ainsi que le captage et stockage de CO_2 émanant de centrales électriques, sont considérés comme alternatives prometteuses. Afin de concevoir de tels systèmes intégrés de conversion d'énergie et d'évaluer leur compétitivité, une comparaison systématique considérant des aspects thermodynamiques, économiques et environnementaux est requise. Cette thèse présente le développement d'une stratégie d'optimisation thermo-environomique systématique pour la modélisation, la comparaison et l'optimisation cohérente de procédés de décarbonisation. Le bénéfice environnemental et les coûts énergétiques et économiques du captage de CO_2 sont évalués pour diverses options du procédé et différents systèmes énergétiques, incluant la production d'H_2 et/ou d'électricité à partir de gaz naturel ou de biomasse et prenant en compte différentes technologies pour le captage du CO_2. La performance des procédés est comparée systématiquement et les compromis sont relevés en vue d'assister dans la prise de décisions et d'identifier des configurations de procédés optimaux en termes de polygénération d'H_2, d'électricité et de CO_2 capturé.

Les résultats des études systématiques de conception et de comparaison de procédés ont démontrés l'importance de l'intégration énergétique, maximisant la récupération d'énergie par cogénération, dans la synthèse de procédés de décarbonisation efficaces. En plus, il est mis en évidence comment les scénarios économiques influencent la compétitivité des procédés et donc la conception optimale du procédé. Il s'avère que les diverses options de procédés sont en compétition, même avec des centrales électriques conventionnelles sans captage de CO_2 lorsqu'une taxe de carbone est introduite. Le choix de la configuration optimale est défini par le but de production et les priorités données aux différents critères thermo-environomiques.

Mots-clés : Captage et stockage du CO_2, hydrogène, biomasse, centrale électrique, conception de procédés, modélisation de procédés, intégration énergétique, optimisation multi-objective.

Contents

Acknowledgements **v**

Abstract (English/Français) **vii**

Introduction **1**

Context 1

CO_2 capture and storage principles 2

CO_2 capture 3

Thermo-environomic evaluations of fuel decarbonisation processes 6

Comprehensive assessment 6

Systems assessment methodologies 8

Conclusions 9

Objectives 11

Outline 13

1 Thermo-environomic optimisation methodology **15**

1.1 Introduction 15

1.2 Strategy 16

1.3 Thermo-environomic modelling 17

1.3.1 Process superstructure 17

1.3.2 Energy-flow model 17

1.3.3 Energy integration model 18

1.3.4 Performance evaluation model 19

1.4 Multi-objective optimisation 26

1.4.1 Performance indicators 26

1.4.2 Optimisation problem definition 28

1.5 Conclusions 29

2 Process models development for CO_2 capture technologies **31**

2.1 Introduction 31

2.2 CO_2 separation technologies 32

2.2.1 Principles 32

2.2.2 Technologies description 32

2.3 CO_2 capture process modelling 37

2.3.1 Chemical absorption 37
2.3.2 Physical absorption 41
2.3.3 Pressure swing adsorption 42
2.3.4 Membrane processes 42
2.4 Conclusions 43

3 Thermo-economic analysis of pre-combustion CO_2 capture processes 45
3.1 Introduction 45
3.2 Pre-combustion CO_2 capture processes description 46
3.2.1 Pre-combustion CO_2 capture process layout 46
3.2.2 Pre-combustion CO_2 capture process technologies 46
3.3 Pre-combustion CO_2 capture process modelling 50
3.3.1 Syngas production 51
3.3.2 Gas treatment and purification 53
3.3.3 H_2 applications 54
3.4 Thermo-economic evaluation of pre-combustion CO_2 capture processes 54
3.4.1 Multi-objective optimisation of pre-combustion CO_2 capture in H_2 processes 55
3.4.2 Pre-combustion CO_2 capture process performance: H_2 production . . . 58
3.4.3 Multi-objective optimisation of pre-combustion CO_2 capture in power plants 64
3.4.4 Pre-combustion CO_2 capture process performance: Electricity generation 64
3.5 Conclusions 67

4 Thermo-economic comparison of CO_2 capture technologies in pre-combustion CO_2 capture processes 69
4.1 Introduction 69
4.2 Process description: Pre-combustion CO_2 capture 70
4.3 Performance of H_2 production processes with different CO_2 capture technologies 70
4.4 Performance of electricity generating processes with different pre-combustion CO_2 capture technologies 74
4.4.1 Influence of feedstock type 75
4.4.2 Influence of reforming technology 77
4.4.3 Influence of hydrogen purity 77
4.4.4 Influence of CO_2 capture technology 78
4.5 Conclusions 79

5 Thermo-economic analysis of post-combustion CO_2 capture processes 81
5.1 Introduction 81
5.2 Post-combustion CO_2 capture process description 82
5.3 Post-combustion CO_2 capture process modelling 82
5.3.1 Power plant model 82
5.3.2 CO_2 capture model 84

5.3.3 Steam network model 84
5.4 Performance evaluation of post-combustion CO_2 capture processes 84
5.4.1 CO_2 capture impact 85
5.4.2 Flue gas recirculation impact 86
5.4.3 Multi-objective optimisation of post-combustion CO_2 capture processes 88
5.4.4 Energy integration improvement: District heating 89
5.5 Conclusions 90

6 Thermo-economic comparison of post-combustion CO_2 capture by amines and chilled ammonia 91
6.1 Introduction 91
6.2 Post-combustion CO_2 capture process performance comparison: Amines versus chilled ammonia 92
6.2.1 Energy integration 93
6.2.2 Economic performance 95
6.3 Multi-objective optimisation: Amines versus chilled ammonia 95
6.4 Chilled ammonia process improvement 96
6.4.1 Energy integration improvement: Absorber design 96
6.4.2 Energy integration improvement: Refrigeration unit design 101
6.5 Conclusions 108

7 Process design optimisation strategy to develop energy and cost correlations of CO_2 capture processes 109
7.1 Introduction 109
7.2 Process design optimisation strategy 110
7.2.1 Subproblem optimisation 111
7.2.2 Surrogate model development 112
7.3 Application: NGCC with post-combustion CO_2 capture 115
7.3.1 Base case comparison 115
7.3.2 Global problem optimisation 116
7.4 Conclusions 119

8 Systematic comparison of CO_2 capture options 121
8.1 Introduction 121
8.2 Performance comparison of CO_2 capture in power plants 122
8.2.1 Thermo-economic performance 122
8.2.2 Environmental performance 124
8.3 Influence of the economic scenarios on the competitiveness of the configurations 131
8.3.1 Sensitivity analysis 132
8.3.2 Economic scenarios influence 133
8.4 Market competition of CO_2 capture in power plants 146
8.5 Conclusions 148

Conclusions **149**

References **155**

Appendix **169**

A Cost correlations comparison **169**

B Process units flowsheets **173**

C Objective function choice **177**

D Compromise process configurations **181**

E H_2 processes: Environmental impacts **187**

F Parameterised CO_2 capture models **191**
F.1 Polynomial fit 191
F.2 Shortcut fit 192

G Economic Scenarios **193**
G.1 Market price evolution 193
G.2 Distribution functions 195

Nomenclature **199**

List of figures **203**

List of tables **215**

Curriculum vitae **221**

Introduction

Context

Actually the world is facing a dual challenge with regard to sustainable energy supply and greenhouse gas emissions reduction. The complexity consists in supplying more abundant and clean energy, consuming fewer fossil resources and finding appropriate solutions to reduce the emissions while also satisfying the energy requirement. Between 1971 and 2009, global CO_2 emissions doubled and until 2035 an additional increase of 22.4% is predicted due to the growing population and energy consumption. This increase of the greenhouse gas emissions produced by human activities contributes to the global warming which causes climate change. In 2010, fuel combustion emitted worldwide 30 Gt of CO_2, which were mainly attributed to coal 43%, oil 37% and gas resources 20% (IEA (2011a, 2012)). Figure 1 shows that the largest part of the global CO_2 emissions from fuel combustion is related to electricity generation and transport; two sectors consuming primarily fossil fuel resources. In pair with the CO_2 emissions increase, the total primary energy supply increased by nearly 50% between 1973 and 2010 to 12717 Mtoe (147PWh) (IEA (2012)). It is pointed out in Figure 2 that over 80% of the world primary energy is supplied by fossil resources, which will be depleted in the long term, and only a small part by renewable resources. These trends illustrate the need for a more sustainable energy future.

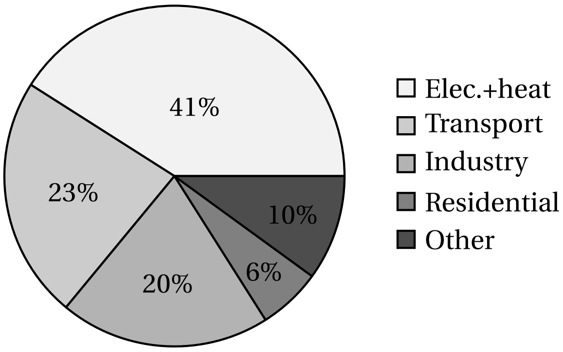

Figure 1: World CO_2 emissions from fuel combustion by sector in 2010 (IEA (2011a)).

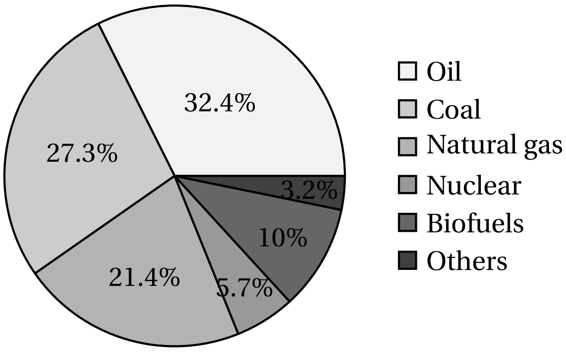

Figure 2: World total primary energy supply by fuel in 2010 (IEA (2012)). Others: 2.3% Hydro.

To meet these challenges of climate change mitigation and sustainable energy supply, several proposals have been investigated, particularly since the Kyoto Protocol in 1997, such as reducing the energy consumption, improving the energy efficiency, changing to less carbon intensive fuels and finally switching to renewable fuels. In the short to medium term, CO_2 emissions reduction by carbon capture and storage (CCS), is considered as a promising option for power plants applications, since fossil fuels will still be dominant. A general overview of the main features of CCS is given in the IPCC report (Metz et al. (2005)). In predictions for post 2020 scenarios (ZEP (2012), Finkenrath (2011), European Commission (2011)), CCS is regarded as cost-competitive compared to other low-carbon alternatives including wind and solar power.

The analysis, comparison and optimisation of fuel decarbonisation processes, capturing CO_2 *in electricity and/or* H_2 *generating processes, is the major topic of this thesis. The next sections briefly introduce the principles of CCS and give an overview of fuel decarbonisation research. Based on the outcomes of the state-of-the-art review, the objectives of this thesis are formulated and finally the thesis content is outlined.*

CO_2 capture and storage (CCS) principles

CCS could provide up to 20% of the targeted CO_2 emissions reductions until 2050 to keep global warming below 2^oC (ZEP (2012)). Therefore a rapid and widespread deployment of CCS is required from small-scale to commercial scale. The major steps of CCS, summarised in Figure 3, are:

- Capture: Gas separation techniques are applied to capture up to 90% of the CO_2 emissions from power plants and heavy industries.
- Transport: The captured CO_2 is first compressed into a liquid state and dehydrated for transport and storage, and then transported to the storage site by pipeline or ship.
- Storage: Potential storage methods are injection into underground geological formations, injection into the deep ocean, or industrial fixation in inorganic carbonates. Natural trapping mechanisms are applied for the safe and permanent CO_2 storage in geological formations, such as deep saline aquifers or depleted gas and oil fields (enhanced oil recovery EOR). These mechanisms include residual, dissolution and mineral trapping. A suitable CO_2 reservoir needs a layer of porous rock to absorb the CO_2 at the right depth (700-5000m) and an impermeable layer of cap rock to seal the porous layer (Metz et al. (2005), ZEP (2012)).

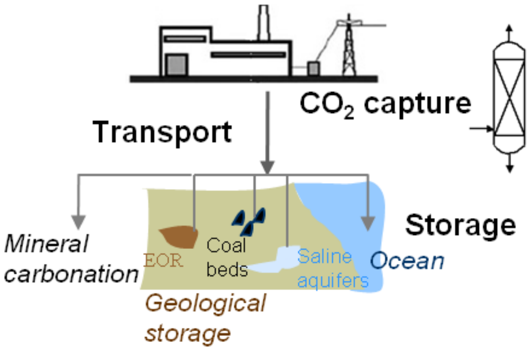
CO$_2$ capture
Transport
Storage
Mineral carbonation
EOR
Coal beds
Saline aquifers
Ocean
Geological storage

Figure 3: CO$_2$ capture and storage principle.

CO$_2$ capture

Three different concepts are distinguished for CO$_2$ capture in power plants, namely post-, oxy-fuel and pre-combustion, illustrated in Figure 4.

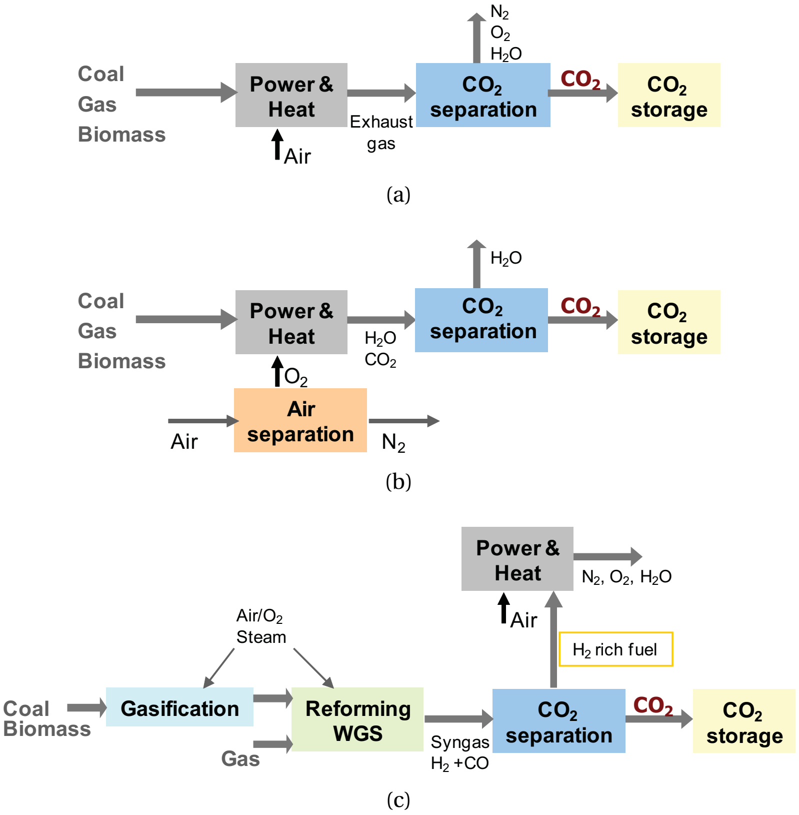
Coal
Gas
Biomass
Power & Heat
Air
Exhaust gas
N$_2$
O$_2$
H$_2$O
CO$_2$ separation
CO$_2$
CO$_2$ storage
Coal
Gas
Biomass
Power & Heat
O$_2$
H$_2$O
CO$_2$
H$_2$O
CO$_2$ separation
CO$_2$
CO$_2$ storage
Air
Air separation
N$_2$
Power & Heat
N$_2$, O$_2$, H$_2$O
Air
Air/O$_2$
Steam
H$_2$ rich fuel
Coal
Biomass
Gasification
Reforming WGS
Gas
Syngas
H$_2$ +CO
CO$_2$ separation
CO$_2$
CO$_2$ storage

(a)

(b)

(c)

Figure 4: CO$_2$ capture concepts: (a) Post-combustion CO$_2$ capture. (b) Oxy-fuel combustion. (c) Pre-combustion CO$_2$ capture.

Post-combustion is an end of pipe capture scheme, illustrated in Figure 4 (a), where after the primary fuel combustion with air, the flue gas consisting of CO_2, N_2 and H_2O is treated in order to capture the CO_2. The design challenge of post-combustion CO_2 capture is related to the low partial pressure of the CO_2 in the flue gas (typically 4-14%vol). Potential separation technologies are chemical absorption, gas separation membranes and cryogenic distillation. The low CO_2 concentration leads to large volumes to be treated and requires a high-capacity chemical solvent.

Oxy-fuel combustion. The CO_2 is captured during the combustion burning primary fuel in pure oxygen instead of air as described in Figure 4 (b). The oxygen is produced in an air separation unit removing the nitrogen either by cryogenic air distillation or by membrane processes. The flue gas consists mainly of H_2O and CO_2 (>80%vol) which is then compressed and dehydrated for transport and storage. One drawback of burning fuel in pure oxygen is that a high flame temperature is required. This impact can however be moderated by recycling CO_2 and/or H_2O-rich flue gas to the combustor. In addition, large amounts of oxygen are required and have to be produced by air separation, which is an energy and cost intensive process. Compared to post-combustion CO_2 capture, the main advantage is that the CO_2 needs only to be purified and that nearly no NOx are formed.

A new emerging concept with internal CO_2 capture is chemical looping combustion (CLC) using an oxygen carrier to bring the oxygen from the air to the fuel. Potential oxygen carriers are metal oxides such as Fe_2O_3, NiO, CuO or Mn_2O_3 (Metz et al. (2005)).

Pre-combustion. The CO_2 is captured before the fuel is burned. As detailed in Figure 4 (c), syngas, a mixture of H_2 and CO, is generated by reforming or gasifying fuel with oxygen or air. Then steam is added to the syngas in a water-gas-shift (WGS) reactor to convert the carbon monoxide CO to CO_2 and additional H_2. Candidate gas separation technologies are chemical and physical absorption and adsorption processes. The H_2-rich fuel can be used as fuel in boilers, furnaces, gas turbines, engines and fuel cells for power and/or heat generation. The captured CO_2 is compressed and dehydrated for transport and storage. The pre-combustion route is often referred to as 'Hydrogen route' since the generation of a H_2-rich fuel has many parallels with H_2 production by thermo-chemical conversion of hydrocarbons and purification by CO_2 separation. This has the advantage that the reforming and separation technology is commercially available. Especially physical solvents units (Rectisol, Selexol), which are well suited for high partial pressure CO_2 separation, are currently in operation. However, some developments are still required to adapt the gas turbine technology for H_2-rich fuel operation. An additional challenge is, as for the other concepts, the reduction of the efficiency penalty of CO_2 capture, for example by improved solvents, advanced shift with reduced steam consumption or simultaneous integration of the reaction and separation in a sorption-enhanced reactor.

Hydrogen has various applications as chemical for the production of ammonia and methanol and for hydrogenation, but also as energy carrier for transport, power generation and distributed heat production. This has led to the 'Hydrogen Economy' vision (Ball and Wietschel (2009), Ramage (2004)). Produced from a variety of widely available primary energy sources (i.e. renewable and fossil), this secondary energy carrier can supply clean, reliable and affordable energy and displace some demands for fossil fuels in the actual energy system. H_2 can be directly combusted in an internal combustion engine or electrochemically converted to electricity in a fuel cell system with a high efficiency reaching 50 to 60% (Stolten (2010)). When produced from renewable resources, the question of venting or capturing CO_2 is of concern. In this perspective, the pre-combustion or hydrogen routes have to be investigated with regard to the different competing outputs, H_2, heat and power and captured CO_2, and their interactions in polygeneration.

Not all the CO_2 capture concepts are compatible with each type of power plant to capture about 85-95% of the plant's CO_2 emissions. The choice of a specific capture technology is determined largely by the technology availability, the process operating conditions, the amount of CO_2 to be captured, the composition of the gas mixture and the energy requirement. The capture costs depend upon technical, economic and financial factors related to the design and operation of the production process or the power system of interest, and the applied CO_2 capture technology. Table 1 summarises and compares the characteristics of the different CCS schemes. Regarding the widespread commercialisation of large scale installations for CO_2 capture, several challenges have to be addressed and some developments have to be done to improve the technology availability.

Fuel decarbonisation in power plants applications can contribute to the reduction of the environmental impacts, however the power generation efficiency is decreased by up to 10%-points and the production costs are increased by over 30% due to the additional energy requirement and equipment costs for the CO_2 capture and compression. The challenge for R&D in future energy systems design consists therefore in minimising the penalties of CCS by rendering these processes energetically, economically and environmentally competitive by the means of process integration and improvements relative to the resources, technologies, operating conditions and targeted production goal.

Table 1: Comparison of CO_2 capture processes (Figueroa et al. (2008), Kanniche et al. (2010), Radgen et al. (2005), Olajire (2010)).

Concept	Post-combustion	Pre-combustion	Oxy-fuel combustion
Gas separation	CO_2 / N_2	CO_2 / H_2	O_2/N_2
Technology (preferred)	Chemical absorption	Physical/chemical ad-/absorption	Distillation
Technology (alternative)	Membrane /PSA	Membrane	Air separation membrane
Application	PC, NGCC	IGCC, NGCC	PC, NGCC
Advantage	Retrofit technology	High CO_2 partial pressure Compression costs/loads reduction	Flue gas concentrated in CO_2 Retrofit, repowering technology
Disadvantage	Low CO_2 partial pressure Solvent degradation Solvent regeneration	Fuel processing Availability	O_2 production requirement Cooled CO_2 recycle to maintain temperature
Developments	Absorbents	H_2 GT, membranes, gasifier	Burner, membranes
Cost influence	Absorber/compressor	Reformer	Air separation unit

Thermo-environomic evaluation of fuel decarbonisation processes

In the perspective of a sustainable energy future driven by greenhouse gas constraints, alternative energy systems and renewable resources, various ways of fuel decarbonisation by CO_2 capture and storage from large-point source emitters, especially power generation plants, have been studied over the last decades. Several research studies have been performed within the scope of identifying promising CCS processes for fossil fuel conversion into electricity and hydrogen. Some are based on fundamental considerations, while others report on results from basic engineering design. A review of the different process analysis studies is made here, before assessing in more detail the various methodologies that have been applied for the systems analysis and comparison.

Comprehensive assessment

Hydrogen economy. The challenges and opportunities for a future hydrogen economy are widely discussed in literature. The book edited by Ball and Wietschel (2009) was the first to cover H_2 in a holistic manner from a technical, environmental and socio-economic perspective by discussing issues like hydrogen infrastructure strategies and supply scenarios, interactions between H_2 and electricity, and the potential of H_2 as alternative fuel in the transportation sector. Winter (2009) addressed the features of H_2 in view of a change of the energy system with respect to the environmental and climatic relevance, the effect on fossil fuel decarbonisation and the exergy efficiency. The challenges of H_2 production, storage and infrastructures, and of fuel cell applications are addressed in Stolten (2010). The economic aspects of the hydrogen economy are investigated in Ramage (2004). A general overview of H_2 properties, applications and production routes is given in Häussinger et al. (2000).

Power plants with CCS. Technologies for CO_2 capture were explored since the 1970s with the objective of enhanced oil recovery rather than reducing greenhouse gas emissions. Economic, environmental and social issues for the comprehensive understanding of CCS technology are discussed in the IPCC report (Metz et al. (2005)), while the status of CCS in Switzerland is addressed in Wallquist and Werner (2008). The progress of CCS research and engineering is reviewed in Yang et al. (2008) and Figueroa et al. (2008). In the light of power plants performance improvements, a number of research projects were conducted in the field of fuel decarbonisation. CCS costs in the European Union are studied by the ZEP project (ZEP (2011)). For the oxy-fuel combustion concepts, many cycle configurations have been proposed; the AZEP scheme (Griffin et al. (2005)), the Graz cycle (Jericha et al. (2004)), the Matiant cycle (Mathieu and Nihart (1999)), the semi-closed CO_2-based power cycle (Bolland and Mathieu (1998)) and alternatively the chemical looping combustion (Chiesa et al. (2008)). Post-combustion CO_2 capture concepts were evaluated for natural gas fuelled power plants in Li et al. (2006) and Bernier et al. (2010) based on a multi-objective optimisation strategy and for coal based-power plants in Rao and Rubin (2002) based on stochastical modelling. Performance analyses of pre-combustion CO_2 capture concepts were investigated among others in Andersen et al. (2000), Lozza and Chiesa (2002a,b), Corradetti and Desideri (2005), Hetland (2009) and Romano et al. (2010). Different CCS concepts for natural gas fired power plants were evaluated and compared in Chiesa and Consonni (2000), Bolland and Undrum (2003), Kvamsdal et al. (2007) and Meerman et al. (2012), and for coal and gas power plants in Göttlicher (1999), Rubin et al. (2007) and Kanniche et al. (2010). A comparison of power plants using different resources is made in Parsons et al. (2002). In these studies the performance, efficiency and CO_2 emissions, are assessed essentially by mass- and heat balance simulations and cost estimations. In Zhang and Lior (2008) the process integration dimension was included through a graphical exergy analysis using exergy utilisation diagrams. Thermodynamic losses of fuel decarbonisation processes were quantified and localised extensively in Ertesvåg et al. (2005) and Petrakopoulou and Tsatsaronis (2012) through rigorous exergy analyses.

Co-production of electricity and H_2. Instead of focusing exclusively on power generation with reduced CO_2 emissions, several process simulation studies have looked at possibilities for electricity and H_2 co-generation with CCS and have identified the benefits and interactions between H_2 production and electricity generation. Based on performance and cost data of natural gas fired plants Davison et al. (2009, 2010) have revealed how synergies within the plant can be provided by co-production and face the variability in demand for the two products. The influence of the process configuration on the efficiency, costs and emissions of the co-production of H_2 and electricity from coal is addressed in Chiesa et al. (2005a) and Kreutz et al. (2005). Whereas the thermodynamic features of H_2 and electricity co-production from natural gas were investigated essentially through energy and exergy efficiencies assessments, irrespective of economic considerations in Consonni and Viganò (2005). Instead of extensive flowsheet calculations a data normalisation and standardisation method was applied in Damen et al. (2006, 2007) to make a consistent techno-economic comparison of several decarbonisation concepts and CO_2 removal technologies for state-of-the art and advanced coal and natural gas based power and H_2 plants. In Cormos (2010) process integration is applied to maximise the overall plant energy efficiency. These studies address the questions whether the co-production can be beneficial in terms of primary energy consumption and/or

CO_2 emissions and whether such practice is subject to technological and/or thermodynamic constraints.

H_2 production. In the field of hydrogen production, the influence of various operating parameters and technologies on the process performance was studied. H_2 process parameters were already optimised in 1983 for different objectives in van Weenen and Tielrooy (1983). H_2 supply evaluation based on the development of cost estimations was the scope of Simbeck and Chang (2002). Techno-economic analyses were conducted in Tarun et al. (2007) for the production of H_2 from natural gas and in Mueller-Langer et al. (2007) for the production of H_2 from fossil and renewable resources. Fossil fuel routes are compared explicitly in Longanbach et al. (2002), while technical and economic prospects of future production of H_2 from biomass were evaluated in Hamelinck and Faaij (2002), Cohce et al. (2010) and Toonssen et al. (2008). The economics of producing H_2 from fossil and renewable resources are compared in detail in Bartels et al. (2010). Environmental impacts were assessed rigorously by a life cycle assessment (LCA) approach in Spath and Mann (2001), Koroneos et al. (2004, 2008) and Dufour et al. (2012) for different H_2 production routes. Particular interest on the thermal efficiency (i.e. reaction characteristics) was paid in Seo et al. (2002), Lutz et al. (2003, 2004) and Chen et al. (2010b) by examining extensively the thermodynamics of reforming and partial oxidation of natural gas to identify favourable operating conditions yielding the lowest energy cost. The thermodynamics of biomass based processes for H_2 production are studied in Cohce et al. (2010). The importance of energy and exergy analyses for the thermodynamic performance and process improvements was revealed in Rosen (1996), Rosen and Scott (1998), where energy analysis indicates that wastes are valuable, while exergy analysis shows that internal consumption must be reduced to increase the efficiency considerably. In Chen et al. (2010a) it is shown how heat recovery for reactants preheating can increase the H_2 yield by 10%. These researches reveal the importance of the analysis of multiple criteria to identify process improvements and optimal process designs.

Systems assessment methodologies

Several comparison, optimisation and selection methods were developed and applied to H_2 and fuel decarbonisation processes for different resources, technologies and operating conditions based on at least one of the following performance indicators; energy efficiency or penalty, economic profit and environmental impact. Most of them applied extensive flowsheet simulation methods (Tarun et al. (2007), Kvamsdal et al. (2007)) and for multi-objective optimisation non-dominated sorting genetic algorithms (NSGA) (Rajesh et al. (2001), Oh et al. (2001), Oh et al. (2002)) to understand the trade-off, for example between H_2 production and steam exportation. Pilavachi et al. (2009) applied the 'analytic hierarchy process' a structured tool that supports complex decisions by building a hierarchy based on the goal, criteria and decision alternatives. A steady-state off-design calculation method for studying the part load operation flexibility of CO_2 capture cycles was developed in Nord et al. (2009). Rubin et al.

(2007) applied the Integrated Environmental Control Model (IECM) for calculating under several conditions the performance, emissions and costs of fossil fuelled power plants. Only few methods included second law efficiency evaluations. Exergy efficiency was considered in the multi-criteria assessment in Ridolfi et al. (2009). Moreover, only restricted energy integration was performed in these strategies. In Romeo et al. (2008) several possibilities to integrate power plant and amine scrubbing were proposed to reduce the energy requirement, however no systematic energy integration technique was applied. Although, Yuan et al. (2008) developed an integrated system engineering strategy for modelling, integration and optimisation of hydrogen polygeneration plants considering thermal pinch analysis to identify the minimum energy requirement and applying the waste reduction algorithm for environmental performance estimation. These few studies including process integration aspects revealed the potential improvement of H_2 processes by energy recovery.

Conclusions

Multiple research studies have been carried out in the field of fuel decarbonisation by CCS in power and H_2 plants. Nevertheless, some gaps in technology knowledge have to be overcome and some technology developments have to be done (i.e. high-capacity and energy-efficient solvents, H_2 fuelled gas turbine,...) in the future for large scale commercialisation reliably establishing cost and thermo-environmental performance. Technologies for CO_2 capture are relatively well understood today. However, R&D of emerging concepts and enabling CCS technologies has to be pursued with emphasis on costs, fuel availability, primary energy demand and sustainability. To understand entirely the role the different CCS schemes could play in reducing greenhouse gas emissions, a number of issues need to be addressed simultaneously; like the assessment of all resulting emissions, the energy requirement and the costs of implementation. Considering the characteristics of H_2 as an alternative energy carrier, previous studies have shown the importance to address different process configurations with regard to the targeted production scope; either H_2 or electricity or co-production of both. Some performance results reported for different process configurations without and with CO_2 capture are summarised in Tables 2 and 3.

In each of these studies, the level of detail and the data quality alters considerably due to the variety of technologies and operating conditions considered, the assumptions made, the methodologies applied, the thermodynamic properties models and the software tools used. This yields a large range of performance results making a consistent comparison difficult. Thermodynamic, economic and environmental criteria are generally addressed in a non-integrated fashion to define the synthesis, design and operational mode of process systems due to the lack of a unified approach handling different criteria simultaneously. Most economic studies comparing H_2 and/or electricity generation processes using various resources and technologies are mainly based on a literature survey with regard to the production costs and do not include extensive process modelling and optimisation. Whereas, studies focusing on thermodynamic analysis, rarely include economic analysis, energy integration and environmental aspects.

Table 2: Performance of state-of-the-art power plants configurations with and without CO_2 capture based on references: Kanniche et al. (2010), Parsons et al. (2002), Rubin et al. (2007), Damen et al. (2006), Kvamsdal et al. (2007), Bolland and Undrum (2003), Chiesa and Consonni (2000), Zhang and Lior (2008), Lozza and Chiesa (2002b,a), Mann and Spath (1997), Carpentieri et al. (2005).

Feedstock	Conversion technology	CO_2 capture technology	Net elec. efficiency [%]	CO_2 capture rate [%]	CO_2 emissions [kg/GJ_e]	Cost (Metz et al. (2005)) [\$/$t_{CO2,captured}$]
Coal	PC	No capture	45/39	0	204-231	-
	PC	Post-comb.	30-35/27.7	85-90	16.1	23-35
	PC	Oxy-comb.	35	85-90		
	IGCC	No capture	41-46	0	189-235	-
	IGCC	Pre-comb.	32-35	85	105	3-9
Natural gas	NGCC	No capture	56-60	0	95-105	-
	NGCC	Pre-comb.	45-48	85-90	11-12	
	NGCC	Post-comb.	47-51	85-90	10-12	33-57
	NGCC	Oxy-comb.	47-51	85-90		
	AZEP	Oxy-fuel	50	100	17	
Biomass	IBGCC	No capture	37(HHV)	0	18.7	-
	IBGCC	Pre-comb.	33.94	80	178	-

Table 3: Performance of state-of-the-art H_2 plants configurations with and without CO_2 capture based on references: Longanbach et al. (2002), Bartels et al. (2010), Toonssen et al. (2008) and Hamelinck and Faaij (2002).

Process	CO_2 capture rate [%]	Energy efficiency [%]	Production costs [\$/GJ_{H2}]	Productivity [t_{H2}/d]	Resource price
Natural gas	0	83.9 (HHV)	5.2	418	3\$/GJ_{NG}
Natural gas	71	78.6 (HHV)	5.6	418	3\$/GJ_{NG}
Coal (Texaco gasif.)	0	63.7 (HHV)	8.7	309	29\$/t_{Coal}
Coal (Texaco gasif.)	87	59 (HHV)	10.5	281	29\$/t_{Coal}
Biomass (FICFB, CGC)	-	57.7	-	-	-
Biomass	-	51-60	8-11	90-184	2\$/GJ_{BM}

However, to identify process improvements and optimal process designs it is important to make a consistent comparison using the same methodology and uniform assumptions, and to take into consideration multiple criteria simultaneously. In doing so, different process options can be evaluated against each other and ranked for decision-making. When process designs are only evaluated with regard to one criterion, for example maximum energy efficiency, there is a risk to promote expensive and environmentally harmful processes. Consequently, the process competitiveness needs to be rated by multiple criteria. Several methods have recently been developed to support planning and decision-making essentially in the field of H_2 infrastructures design and to estimate the energy and economic consequences taking into account multiple parameters. So far, only reduced multi-criteria assessments and multi-objective optimisations were applied to power plants with CCS in general. Moreover, in the multi-objective optimisations performed in this field, economic, thermodynamic and/or environmental objectives are chosen generally without considering the use of energy integration techniques and without including rigorous life cycle assessment (LCA). Only few evaluations consider thermodynamic and exergy analyses extensively. In the view of increasing the energy conversion efficiency, process integration maximising the heat recovery and minimising the energy losses is however inevitable. Therefore, the development of a comprehensive comparison framework for fuel decarbonisation processes comparison and optimisation is needed.

Objectives

To overcome the difficulties of comparing processes with regard to multiple criteria and different assumptions, the goal of this thesis is to propose a comprehensive comparison framework for the quantitative and consistent comparison and optimisation of process options. The objective is to use a uniform methodology for the systematic comparison and optimisation of different fuel decarbonisation process configurations. By combining thermo-economic models, energy integration techniques, and economic and environmental performance evaluations simultaneously, the developed platform based on computer-aided tools will support the decision-making process for H_2 and fuel decarbonisation process development, design and operation with regard to several criteria. Special interest is given to the effect of polygeneration of H_2 fuel, captured CO_2, heat and power, in order to identify its advantages and constraints, and to better understand the trade-offs between efficiency, investment and emissions.

The approach has to be systematic and has to provide a fast, comprehensive and optimal reassessment of design options when conditions change. A methodology able to generate optimal process configurations by taking into account the thermodynamic efficiencies based on process integration techniques, the economic performance and the environmental impacts from LCA results will be beneficial from a sustainability and process engineering point of view to identify possibilities to enhance the competitiveness of power plants and H_2 systems with CCS. The usefulness of an optimisation framework including process integration and considering multiple criteria has already been proven in the field of biomass conversion into biofuels (Gassner and Maréchal (2009a), Gerber et al. (2011), Tock et al. (2010)) and in a previous study of the optimisation of a post-combustion process in Bernier et al. (2010).

Based on the development and application of a consistent evaluation and optimisation methodology, this thesis intends to study and understand the competing energetic, economic and environmental costs of carbon capture for greenhouse gas mitigation and sustainable energy supply in actual and future energy systems. It is focused on two types of feedstocks for the generation of H_2 and electricity: namely fossil natural gas and renewable woody biomass. CO_2 transport and sequestration issues are beyond the scope of this thesis and hence not investigated in detail, however it is accounted for CO_2 compression to 110 bar for subsequent transportation. The potential of CO_2 sequestration in Switzerland is investigated in Chevalier et al. (2010) and a cost estimation of CO_2 storage in the EU is made in ZEP (2011). In Norway, Canada and Algeria industrial-scale storage projects are successfully in operation (Metz et al. (2005)).

This research aims at answering the following questions: What defines the economic and environmental cost of fuel decarbonisation? What is the influence of the technology choice and the economic scenario? What is the benefit from process integration implementation? What is the effect of the installation size? What causes the trade-off between the objectives and what are the consequences on the decision-making? What are the technological challenges to be addressed in the future? What are the bottlenecks of this technology to penetrate the market?

In order to address these questions the main challenges and objectives of this research are:

(i) The development of a **systematic framework** for the thermo-economic modelling, analysis and optimisation. By separating the technology models from the analysis models, models developed with different software can be assembled in large superstructures from which process designs can be extracted and optimised systematically with regard to competitive objectives including energetic, economic and environmental considerations.

(ii) The development of **flowsheets** to simulate accurately the chemical and physical transformations in fuel decarbonisation processes using different resources and technologies. The challenge of the process operation unit model development is to generate a coherent representation of the existing technologies with the appropriate assumptions and at the same time to include sufficient details to be accurate and flexible but avoid complexity. In addition, these models have to reflect the influence of the design parameters on the chemical conversion and on the energy demands.

(iii) To identify possibilities for process improvements by **energy integration**. By applying pinch analysis, it will be shown how the quality of the process integration influences the competitiveness of the process configurations; i.e. opportunities for maximising the internal heat exchange and optimising the valorisation of excess heat for combined heat and power generation are revealed.

(iv) To make a **consistent economic evaluation** (i.e. uniform approach and assumptions) taking into account the variability of the market conditions, the resource prices, the operation time and the interest rate. The main challenge of comparing literature data is primarily related to the various assumptions made, especially in the costs assessment, therefore this systematic evaluation step is crucial in the rational process design methodology. With regard to the CO_2 capture competitiveness, the question of the introduction of a carbon tax has to be assessed.

(v) To perform **life cycle assessment** to assess the advantage of CO_2 capture with regard to the environmental impacts. This will allow to answer the question of how processes using biomass perform compared to processes using natural gas or coal and compared to alternative renewable processes such as solar or hydroelectricity.

(vi) To carry out **multi-objective optimisation** to identify optimal process configurations and **support decision-making**. Multi-objective optimisation has the advantage to assess the trade-off between competing objectives with regard to different decision variables including the process configuration and the design parameters (i.e. operating conditions).

(vii) Evaluate the impact of CO_2 capture on the thermodynamic, economic and environmental performance of H_2 and power generation plants by comparing and optimising different CO_2 capture concepts and technologies. For different feedstocks (i.e. natural gas and biomass) and technologies the optimal process design and performance is determined for different economic scenarios. This allows to answer the question of the potential and **competitiveness of CO_2 capture** in processes producing hydrogen and/or electricity based on fossil or renewable resources. The break even economic conditions (i.e. carbon tax and resource price) making these options competitive in a more sustainable energy future can be identified.

Outline

The methodology developed for the design, optimisation and comparison of fuel decarbonisation processes is described in detail in Chapter 1. Different technologies for CO_2 capture are introduced in Chapter 2 and the respective thermo-economic models are set up. In Chapters 3-6, the presented methodology is applied to study pre- and post-combustion CO_2 capture processes. In Chapter 3, the performance of different pre-combustion CO_2 capture process configurations producing H_2 and/or electricity from biomass or natural gas is assessed and optimised. The detailed comparison of different CO_2 separation technologies applied to pre-combustion CO_2 capture processes in Chapter 4 reveals the importance of process integration. The impact of post-combustion CO_2 capture with chemical absorption with amines and of flue gas recirculation in natural gas combined cycle plants (NGCC) is assessed in Chapter 5. In Chapter 6, the energy and cost penalty of chemical absorption with amines and of chilled ammonia applied to NGCC plants are compared. It is pointed out how process improvements can be identified from the energy integration results. A methodology for developing surrogate models of CO_2 capture technologies predicting accurately the costs and energy demands with a reduced computation time is established in Chapter 7. The optimal process configurations for electricity generation by the different pre- and post-combustion CO_2 capture processes are compared in detail in Chapter 8 with regard to the life cycle environmental impacts and with regard to different economic scenarios. In addition, an approach to support decision-making based on the Pareto results is presented in Chapter 8. Finally, conclusions on the potential of these options in an sustainable energy future and on the R&D challenges of CCS are drawn.

1 Thermo-environomic optimisation methodology

This chapter describes the thermo-environomic (i.e. energetic, economic and environmental) evaluation and optimisation strategy that has been applied throughout the thesis. The basis of the strategy has been published in Tock and Maréchal (2012e).

1.1 Introduction

To design complex integrated energy conversion systems, such as power plants with CCS, taking into account energetic, economic and environmental considerations, a systematic approach is developed. The methodology relies on previous developments presented in Bolliger et al. (2009), Bolliger (2010), Gassner and Maréchal (2009a) and Gerber et al. (2011). Bolliger et al. first presented a generic approach to analyse energy conversion systems by separating the process unit models from the data needed to model the energy and mass integration in the system. Following this approach, models can be assembled in large superstructures from which system configurations can be extracted and optimised systematically with regard to competitive objectives. Dissociating system models from the system design methods is the main advantage compared to other platforms such as DOME (Pahng et al. (1998)) and CAPE-OPEN (Dickinson (2008)) dealing essentially with the flowsheeting and requiring an explicit definition of the interconnections.

The development of this platform is motivated by the need of a flexible tool for the conceptual process design combining thermodynamic analysis, energy integration, performance evaluation and multi-objective optimisation strategies. Such a systematic methodology has previously been applied successfully to study biofuel production systems (Gassner and Maréchal (2009a,b), Tock et al. (2010)) and fuel cell systems (Facchinetti et al. (2011), Maréchal et al. (2005), Autissier et al. (2007)). For H_2 and power generation plants with CCS, such an consistent approach has not been applied yet. This chapter introduces the developed thermo-environomic (i.e. thermodynamic, economic and environmental) evaluation and optimisation strategy for studying CO_2 capture options in H_2 and power generation plants.

1.2 Strategy

The process design methodology combines process modelling, using established flowsheeting tools, and process integration models in a multi-objective optimisation framework following the approach presented in Gassner and Maréchal (2009a). The main features of the methodology are summarised in Figure 1.1. Technology models representing the physical behaviour are separated from the thermo-economic analysis models and the multi-objective optimisation including energy integration, economic evaluation and environmental impact assessment. Through a MATLAB-language based platform (MathWorks Inc.), structured data is transferred between the different models. The advantage of dissociating the technology models from the analysis models is that process unit models developed with different software can be assembled in a superstructure for subsequent large processes design and optimisation.

First a block flow diagram of the studied conversion process is set up and suitable technologies are summarised in a superstructure. For each building block of the process superstructure, chemical and physical models of process units are developed and the heat transfer requirement is defined. The energy-integration model optimises the heat recovery in the system and the combined heat and power production by applying the pinch analysis concept. Knowing the flows and operating conditions in the selected units of the energy system, the size and equipment costs are estimated in order to calculate the economic and environmental performance. The trade-off between competing performance indicators is assessed by sensitivity analysis and multi-objective optimisation defining the optimal values of the decision variables and of the system design. The platform consists hence of different layers: the model, the computation type (i.e. optimisation, sensitivity analysis, one run) and the results extraction.

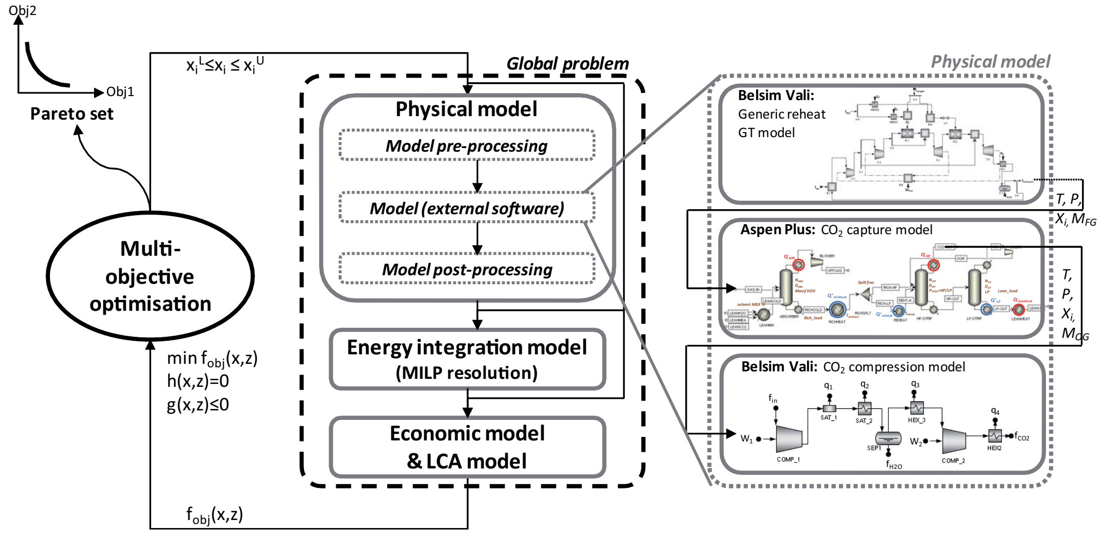
Obj2
Obj1
Pareto set
Multi-objective optimisation
$x_i^L \le x_i \le x_i^U$
min $f_{obj}(x,z)$
$h(x,z)=0$
$g(x,z)\le 0$
$f_{obj}(x,z)$
Global problem
Physical model
Model pre-processing
Model (external software)
Model post-processing
Energy integration model
(MILP resolution)
Economic model
& LCA model
Physical model
Belsim Vali:
Generic reheat
GT model
T, P, X_i, M_{FG}
Aspen Plus: CO_2 capture model
T, P, X_i, M_{CG}
Belsim Vali: CO_2 compression model
f_{in}
q_1
q_2
q_3
q_4
W_1
W_2
SAT_1
SAT_2
HEX_3
HEX2
SEP1
COMP_1
COMP_2
f_{H2O}
f_{CO2}

Figure 1.1: Illustration of the developed platform for studying energy conversion systems.

1.3 Thermo-environomic modelling

1.3.1 Process superstructure

For the process design, a block flow diagram of the conversion process to be studied is first set up. Therefore, the available feedstocks and energy resources, the products and by-products specifications, the main process steps and the thermodynamically and technically feasible operating conditions are identified based on a literature survey. For the different process unit operations, such as feed preparation, thermo-chemical conversion/synthesis, gas treatment, and purification, candidate process technologies are assembled in a process superstructure. The superstructure is completed with technology options for the heat recovery and the optimal energy conversion system, such as gas turbines, heat pumps and Rankine cycles. Such a superstructure is illustrated for pre-combustion CO_2 capture processes in Chapter 3 Figure 3.1.

1.3.2 Energy-flow model

Process models are developed within specially tailored modelling languages using numerical solvers to solve the set of equations describing the thermo-physical and chemical conversion operations of the technology for a given set of decision variables and unit model parameters. The variables to be specified are defined by a degree of freedom analysis. Each model follows this calling sequence: pre-processing, simulation, post-processing. The pre-processing phase selects the process model, collects necessary parameters and transfers the decision variables to the model. The simulation phase calculates the process unit using an external flowsheeting software; for example *Belsim Vali* (Belsim S.A.) which is suitable for design as well as for data reconciliation purposes and uses a simultaneous resolution approach, or *Aspen Plus* (AspenTech, Aspen Technology Inc.) using a sequential resolution approach for process simulation. The post-processing phase extracts from the simulation results, the data needed to define the unit interface with the rest of the process. Since each model is organised as an input (decision variables) - output entity, the internal mathematical formulation appears as a black box for the process synthesis model. The asset of defining the models in this way is that process unit models developed with different software can be combined. The communication between different models, the calculation sequence and the process synthesis model set-up is organised in a MATLAB-language code (MathWorks Inc.).

In the physical model, the thermodynamic state of the process unit operations are calculated based on mass and energy balances. Each process unit carries decision variables whose value will be fixed by optimisation. The challenge of the process modelling is to generate a coherent representation of the existing technologies that reflects the influence of the operating conditions accurately. For the developed models, the modelling assumptions and operating ranges are essentially based on literature data, due to lack of experimental data. However, if experimental results are available a systematic parameter validation of the developed models can be performed, which then could also be used for the design of experiments. The platform extracts the data required for the analysis models, such as the material conversion and the heat and power requirement. The characteristics of the hot and cold streams are required for the energy integration. The flowrates, material, pressure and temperature are needed for the cost estimation and the life cycle inventory.

1.3.3 Energy integration model

Once the chemical and physical transformations and the heat transfer requirements are determined, energy integration can be performed. The energy consumption of the process is minimised by calculating thermodynamically feasible energy targets and achieving them by optimising the heat recovery and the combined heat generation. The systematic combination of the different options for fuel conversion for combined heat and power integration is developed using the superstructure concept and the optimal system configuration is then defined by selecting the most profitable energy conversion system. The problem is solved as a Mixed Integer Linear Programming Problem (MILP) minimising the operating costs, while computing the mass balances and the heat cascade as explained in Maréchal and Kalitventzeff (1998) and Gassner and Maréchal (2009a).

The energy integration model is based on the definition and the identification of the hot and cold streams temperature-enthalpy profiles and their minimum approach temperature ΔT_{min}. By definition a hot stream needs to be cooled down so it is a heat producer; while a cold stream has to be heated up and consequently is a heat consumer. The temperature of each stream is corrected by the minimum approach temperature ΔT_{min} to assure a feasible heat exchange and to account for different values of the heat transfer coefficients. For hot streams the temperature value is reduced by $\Delta T_{min}/2$ and for cold streams increased by $\Delta T_{min}/2$. $\Delta T_{min}/2$ values of 8, 4 and 2 K are assumed for gaseous, liquid and condensing/evaporating streams, respectively. By solving the combined mass and energy integration, the optimal heat recovery is determined and the combined production of fuel, heat and power is computed.

The composite curves are calculated by assembling the hot and cold streams. The hot composite curve characterised by an enthalpy-temperature diagram (i.e. H-T diagram), represents the heat available in the process and the cold composite curve the heat demands of the process. The composite curves are usually reported in corrected temperature axis (i.e. accounting for the ΔT_{min}). The pinch point is the point where the temperature difference between the hot and cold curve is minimal. The maximum heat recovery is determined by considering that heat exchange can only take place, if the temperature difference between the composite curves is superior to ΔT_{min}. Globally, the process requires energy above the pinch point (i.e. heat sink) and releases energy (i.e. heat source) below the pinch point. The graphical analysis of the composite curves and the identification of the pinch point is applied to propose process improvement options, such as polygeneration including steam cycles, combined heat and power, refrigeration and heat pumping.

The heat required by the cold streams is usually supplied by the conversion of primary energy sources, waste streams, or intermediate process streams and by recovering heat from the hot streams in the heat exchangers. The cooling demand is satisfied by conventional cooling by river water, or by refrigeration cycles if the required temperature is below ambient temperature. After heat recovery, the energy balance can show an excess of heat. This excess heat that is released from the process can be valorised by producing high and low level steam that can be used either as heat source for industrial purposes or in steam turbines to generate additional electricity. To satisfy the energy requirements, the following rules have to be respected:

1) No cold utility used above the pinch point.
2) No hot utility used below the pinch point.
3) No exchanger can transfer heat across the pinch point.

The key points here are to define the superstructure including all potential hot and cold utilities, to determine the best utility operating conditions, to choose adequate minimum approach temperatures with regard to the energy-capital trade-off and to minimise the losses by appropriate process integration with respect to the process operation characteristics. In the following chapters, it is shown how the quality of the process integration determines the process performance.

1.3.4 Performance evaluation model

To assess the process performance several indicators are defined in the performance evaluation model. The competitiveness of the process configurations is primarily evaluated by some thermodynamic, economic and environmental indicators. These indicators are differently weighted combinations of the material, energy and monetary process inputs and outputs determined based on the process flowsheet.

- Energy: chemical efficiency, energy efficiency,...
- Economic: investment cost, operating cost, production cost, CO_2 avoidance cost,...
- Environmental: local CO_2 emissions, life cycle impacts,...

To evaluate these performance indicators, the equipment is sized to estimate the respective costs and the environmental impacts are assessed based on a life cycle inventory (LCI).

Equipment sizing and cost estimation

The economic performance is defined on the one hand by the capital investment and on the other hand by the operation and maintenance costs. The major concern is to make a reliable economic evaluation. Ideally, real market prices for commercial equipment or manufacturer's data for emerging technologies have to be used for an accurate analysis. However manufacturers publish only little information and generally precise information is hardly available.

Therefore, the investment costs are evaluated here by using costs correlations. These estimations are based on the size and the type of construction material of each equipment that depend on the process productivity determined by the decision variables and the operating conditions. For the preliminary rating, equipment design heuristics from literature are used to estimate the size at the given production scale. Following the approach outlined in Turton (2009), the equipment costs are then estimated by applying the correlations given in Turton (2009) and Ulrich and Vasudevan (2003) for a multitude of equipment. In literature various approaches are found to estimate costs (Turton (2009), Ulrich and Vasudevan (2003), Chauvel et al. (2001), Mussatti (2002), Klemeš et al. (2007)). The comparison of these estimations, applied for evaluating the costs of CO_2 capture by chemical absorption in Appendix A, reveals the difficulty of precisely estimating the costs with regard to the technology, size and operating conditions. According to Turton (2009) the accuracy of the estimations is about ±30%. Since this approach, using the uniform assumptions, is systematically applied for evaluating the different process configurations it allows nevertheless to make a consistent comparison of the options and to rank them. The comparison of the results with other published data (Section 8.4) shows all in all a good agreement. With real market data are available, the comparative study made here could be validated.

Investment cost. The equipment purchase costs are estimated by general correlations, assuming atmospheric pressure and carbon steel construction, given by Eq.1.1 (Turton (2009).

$$log C_{pc} = K_1 + K_2 log A + K_3 (log A)^2 \tag{1.1}$$

where K_i are constants and A is the characteristic size parameter (i.e. power for compressors, length/diameter for reactors and heat transfer area for heat exchangers).

Based on these correlations the bare module costs C_{BM}, representing the purchase costs adjusted by material (F_M) and pressure (F_P) factors, that take into account the specific process pressures and materials, are defined by Eq.1.2.

$$C_{BM} = (B_1 + B_2 F_M F_P) I \cdot C_{pc} \tag{1.2}$$

where B_i are constants and I is the actualisation factor expressed by the ratio of the Marshall and Swift Equipment Cost Index at actual time to the cost data's reference year.

The total grass roots costs C_{GR} defining the total investment costs (i.e. initial investment cost C_I) for a new production site are calculated from the bare module cost by using further multiplication factors to take into account indirect expenses like labour, transportation, fees, contingencies and auxiliary facilities (Eq.1.3).

$$C_{GR} = C_I = (1+\alpha_1)\sum_{i=1}^{n} C_{BM,i} + \alpha_2 \sum_{i=1}^{n} C_{BM,n,i} \tag{1.3}$$

where $C_{BM,n,i}$ represents the bare module costs of the i^{th} equipment for the base case conditions (i.e. atmospheric pressure and carbon steel material) and $C_{BM,i}$ the costs at the operating conditions. The two factors represent additional costs related to the construction of the plant being dependent (α_1) or independent (α_2) of the process conditions. According to Turton (2009) conventional values for these factors are: α_1=0.18 (contingencies 0.15 and fees 0.03) and α_2=0.35 (auxiliary facilities, site development and buildings).

Equipment sizing: Reactor. The equipment's size is defined based on the physical quantities computed from the flowsheet models. For example, the size of a reactor is estimated based on an empiric relation (Eq.1.4) between the diameter d, the volumetric flowrate $\dot{V}$ and the mean gas velocity u_{mean}, and an exponential relation (Eq.1.5) between the height h and the volumetric flowrate $\dot{V}$.

$$d = 2\sqrt{\frac{\dot{V}}{\Pi \cdot u_{mean}}} \tag{1.4}$$

$$h = h_o \dot{V}^b \tag{1.5}$$

For shell and tube reactors with catalysts the sizing and cost estimation method reported in Maréchal et al. (2005) is applied. The costs are mainly defined by the carbon conversion and the flowrate in the reactor. The cost evaluation comprises the catalyst volume and cost estimation, and the reactor volume and cost assessment.

The volume of the catalyst in the reactor k, $V^k_{catalyst}$, corresponds to the volume required to achieve the target conversion of reactant X and is computed from the reaction kinetics $-r^k_r$.

$$V^k_{catalyst} = \frac{\dot{n^k_{r,in}}}{\rho^k_B} \int_0^X \frac{dX}{-r^k_r} \tag{1.6}$$

where $n^k_{r,in}$ is the molar flow rate of reactant coming out of reactor k [mol/s] and ρ^k_B the bulk density of catalyst used in reactor k [kg/m^3].

The catalyst costs are then evaluated from the volume by knowing the volume cost $\pi^k_{catalyst}$:

$$C^k_{catalyst} = V^k_{catalyst} \cdot \pi^k_{catalyst} \tag{1.7}$$

The volume of the reactor V^k_{Rct} is estimated from the catalyst volume by introducing a proportionality constant F^k_V.

$$V^k_{Rct} = F^k_V \cdot V^k_{catalyst} \tag{1.8}$$

Finally, the costs of the reactor volume C^k_{volume}, is computed by scaling from a reference case with known costs C^k_{ref} and volume V^k_{ref}.

$$C^k_{volume} = C^k_{ref} \cdot F^k_V \cdot \left(\frac{V^k_{Rct}}{V^k_{ref}}\right)^{\gamma} \tag{1.9}$$

where γ is the scale exponent and F^k_V the proportionality constant taking into account the scaling due to pressure and material factors.

The values for the sizing and costing of the steam methane reformer (SMR) and the water-gas shift (WGS) reactor are summarised in Table 1.1. The appropriate catalyst is chosen in accordance with the process temperature. For the SMR reforming the selected catalyst is Ni/Al_2O_3 and for the water-gas shift reaction at high temperature (HTS) 1%Pd/Al_2O_3 and at low temperature (LTS) 5%Ni/Al_2O_3.

Table 1.1: Assumptions for the sizing of the SMR and WGS reactors (Maréchal et al. (2005)).

Process	SMR	WGS (HTS)	WGS (LTS)
Catalyst	Ni/Al_2O_3	1%Pd/Al_2O_3	5%Ni/Al_2O_3
α	-	0.14	-0.14
β	-	0.38	0.62
k [kmol/kgs]	227.8	1.93	39
Bulk density ρ_B [kg/m^3]	1200	1200	1200
Activation energy [J/mol]	129790	79967.8	78293
$\pi^k_{catalyst}$ [\$/m^3]	100000	16800	16800
C^k_{ref} [\$]	21936	5774.6	5774.6
V^k_{ref} [m^3]	0.0167	0.104	0.104
F^k_V	1.17	1.17	1.17
Scale exponent γ	0.6	0.6	0.6

Equipment sizing: Columns. According to Turton (2009) and Ulrich and Vasudevan (2003) the costs of distillation columns with tower packings are evaluated as the sum of the cost of the vertical vessels and the packings. Alternative approaches are presented in Appendix A. For packed towers the active tower height (H$_a$) is defined by Eq.1.10 and the diameter d is calculated (Eq.1.11) based on the gas mass flowrate [kg/s] ($\dot{m}_{gas}$), gas density [kg/m^3] (ρ_{gas}) and the vapour flow velocity [m/s] (u$_g$) (Ulrich and Vasudevan (2003)). The vapour flow velocity is estimated based on the Souders-Brown relation K$_{SB}$ and the gas and liquid densities

(ρ_l= 1013kg/m^3 for monoethanolamine (Radgen et al. (2005))) (Eq.1.12).

$$H_a = N_{stages} \cdot HETP \tag{1.10}$$

$$d = 2\sqrt{\frac{\dot{m}_{gas}}{\rho_{gas} \cdot \Pi \cdot u_g}} \tag{1.11}$$

$$u_g = K_{SB}\sqrt{\frac{\rho_l - \rho_g}{\rho_g}} \tag{1.12}$$

For the columns a maximal diameter of 5m is considered as construction constraint. If the calculated value by Eq.1.11 is higher, several units operating in parallel are considered. To calculate the height equivalent to a theoretical plate HETP the following relations are considered with ϵ being the tray efficiency (considered 90%) (Ulrich and Vasudevan (2003)).

$$HETP = 0.5d^{0.3}/\epsilon \quad d > 1m \tag{1.13}$$

$$HETP = 0.4d/\epsilon \quad d < 1m \tag{1.14}$$

The costs of the vessel and of the packings are defined by correlations taking into account the height, the diameter and the material (here cast steel) and the pressure by the corresponding factors.

Equipment sizing: Heat Exchanger. The capital cost estimation of the heat exchanger network is based on the average surface area and the number of units necessary to satisfy the minimum energy requirements computed by the energy integration. Since this approach does not include the actual heat exchanger network design, the cost estimation is not based on the proper sizing of each equipment and therefore the costs are overestimated because the minimum energy requirement generally results in a greater number of units having smaller surface areas. The disadvantage of this method is, that it does not account for the specific process conditions. However, for heat exchangers operating in the range of 1-50 bar, this influence is negligible. The costs of the heat exchangers are given by the correlation for a fixed tube sheet heat exchanger. The overall costs are assessed by the average value of the costs of a heat exchanger operating at high pressure (construction material nickel alloy) and one at low pressure (construction material carbon steel) multiplied by the minimal number of heat exchangers.

Production costs. The production costs C$_P$, expressed in \$/GJ$_e$ or \$/GJ$_{H2}$, are evaluated by Eq.1.15 dividing the total annual costs of the system consisting of annual investment (C$_{I,d}$) and operating and maintenance costs (COM) by the annual production of electricity or fuel (P$_a$). All the costs have been updated to year 2011 by using the Marshall and Swift Index (Table 1.2).

The operating and maintenance costs (COM) consist of the costs of raw materials (C_{RM}), utilities (i.e. electricity demand) (C_{UT}), labour (C_{OL}) and maintenance (C_M) calculated based on Eqs.1.16-1.21. By using this method, it is possible to study the balance between the costs arising from the initial investment and the performance of the equipment with regard to the consumption of resources.

$$C_P = C_{I,d} + COM \tag{1.15}$$

$$COM = C_M + C_{OL} + C_{UT} + C_{RM} \tag{1.16}$$

$$C_{I,d} = \frac{i_r \cdot (1+i_r)^n}{(1+i_r)^n - 1} \cdot \frac{C_I}{P_a} \tag{1.17}$$

$$C_M = 0.05 \cdot \frac{C_I}{P_a} \tag{1.18}$$

$$C_{OL} = \frac{C_{salaries}}{P_a} \tag{1.19}$$

$$C_{RM} = GJ_{RM,consumed} \cdot c_{RM} \tag{1.20}$$

$$C_{UT} = GJ_{e,consumed} \cdot c_{el} \tag{1.21}$$

The discounted investment costs (i.e. annual investment costs) $C_{I,d}$ take into account the technical and economic lifetime n of the installation and the interest rate i_r. The annual maintenance costs C_M are supposed to amount to 5% of the initial investment. Unitary prices for raw material and electricity are termed c_{RM} and c_{el} respectively. The different assumptions for the economic analyses are reported in Table 1.2.

Table 1.2: Assumptions for the economic analysis.

Parameter	Value
Marshall and Swift index	1473.3
Dollar exchange rate	1.2 \$/€
Expected lifetime	25 years
Interest rate	6%
Yearly operation	7500h/y
Operators[a]	4[b] p./shift
Operator’s salary	91’070 \$ /y
Wood price (θ_{wood}=50%wt)	13.9 \$ /GJ_{BM}
Electricity price (green)	75 \$ /GJ_e
MEA price	0.970 \$/kg_{MEA}
Natural gas price	9.7 \$/GJ_{NG}

[a] Full time operation requires three shifts per day. With a working time of five days per week and 48 weeks per year, one operator per shift corresponds to 4.56 employees.

[b] For a plant size of 20 $MW_{th,wood}$. For other production scales, an exponent of 0.7 with respect to plant capacity is used.

For the processes generating electricity as the main product, the production costs C_P correspond to the electricity production costs known as COE (cost of electricity) and C_{UT} is considered to be zero (i.e. no electricity purchase). In Chapter 8 it is shown how these economic assumptions influence the competitiveness of the process configurations.

Environmental impacts evaluation

With regard to CO_2 emissions mitigation, an assessment of the overall life cycle environmental impacts from the resource extraction along the production chain to the final product, including off-site emissions and construction emissions, is essential. Life cycle assessment (LCA) has been proven to be suitable for this scope. LCA is a well-established method, standardised in ISO 14040 & 14044 (ISO (2006a,b)), that allows to assess the environmental performance of a product, a system or a service accounting for its full life cycle and related to its function. LCA consists of four main stages; the goal and scope definition, the life cycle inventory (LCI), the impact assessment (LCIA) and the interpretation.

In the goal and scope definition step, the function of the studied system is defined and quantified by the functional unit (FU) and the systems boundaries are defined. Common choices for the functional units are the unitary consumption of the feedstock (e.g 1 MW of natural gas) or the unitary production of the main product (e.g. 1 kg of H_2 or 1 GJ of electricity).

In the life cycle inventory phase (LCI), the extractions, resources and emissions involved in the process are identified and quantified.

In the life cycle impact assessment (LCIA), the cumulated emissions and extraction inventory is then aggregated in more global indicators, having an environmental significance. Typical indicators are the global warming potential, the resources depletion, the acidification and eutrophication potential.

The interpretation phase has as a goal to identify, quantify, check, and evaluate information from the results of the life cycle inventory and/or the life cycle impact assessment in order to support decision-making.

As shown by Gerber (Gerber (2012), Gerber et al. (2011)), life cycle assessment can be included in the thermo-economic models. For this purpose, the LCI is written as a function of the characteristics (i.e. design variables, mass and energy balances, equipment size) of the thermo-economic model. The influence of the process scale is included by scale-up laws similar to the costing. The results from the energy flow and energy integration models are used to perform the LCI of emissions and extraction flows from the process operation and equipment in the considered system boundary illustrated in Figure 1.2. Based on the LCI, a LCIA is performed and the impact categories defining the environmental performance can be included as an objective in the multi-objective environomic optimisation. The choice of the system boundary, the functional unit and the impact method are very important for a consistent comparison and ranking of process options with regard to both environmental and economic performance. More details of this methodology are found in Gerber (2012) with an application to biofuel processes and geothermal systems.

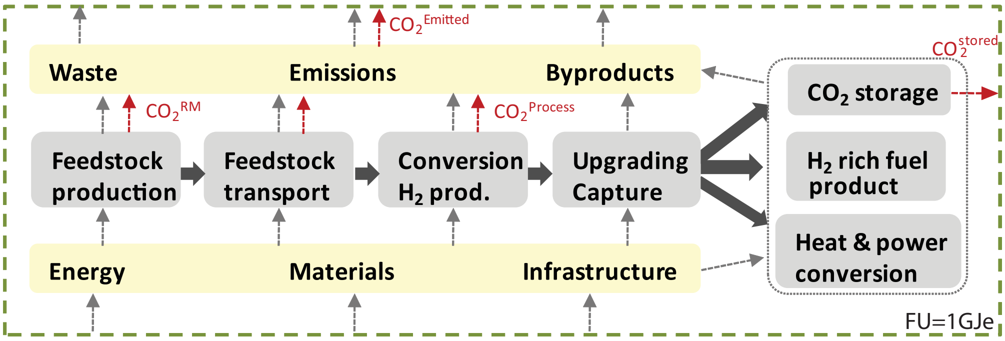
$CO_2^{Emitted}$
CO_2^{stored}
Waste
Emissions
Byproducts
CO_2^{RM}
$CO_2^{Process}$
CO₂ storage
Feedstock production
Feedstock transport
Conversion H₂ prod.
Upgrading Capture
H₂ rich fuel product
Heat & power conversion
Energy
Materials
Infrastructure
FU=1GJe

Figure 1.2: Typical system's boundary for the life cycle inventory.

1.4 Multi-objective optimisation

1.4.1 Performance indicators

The performance of different process options is evaluated by thermodynamic, economic and environmental performance indicators defined from the thermo-environomic process model. The energetic performance depends on the one hand on the efficiency of the chemical conversion into fuel defined by the technology choice, the operating conditions, the stoichiometry and the product type, and on the other hand on the quality of the process integration that depends on the energy conversion technologies, the heat recovery and the combined heat and power production. The energetic performance is defined generically based on the schematic process description reported in Figure 1.3 (a).

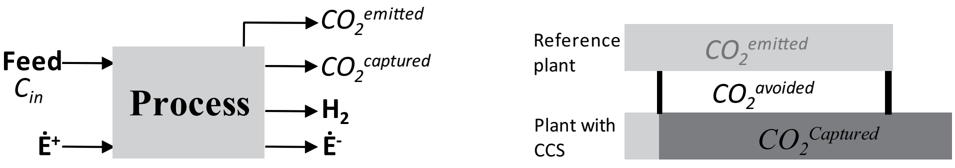
Feed
C_{in}
$\dot{E}^+$
Process
$CO_2^{emitted}$
$CO_2^{captured}$
H₂
$\dot{E}^-$
Reference plant
$CO_2^{emitted}$
$CO_2^{avoided}$
Plant with CCS
$CO_2^{Captured}$

(a) (b)

Figure 1.3: (a) Schematic process description. (b) Avoided CO_2 definition illustration.

The first law energy efficiency ϵ_{tot} calculated by Eq.1.22, takes into account the energy of the products and the resources, and considers thermal and mechanical energy as being equivalent. In order to take into account the difference of the quality of the energy, the natural gas equivalent efficiency ϵ_{eq} is defined by Eq.1.23. In this definition, the consumed electricity is presented by the net electricity output ($\Delta\dot{E}^- = \dot{E}^- - \dot{E}^+$). The net electricity output is substituted by an equivalent amount of natural gas required for generating the same amount of electricity in a combined cycle with an energy efficiency η of 57.3%. The ϵ_{tot} expression is reduced to Eq.1.24 for power plants applications. The reported efficiencies are expressed on the basis of the lower heating value (Δh^0, LHV).

$$\epsilon_{tot} = \frac{\Delta h^0_{H2,out} \cdot \dot{m}_{H2,out} + \dot{E}^-}{\Delta h^0_{feed,in} \cdot \dot{m}_{feed,in} + \dot{E}^+} \tag{1.22}$$

$$\epsilon_{eq} = \frac{\Delta h^0_{H2,out} \cdot \dot{m}_{H2,out} + \frac{1}{\eta}\Delta\dot{E}^-}{\Delta h^0_{feed,in} \cdot \dot{m}_{feed,in}} \tag{1.23}$$

$$\epsilon_{tot} = \frac{\Delta\dot{E}^-}{\Delta h^0_{feed,in} \cdot \dot{m}_{feed,in}} \tag{1.24}$$

To assess the CO_2 mitigation potential, the CO_2 capture rate is defined in Eq.1.25 by the molar ratio between the CO_2 captured and the carbon entering the system (Figure 1.3 (a)). For electricity import in H_2 production processes, green electricity is considered since the aim is to evaluate the potential CO_2 emissions reduction. Consequently no local carbon emissions have been accounted for electricity importation. The CO_2 capture cost is evaluated by the CO_2 avoidance costs, which are expressed in Eq.1.26 by the difference of the emissions and the difference of the total production cost with regard to a reference plant without CO_2 capture. Figure 1.3 (b) illustrates the definition of the avoided CO_2 emissions. For the reference plant the performance data reported in Table 1.3 are considered in the following chapters. In addition, the life cycle impacts of the whole process chain are considered to evaluate the environmental performance indicators (e.g. global warming potential, resources extraction) as explained in Sections 1.3.4 and 8.2.2.

$$\eta_{CO2} = \frac{\dot{n}_{C_{captured}}}{\dot{n}_{C_{in}}} \cdot 100 \tag{1.25}$$

$$\$/\,t_{CO2,avoided} = \frac{C_{P_{CC}} - C_{P_{ref}}}{\dot{m}_{CO_{2,emitted_{ref}}} - \dot{m}_{CO_{2,emitted_{CC}}}} \frac{[\$/GJ]}{[t_{CO2}/GJ]} \tag{1.26}$$

The economic performance is evaluated by the capital investment and the production costs following the approach described in Section 1.3.4.

Table 1.3: Reference plants performance considered for the CO_2 avoidance costs assessment.

Process	H_2	NGCC	NGCC
Reference	Metz et al. (2005)	Finkenrath (2011)	this work chap. 5& 6
ϵ_{tot}	-	57 %	58.9%
CO_2 emissions	137 kg_{CO2}/GJ$_{H2}$	100kg_{CO2}/GJ$_e$	105kg_{CO2}/GJ$_e$
C$_{P,ref}$	7.8 \$/GJ$_{H2}$	21 \$/GJ$_e$	18.3\$/GJ$_e$

1.4.2 Optimisation problem definition

In order to define optimal conceptual process designs based on the competing performance indicators (objectives), multi-objective optimisation techniques are applied. The major steps to set up the optimisation problem are the decision variables definition, the problem formulation (i.e. objective functions), the problem resolution and the comprehensive analysis. By combining the decision variables of the process operating conditions (i.e. design) with the integer decision variables related to the technology choice (unit existence) and the interconnections (i.e. process configuration), the problem becomes a mixed integer non-linear programming and differentiable problem that is solved with an evolutionary multi-objective optimisation algorithm described in Molyneaux et al. (2010). The use of an evolutionary algorithm makes the approach less sensitive to non-convergence problems and the proper definition of the decision variables allows to stabilise the robustness of the model. Compared to other algorithms requiring the calculation of derivatives, this kind of evolutionary algorithms based on biological mechanisms, such as crossover and mutation techniques, are more suitable for non-linear, non-continuous optimisation problems. Evolutionary algorithms working with populations instead of a single data point, generate multiple promising solutions in the form of a Pareto optimal frontier. The Pareto optimal configurations correspond to the configurations for which it is not possible to improve one objective without simultaneously downgrading one of the other objectives. During the Pareto frontier generation infeasible solutions are avoided through heuristics embedded in the sizing and cost estimation models. Figure 1.4 illustrates the thermo-environomic optimisation strategy including the data exchange between the thermodynamic and analysis models.

In the multi-objective optimisation procedure the goal is to find the set of optimal solutions $\left\{\vec{z_0}\right\}$ in the space of the decision variables that minimises/maximises the objective function $F(\vec{z},\vec{y})$. The multi-objective optimisation problem is written as follows:

$$
\begin{aligned}
min_{\vec{z}} F(\vec{z},\vec{y}) \text{ subject to:}\\
\vec{h}\,(\vec{z},\vec{y}) &= 0\\
\vec{g}\,(\vec{z},\vec{y}) &\leq 0\\
\vec{L}\,(\vec{z},\vec{y}) &= \text{True}
\end{aligned}
$$

In multi-objective problems $F(\vec{z},\vec{y})$ has more than one dimension and the optimisation yields a set of solutions $\left\{\vec{z_0}\right\}$ reflecting the compromise between the objectives. F is optimised under the constraints of the model equations including the equalities ($\vec{h}\,(\vec{z},\vec{y})$=0), the inequalities ($\vec{g}\,(\vec{z},\vec{y})\leq 0$) and logical equations ($\vec{L}\,(\vec{z},\vec{y})$=True). For a given value of the decision variables $\vec{z}$, the dependent variables $\vec{y}$ are computed by solving the model equations.

The objective functions definition is a key point in the competitiveness evaluation. In fact, the choice of the adequate objective function depends on the aspired target, for example; maximal electricity or H_2 production, maximal energy efficiency, maximal CO_2 capture rate/ minimal

CO_2 emissions, lowest investment or production costs. The optimal process configuration will consequently change with regard to the objective. The question of either optimising the global problem or the CO_2 capture subproblem can arise (Chapter 7). The comprehensive analysis of the multi-objective optimisation results helps to identify and understand the trade-off between thermodynamic, economic and environmental considerations. These results can support decision-making by selecting the optimal process configuration from the Pareto-optimal results. Since each solution included in the Pareto frontier is optimal with regard to the chosen objectives, it is not obvious which specific solution has to be selected. The analysis made in Chapter 8 and the proposed approach show how to support decision-making under different economic conditions.

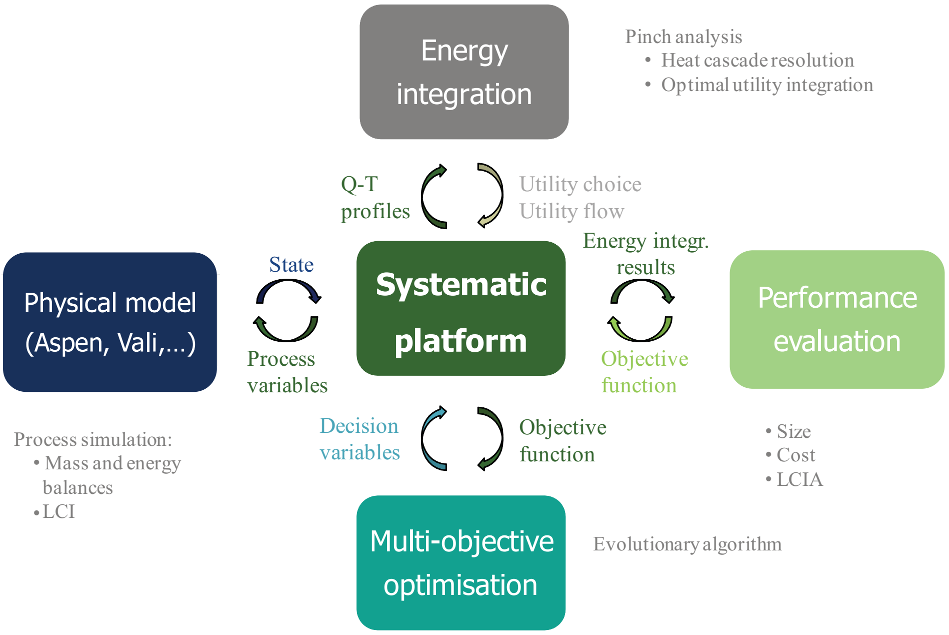
Energy integration
Pinch analysis
• Heat cascade resolution
• Optimal utility integration
Q-T profiles
Utility choice
Utility flow
State
Energy integr. results
Physical model (Aspen, Vali,...)
Systematic platform
Performance evaluation
Process variables
Objective function
Decision variables
Objective function
Process simulation:
• Mass and energy balances
• LCI
• Size
• Cost
• LCIA
Multi-objective optimisation
Evolutionary algorithm

Figure 1.4: Schematic illustration of the thermo-environomic optimisation strategy.

1.5 Conclusions

A MATLAB-language based platform (MathWorks Inc.) for studying, designing and optimising complex integrated energy systems is developed. The main goal is to have a flexible tool for the conceptual process design combining flowsheeting models using commercial packages, energy integration, performance evaluation (i.e. economic and environmental) and multi-objective optimisation strategies. In the proposed approach physical models are separated from the design and integration methods. A key feature is the possibility to connect process unit models developed with different software and to make a consistent comparison on a common basis. The advantage of including the process integration model in the design process is that the influence of the design and operation is reflected on the thermo-environomic performance of an energy balanced system. It turns out that the availability of reliable cost data is a major concern for the economic performance evaluation. The choice of the objective functions for the multi-objective optimisation is of importance in order to assess the trade-off between competing objectives and to support decision-making. The developed platform is applied to study the thermo-economic and environmental impacts of the integration of a CO_2 capture in H_2 and power generation plants in the following chapters.

2 Process models development for CO_2 capture technologies

For CCS the main step is the separation of CO_2 from the flue gas. Different technologies are suitable for this purpose. Here the principles of the different technologies are described and the advantages and disadvantages of each technology are pointed out for H_2 and electricity production applications. Thermodynamic models are developed for the most important candidate technologies. These models have been developed for the studies made in Tock and Maréchal (2012c) and Tock and Maréchal (2012d).

2.1 Introduction

Introducing CCS in power plants leads to an efficiency decrease and cost increase. The performance penalty depends on several factors, primarily related to the applied CO_2 separation technology. The relevant technologies summarised in Figure 2.1 are based on the reviews made in Figueroa et al. (2008), Metz et al. (2005), Radgen et al. (2005), Yang et al. (2008), Olajire (2010) and MacDowell et al. (2010). In the following sections the different technologies are described and the developed thermodynamic models are presented.

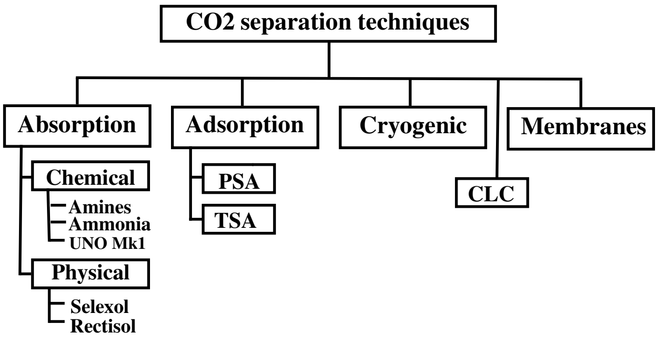
CO2 separation techniques
Absorption
Chemical
Amines
Ammonia
UNO Mk1
Physical
Selexol
Rectisol
Adsorption
PSA
TSA
Cryogenic
CLC
Membranes

Figure 2.1: CO_2 separation technologies.

2.2 CO_2 separation technologies

2.2.1 Principles

CO_2 can be separated from the flue gas by gas separation techniques that are based on the differences in volatilities, dissolution, diffusion and permeation. General information about gas separation principles are given in Bart and von Gemmingen (2005), Hiller et al. (2006) and Schlauer (2008).

2.2.2 Technologies description

Chemical absorption

Chemical absorption is a gas-liquid contacting and separating equipment using aqueous solutions for scrubbing acidic gases like CO_2 from the flue gas. This process schematically presented in Figure 2.2 typically comprises two operations; absorption and desorption (i.e. solvent regeneration). The flue gas raises in the absorber column, while the chemical solvent trickles down in counter-current and acts as a weak base, neutralising the acidic compounds to turn the molecules into ions (i.e. CO_2 into HCO_3^-) and dissolving them in the gas-scrubbing solution. The solvent entering the column at the top is referred as 'lean', since it contains none or little of the component to be absorbed. The column includes horizontal trays or packing material to ensure sufficient mixing and contacting. After the extraction of the CO_2 from the gas stream, the saturated 'rich' solution leaving the bottom of the column is heated and passes a regeneration column with a condenser at the top and a reboiler at the bottom. The reboiler heats the liquid stream to up to 150^oC(Radgen et al. (2005)) in order to break the chemical bounds and release the pure acid gas from the solvent. The lean aqueous solution is recovered and reused in the absorber. The heat requirement consists of the sensible heat, the heat of vaporisation and the heat of reaction. The key energy penalty of the chemical absorption process arises from the solvent regeneration (approximately 3-5GJ/t_{CO2} at 150^oC), the compression of the flue gas and the pumping of the solvent through the removal plant (0.5-1.5GJ/t_{CO2}) (Radgen et al. (2005)).

The process is suited for gas streams with low partial pressure of CO_2. However, high solvent flowrates are required to achieve high CO_2 capture rates. The main advantage is the high capture efficiency and selectivity, while the main disadvantage is the high energy requirement. The solvent determines the thermodynamic and kinetic limits of the process. The choice of the solvent depends on many different factors such as the flue gas composition, the required CO_2 recovery and purity, the solvent regeneration, the sensitivity to impurities, and the capital and operation costs. Amine solvents are preferably used. Recent researches focus on the development of new advanced CO_2 absorption solutions like blends and sterically hindered amines. Alternatively, the use of ionic liquids (i.e. liquids composed entirely of ions with a melting point below 100^oC) is studied in Wappel et al. (2010) and Heldebrant et al. (2009) and possible energy savings between 12 and 16% are predicted for 60 %wt ionic liquid solutions.

The ideal chemical solvent should have the following characteristics; high reactivity with respect to CO_2, low heat of reaction with CO_2, high absorption capacity, high stability (i.e. low thermal and chemical degradation), low environmental impact and low costs.

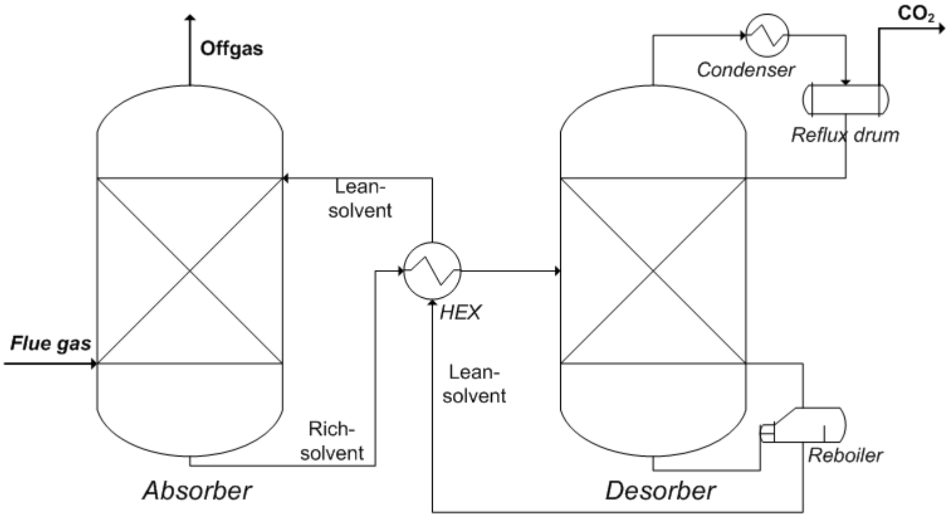

Figure 2.2: Schematic flowsheet of the chemical absorption process (omitting pressure change devices).

Chemical absorption with amines is a mature commercialised technology used over many decades in natural gas industry. Aqueous solutions of ethanolamines like mono- (MEA), di- (DEA) and triethanolamines (TEA) are commonly used to remove CO_2 from flue gases. The acid-base neutralisation reaction is given by Eq.2.1 where R is any alkanol group. The absorber typically operates between 40 and 60^oC (Metz et al. (2005)). The temperature for the amine regeneration is around 100-140^oC (1.5-2 bar) and the heat requirement depending on the purity constraints, is in the range of 1.5-3.4GJ/t_{CO2} (Metz et al. (2005)). Typical values for the electricity requirement are 0.06-0.11 GJ_e/t_{CO2} for post-combustion CO_2 capture in coal-fired power plants and 0.21-0.33 GJ_e/t_{CO2} for post-combustion CO_2 capture in natural gas fired combined cycles (Metz et al. (2005)).

$$CO_2 + R - NH_2 + H_2O \quad \rightleftharpoons \quad R - NH_3HCO_3 \tag{2.1}$$

The major drawbacks of the MEA process in power plants applications are the low CO_2 loading capacity, the equipment corrosion, the thermal and oxidative degradation of amines by SO_2, NO_2 and oxygen (Gouedard et al. (2012)), and the large energy requirement for the solvent regeneration. Reported amine solvent makeup due to degradation losses is around 0.5-3.1kg_{MEA}/t_{CO2} (Rao and Rubin (2002)). Given the relative low degradation temperatures of amines the solvent regeneration operates at low pressure compared to the one required for CO_2 transport and storage. Consequently, considerable energy and costs penalties are induced by CO_2 compression to 110 bar. The electricity consumption for the CO_2 compression from 1 to 100 bar is in the order of $0.4GJ_e/t_{CO2}$ (Metz et al. (2005)). This leads to an electrical production efficiency decrease of about 2%-points in an NGCC plant.

Chemical absorption with chilled ammonia. As a possible alternative to amine solvents, ammonia is identified, since it satisfies some of the ideal solvent characteristics such as energy efficient CO_2 capture, i.e. high CO_2 absorption capacity and low regeneration energy, stable (no degradation) and globally available low-cost reagent. The chilled ammonia process (CAP) patented by Gal (2006) is developed by *Alstom Power* for CO_2 capture in power plants and tested at the AEP Mountaineer plant. In this process the absorption operates at low temperature 0-20^oC. The operation at low temperature has the advantage of decreasing the NH_3 slip in the absorber and the flue gas volume. The cooled flue gas is contacted in the absorber with the lean solvent composed of 28%wt NH_3 and having a CO_2 loading (CO_2/NH_3 molar ratio) of 0.25-0.67 and preferably in the range of 0.33-0.67. A high loading increases the vapour pressure of CO_2 and decreases the capture efficiency, while a low loading increases the vapour pressure of NH_3 leading to NH_3 losses by evaporation. In these operating ranges the solubility limits may be reached and solid particles such as ammonium bicarbonate (NH_4HCO_3) precipitate. Hence the CO_2 rich stream is a slurry that has a CO_2 loading of 0.5-1 (preferably 0.67-1). The CO_2 rich stream is pressurised and heated up before entering the desorber. In the stripper operating at 50-200^oC (preferably 100-150^oC) and 2-137 bar, the CO_2 is evaporated from the solution. The high purity CO_2 is released and the lean solution is recycled back to the absorber. The desorption operation at high pressure has the advantage that the released CO_2 has to be compressed less for CO_2 transport and storage. In addition, the vaporisation of water and ammonia is limited at these conditions and hence the energy consumption is reduced. According to Jilvero et al. (2012) the heat requirement for the regeneration of aqueous ammonia is around $2.5GJ/t_{CO2}$. Compared to MEA processes the heat of reaction is similar, however the lower water evaporation during the pressurised regeneration with ammonia results in a lower energy requirement and makes absorption of CO_2 by ammonia beneficial.

Physical absorption

In physical absorption, the acidic gas is physically bound to the organic solvent (rather than reacting chemically) by absorption at high pressure and low temperature and the solvent is regenerated by heating or release of pressure. The regeneration is often performed in multiple flash drums. The physical absorption of CO_2 is driven by the solubility of CO_2 within the solvent and hence depends on the partial pressure and temperature. Consequently, it is applicable to gas streams which have high CO_2 partial pressure (>15%vol) since the solubility of CO_2 in physical solvents increases linearly with its partial pressure. The interaction between the CO_2 and the absorbent is weak compared to chemical absorption, which leads to a lower energy requirement for the solvent regeneration. The main energy requirement is related to the flue gas pressurisation. Commercial applications of this process are the removal of CO_2 and H_2S in natural gas processing and the removal of CO_2 from syngas in hydrogen, ammonia and methanol production. Common commercially available solvents are Rectisol (based on methanol developed by Lurgi and Linde), Selexol (DEPG: polyethylene glycol dimethyl ether manufactured by Union Carbide and Dow) and Purisol (NMP: N-methyl-2-Pyrrolidone licensed by Lurgi AG). Different solvents and the corresponding gas solubility are compared in Burr and Lyddon (2008).

In the Selexol process the absorption operates at low temperature 0-40^oC (20-30 bar). Selexol has a high viscosity (0.0058 Pa·s (Burr and Lyddon (2008)) which reduces mass transfer rates and tray efficiency and increases packing or tray requirement. The Selexol solvent has the advantage of having chemical and thermal stability and being non-corrosive and inherently non-foaming.

In the Rectisol process, chilled methanol is used as a solvent and the absorption normally operates at -60 to -30^oC(>20 bar) because of the high vapour pressure of methanol (boiling point 65^oC). The rich solvent is regenerated by flashing at low pressure, consequently there is no reboiling heat requirement. The methanol solvent has the advantage of having a high thermal and chemical stability and being non-corrosive. The main disadvantage is that the solvent needs to be cooled down which results in high capital and operating costs for the refrigeration. However, this can be balanced by a lower solvent flowrate for CO_2 separation compared to other solvents. The Rectisol process layout is flexible and many different flow schemes can be applied. Water washing of effluent flows is often introduced to recover methanol.

Physical adsorption

Adsorption is a physical process based on the attachment of a gas or liquid to a solid surface. The attachment can be either physical (physisorption) or chemical (chemisorption). Fundamentals about adsorption processes are reported in Bart and von Gemmingen (2005). The basic steps of this cyclic process are an adsorption step in which the more adsorbable specie is selectively removed from the feed gas and a regeneration (desorption) step where these species are removed from the adsorbent which is then reused for the next cycle. The process is enhanced by high pressure and low temperature, accordingly adsorption and regeneration are achieved through pressure (pressure swing adsorption PSA) or temperature (temperature swing adsorption TSA) cycles. The solvent choice depends on the adsorption capacity, as well as on the relative diffusion velocities of the species. Potential adsorbents for CO_2 capture are activated carbon, zeolites, alumina and metallic oxides.

Pressure swing adsorption (PSA) is described in detail in Barg et al. (2000), Malek and Farooq (1998), Ritter and Ebner (2007) and Sircar and Golden (2000). PSA is based on the use of anhydrous organic solvents such as activated carbon and zeolites which dissolve the acids and can be stripped by reducing the acid-gas partial pressure without the application of heat. The separation principle is that adsorbent beds adsorb more impurities at high gas-phase partial pressure than at low partial pressure (Longanbach et al. (2002)). For H_2 purification, the gas stream passes through adsorption beds at 15-28 bar, and the impurities are purged from the beds at around 0.2 bar to obtain a high recovery of H_2. The minimum pressure ratio between the feed and purge gas of the PSA unit is about 4:1. The PSA process operates on a cyclic basis. The adsorption temperature influences also the efficiency. In fact, fewer impurities are adsorbed at higher temperatures because the equilibrium capacity of the molecular sieves decreases with increasing temperature. With PSA H_2 purities of over 99%mol can be reached. Regarding PSA applications for pre-combustion CO_2 capture extensive experimental and modelling research is done by Schell et al. (2012) and Casas et al. (2012). The main challenge of current adsorption systems for large-scale power plants applications is the low absorption capacity and low selectivity of the available adsorbents at low to moderate CO_2 concentration.

Membrane technology

A relative novel capture concept is the use of selective membranes to separate one component from a gas stream. This could be applied in post-combustion systems to remove CO_2 from the flue gas, in pre-combustion systems to remove CO_2 from hydrogen and in oxy-fuel combustion systems to remove O_2 from N_2. These technologies are described in detail in Brunetti et al. (2010), Bredesen et al. (2004), Ockwig and Nenoff (2007), Adhikari and Fernando (2006) and Stolten (2010).

For membrane separation there are different mechanisms that can operate; Knudsen diffusion, molecular sieving, solution-diffusion separation, surface diffusion and ionic transport. Different types of materials find applications in gas purification. The membranes are either organic (i.e. polymeric) or inorganic (i.e. carbon, zeolite, ceramic or metallic) and can be porous or non-porous. The membrane performance is defined by the permeability and the selectivity. The membrane acts as a filter separating one or more gases from a gas mixture based on selective permeation. The partial pressure difference between the feed and the permeate is the driving force for membrane separation, therefore high-pressure streams are preferred. Consequently, the selectivity for CO_2 capture is low and thus only a small fraction is captured and the purity is low (Yang et al. (2008)). To increase the CO_2 capture, multi-stage membrane separation has to be included which adds additional energy demand and cost. Moreover, membranes are sensitive to sulphur compounds.

Cryogenic distillation

The separation by cryogenic distillation is a low temperature separation process based on the boiling temperature difference of the compounds of the gas mixture. Cryogenic separation is not applicable for atmospheric pressure exhaust gases containing a low amount of CO_2 because it requires too much energy for refrigeration and is too expensive. However, for high pressure, high CO_2 content gas mixtures it is possible to liquefy it by cooling without requiring too much energy. Cyrogenic distillation is a commercial process used for air separation and for liquefying and purifying high purity CO_2 (>90%mol). Consequently, this process is well suited for oxy-fuel processes. This process has the advantage that the pure CO_2 is recovered in liquid form and can be transported easily. Applied to hydrogen separation, it yields hydrogen with moderate purity <95%mol.

Performance comparison

Key features and operating conditions of CO_2 capture technologies are summarised in Table 2.1.

Table 2.1: Comparison of the physical and chemical ab- and adsorption processes for CO_2 separation (Göttlicher (1999)).

Process	Conditions	Gas removed	Thermal energy [kWh/kg$_{CO2}$]	Mechanical work [kWh/kg$_{CO2}$]	CO_2 purity [%mol]
Rectisol	$T_{abs} \approx -10/-70^oC$	CO_2 , NH_3	0.025	0.038	<90%
	p_{CO2} >10 bar	H_2S, COS, HCN			
Selexol	p_{CO2} ≈7-30 bar	CO_2 , NH_3	0.016-0.024	0.03-0.06	
		H_2S, COS, HCN			
MEA	$T_{abs} \approx 40^oC$, 1-5 bar	CO_2 ,CS_2	2.3	0.05-0.3	< 99%
	$T_{desorb} = 95-120^oC$	H_2S, SO_2, COS	(≈0.48kWh$_e$/kg$_{CO2}$)		
PSA-Flue gas	P_{ads}=1 bar	CO_2	0.16-0.18		
28-34% CO_2	P_{desorb}=0.05-0.9 bar				
PSA - syngas	P_{ads}=13-21 bar	CO_2	-	-	>90%
	P_{desorb}<1 bar				

2.3 CO_2 capture process modelling

For the different CO_2 capture technologies discussed previously, thermodynamic models are developed here to be used in the subsequent pre- and post-combustion CO_2 capture processes optimisation.

2.3.1 Chemical absorption

Amines: MEA

The flowsheet of the CO_2 capture process by chemical absorption with MEA illustrated in Figure 2.3 is based on the one developed by Bernier et al. (2010).

The model developed in Aspen Plus (AspenTech) is adapted from the default rate-based model available from *AspenTech* . In the thermodynamic model, the electrolyte NRTL method is used for the liquid phase and the Redlich-Kwong method for the vapour phase. The electrolyte solution chemistry is defined by the equations Eqs.2.2-2.9.

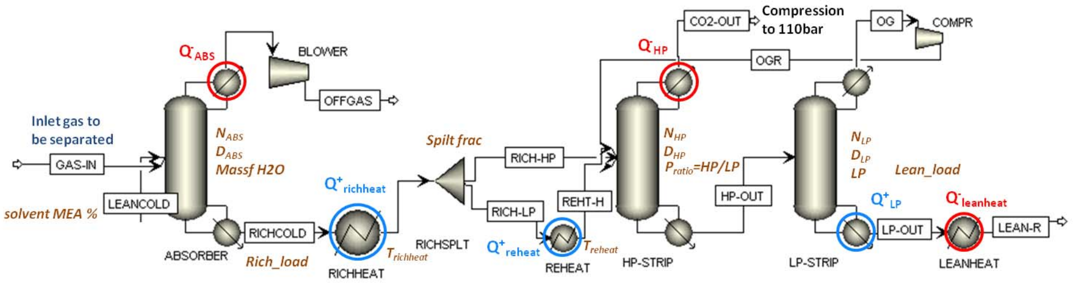
Q⁻ABS
BLOWER
OFFGAS
Inlet gas to be separated
GAS-IN
N ABS
D ABS
Massf H2O
solvent MEA %
LEANCOLD
ABSORBER
RICHCOLD
Rich_load
Q⁺ richheat
RICHHEAT
T richheat
Spilt frac
RICHSPLT
RICH-HP
RICH-LP
Q⁺ reheat
REHEAT
T reheat
REHT-H
Q⁻HP
CO2-OUT
Compression to 110bar
OGR
N HP
D HP
P ratio=HP/LP
HP-STRIP
HP-OUT
OG
COMPR
N LP
D LP
LP
Lean_load
LP-STRIP
Q⁺ LP
LP-OUT
Q⁻leanheat
LEANHEAT
LEAN-R

Figure 2.3: Process model of the CO$_2$ capture by chemical absorption with amines. Decision variables reported in Table 2.2 and heat exchanges (i.e. hot stream: red, cold stream: blue) are depicted.

$$\begin{aligned}
2H_2O &\rightleftharpoons H_3O^+ + OH^- && (2.2)\\
CO_2 + 2H_2O &\rightleftharpoons H_3O^+ + HCO_3^- && (2.3)\\
HCO_3^- + H_2O &\rightleftharpoons H_3O^+ + CO_3^{2-} && (2.4)\\
MEAH^+ + H_2O &\rightleftharpoons MEA + H_3O^+ && (2.5)\\
MEACOO^- + H_2O &\rightleftharpoons MEA + HCO_3^- && (2.6)\\
H_2O + H_2S &\rightleftharpoons HS^- + H_3O^+ && (2.7)\\
H_2O + HS^- &\rightleftharpoons S^{2-} + H_3O^+ && (2.8)
\end{aligned}$$

The absorber and desorber are modelled by a rate based RadFrac column including reaction kinetics. The considered reactions include the reaction between MEA and CO$_2$ given by Eq.2.9. The CO$_2$ capture rate is defined by the columns design (i.e. number of stages, diameter, etc.) and the operating conditions. CO$_2$ compression to 110 bar for subsequent CO$_2$ transport and storage is modelled separately in *Belsim Vali* (Belsim S.A.) by a two stage compressor with intercooling. Table 2.2 summarises the decision variables and the corresponding variation range for optimisation.

$$MEA + CO_2 + H_2O \rightleftharpoons MEACOO^- + H_3O^+ \qquad (2.9)$$

Table 2.2: Decision variables and feasible range for optimisation for the chemical absorption process using an aqueous MEA solution.

Operating parameter	Value	Range
Lean solvent CO_2 loading [kmol/kmol]	0.2	[0.18-0.25]
Rich solvent CO_2 loading [kmol/kmol]	0.48	[0.4-0.5]
Split fraction [-]	0.5	[0-0.7]
Rich solvent pre-heat T [^oC]	105	[95-105]
Rich solvent re-heat T [^oC]	125	[115-125]
LP stripper pressure [bar]	1.98	[1.7-2.1]
HP / LP pressure ratio [-]	1.5	[1-1.5]
Nb stages absorber	15	[10-17]
Nb stages HP stripper	11	[8-15]
Nb stages LP stripper	8	[6-10]
Absorber diameter [m]	8	[6-12]
HP stripper diameter [m]	6	[3-6]
LP stripper diameter [m]	3	[2-5]
MEA concentration in solvent [- wt]	0.35	[0.3-0.35]
Absorber steam out [kg$_{H2O}$/t$_{FG}$]	307	[306-309.5]

Amines: TEA

The model for the chemical absorption with TEA is similar to the one presented for MEA and is illustrated by Appendix Figure B.1. While MEA is suited for capturing CO_2 from flue gas, TEA is more appropriate to separate CO_2 from a H_2-rich fuel. The model is adapted from the default rate-based model available from *AspenTech* . The absorber is modelled by an equilibrium RadFrac column and the desorber by a single stage flash unit. The lean solvent recycling is not modelled explicitly, but by imposing design specifications it is ensured that the streams are identical after solvent make-up. The main decision variables are summarised in Table 2.3. The CO_2 capture rate is defined by the flowrate of the lean solvent and the columns design.

Table 2.3: Decision variables and feasible range for optimisation for the chemical absorption process using an aqueous TEA solution.

Operating parameter	Value	Range
TEA concentration [%wt]	35	[25-40]
H_2/TEA ratio [kg/kg]	0.049	[0.035-0.055]
Absorber T [^oC]	40	[20-45]
Absorber P [bar]	28.8	[15-30]
Nb stages absorber	25	-
Absorber packing	Pall ring & Ralu-ring (rasching)	
Regeneration P [bar]	2	[1-130]
Regeneration T [^oC]	67	[25-120]
CO_2 compression [bar]	110	-

Chilled ammonia

Process models of chilled ammonia systems have recently been developed in a few research studies (Mathias et al. (2010), Darde et al. (2010, 2012), Valenti et al. (2009), Jilvero et al. (2011), Dave et al. (2009)). The vapour-liquid equilibrium of the CO_2-NH_3-H_2O system was extensively studied in Göppert and Maurer (1988) and Kurz et al. (1995) based on experimental data and a thermodynamic model was proposed by Thomsen and Rasmussen (1999).

The thermodynamics of the CO_2-NH_3-H_2O system is complex since it is a vapour-liquid-solid system with electrolytes present in the liquid state. The electrolyte NRTL model available in *Aspen Plus* (AspenTech) is used to model this system based on the data published by Pinsent et al. (1956), Göppert and Maurer (1988) and Kurz et al. (1995). This model represents adequately the vapour-liquid equilibrium and the precipitation of solids (i.e. ammonium bicarbonate NH_4HCO_3) based on the chemistry model given by Eqs.2.10-2.15, including auto-pyrolysis of water, dissociation of ammonia and carbon dioxide, and formation of carbonate.

$$2H_2O \rightleftharpoons H_3O^+ + OH^- \tag{2.10}$$

$$CO_2 + 2H_2O \rightleftharpoons H_3O^+ + HCO_3^- \tag{2.11}$$

$$HCO_3^- + H_2O \rightleftharpoons H_3O^+ + CO_3^{2-} \tag{2.12}$$

$$NH_3 + H_2O \rightleftharpoons NH_4^+ + OH^- \tag{2.13}$$

$$NH_3 + HCO_3^- \rightleftharpoons H_2NCOO^- + H_2O \tag{2.14}$$

$$NH_4HCO_3(s) \rightleftharpoons NH_4^+ + HCO_3^- \tag{2.15}$$

The developed flowsheet for the chilled ammonia process, illustrated in Appendix Figure B.2, includes the following steps: CO_2 absorption, NH_3 stripping from vent gas, CO_2 desorption and solvent regeneration, and CO_2 compression. The absorber and the desorber are modelled by a single flash stage assuming physical and chemical equilibrium. The main design specifications and decision variables are given in Table 2.4. In the absorber the CO_2 capture rate is defined by the lean solvent flowrate. The NH_3 concentration in the aqueous solution (without CO_2) and the CO_2 loading of the lean solution (i.e. CO_2/NH_3 molar ratio) highly influence the separation performance. Since the NH_3 slip from the absorber is in the range of 500-3000ppm$_v$, which is much too high for gases vented to the atmosphere, a water wash column is introduced in order to reduce the level to 10ppm$_v$. The vent gas is heated up to around 45^oC in order to satisfy flume conditions before being released to the atmosphere. The rich solvent passes a pump and an heat exchanger before entering the regeneration column. The temperature of the heat exchanger is defined such that all the ammonium bicarbonate is dissolved before entering the flash column in order to have no fouling issues. The reboiler temperature is defined such that the required CO_2 regeneration is achieved. The recycling of the solvent is defined by a design specification assuring that the input lean solvent equals the output lean solvent after the addition of the stripped NH_3 after the water wash of the vent gas and of fresh NH_3. The cooling down below atmosphere to the absorber temperature is modelled in the energy integration by a refrigeration cycle.

Table 2.4: Decision variables and feasible range for optimisation for the chilled ammonia process.

Operating parameter	Value	Range
NH_3 concentration [%wt]	28	-
CO_2 capture rate [%]	90	[85-95]
Lean CO_2 loading [kmol/kmol]	0.4	[0.33-0.67]
Absorber T [^oC]	5	[0-10]
Absorber P [bar]	1	-
Regeneration P [bar]	30	[2-136]
CO_2 compression [bar]	110	-

2.3.2 Physical absorption

Compared to chemical absorption the thermodynamic modelling of the physical absorption is less complex since no ions are involved and no chemical reactions take place in the absorber/desorber. The model is adapted from the default models for physical solvents available from *AspenTech*. To model the thermo-physical properties the PC-SAFT equation of state model for vapour pressure, liquid density, heat capacity and phase equilibrium is used. The absorber is modelled as a RadFrac column and the desorber as a single stage flash unit. Again the solvent recirculation is defined by a design specification and is not modelled explicitly. The CO_2 capture rate is defined by the flowrate of the lean solvent and the columns design. The flowsheet of the Rectisol and Selexol processes are illustrated in Appendix Figures B.4 & B.3. The main design specifications and decision variables of the physical absorption process are given in Table 2.5 for the Rectisol solvent and in Table 2.6 for the Selexol solvent.

Table 2.5: Decision variables and feasible range for optimisation for the physical absorption process using the Rectisol solvent.

Operating parameter	Value	Range
MeOH/CO_2 ratio [kmol/kmol]	13.6	[10-15]
Absorber T [^oC]	-37	[-70-0]
Absorber P [bar]	27.5	[15-60]
Absorber packing	Ceramix intalox saddles	
Nb stages absorber	10	-
Regeneration P [bar]	1	[1-10]
Regeneration T [^oC]	40	[20-100]
CO_2 compression [bar]	110	-

Table 2.6: Decision variables and feasible range for optimisation for the physical absorption process using the Selexol solvent.

Operating parameter	Value	Range
DEPG/CO_2 ratio [kg/kg]	12	[8-14]
Absorber T [^oC]	-16	[-18-173]
Absorber P [bar]	16	[10-60]
Nb stages absorber	10	-
Absorber packing	Pall ring	
Regeneration P [bar]	1.2	[1-10]
Regeneration T [^oC]	31	[25-100]
CO_2 compression [bar]	110	-

2.3.3 Pressure swing adsorption

For the pressure swing adsorption model, the approach outlined in Gassner and Maréchal (2009b) is adapted for the H_2/CO_2 separation based on data from Jee et al. (2001). The purity and the amount of H_2, and the CO_2 recovered in the respective outlet streams is defined by the PSA cycle design, namely the durations of the adsorption, recycling and purging periods. Depending if the objective is to generate highly pure H_2 or highly pure CO_2, the PSA setup has to be modified. To define the relative durations of these periods the parameters t_{r1} and t_{r2} are introduced. The time-averaged flow of species i that leaves the adsorber system ($\dot{m}_{i;out}$) or is recycled to its inlet ($\dot{m}_{i;rec}$) is determined by the equations Eqs.2.16-2.18 based on a regression $f(i,tr)$ on data from Jee et al. (2001):

$$\dot{m}_{i;out} = f(i,t_{r1})\dot{m}_{i;in} \tag{2.16}$$

$$\dot{m}_{i;rec} = f(i,t'_{r2})\dot{m}_{i;in} - \dot{m}_{i;out} \tag{2.17}$$

$$t'_{r2} = (1-t_{r1})t_{r2} + t_{r1} \tag{2.18}$$

2.3.4 Membrane processes

The membrane process has been modelled in a preliminary study as two subsequent membranes following the approach of Gassner et al. (2009) with the data of Franz and Scherer (2010) for a CO_2 selective Pebax membrane. The decision variables are the pressure and the stage cuts. The results yield low H_2 process efficiencies due to the low H_2 purity that has been achieved with this membrane design. This process has to be further optimised following the design approaches reported in Gassner et al. (2009) and Pathare and Agrawal (2010). Due to time constraints this future technology for CO_2 capture was not addressed further in this thesis. However, regarding the advances in membrane research and the relative low energy penalty of this technology it might become a competitive options which has to be investigated in more detail.

2.4 Conclusions

Based on a technology review, the most important candidate technologies for CO_2 separation from other gases are identified and thermo-economic models are developed for the different options. With regard to H_2 and power production applications the choice of one specific technology depends on the gas composition, the required CO_2 recovery and purity, the energy requirement and the capital and operation costs. The energy penalty of the CO_2 capture is a key concern for the competitiveness and deployment of CCS. In addition, the energy requirement for CO_2 compression for transportation and storage is not negligible with 0.4 GJ_e/t_{CO2} for the compression from 1 to 110 bar. In fact, in power plants CO_2 capture and compression leads to a reduction of the electrical production efficiency up to 10%-points, whereof 2%-points are on account of CO_2 compression.

The different CO_2 capture process models are applied in the following chapters to evaluate, compare and optimise pre- and post-combustion CO_2 capture processes. Based on the simulation models, the hot and the cold streams are computed for subsequent process integration and the equipment sizes are calculated for the cost estimation as explained in Section 1.3.4. The advantage of this modelling approach is that the impact of the operating conditions on the process integration and on the investment cost is taken into account. Consequently, the models are well adapted for thermo-economic optimisations.

3 Thermo-economic analysis of pre-combustion CO_2 capture processes

In this chapter the thermo-environomic modelling of processes generating H_2 and/or electricity with CO_2 capture are presented. Different process options using natural gas or biomass as a resource are analysed, compared and optimised as in the published versions (Tock and Maréchal (2012a,b)).

3.1 Introduction

Several research studies have already identified promising fuel decarbonisation processes for H_2 production and/or electricity generation using different resources. Reported efficiencies range from 69 to 80% for fossil fuel H_2 production (Longanbach et al. (2002), Damen et al. (2006), Consonni and Viganò (2005)) and from 51 to 60% for biomass fed H_2 processes (Hamelinck and Faaij (2002), Toonssen et al. (2008)) (Table 3). Whereas for pre-combustion CO_2 capture in natural gas combined power plants, efficiencies of 42-48% are reported and of 33% for integrated biomass gasification combined cycle plants (Table 2). CO_2 capture reduces the efficiency of power plants by around 10%-points and increases the production costs by 30% due to the energy consumption for CO_2 capture and compression. This yields CO_2 avoidance costs in the range of 13-75$/t$_{CO_{2,avoided}}$ according to Metz et al. (2005). In each study, different assumptions are made and different technologies are considered. This adds up in a large range of performance results making a consistent comparison difficult. Therefore, the objective is to apply the developed systematic methodology to compare and optimise pre-combustion fuel decarbonisation process configurations for H_2 and electricity generation with regard to energy, economic and environmental considerations. Special interest is given to the effect of polygeneration of H_2-fuel, captured CO_2, heat and power, in order to identify its advantages and constraints, and to better understand trade-offs between efficiency, costs and emissions.

3.2 Pre-combustion CO_2 capture processes description

3.2.1 Pre-combustion CO_2 capture process layout

The general superstructure presented in Figure 3.1 summarises the different technological options that are considered for pre-combustion CO_2 capture process designs. The main process steps are resource extraction and treatment, syngas (i.e. H_2 and CO) generation by natural gas (NG) reforming or biomass (BM) (i.e. wood) gasification, gas cleaning and treatment, H_2 purification and/or H_2 burning for electricity generation. In both natural gas and biomass based H_2 pathways, a CO_2 removal step is included during the H_2 purification which allows for CO_2 capture (CC) and further sequestration for greenhouse gas mitigation. The energy demand of the process can be satisfied by importing electricity or by burning part of the H_2-fuel in a gas turbine (GT) to close the balance. Alternatively, the H_2-fuel could be used for fuel cell applications. Consequently, depending on the production purpose, the process produces either H_2 with and without captured CO_2, imports electricity or is self-sufficient in terms of power, or exports electricity if all the H_2-fuel is burnt. When CO_2 is captured, CO_2 pressurisation to 110 bar is taken into account to satisfy the conditions for transport and sequestration.

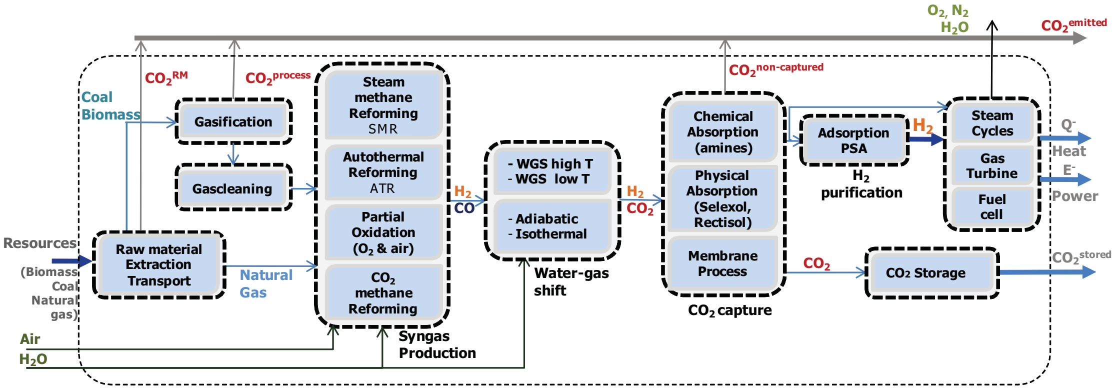
O_2, N_2
H_2O
$CO_2^{emitted}$
CO_2^{RM}
$CO_2^{process}$
$CO_2^{non-captured}$
Coal
Biomass
Gasification
Gascleaning
Steam methane Reforming SMR
Autothermal Reforming ATR
Partial Oxidation (O_2 & air)
CO_2 methane Reforming
H_2
CO
- WGS high T
- WGS low T
- Adiabatic
- Isothermal
Water-gas shift
H_2
CO_2
Chemical Absorption (amines)
Physical Absorption (Selexol, Rectisol)
Membrane Process
CO_2 capture
Adsorption PSA
H_2 purification
H_2
Steam Cycles
Gas Turbine
Fuel cell
Q^-
Heat
E^-
Power
CO_2
CO_2 Storage
CO_2^{stored}
Resources
(Biomass
Coal
Natural
gas)
Raw material Extraction Transport
Natural Gas
Air
H_2O
Syngas Production

Figure 3.1: Process superstructure of the pre-combustion CO_2 capture process options.

3.2.2 Pre-combustion CO_2 capture process technologies

The main feature of pre-combustion CO_2 capture processes is the generation of an intermediate fuel mixture of H_2 and CO (syngas) from which H_2 and CO_2 can be separated after gas treatment and purification. Syngas can be produced from nearly any carbon containing fuel ranging from natural gas, coal and oil products to biomass. If the feed has a high sulphur content, a desulphurisation step is required to prevent catalyst poisoning. The main technologies and chemical reactions are discussed in the following sections.

Natural gas reforming

Presently, natural gas is the dominant feedstock to produce H_2. The most common method to produce syngas from natural gas is steam methane reforming (SMR) expressed by Eq.3.1. SMR is an endothermic process that takes place in the presence of a Ni-catalyst and is favoured at low pressure, high temperature and low steam-to-carbon ratio. Typical operating pressures are 10-40 bar since pressurisation yields an economic advantage due to the smaller equipment size. Common operating temperatures are 830-1000^oC and steam to carbon ratios of 2-6 to prevent coking (Spath and Dayton (2003), Stolten (2010)). In the reformer, the water-gas shift reaction Eq.3.4 occurs simultaneously which leads to the overall equation described by Eq.3.2. The reforming reaction yields a H_2/CO ratio close to 3. This ratio can however be varied over a large range, since the reforming reaction is coupled to the shift reaction. The reactor is a tubular reformer composed of catalyst-filled alloy steel tubes that are surrounded by a firebox providing the heat necessary for the endothermic reforming reaction. A large variety of reformer designs exist and can be used in various process configurations described in Häussinger et al. (2000). The main components of the reformer furnace are a combustion chamber, a radiant heat transfer section, and a convection section. The radiant section supplies heat to the catalyst tubes by burning the air/fuel (i.e. recycled syngas from the hydrogen purification) mixture and the convection section recovers heat by cooling down the flue gases (Spath and Dayton (2003)). The syngas leaves the reformer tubes close to thermodynamic equilibrium. If a desulphurisation unit is required before the reformer unit to avoid catalyst degradation by sulphur compounds, it usually consists of a hydrogenator followed by a zinc oxide bed (Spath and Dayton (2003)).

An alternative to steam reforming is partial oxidation (POX) of the fuel with air or pure O_2 according to Eq.3.3. Since the reaction is exothermic, there is no need for a complex heated reactor. There are three ways to carry out POX; non-catalytic partial oxidation, autothermal reforming (ATR) and catalytic partial oxidation (CPO). In the non-catalytic POX, high temperatures are required to yield high conversion of methane and avoid soot formation (Stolten (2010)). The benefit of this process is that it can be operated at high temperatures without the use of catalysts (i.e. 1600-1350^oC, 150 bar). However, high combustion temperatures cause problems with NOx formation. The POX reaction together with WGS produces however less H_2 than the reforming reaction. In an autothermal reformer (ATR) the endothermic steam reforming (Eq.3.1) is combined with the exothermic partial oxidation (POX) (Eq.3.3). The oxygen for the reaction can be supplied either by air or pure O_2. The advantage of adding pure O_2 is that no N_2 is present in the downstream process which reduces the installation size and facilitates CO_2 capture. However, air separation by cryogenic distillation or oxygen transfer membranes consumes energy and adds additional costs. To maximise the H_2 production, the ATR reactor is typically operated at high temperature (900-1100^oC) and S/C ratio of 1 to 3.7. The autothermal reformer consists of a specially designed burner and a fixed catalyst bed in a brick-lined reactor (Stolten (2010)). The syngas composition is defined by the thermodynamic equilibrium at the exit temperature and pressure. In the catalytic partial oxidation the fuel and the air/O_2 are premixed and fed to a catalytic reactor (Rh-catalyst) without a burner. The partial oxidation reaction (Eq.3.3) is typically operated around 950^oC. In practice the reaction is accompanied by SMR and WGS reactions and at high conversions the syngas is close to thermodynamic equilibrium (Stolten (2010)).

$$CH_4 + H_2O \leftrightarrow CO + 3H_2 \quad \Delta\tilde{h}_r^o = 206kJ/mol \tag{3.1}$$

$$CH_4 + 2H_2O \leftrightarrow CO_2 + 4H_2 \quad \Delta\tilde{h}_r^o = 165kJ/mol \tag{3.2}$$

$$CH_4 + \frac{1}{2}O_2 \leftrightarrow CO + 2H_2 \quad \Delta\tilde{h}_r^o = -36kJ/mol \tag{3.3}$$

$$CO + H_2O \leftrightarrow CO_2 + H_2 \quad \Delta\tilde{h}_r^o = -41kJ/mol \tag{3.4}$$

Biomass gasification

Biomass-based technologies gained considerable attention in the last years, because they use renewable resources and emit no or very few net CO_2 emissions, if carefully managed, since the released CO_2 was previously fixed in the plant as hydrocarbon by photosynthesis. H_2 production from biomass can be divided into two categories; thermo-chemical processes (i.e. biomass gasification and pyrolysis) and biological processes (i.e. biophotolysis and fermentation). An overview of these processes and their economics is given in Bartels et al. (2010). Here it is focussed on the thermochemical lignocellulosic biomass gasification processes using wood as a resource.

After biomass handling, the wood has to be dried because the high moisture content would reduce the gasifier performance. Steam and air drying are reported to be the most common technologies. Their performance depends on the energy integration with the rest of the process and on the potential heat recovery. Optionally the biomass feed can be treated in a thermochemical torrefaction or pyrolysis step to improve the thermal and mechanical properties by drying the biomass further and breaking the feedstock down (Gassner and Maréchal (2009b)). During wood gasification, the solid macromolecules are broken into H_2, CO, CO_2 hydrocarbons, tars and ash in the presence of steam or oxygen as gasifying agent. The heat for this endothermal process can be delivered by different gasifier technologies such as indirectly or directly heated entrained or fluidised bed gasifiers. When the heat is provided by partial oxidation using air/O_2 the process is known as autothermal. An example of directly heated gasification is the Viking reactor and of indirectly heated gasification the fast internally circulating fluidised bed (FICFB) gasifier studied in Gassner and Maréchal (2009). A detailed technology description, as well as the advantages and disadvantages of the different gasifier technologies are reported in Olofsson et al. (2005) and Spath and Dayton (2003). The generated producer gas (PG) consists mainly of CO, CH_4 and other hydrocarbons, consequently these components need to undergo gas cleaning and conversion via steam reforming (Eq.3.1) and shift reactions (Eq.3.4) to generate a $H_2/CO/CO_2$ mixture. The particulates are removed through cyclone separators in a cold gas cleaning step and the produced char is burnt to generate heat that can be reused in the process.

Water gas shift reactor

The syngas (H_2-CO mixture) generated by reforming or gasification is cooled down for heat recovery purposes and catalytically reacted with H_2O in a water gas shift (WGS) reactor to increase the H_2 and CO_2 content according to Eq.3.4. The WGS reaction is exothermic and proceeds nearly to completion at low temperature and is independent of pressure. Conventionally, a dual shift reactor realising the shift in a successive high temperature (HTS) (i.e. T=350-420^oC) and low temperature (LTS) (i.e. T=200-250^oC) reactor is applied to increase the CO conversion and profit from the high temperatures (Longanbach et al. (2002)). The steam to carbon ratio S/C is an important parameter for this reaction. In practice, the ratio is set between 1 and 4. A high S/C ratio favours the conversion, but on the other hand the production of steam is energy consuming. Typically reaction pressures are in the range of 1-30 bar. For HTS iron oxide or chromium oxide catalysts are used, while for LTS a catalyst mix of zinc oxide, copper oxide and aluminium oxide catalysts are preferred.

Purification and CO_2 capture

After the shift section, the H_2/CO_2 mixture is separated. First water is removed by condensation to avoid a decrease of the separation efficiency due to high water contents. To generate high purity H_2 and CO_2 simultaneously, chemical absorption with amines or physical absorption is followed by a pressure swing absorption step. These processes have been described in detail previously in Section 2.2.2.

H_2 applications

After the separation of H_2, the H_2-rich fuel can be used as fuel in boilers, furnaces, gas turbines, engines and fuel cells for power and/or heat generation, or as chemical for other applications. Fuel cell applications are reviewed in Stolten (2010). Thermo-economic analysis of fuel cell systems have previously been made in Facchinetti et al. (2011), Maréchal et al. (2005), Autissier et al. (2007), van Herle et al. (2003) and Morandin et al. (2009). Using H_2 in combustion systems is challenging, because compared to other hydrocarbons H_2 has an higher specific heat, higher diffusivity, larger flammability limits and higher laminar flame speed (McDonell (2006)). In Chiesa et al. (2005b) the issues of burning H_2 in a heavy-duty gas turbine designed for natural gas are discussed and some adaptation techniques are proposed especially also with regard to NOx control. The most relevant effects of the variation of the flowrate and of the thermo-physical properties are on the matching between turbine and compressor and on the cooling system. Within the objective to produce electricity with CO_2 capture, it is focused here on pre-combustion systems burning H_2-rich fuel in a gas turbine. The options of burning the H_2-rich fuel after CO_2 separation by chemical absorption and/or after H_2 purification by PSA are considered.

3.3 Pre-combustion CO_2 capture process modelling

The developed models for the different technological options of processes producing H_2 and/or electricity with pre-combustion CO_2 capture are based on literature data. Details for each process unit are given hereafter with regard to the different resources being either biomass or natural gas. The natural gas fed process layout illustrated in Figure 3.2 is established using mainly literature data from Longanbach et al. (2002), Damen et al. (2006), Consonni and Viganò (2005), Romano et al. (2010) and Maréchal et al. (2005).

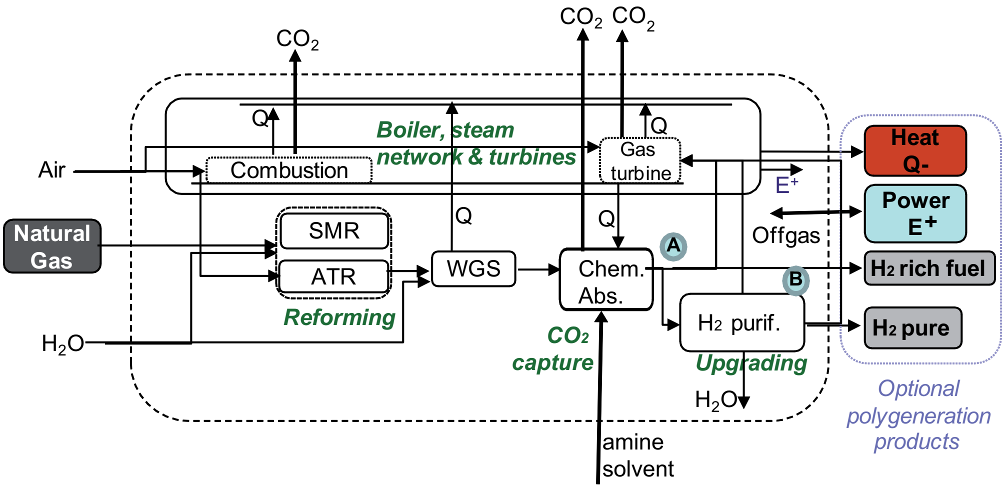
CO2
CO2 CO2
Q
Boiler, steam network & turbines
Q
Gas turbine
Air
Combustion
E+
Natural Gas
SMR
Q
Q
ATR
WGS
Chem. Abs.
A
Offgas
Reforming
B
H2O
CO2 capture
H2 purif.
Upgrading
H2O
amine solvent
Heat Q-
Power E+
H2 rich fuel
H2 pure
Optional polygeneration products

Figure 3.2: Process layout of the natural gas reforming processes with pre-combustion CO_2 capture. The products are defined by the decisions made at the cross points A and B.

The biomass conversion processes outlined in Figure 3.3 rely mainly on previous works (Gassner and Maréchal (2009b), Gassner and Maréchal (2009), Tock et al. (2010)) and on literature data (Hamelinck and Faaij (2002), Spath et al. (2005), Carpentieri et al. (2005)).

The detailed process flowsheets of the each process step are developed within the *Belsim Vali* (Belsim S.A.) software. Tables 3.1 and 3.2 summarise the different modelling assumptions and the nominal operating conditions, respectively. To predict accurately the thermodynamic properties, such as fugacity, enthalpy and molar volume different methods are chosen. For pure compounds the fugacity is calculated by the Raoult law for the liquid phase and by the ideal gas law for the gas phase. For mixtures the fugacity is calculated by the Peng-Robinson equation of state. The Lee-Kesler method is applied for the enthalpy and vapour volume calculation and the Gunn Yamada method for the liquid volume. For the gas separation units, the specific models described in Section 2.3 are considered.

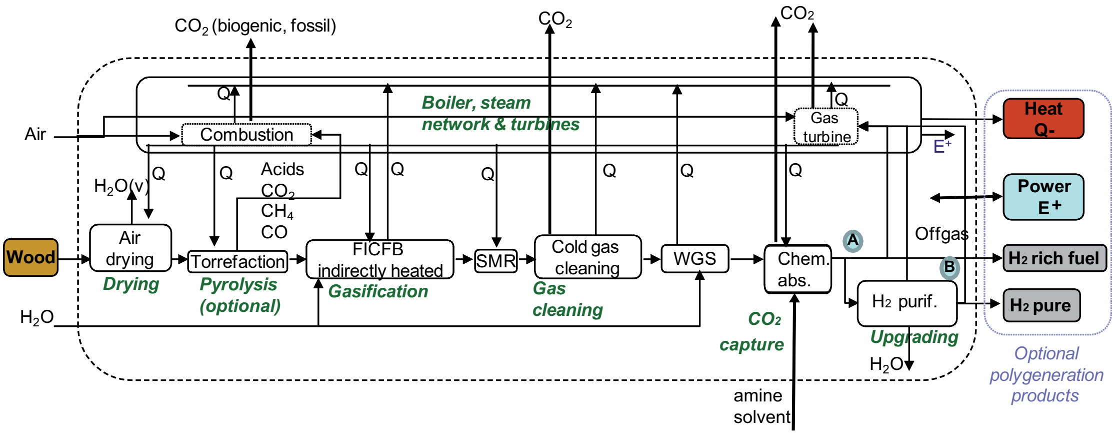
CO_2 (biogenic, fossil)
CO_2
CO_2
Air
Q
Combustion
Boiler, steam network & turbines
Q
Gas turbine
E^+
Heat Q-
Power E+
$H_2O(v)$
Q
Q
Acids CO_2 CH_4 CO
Q
Q
Q
Q
Q
Q
Wood
Air drying
Torrefaction
FICFB indirectly heated
SMR
Cold gas cleaning
WGS
Chem. abs.
A
Offgas
B
H_2 rich fuel
H_2 purif.
H_2 pure
Drying
Pyrolysis (optional)
Gasification
Gas cleaning
CO_2 capture
Upgrading
H_2O
H_2O
amine solvent
Optional polygeneration products

Figure 3.3: Process layout of the biomass conversion processes with pre-combustion CO_2 capture. The products are defined by the decisions made at the cross points A and B.

Table 3.1: Parameters for the energy-flow models of the pre-combustion CO_2 capture processes using natural gas or biomass as a feedstock.

Section	Specification	Value
Biomass feedstock	Composition	C=51.09%, H=5.75%
	[%wt]	O=42.97%, N=0.19%
	$\theta_{wood,in}$	50%wt
Natural gas feedstock	Composition	CH_4= 100 %
Chemical absorption	$\dot{Q}$ @ 423 K	3.7MJ/kg_{CO2}
(95% efficiency) (Radgen et al. (2005))	Electric Power	1.0MJ_e/kg_{CO2}
Physical adsorption	Adsorption P	10 bar
	Purging P	0.1 bar
	H_2 recovery	90%
CO_2 compression	Pressure	110 bar
	$\eta_{compressor}$	85%
Gas turbine	$\eta_{compressor}$	85%
	$\eta_{turbine}$	90%

3.3.1 Syngas production

Natural gas reforming

With regard to feedstock pretreatment, it is assumed that the sulphur content is low and consequently desulphurisation is omitted and has not been modelled. The natural gas reforming reactor is modelled as an isothermal reactor indicating that the reaction is performed at constant temperature. For the reactor modelling the approach described in Maréchal et al. (2005) applying the minimum exergy losses representation is followed. This modelling approach allows to decouple the heat transfer from the chemical reaction heat and consequently to maximise the energy recovery for power generation. It is assumed that the reactions (Eqs.3.1&3.4) reach thermodynamic equilibrium defined by the reaction temperature. In reality it is difficult to achieve isothermal conditions for exothermic or endothermic conditions since heat has constantly to be withdrawn or supplied. However in a shell and tube heat exchanger based reactor, isothermal conditions can be assumed since heat transfer can take place simultaneously as the reaction continues. For the authothermal reforming, the reactor is also modelled as isothermal reactor with equilibrium reactions. The POX reaction (Eq.3.3) using air as an oxidant is modelled as a conversion reaction by imposing complete consumption of the oxygen. The operating pressure, temperature and the steam to carbon ratio are decision variables that are optimised in the multi-objective optimisation.

Table 3.2: Operating conditions and feasible range for optimisation for the pre-combustion CO_2 capture processes using natural gas or biomass as a feedstock.

Section	Specification	Nominal	Range
Biomass drying	T [K]	473	-
Biomass pyrolysis	T [K]	533	-
Biomass gasification	$\theta_{wood,gasif\_in}$ [%wt]	20	[5-35]
	T [K]	1123	[1000-1200]
	P [bar]	1	[1-15]
	Steam/biomass [%wt]	50	-
SMR after gasification	T [K]	1138	[950-1200]
SMR	T [K]	1073	[725-1200]
	P [bar]	11	[1-30]
	S/C [-]	3	[1-6]
ATR	T [K]	1173	[780-1400]
	P [bar]	15	[1-30]
	S/C [-]	2.5	[0.5- 6]
WGS	T_{HTS} (NG/BM) [K]	633/623	[523-683]/[573-683]
	T_{LTS} (NG/BM) [K]	473/453	[423-523]/[423-573]
	P (BM) [bar]	25	[1-25]
	S/C (BM) [-]	2	[0.2-4]
Gas turbine	Combustion inlet T [K]	773	-
	Turbine inlet T [K]	1680	-

Biomass gasification

For the biomass drying and gasification, the models developed in previous works (Gassner and Maréchal (2009b), Tock et al. (2010)) for the production of synthetic natural gas (SNG) and liquid fuels (BtL) have been adapted in accordance with literature data considering biomass conversion into H_2 (Hamelinck and Faaij (2002), Spath et al. (2005)). The model for biomass drying by air or steam is based on the one described in Gassner and Maréchal (2009b) taking into account the wood humidity θ and the mass and heat transfer coefficients. For the gasifier, it is focused on an indirectly heated steam-blown fluidised bed gasifier (FICFB). The heat is supplied by circulating a hot medium between the gasifier vessel and the char combustion chamber and the steam is supplied from the steam cycle. The chemical conversion in the gasifier is modelled by equilibrium relationships with an artificial temperature difference as explained in Gassner and Maréchal (2009b). The gasification temperature and pressure are key decision variables. The cleaning and reforming is modelled according to the previous works (Gassner and Maréchal (2009b), Tock et al. (2010)). The high temperature stage reforming is modelled by considering the reactions at equilibrium. The reforming temperature is a decision variable and the steam to carbon (S/C) ratio is fixed by the amount of steam supplied to the gasifier.

3.3.2 Gas treatment and purification

Water gas shift

For the water gas shift reactor, the option to include one reactor operating at intermediate temperature or to include a dual shift reactor consisting of one reactor operating at high temperature and one at low temperature is considered. The WGS reactor is modelled as an isothermal reactor and it is assumed that the WGS reaction (Eq.3.4) reaches thermodynamic equilibrium at the specified reaction temperature which is a decision variable. Similar to the reforming reactor modelling, the isothermal modelling of the reactor follows the approach outlined in Maréchal et al. (2005). No additional water is added at this stage for the natural gas fed process. The amount of water that is available is defined by the S/C ratio of the reforming section. However, for the biomass fed process additional water can be fed to the WGS reactor. The optimal amount is defined by optimisation.

CO_2 removal and H_2 purification

In the purification section, chemical absorption with amines is followed by a pressure swing absorption step (PSA) to generate high purity H_2 and CO_2 simultaneously. In a first approach, the CO_2 capture unit is modelled as a blackbox using the average data reported in Table 3.1. This simplified model does not represent the influence of decision variables that are inherent to the CO_2 removal process and could allow to increase the CO_2 capture efficiency. However, it gives a first prospect of the penalty of CO_2 capture in Section 3.4. The influence of the CO_2 capture unit design is investigated in more detail in Chapter 4 and in Tock and Maréchal (2012c).

The PSA model is based on the one described in Section 2.3.3 with the assumptions given in Table 3.1. The targeted H_2 purity is above 95%mol.

After the CO_2 capture unit, the H_2-rich gas exits at the process pressure and after the PSA unit at atmospheric conditions or lower. No H_2 compression for storage and transportation has been included in this study. If CO_2 sequestration is considered, CO_2 compression up to 110 bar by a two stage compression with intermediate cooling is included. It has to be noted that the CO_2 purification step possibly required before the CO_2 compression to reach the purity characteristics for transportation and storage (min 95%vol) has not been included.

3.3.3 H_2 applications

Gas turbine

Within the objective to produce electricity with CO_2 capture, the burning of H_2 fuel in a gas turbine is investigated. The options of burning the H_2-rich fuel after CO_2 separation by chemical absorption and/or after H_2 purification by PSA are considered (Figures 3.2 & 3.3). Even if in practice there are still some concerns with regard to flame stability which have to be addressed for pure H_2 combustion, it is assumed in the modelling that by some technology adaptations it will be feasible in the future. In the gas turbine model, the oxidant is air which is first compressed and is then preheated to the combustion temperature. The preheating temperature is optimised in the energy integration. The preheated fuel is completely oxidised in the combustion chamber. It is modelled by an adiabatic reactor taking into account atomic balances and by a heat exchanger cooling the gas down to the turbine inlet temperature. For the compressor and the turbine isotropic efficiencies of 85% and 90% respectively, are considered. The combustion and turbine inlet temperatures are decision variables that will be optimised. The model is applied for natural gas, as well as for impure and pure H_2 burning.

Fuel cells

The usage of H_2 in fuel cells has been studied in previous works (Maréchal et al. (2005), Facchinetti et al. (2011, 2012), Autissier et al. (2007), van Herle et al. (2003), Morandin et al. (2009)) and has not been addressed here in detail. The results are included in the discussion part for comparison purpose.

3.4 Thermo-economic evaluation of pre-combustion CO_2 capture processes

To assess the impact of pre-combustion CO_2 capture, different scenarios for H_2 and/or electricity generation are studied. These scenarios include:

- biomass gasification (BM)
- natural gas reforming by SMR
- natural gas reforming by ATR

For H_2 generation processes, the possibility to import electricity (E_{imp}) or to burn part of the H_2-rich gas to satisfy the process power demands (self-sufficient, $self$) is considered. The H_2 production is compared with the production of electricity burning the H_2-rich fuel in a gas turbine (GT) after capturing the CO_2. Each scenario integrates a combined steam cycle. The performance analyses are performed for a plant capacity of 725MW$_{th,NG}$ of natural gas and 380MW$_{th,BM}$ of dry biomass, respectively. The biomass installation size is chosen in accordance with Hamelinck and Faaij (2002). Larger plants would be favourable in terms of annual production and infrastructure's cost, but are penalised by the logistics of wood transport depending on the average collection distance related to the plant size (Gerber et al. (2011)). The competitiveness of H_2 and electricity generation processes is evaluated by the performance indicators defined in Section 1.4.1 for the economic assumptions reported in Table 1.2. A multi-objective optimisation is performed to assess the trade-off of competing factors defining the process performance of the H_2 and electricity generation with CO_2 capture. The maximisation of the overall energy efficiency ϵ_{tot} (Eq.1.22) and the maximisation of the overall carbon capture rate η_{CO2} (Eq.1.25) are chosen as objectives within the aim of optimising the CO_2 capture integration. The key process operating conditions given in Table 3.2 are chosen as decision variables.

3.4.1 Multi-objective optimisation of pre-combustion CO_2 capture in H_2 processes

The Pareto optimal frontiers generated by the multi-objective optimisation of CO_2 capture in different H_2 production processes reveal in Figure 3.4 the efficiency decrease with increasing CO_2 capture rate. Due to the energy consumption for CO_2 capture and compression, the net electricity output is decreased and consequently the overall energy efficiency also. The increase of the power consumption with regard to the CO_2 capture rate is illustrated in Figure 3.5.

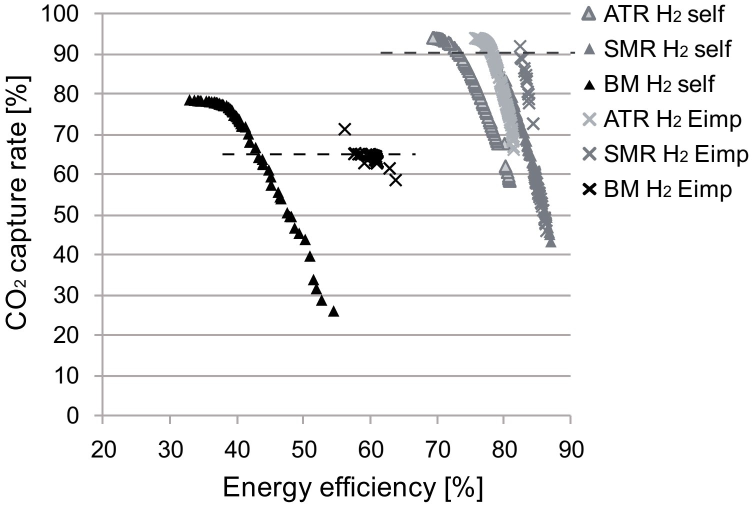

Figure 3.4: Pareto optimal frontiers for CO_2 capture in H_2 production processes maximising the energy efficiency and the CO_2 capture rate. Dashed lines represent the CO_2 capture level of configurations yielding a compromise with regard to both objectives.

For the natural gas fed H_2 processes with CO_2 capture the trade-off between efficiency, CO_2 capture and production costs is presented in Figure 3.6. High efficiencies and low production costs are reached for process configurations with low CO_2 capture rates. These solutions having a higher H_2 productivity release however more CO_2 emissions. While high CO_2 capture rates, reduce the efficiency and increase the production costs due to the additional investment and the increase of the energy demand for CO_2 capture (Figure 3.5).

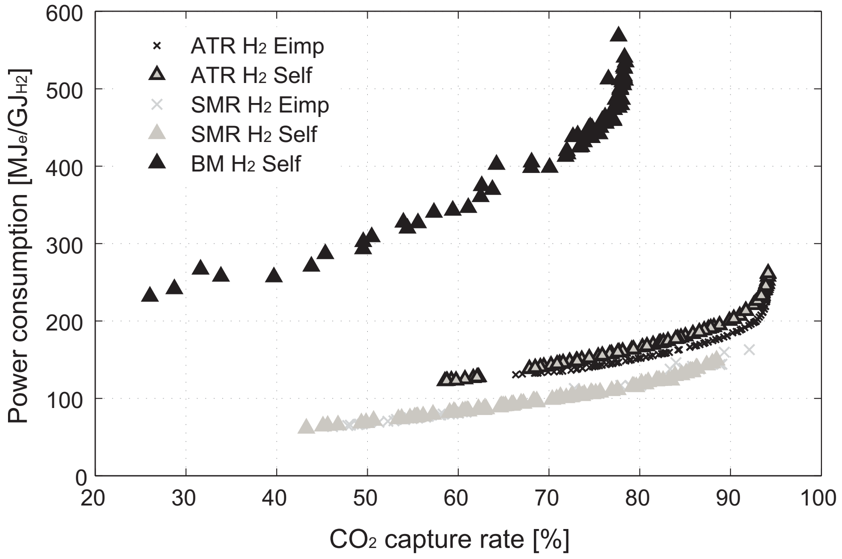

Figure 3.5: Multi-objective optimisation results of CO_2 capture in H_2 production processes: Trade-off between CO_2 capture rate and power consumption.

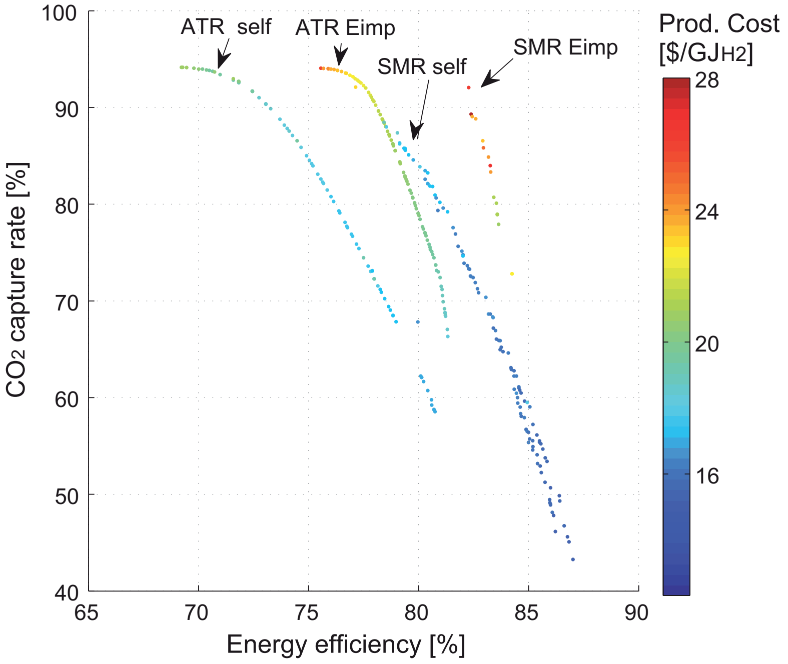

Figure 3.6: Multi-objective optimisation results of CO_2 capture in natural gas fed H_2 production processes: Trade-off between efficiency, CO_2 capture rate and production costs.

Self-sufficient H_2 production processes *(self)* with CO_2 capture yield lower efficiencies and lower costs than scenarios importing electricity from the grid (*Eimp)*. For self-sufficient H_2 production processes with CO_2 capture part of the H_2-rich fuel has to be burnt in a gas turbine to close the power balance, which reduces the H_2 productivity and hence the overall energy efficiency. The increase in power generation by the gas turbine fed with H_2-rich fuel with the increasing CO_2 capture rate is illustrated in Figure 3.7. In H_2 production processes importing electricity, only a small amount of the H_2-rich fuel has to be burnt at high capture rates in order to deliver the heat required for the CO_2 capture. From an energy integration point of view, configurations satisfying the thermal energy demand by the heat from the steam network and by the combustion of waste and product streams are preferred.

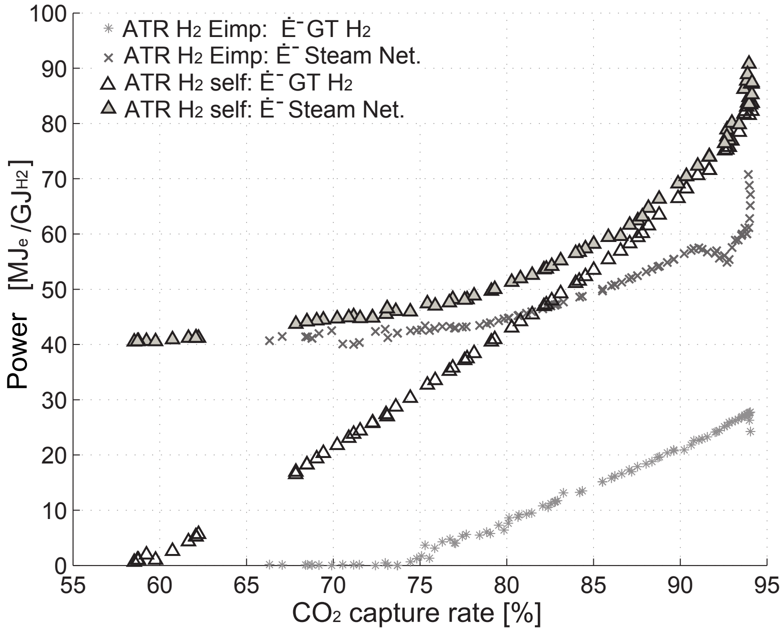

Figure 3.7: Power generation by the steam network and by the H_2-rich fuel gas turbine along the Pareto optimal frontiers of the H_2 production by ATR (self and Eimp) with CO_2 capture.

For each scenario one configuration yielding a compromise between efficiency and CO_2 capture is chosen in order to compare in detail the performance of the different process configurations. For natural gas fed processes the Pareto optimal configuration corresponding to a capture rate of 90% is chosen, while for biomass conversion processes the one with 65% capture rate is selected. For biomass conversion a lower capture rate can be considered in order to reach a higher efficiency ϵ_{tot}, because it corresponds to the capture of biogenic CO_2. CO_2 capture generates in this case a negative balance since the captured carbon comes from the CO_2 assimilated in the biomass by photosynthesis. The specific performance results of the selected configurations expressed per GJ of H_2 produced (based on the lower heating value) are summarised in Table 3.3 and the corresponding operating conditions are reported in Appendix Table D.1.

Table 3.3: Performance of H_2 process configurations with pre-combustion CO_2 capture. The net electricity output expressed in MJ of electricity per GJ of hydrogen is negative when the integrated process requires electricity importation and positive when it generates electricity. The corresponding operating conditions are reported in Appendix Table D.1.

Process	ATR self	ATR self no MVR	SMR self	BM self	ATR E_{imp}	SMR E_{imp}	BM E_{imp}	BM E_{imp} no CC	BM E_{imp} no MVR
Feed [$MW_{th,NG/BM}$]	725	725	725	380	725	725	380	380	380
CO_2 capture [%]	89.9	89.9	88.5	64.3	89.6	89.3	65	0	47
Power Balance									
Net electricity [MJ_e/GJ_{H2}]	0	0	0	0	-95.1	-146.7	-283.2	-57.1	-230.9
$\dot{E}^{+}_{Consumption}$[$MJ_e/GJ_{H2}$]	240.3	206	184.3	508.3	221.6	172.4	309.24	103.3	248.8
$\dot{E}^{-}_{SteamNetwork}$ [MJ_e/GJ_{H2}]	69.1	52.2	44.3	155.4	55.4	0	8.1	0	0
$\dot{E}^{-}_{GasTurbine}$ [MJ_e/GJ_{H2}]	171.2	153.8	140	352.9	71.1	25.7	17.9	46.2	17.9
Performance									
Product [MJ_{H2}/GJ_{res}]	732.8	703.2	784.2	432.5	844.6	937.2	724.2	631.2	527.1
H_2 purity [%mol]	96.3	96.3	99.8	99.5	96.3	99.9	99.6	77.9	99.6
H_2 production [t_{H2}/d]	382.5	367.1	409.3	118.3	440.9	489.2	197	165.2	143.4
$CO_{2,emitted}$ [kg/GJ_{H2}]	7.5	7.9	8.1	-149	6.7	6.3	-90	0	-90
ϵ_{tot} [%]	73.3	70.3	78.4	43.2	78.2	82.4	60.1	60.9	46.9
ϵ_{eq} [%]	73.3	70.3	78.4	43.2	70.4	69.7	36.6	56.8	31.4
Economics (Assumptions Table 1.2)									
Investment [$\$/kW_{H2}$]	770.7	671.9	1127.8	2857.0	600.6	1921.8	1803.0	1667	2063
Annualised Inv. [$\$/GJ_{H2}$]	2.2	1.9	3.3	8.3	1.8	5.6	5.2	4.8	6
Maintenance [$\$/GJ_{H2}$]	2.7	2.6	3.3	8.2	2.2	4.6	5.1	5.1	6.2
Resource cost [$\$/GJ_{H2}$]	13.3	13.8	12.4	32.1	11.5	10.4	18.9	21.6	25.9
Electricity cost [$\$/GJ_{H2}$]	0	0	0	0	5.9	10.2	20.9	4.2	17
Prod. cost [$\$/GJ_{H2}$]	18.2	18.4	19	48.6	21.4	30.8	50.1	35.7	55.1
$\$/t_{CO2,avoided}$	80.7	82	86.7	142	105	175	186	204	208
Costs variation: 5.5-19.5$/$GJ_{res}$, 41.7-75$/GJ_e									
Prod. cost [$\$/GJ_{H2}$]	12.5-31.5	12.5-32.2	13.6-31.4	29.3-61.4	13.9-33.6	21.7-42.2	22.6-54.2	15.8-43.7	22.5-59.2
$\$/t_{CO2,avoided}$	36-183	36-189	45-182	75-187	46-198	106-263	65-204	-	64-226

3.4.2 Pre-combustion CO_2 capture process performance: H_2 production

The comparison of the H_2 production processes with CO_2 capture using different resources and importing electricity (E_{imp}) or being self-sufficient (self) in terms of power shows that the highest efficiency is reached for the natural gas SMR process importing electricity (Figure 3.4). The performances summarised in Table 3.3 are analysed and discussed in detail in the following paragraphs.

Energy integration

For self-sufficient H_2 production processes with CO_2 capture using different resources the variation in terms efficiency is highly linked to the difference in the energy demands illustrated in Figure 3.8 by the composite curves resulting from the energy integration.

The endothermic gasification and SMR processes require heat supply for the syngas generation, while in the ATR process the heat is delivered internally by a POX reaction. As a consequence, the ATR process requires the lowest amount of hot utility. The heat demands above the pinch point are satisfied by the combustion of offgases and, if necessary, of part of the H_2-rich gas. In the purification step, the CO_2 separation by chemical absorption requires a large amount of energy for the amine-solvent regeneration. Below the pinch point, the heat excess is valorised in a steam network for electricity generation. In these configurations, the quality of the energy integration is improved by introducing a mechanical vapour recompression (MVR) between the absorber (condensation at 429 K) and the stripper (evaporation at 378 K) of the chemical absorption unit for CO_2 capture.

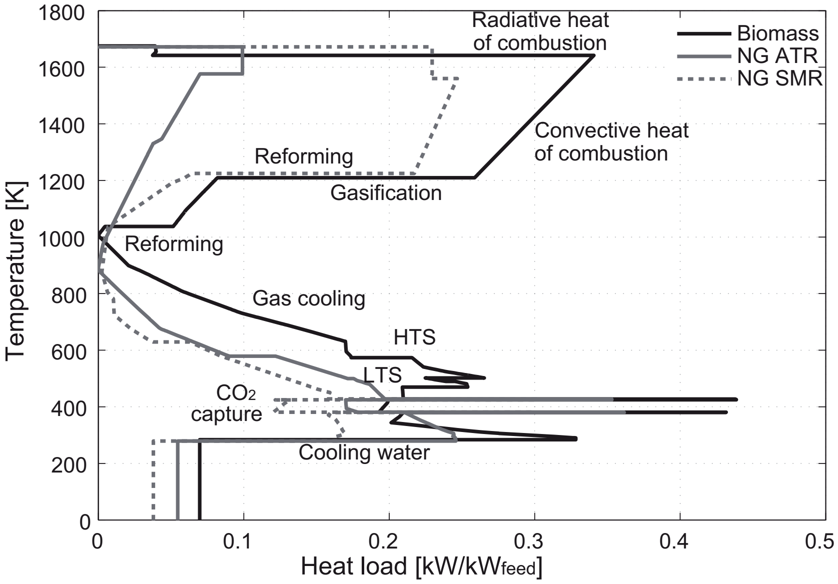

Figure 3.8: Integrated composite curves of self-sufficient H_2 production processes with CO_2 capture using different resources reported in Table 3.3 (ATR self, SMR self, BM self). The steam network integration is omitted on the figure for clarity.

The composite curves illustrated in Figures 3.9& 3.10 clearly reveal the benefit of introducing MVR in self-sufficient natural gas fed H_2 production process (ATR) with CO_2 capture by chemical absorption. The integration of the MVR is reported by the integrated composite curve in Figure 3.10. Although it is realised below the pinch point, the MVR integration appears to be energetically needed because the combined production of heat and power creates a utility pinch point at the level of the desorption. Introducing the MVR, reduces the medium pressure steam usage needed for the CO_2 desorber. This steam can be expanded to very low pressure in the condensing turbine stage which maximises the combined production of power. The increase of the mechanical power production is larger than the amount required to compensate the mechanical power needed by the compression in the MVR. The efficiency is increased by 3%-points through the conversion of waste heat into mechanical power (Table 3.3). Even if the productivity is increased, the production costs remain nearly constant due to the increased capital costs for the compressor purchase around 98.8M$/kW$_{H2}$.

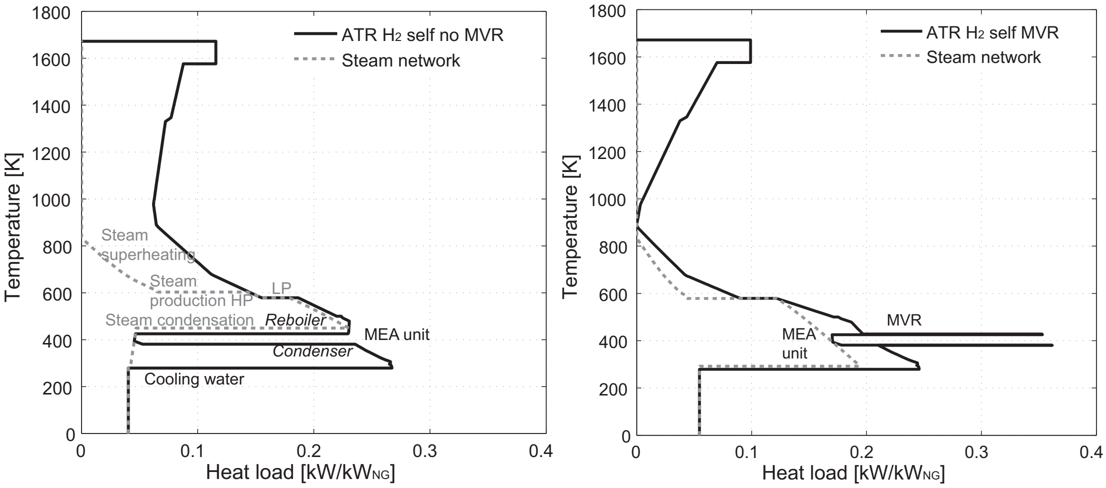

Figure 3.9: Integrated composite curves of the self-sufficient natural gas fed H_2 production process with CO_2 capture without (left) and with MVR integration (right) reported in Table 3.3 (ATR self and ATR self no MVR).

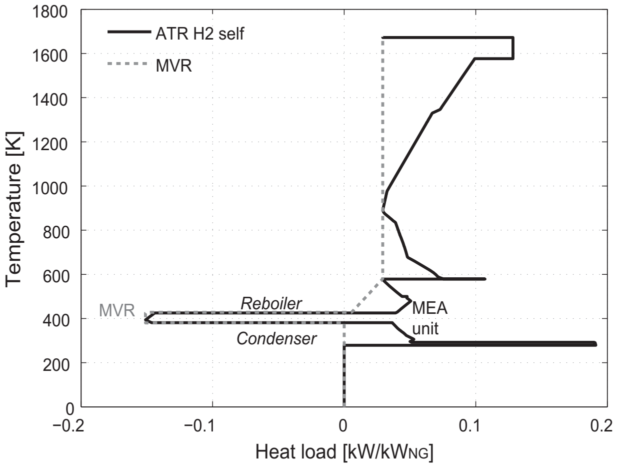

Figure 3.10: MVR integration for the self-sufficient natural gas fed H_2 production process with CO_2 capture (Table 3.3 ATR self).

For biomass fed H_2 production processes with CO_2 capture, the impact of CO_2 capture and MVR on the energy integration is illustrated in Figure 3.11 for the compromise process configuration importing electricity from the grid. The corresponding performance results are summarised in Table 3.3. For the biomass fed H_2 processes purifying H_2 by PSA without or with CO_2 capture, there is a pinch point at low temperature created by the drying, respectively by the chemical absorption for CO_2 capture (Figure 3.11 (left)). Consequently, there is no heat excess available for cogeneration. By introducing mechanical vapour recompression, excess heat from below the pinch can be transferred to a higher temperature for valorisation in a Rankine cycle and consequently the energy integration of the CO_2 capture unit is improved as shown in Figure 3.11 (right). Through H_2 purification by CO_2 capture, the H_2 yield is increased by over 10% and the environmental impact is decreased by 90kg_{CO2}/GJ_{H2}.

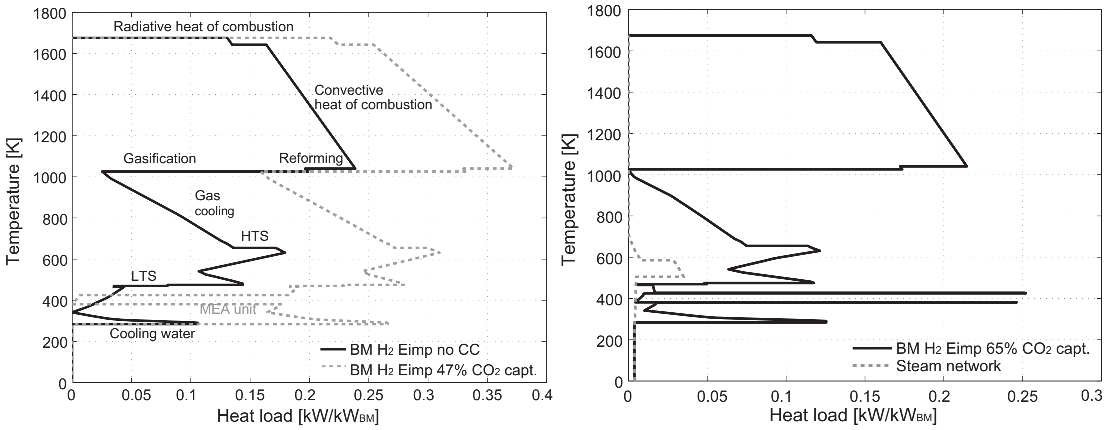

Figure 3.11: Integrated composite curves for the biomass fed H_2 production process (with electricity import) without and with CO_2 capture (left) and with MVR (right) reported in Table 3.3 (BM Eimp, no CC and no MVR).

Power balance

The variation of the H_2 production processes efficiency summarised in Table 3.3, reflects the difference in the power demand and supply. The power balance reported in Figure 3.12 shows that the largest power demand is attributed to gas treatment and purification including CO_2 capture and compression. Moreover, the heat pumping by MVR improving the capture unit integration requires power for the compression. Power is generated by the steam network and by the gas turbine burning offgases. For self-sufficient configurations, the balance is closed by burning part of the H_2 product in a gas turbine, while for the other scenarios electricity is imported from the grid.

For the H_2 procduction by ATR processes, using air as oxidant, some N_2 remains in the products yielding a H_2 purity around 96%mol compared to over 99.5%mol for SMR and biomass based processes. The purification of the syngas produced by ATR is more power demanding and more expensive due to the larger flows to be treated. In addition, air has to be compressed to the operating pressure explaining the larger power demand for the synthesis. Feeding the ATR with pure O_2 might become an alternative if purities over 99%mol H_2 are mandatory. Adding pure O_2 has the advantage that no N_2 is present in the downstream process which reduces the equipment size and facilitates CO_2 capture. However, it requires pure O_2 to be produced in an air separation unit consuming a large amount of energy. This trade-off remains to be investigated in future studies.

Comparing the self-sufficient H_2 processes including CO_2 capture, the natural gas fed SMR process has the lowest power consumption (Figure 3.12) explaining the higher efficiency (ϵ_{tot}=78%), even if the thermal energy demand is larger (Figure 3.8). The power demand is reduced by 18% and 34% when compared with the ATR and the biomass fed process respectively. Since less process gas has to be burnt in a gas turbine for power generation more H_2 is produced. The H_2 productivity is decreased by 6% for the ATR and by 45% for the biomass based process. The lower efficiency of the biomass fed process is related to the lower energy content compared to the natural gas resource and to the endothermic gasification. These trends are also reflected by the difference in the production costs reported in Figure 3.13.

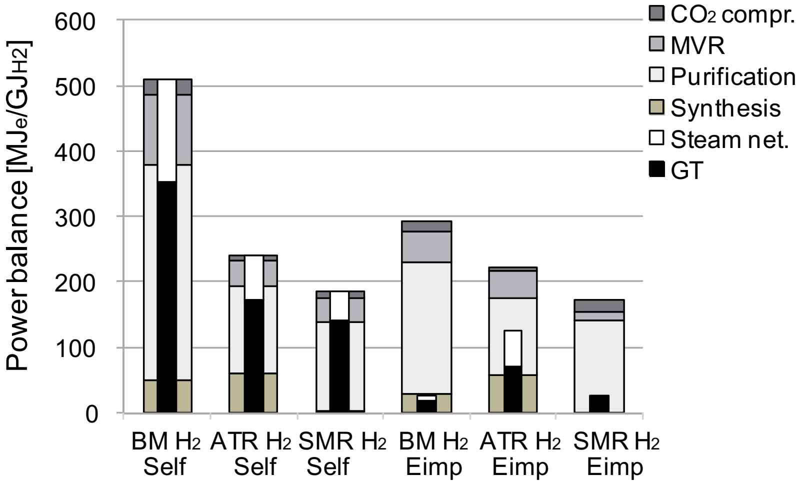

Figure 3.12: Power balance of the different H_2 process configurations with CO_2 capture reported in Table 3.3.

When electricity is imported from the grid, the energy efficiency ϵ_{tot} of the ATR process is increased by nearly 5%-points and of the biomass fed process by more than 16%-points, because more H_2 is produced since none has to be burnt for power generation. However, expressed in terms of natural gas equivalent efficiency given by Eq.1.23, the efficiency of the self-sufficient scenario is nearly 3%-points higher for the ATR process and over 6%-points for the biomass based process. This shows that the internal electricity generation is more efficient than the separate production of electricity from natural gas. The marginal production expressed by $\Delta\dot{E}/\Delta H_2$ is around 70% for the ATR and biomass based processes. Even if, 13% more H_2 is produced for the ATR process with electricity import, Figure 3.13 shows that the production costs are around 15% higher due to the electricity purchase at the price of green electricity being $75\$/\mathrm{GJ}_e$. An electricity purchase price of around $34.7\$/\mathrm{GJ}_e$ would make both solutions equivalent.

Economic performance

The economic performance expressed in terms of production costs in Figure 3.13 is related to the productivity. The natural gas fed H_2 production processes have lower production costs because of the higher H_2 yield. The H_2 production costs are composed mainly of the resource purchase, the annual investment and the electricity purchase for configurations importing electricity. The H_2 production costs of the biomass gasification processes are high because of the lower efficiency and the larger investment required especially for the gasifier purchase that corresponds to about 1/3 of the capital investment costs. The capital investment costs buildup in Figure 3.14 emphasis the large contribution of the gasifier costs to the syngas generation costs. For the natural gas fed H_2 production processes, the investment costs for CO_2 capture and compression are more important since the capture rate is higher. It is to note that the equipment sizing and costing method might overestimate the equipment costs; nevertheless biomass gasification being an emerging technology is as a matter of cause more expensive than the well-established reforming technology.

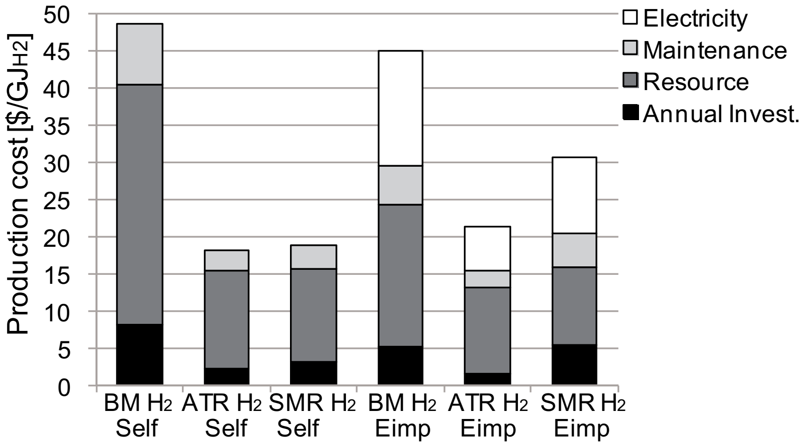

Figure 3.13: Production costs buildup for the different H_2 process configurations with CO_2 capture reported in Table 3.3 based on the base case economic assumptions given in Table 1.2.

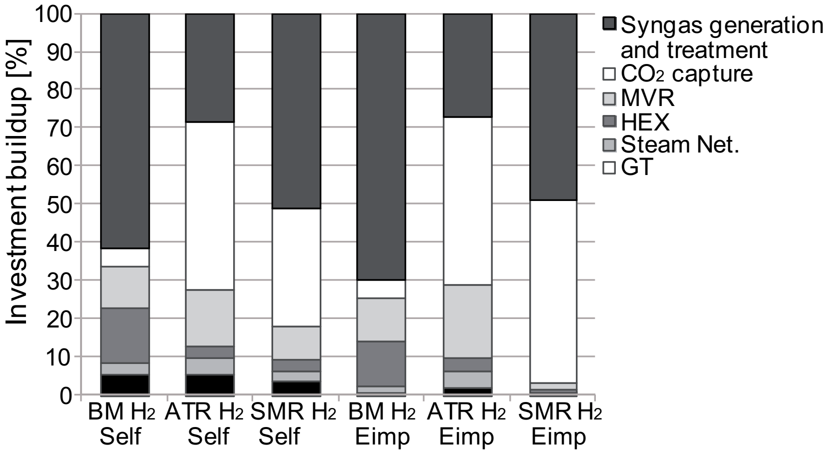

Figure 3.14: Capital investment buildup for the different H_2 process configurations with CO_2 capture reported in Table 3.3.

Taking into account a variation of the resource price between 5.5 and 19.5$/GJ$_{res}$, the assessed H_2 production costs in the range of 12.5-61$/GJ$_{H2}$ are comparable to the one reported in Bartels et al. (2010) for fossil and renewable resources and competitive with the costs of 7.5-14$/GJ$_{H2}$ assessed in the IPCC report (Metz et al. (2005)) for a CO_2 capture in natural gas fuelled H_2 plants yielding an efficiency in the order of 52-68%. These reference processes published in Metz et al. (2005) feature a lower efficiency than the one in this study (73-78%). This efficiency increase can be explained by the improved quality of the process integration. Biomass gasification technology development could lead to a capital costs reduction and consequently to more competitive biomass based H_2 production processes in the future.

Considering as a reference a H_2 plant without CO_2 capture from Metz et al. (2005) (producing 1530MW_{H2}) from natural gas with a cost of 7.8$\$/GJ_{H2}$ (with 5$\$/GJ_{NG}$) and emissions of 137$kg_{CO2,emitted}/GJ_{H2}$, the computed CO_2 avoidance costs 36-263$\$/t_{CO2,avoided}$ are comparable to the ones reported in Metz et al. (2005) (2-56$\$/t_{CO2,avoided}$) with a resource price around 5$\$/GJ_{Res}$. With CO_2 capture, CO_2 emissions in H_2 plants using natural gas can be reduced to around 7.5$kg_{CO2,emitted}/GJ_{H2}$, while for the biomass fed H_2 production process the CO_2 emissions are biogenic and consequently accounted as being null or even negative if CO_2 is captured. The introduction of a carbon tax will promote these solutions even more as discussed in Chapter 8. In addition, the environmental benefit of capturing CO_2 in H_2 production processes is clearly revealed by the life cycle assessment results reported in Appendix E.

This reveals that fuel decarbonisation for H_2 production is not only competitive with regard to environmental considerations but also with regard to the energetic and economic performance for specific resource prices.

3.4.3 Multi-objective optimisation of pre-combustion CO_2 capture in power plants

Instead of generating pure H_2, the option to generate electricity by burning the H_2-fuel in a gas turbine after CO_2 capture is investigated. The trade-off between CO_2 capture, energy efficiency and costs revealed by multi-objective optimisation is reported in Figure 3.15 (left). CO_2 capture reduces the efficiency due to the additional power consumption for CO_2 capture and compression decreasing the net electricity output (Figure 3.15 (right)). As for the H_2 production processes, MVR is introduced in order to improve the energy integration of the chemical absorption unit for CO_2 capture.

The performance results of the compromise power plant scenarios capturing 90% of the CO_2 emissions for natural gas fed processes and 65% for biomass based ones are compared in Table 3.4 and discussed in detail hereafter. The operating conditions are summarised for each process configuration in Appendix Table D.2.

3.4.4 Pre-combustion CO_2 capture process performance: Electricity generation

For the different power plants configurations with pre-combustion CO_2 capture, the difference in the energy demands is illustrated in Figure 3.16 by the composite curves resulting from the energy integration. As for the H_2 production scenarios, the difference between SMR and ATR is clearly seen by the hot utility requirement. In addition, the difference in the cogeneration

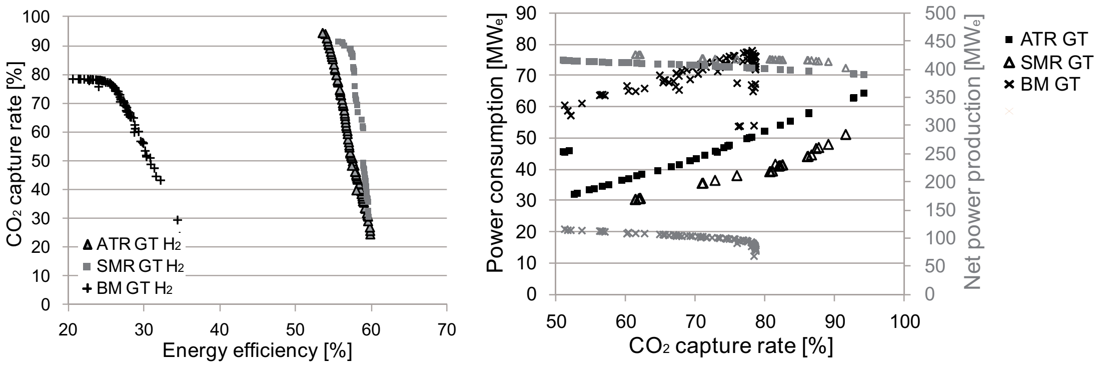

Figure 3.15: Multi-objective optimisation results of power plant's configurations with pre-combustion CO_2 capture (left). Net electricity generation and power consumption variation with the CO_2 capture rate along the Pareto optimal frontiers (right).

Table 3.4: Performance of the compromise power plants configurations with pre-combustion CO_2 capture. The electricity balance is expressed in MJ of electricity per GJ of net electricity produced. The corresponding operating conditions are summarised in Appendix Table D.2.

Process	ATR GT	SMR GT	BM GT
Feed [MW$_{th,NG/BM}$]	725	725	380
CO_2 capture [%]	89.2	90	65.6
	Power Balance		
Net electricity [MW$_e$]	389	403	106.8
$\dot{E}^+_{Consumption}$ [MJ$_e$/GJ$_{e,net}$]	152.3	125.2	643.9
$\dot{E}^-_{SteamNetwork}$ [MJ$_e$/GJ$_{e,net}$]	151.7	131.3	524.7
$\dot{E}^-_{GasTurbine}$ [MJ$_e$/GJ$_{e,net}$]	1000.6	993.9	1119.2
	Performance		
Product [MJ$_e$/GJ$_{res}$]	544.4	564.3	281.1
H_2-rich fuel [H_2 %mol]	65	98.2	89.5
$CO_{2,emitted}$ [kg/GJ$_e$]	11	9.8	-294
ϵ_{tot} [%]	54.4	56.4	28.1
	Economics (Assumptions Table 1.2)		
Investment [\$/kW$_e$]	2195.4	2750.2	4721.6
Annualised Inv. [\$/GJ$_e$]	6.4	8.1	13.7
Maintenance [\$/GJ$_e$]	5.9	6.9	13.2
Resource cost [\$/GJ$_e$]	18.1	17.5	49.4
Prod. cost [\$/GJ$_e$]	30.4	32.5	76.3
\$/t$_{CO2,avoided}$	99	119	156
	Costs variation: 5.5-19.5\$/GJ$_{res}$		
Prod. cost [\$/GJ$_e$]	22.7-48.6	24.9-49.9	46.6-96.1
\$/t$_{CO2,avoided}$	14-296	38-306	72-212

potential is revealed by the heat excess at low temperature.

Compared to a conventional natural gas plant (NGCC) without CO_2 capture generating electricity with an efficiency of 55-58%, production costs of 18-24\$/GJ$_e$ and CO_2 emissions of 100-105kg$_{CO2}$/GJ$_e$ (Finkenrath (2011)), CO_2 mitigation reduces the efficiency by around 8%-points and increases the costs by over 20% due to the energy demand and the costs of CO_2

capture by chemical absorption and of CO_2 compression. With pre-combustion CO_2 capture, electricity production costs in the range of 22.7-50$/$GJ_e$ are assessed for natural gas based processes with an efficiency of around 55%, compared to 28% and 46.6-96$/$GJ_e$ for biomass fed processes taking into account a resource price variation from 5.5 to 19.5$/$GJ_{res}$. With CO_2 avoidance costs of 14-306$/$t_{CO2,avoided}$ and 72-212$/$t_{CO2,avoided}$ for natural gas and biomass fed electricity production processes respectively, CO_2 capture is promising with regard to the future energy market, especially when high CO_2 taxes are imposed. The use of biomass becomes competitive compared to fossil resources from environmental point of view and even from an economical one if gasifier costs can be reduced. The analysed pre-combustion CO_2 capture processes reveal to be competitive compared to an NGCC power plant with post-combustion CO_2 capture yielding an efficiency of about 50%, production costs in the range of 23-35$/$GJ_e$ (with 9.7$/$GJ_{NG}$) and CO_2 avoidance costs around 62-128$/$t_{CO2,avoided}$ (Finkenrath (2011)). Depending on the production purpose and the market scope, the decision between generating electricity or H_2 with electricity import or self-sufficient, with or without CO_2 mitigation can be made with the developed thermo-environomic models.

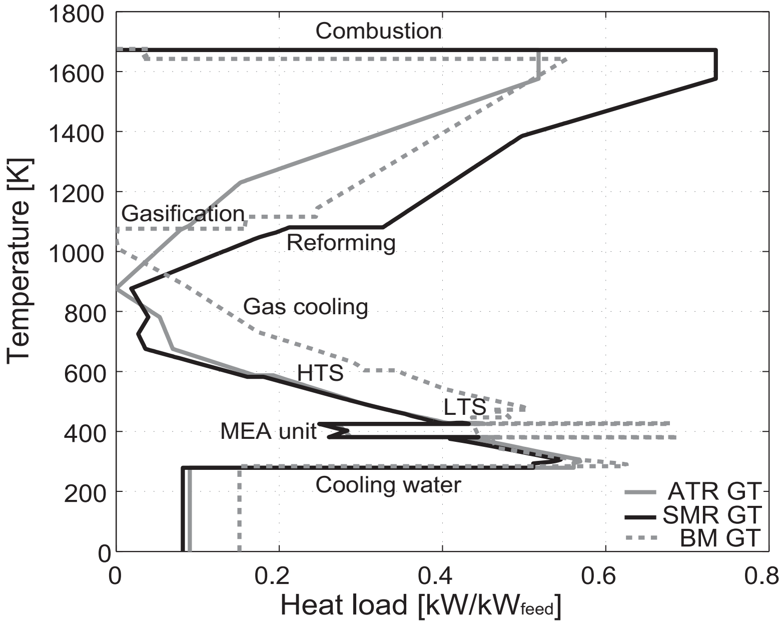

Figure 3.16: Integrated composite curves of power plant's configurations with pre-combustion CO_2 capture using different resources (Table 3.4). The steam network integration is omitted on the figure for clarity.

The competitiveness of different power plant designs with pre-combustion CO_2 capture is investigated more in detail in Chapter 4 and the influence of the economic assumptions (i.e. resource price, carbon tax) is assessed in Chapter 8.

3.5 Conclusions

This chapter presented the development of thermo-economic models for the conceptual design and comparison of fuel decarbonisation processes producing H_2 and/or electricity from either natural gas or biomass resources with CO_2 capture by chemical absorption. The competitiveness of different process configurations is evaluated consistently with respect to energy efficiency, costs and environmental impacts. It is highlighted in particular, how appropriate energy integration and operating conditions optimisation improve the process performance by maximising the combined production of fuel, heat and power. Using natural gas as a resource overall energy efficiencies in the range of 73-82% are reached for H_2 production with CO_2 capture and 43-60% for biomass fed processes. Under selected economic assumptions, CO_2 avoidance costs in the range of 36-263$/t$_{CO2,avoided}$ are obtained for H_2 producing plants and 14-306$/t$_{CO2,avoided}$ for power plants. It is shown that the competitiveness of the process configurations highly depends on the resource price, the imposed CO_2 taxes and the production scope. With regard to climate change mitigation, fuel decarbonisation for H_2 and/or electricity generation using fossil and even renewable resources can become competitive under given economic scenarios. This aspect is further studied in Chapter 8.

4 Thermo-economic comparison of CO_2 capture technologies in pre-combustion CO_2 capture processes

In the previous chapter, the energy and cost penalty of CO_2 capture by chemical absorption in pre-combustion CO_2 capture processes has been highlighted based on a simplified chemical absorption model. In this chapter different CO_2 capture technologies, i.e. chemical and physical absorption, are compared more in detail based on accurate flowsheeting models in order to evaluate the impact on the performance of pre-combustion CO_2 capture processes producing H_2 or electricity. The results presented for the H_2 production processes have been published in Tock and Maréchal (2012c) and the one for the electricity production processes partly in Tock and Maréchal (2012f).

4.1 Introduction

Since CO_2 capture affects the process performance through the thermal and mechanical energy requirement for CO_2 capture and the related investment, it is of interest to evaluate the impact of different technology options. The efficiency and competitiveness of these processes is highly defined by the quality of the energy integration, however in most of the studies this aspect is not investigated in detail. In Lozza and Chiesa (2002a,b) different natural gas fed pre-combustion CO_2 capture process configurations including chemical and physical absorption are compared with regard to the thermodynamic and economic performance. According to their results, systems based on partial oxidation and on chemical or physical absorption yield similar efficiencies (around 48%) and electricity production costs (13.1-13.8$\$/GJ_e$) for a capture rate of 90%. When comparing CO_2 capture by chemical and physical absorption, process integration becomes of importance, since there is a competition between the energy demands. Chemical absorption requires a large amount of energy for solvent regeneration, while physical absorption needs energy for the refrigeration as explained in Section 2.2.2. Consequently, the process integration and performance will be affected differently. The objective is therefore to compare different pre-combustion CO_2 capture process options for H_2 or electricity generation, focusing on the potential performance improvement by process integration. By performing a multi-objective optimisation, the influence of the operating and design conditions of the process units are investigated in order to assess the trade-offs and the competitiveness of the process configurations.

4.2 Process description: Pre-combustion CO_2 capture

The pre-combustion CO_2 capture processes that are considered produce electricity or H_2 from natural gas (725$MW_{th,NG}$) or biomass resources (380$MW_{th,NG}$) by using the same technologies as described in Chapter 3. The investigated technologies for CO_2 capture are chemical absorption with triethanolamine (TEA) and physical absorption with Rectisol or Selexol which have been described previously in Section 2.2.2. The corresponding process flowsheets are illustrated in Appendix Figures B.1, B.3 and B.4. For comparison purpose, some performance results presented in Section 3.4 based on process models considering a simple chemical absorption blackbox model (BBA) for CO_2 capture are included. The thermo-economic models have been described in Section 2.3 for the CO_2 capture technologies and in Section 3.3 for the different syngas production processes. Since the syngas production models are developed with the *Belsim Vali* (Belsim S.A.) software and the CO_2 capture models with the *Aspen Plus* (AspenTech) software, the key feature of the thermo-environomic modelling and optimisation framework allowing to set-up a process model by using parts developed with different flowsheeting software is valuable here. Similar to the H_2 production processes studied in Section 3.4, the process energy demand is satisfied either by importing electricity from the grid (Eimp) or by burning part of the H_2-rich fuel in a gas turbine to be self-sufficient (self) in terms of energy. For the scenarios generating only electricity, the H_2-rich gas leaving the CO_2 capture unit is either burnt directly in a gas turbine or either sent to a hydrogen purification unit (PSA) before being burnt. The competition between the energy demand for the H_2 purification and the gain in the combustion energy is revealed. The removed CO_2 is compressed to 110 bar for transport and storage. The process competitiveness is evaluated based on the performance indicators defined in Section 1.4.1 and the economic assumptions reported in Table 1.2. After briefly investigating H_2 production configurations in Section 4.3, it is focused in Section 4.4 more on the study of electricity generating configurations including different technologies for pre-combustion CO_2 capture.

4.3 Performance of H_2 production processes with different CO_2 capture technologies

Multi-objective optimisation is performed to optimise the CO_2 capture integration in H_2 production processes with regard to the decision variables given in Tables 2.3, 2.5, 2.6 & 3.2. The chosen objectives are the maximisation of the energy efficiency ϵ_{tot} and of the overall CO_2 capture rate η_{CO2}. The trade-off between CO_2 mitigation, efficiency and cost is illustrated for the different H_2 production scenarios in Figure 4.1. CO_2 mitigation reduces the efficiency and increases the costs due to the energy demand for CO_2 capture and compression to 110 bar and the associated costs.

To compare the different processes, configurations with around 85-90% CO_2 capture are selected for the natural gas scenarios and around 60-65% for the biomass scenarios. The performance results are summarised in Table 4.1 and the corresponding operating conditions are given in Appendix Table D.3. The same trends as the one discussed in Section 3.4 are of course identified by comparing biomass and natural gas fed H_2 production configurations, as well as self-sufficient and electricity importing configurations.

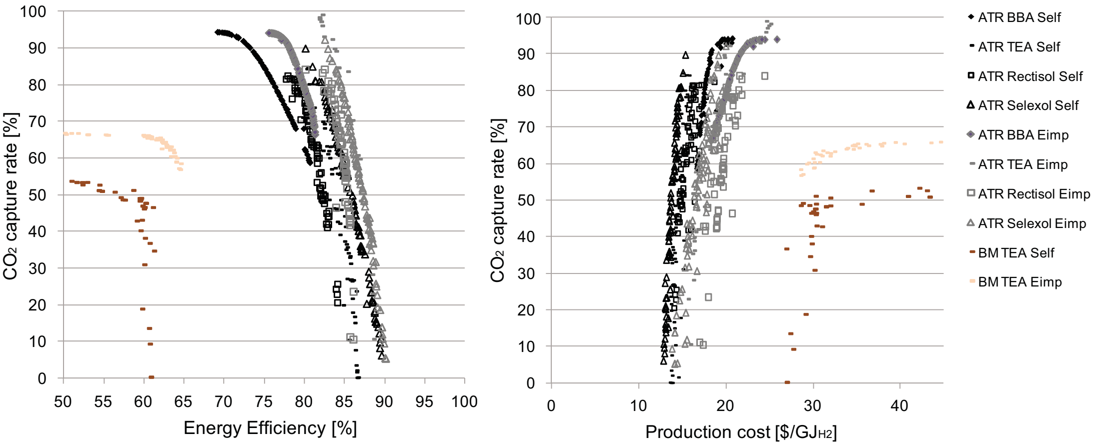

Figure 4.1: Trade-off between CO_2 mitigation, energy efficiency and production cost for H_2 production process configurations including different CO_2 capture technologies.

Table 4.1: Performance of the compromise H_2 production process configurations with CO_2 capture. The specific performances are expressed per GJ of H_2 produced. The corresponding operating conditions are reported in Appendix Table D.3.

			Process Parameters			
Resource	NG	NG	BM	NG	NG	BM
Process	ATR self	ATR self	FICFB self	ATR E_{imp}	ATR E_{imp}	FICFB E_{imp}
Capture technology	TEA	Selexol	Selexol	TEA	Selexol	Selexol
Feed [$MW_{th,NG/BM}$]	725	725	380	725	725	380
CO_2 capture [%]	84.2	89.8	63.7	89.7	89.7	63.4
			Power balance			
Net electricity [MJ_e/GJ_{H2}]	0	0	0	-102.5	-85.9	-130.9
$\dot{E}^{+}_{Consumption}$[$MJ_e/GJ_{H2}$]	143.6	129.7	118.2	151.6	125.9	199.2
$\dot{E}^{-}_{SteamNetwork}$ [MJ_e/GJ_{H2}]	21.7	33.2	69.1	13	15.4	50.7
$\dot{E}^{-}_{GasTurbine}$ [MJ_e/GJ_{H2}]	121.9	96.5	112.1	36.1	24.6	17.6
			Performance			
H_2 purity [%mol]	96.2	96.4	95.3	96.2	96.5	98.9
$CO_{2,emitted}$ [kg/GJ_{H2}]	11.0	7	-108	6.2	6.3	-95.5
ϵ_{tot} [%]	78.9	80.1	59.2	83.6	82.9	61.2
ϵ_{eq} [%]	78.9	80.1	59.2	75.1	75.9	51.3
			Economics (Assumptions Table 1.2)			
Annualised Inv. [$/$GJ_{H2}$]	1.27	1.18	6.37	0.92	1.07	5.37
Maintenance [$/$GJ_{H2}$]	1.92	1.84	6.18	1.54	1.66	5.31
Resource cost [$/$GJ_{H2}$]	12.41	12.24	16.42	10.72	10.97	14.38
Electricity cost [$/$GJ_{H2}$]	0	0	0	6.39	5.35	9.66
Prod. cost [$/$GJ_{H2}$]	15.6	15.26	28.97	19.57	19.05	34.72

With regard to the different CO_2 capture technologies applied to the H_2 production, the difference in the overall efficiencies can be explained by the change in the energy integration. This is illustrated in Figure 4.2 by the comparison of the composite curves for the H_2 production by ATR with 90% of CO_2 capture by chemical absorption with TEA or physical absorption with Selexol. The excess heat available below the pinch point is different, consequently the cogeneration potential changes. For the self-sufficient scenarios, this translates into a variation of the H_2 productivity, since some H_2-rich fuel has to be burnt in order to generate electricity in addition to the steam network to satisfy the process demand as shown in Figure 4.3. Due to the lower energy demand for solvent regeneration, the Selexol physical absorption process yields a slightly higher efficiency for the self-sufficient scenario generating H_2 from natural gas.

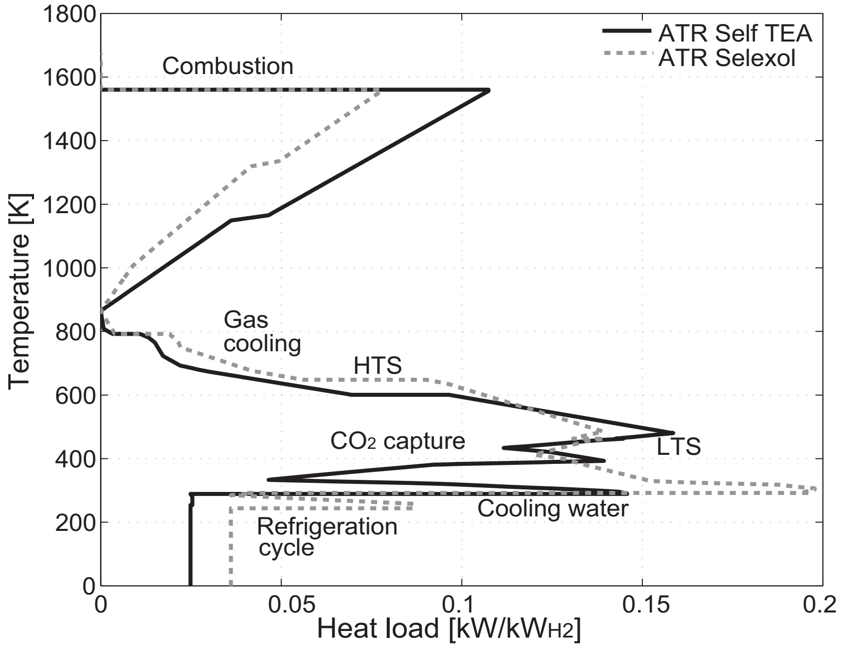

Figure 4.2: Comparison of the composite curves for self-sufficient H_2 production processes capturing 90% of the CO_2 by chemical or physical absorption (Table 4.1: ATR self TEA & Selexol). The steam network integration is omitted on the figure for clarity.

The changes in the H_2 productivity explain also the difference in the H_2 production costs. The H_2 production costs build-up illustrated in Figure 4.4 shows that, the resource purchase contributes to more than two thirds of the production costs. Decreasing the resource price to $5.5\$/GJ_{res}$ will reduce the costs by 30%, while an increase of the resource price to $20\$/GJ_{res}$ will lead to up to 60% higher H_2 production costs. Consequently, the competitiveness of the process configurations is highly influenced by the resource price and the introduction of a carbon tax. This influence of the economic scenario on the economic performance of CO_2 capture in H_2 production processes is illustrated in Appendix Figure E.3 and discussed in detail in Section 8.3 for the power plants competitiveness. The environmental benefit of capturing CO_2 in H_2 production processes is clearly revealed by the LCIA results reported in Appendix E.

Regarding the different impact contributions, the same conclusions as the one discussed in Section 8.3 for the electricity producing processes can be drawn.

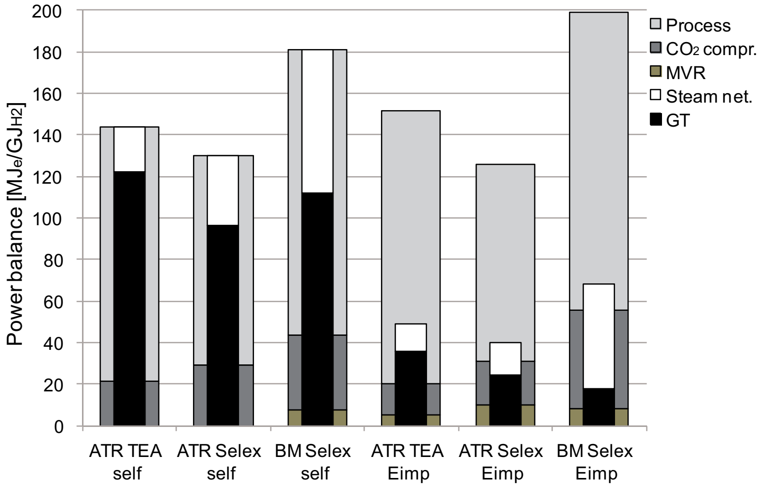

Figure 4.3: Power balance for the different H_2 production process configurations with CO_2 capture reported in Table 4.1.

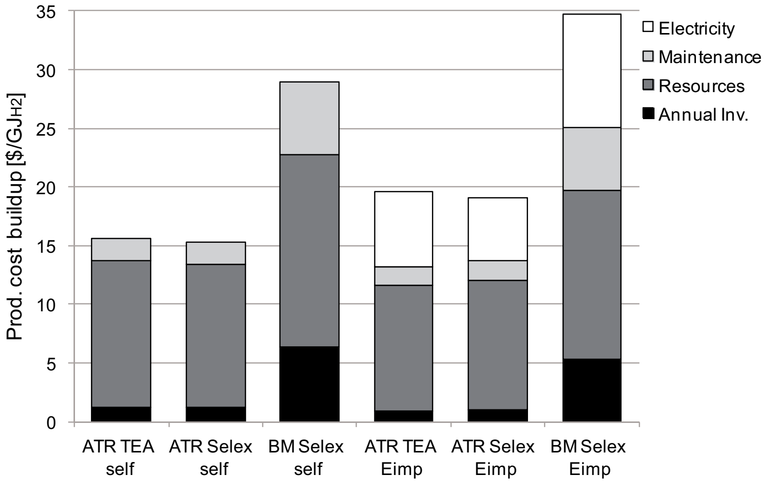

Figure 4.4: Production cost buildup for the different H_2 production process configurations with CO_2 capture reported in Table 4.1.

4.4 Performance of electricity generating processes with different pre-combustion CO_2 capture technologies

To study the influence of pre-combustion CO_2 capture technologies on the power plants performance, different process configurations assembled from the superstructure in Figure 3.1 are analysed in a multi-objective optimisation. The objectives are to maximise the energy efficiency ϵ_{tot} and the overall CO_2 capture rate η_{CO2} with regard to the decision variables given in Tables 2.3, 2.5, 2.6 & 3.2. For generating electricity two different options are considered according to the flowsheet in Figure 3.2. The H_2-rich fuel is either directly burnt in a gas turbine after the CO_2 removal by chemical or physical absorption, or the H_2-rich fuel is further purified by PSA and then supplied to the gas turbine. The trade-off between CO_2 mitigation, efficiency and cost is illustrated for electricity generating configurations including different pre-combustion CO_2 capture technologies in Figure 4.5. The efficiency decrease and the cost increase with the CO_2 capture rate is depicted.

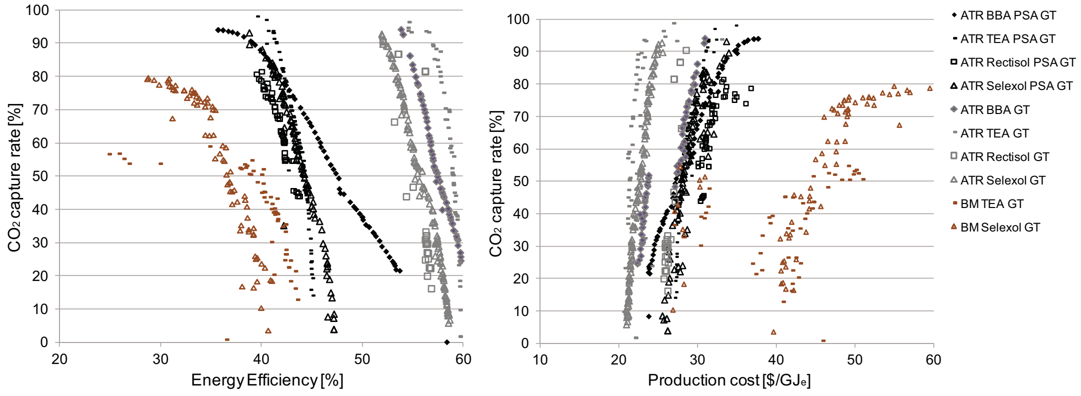

Figure 4.5: Trade-off between CO_2 mitigation, energy efficiency and production cost for power plant configurations including different pre-combustion CO_2 capture technologies.

The different process options are compared in detail in the following sections. The comparison is based on configurations with around 90% CO_2 capture for the natural gas scenarios and around 60% for the biomass scenarios. For biomass feedstock, these kind of electricity generating plants are known as integrated biomass gasification combined cycle (IBGCC) plants. The performance results are summarised in Table 4.2 and Figures 4.6&4.7. For these compromise power plants configurations with pre-combustion CO_2 capture, the optimised operating conditions are reported in Appendix Table D.4.

The comparison of the performance results for the natural gas fed electricity generation process with pre-combustion CO_2 capture assessed in Section 3.4.4 with the simplified chemical absorption model and the one computed here with the detailed chemical absorption model clearly reveals the benefit of optimising the CO_2 capture unit design (Table 4.2: NG ATR BBA vs TEA). The simplified model allows to make a good preliminary estimation of the CO_2 capture penalty. However, by optimising the CO_2 capture design and integration the efficiency can be improved by 2.5%-points and the production costs reduced by 25%.

Table 4.2: Performance of the compromise electricity generation configurations with pre-combustion CO_2 capture. The specific performances are expressed per GJ of electricity produced. The corresponding operating conditions are reported in Appendix Table D.4.

	Process Parameters							
Resource	NG	NG	NG	NG	NG	NG	BM	BM
Process	ATR	ATR	ATR	ATR	ATR	SMR	FICFB	FICFB
Capture technology	TEA	BBA	TEA	Rectisol	Selexol	TEA	TEA	Selexol
Purification	PSA	-	-	-	-	-	-	-
Feed [$MW_{th,NG/BM}$]	725	725	725	725	725	725	380	380
CO_2 capture [%]	90.1	89.2	89.7	90.5	89.1	89.3	59	62.28
	Power Balance							
Net electricity [MW_e]	295.9	389	406.6	372.2	375.8.2	381.3	132.2	137.5
$\dot{E}^+_{Consumption}$ [$MJ_e/GJ_{e,net}$]	284.67	152.3	91.94	125.11	146.64	48.13	342.40	244.10
$\dot{E}^-_{SteamNetwork}$ [$MJ_e/GJ_{e,net}$]	326.52	151.7	200.05	191.48	177.60	143.81	346.20	690.26
$\dot{E}^-_{GasTurbine}$ [$MJ_e/GJ_{e,net}$]	958.15	1000.6	891.89	933.63	969.04	904.32	996.20	533.85
	Performance							
H_2 purity GT_{inlet} [%mol]	96.2	65	63.24	63.34	64.60	99	86.31	89.73
$CO_{2,emitted}$ [kg/GJ_e]	13.3	11	10.11	10.18	11.52	11.22	-170	-164.6
ϵ_{tot} [%]	41.4	54.4	56.9	52.1	52.6	53.3	34.8	36.2
	Economics (Assumptions Table 1.2)							
Annualised Inv. [$\$/GJ_e$]	2.9	6.4	2.22	4.73	2.39	2.35	21.38	11.25
Maintenance [$\$/GJ_e$]	4	5.9	2.97	4.72	3.21	3.16	17.26	10.79
Resource cost [$\$/GJ_e$]	24	18.1	17.47	19.09	18.90	18.63	27.5	26.4
Prod. cost [$\$/GJ_e$]	30.9	30.4	22.7	28.5	24.5	24.1	66.1	48.4

4.4.1 Influence of feedstock type

The performance of power plants with pre-combustion CO_2 capture is influenced by the feedstock type, being either fossil natural gas or renewable woody biomass. The biomass fed processes yield lower efficiencies than the natural gas based processes due to the lower biomass conversion (Figure 4.5). In order to satisfy the energy demand of the gasification, part of the process gas has to be burnt which reduces the amount of fuel sent to the gas turbine and consequently the electricity output (Table 4.2: BM Selexol and TEA). Considering a CO_2 capture rate of 60%, an efficiency around 36% can be reached by the IBGCC plant with physical absorption. CO_2 capture by physical absorption in an IBGCC plant yields a 1.4%-points higher efficiency than chemical absorption with TEA and 28% lower electricity production costs. The computed efficiencies are in the range of the IBGCC power plant efficiency reported in Carpentieri et al. (2005), Corti and Lombardi (2004) and Klimantos et al. (2009). In Carpentieri et al. (2005) an efficiency of 33.9% is assessed with CO_2 capture. The higher efficiency computed here can be explained by the improved quality of the process integration. The electricity production costs for biomass fed processes are much higher than for natural gas fed power plants (Figure 4.7), especially because of the higher investment costs related to the gasifier purchase. However, when a CO_2 tax is introduced, CO_2 capture in biomass based electricity generation processes becomes competitive since the captured CO_2 is biogenic which leads to a net gain from the tax as discussed more in detail in Chapter 8.

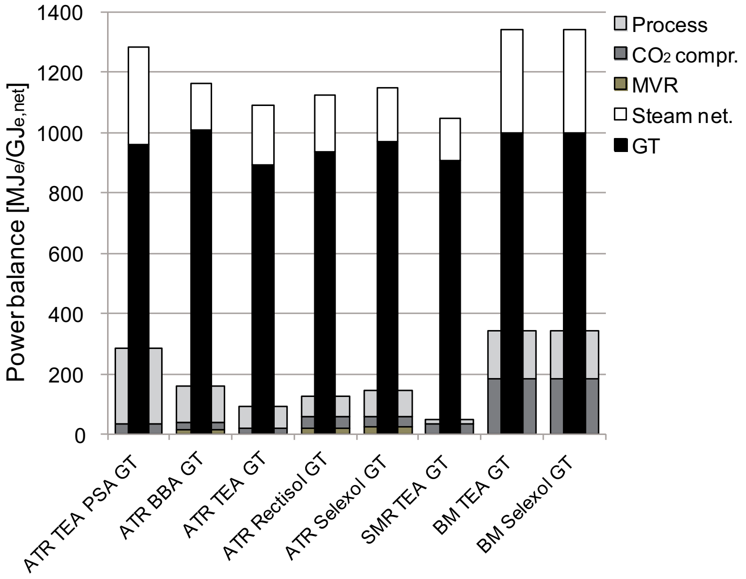

Figure 4.6: Power balance for the different electricity generating configurations with pre-combustion CO_2 capture, reported in Table 4.2.

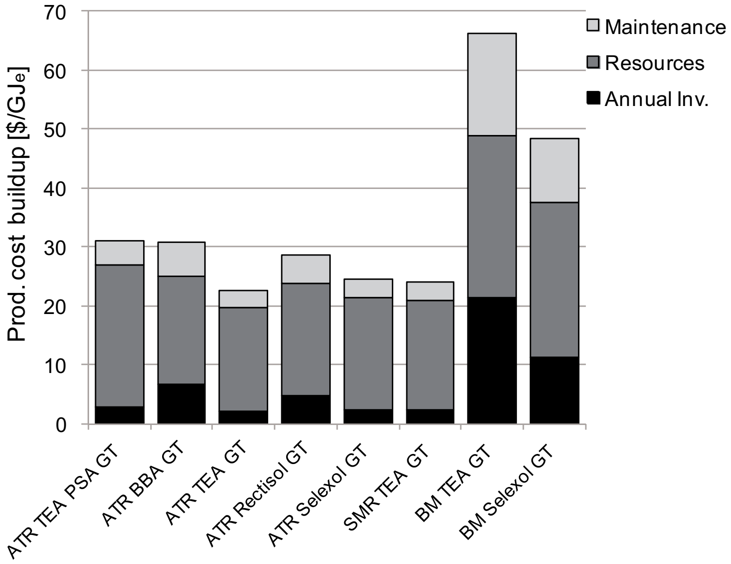

Figure 4.7: Production cost buildup for the different electricity generating configurations with pre-combustion CO_2 capture, reported in Table 4.2.

4.4.2 Influence of reforming technology

For the electricity generation from natural gas two different options can be considered to generate the syngas intermediate in the pre-combustion concepts, either SMR or ATR. The energy demand difference between both process configurations is illustrated in Figure 4.8 for 90% of CO_2 capture by chemical absorption with TEA (ATR TEA GT and SMR TEA GT). The endothermic steam methane reforming requires heat at high temperature which has to be satisfied by combustion. The electricity consumption of the SMR process is nearly half the one of the ATR process requiring air compression (Figure 4.6). These differences in the energy demand lead to a 6% lower net electricity production and a 3%-points lower efficiency for the SMR power plant with pre-combustion CO_2 capture (Table 4.2). Both process options yield comparable electricity production costs, since the resource purchase contributes to nearly 80% of the costs and the specific annual investment is comparable (Figure 4.7).

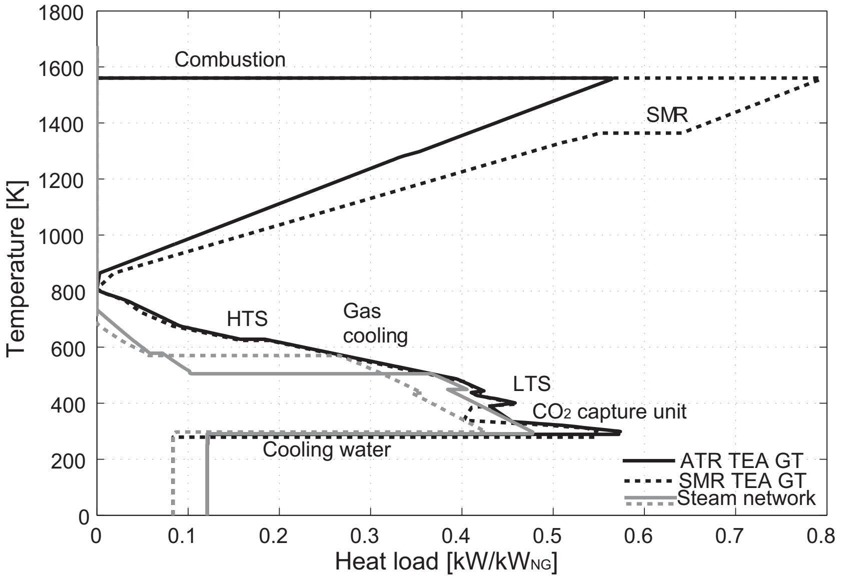

Figure 4.8: Integrated composite curves comparison for electricity generation from natural gas by SMR and ATR with 90% of CO_2 capture by chemical absorption with TEA (Table 4.2).

4.4.3 Influence of hydrogen purity

The Pareto frontiers in Figure 4.5 clearly show the performance difference between pre-combustion CO_2 capture processes burning pure hydrogen after PSA purification (>96%mol) and processes burning the H_2-rich fuel (65% mol) directly in a gas turbine after CO_2 removal. The detailed comparison between two natural gas based electricity generating process options burning pure H_2 after PSA (ATR TEA PSA GT) or burning the H_2-rich fuel after chemical absorption with TEA capturing 90% of the CO_2 (ATR TEA GT) allows to explain this difference. The energy integration result, reported in Figure 4.9, shows that more excess heat is available when H_2 purification is included which leads to a 15% higher electricity generation in the steam turbine. H_2 purification by PSA requires however a large amount of electricity for the compression which leads to an increase of the process power consumption around 50% (Figure 4.6). Since the increase in the electricity generation by high quality fuel combustion does not compensate the electricity consumption for purification, the energy efficiency is reduced by 15.5%-points. The lower electricity output leads to an increase of the electricity production costs around 25% (Figure 4.7). For the subsequent analyses it is hence focussed on pre-combustion power plants generating electricity by burning the H_2-rich fuel after CO_2 removal without an additional H_2 purification step.

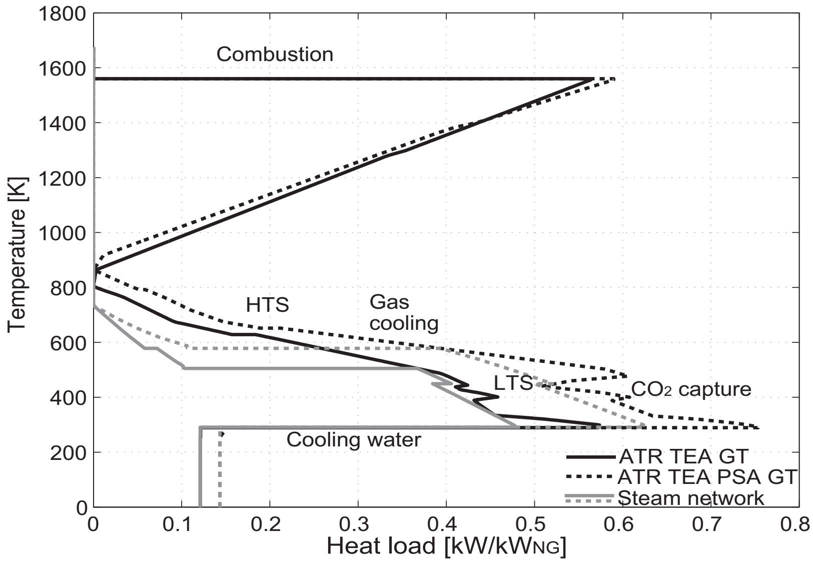

Figure 4.9: Integrated composite curves comparison for electricity generation from natural with 90% of CO_2 capture by chemical absorption with TEA with and without H_2 purification by PSA (Table 4.2).

4.4.4 Influence of CO_2 capture technology

The comparison of the different CO_2 capture technologies that can be applied for pre-combustion power plants concepts yield similar conclusions as for the H_2 production processes. Taken as whole, the different technologies are competitive with regard to energetic, economic or environmental criteria, as reported in Table 4.2. Physical absorption allows to cogenerate more electricity, however the larger power consumption balances this effect and leads to comparable electrical production efficiencies. Physical absorption with Selexol and Rectisol are both competitive in terms of energy efficiency. The economic performance is highly dependent on the resource purchase price. The specific capital investment of the different options is in the same order of magnitude. Since the investment costs estimation takes into account the operating conditions, differences may occur for similar installations such as Selexol and Rectisol. All in all the differences are not significant with regard to the investment costs estimation error in the order of 30% according to Turton (2009). The competitiveness of these pre-combustion CO_2 capture concepts with regard to post-combustion CO_2 capture in power plants depends mainly on the economic scenario as reported in detail in Chapter 8.

4.5 Conclusions

By applying the developed multi-objective optimisation strategy, the competitiveness of different H_2 production process and power plant configurations with pre-combustion CO_2 capture are compared with regard to thermodynamic, economic and environmental criteria. It is highlighted how the production purpose (i.e. H_2 or electricity) and the technology choices affect the performance. Due to the lower energy demand for solvent regeneration, physical absorption processes yield slightly lower efficiency losses for CO_2 capture, however the overall performance is comparable. With 90% of CO_2 capture, efficiencies around 52% are assessed for pre-combustion CO_2 capture processes using natural gas as a feedstock to generate electricity and around 80% for processes generating pure H_2, with production costs in the order of 25\$/GJ$_e$ and $15\$/GJ_{H2}$ respectively. For biomass fed processes with around 60% of CO_2 capture the efficiency and the costs assessed for power and H_2 production plants are 36% and 47\$/GJ$_e$, respectively 60% and $29\$/GJ_{H2}$. The environmental benefit of capturing biogenic CO_2 is assessed in detail by performing a life cycle impact assessment in Chapter 8. Moreover, the competitiveness of these pre-combustion CO_2 capture processes will be compared to post-combustion CO_2 capture processes for electricity generation in Chapter 8 and the influence of the resource price and the CO_2 tax will be evaluated.

5 Thermo-economic analysis of post-combustion CO_2 capture processes

After having studied pre-combustion CO_2 capture processes, post-combustion CO_2 capture options are evaluated here with the aim of making a consistent performance comparison in Chapter 8. Post-combustion CO_2 capture in natural gas combined cycle (NGCC) power plants has been investigated in the frame of the project "Technologies for gas turbine power generation with CO_2 mitigation" funded by Swisselectric research. The outcomes of this project have been published in Tock and Maréchal (2012e) and Griffin and Mantzaras (2012).

5.1 Introduction

With regard to climate change mitigation, post-combustion CO_2 capture is frequently mentioned because it can be applied to retrofit or new plant applications. However, one of the main issues of implementing post-combustion CO_2 capture in natural gas combined power plants is the efficiency decrease and the costs increase by the capture of low partial pressure CO_2. To overcome this, one proposed solution is to introduce flue gas recirculation (FGR) that increases the CO_2 concentration in the flue gas and reduces the volume of the flue gas to be treated in the CO_2 capture plant. Consequently, the efficiency and economics of CO_2 mitigation in gas turbine combined cycle power plants could be improved. This process including the gas turbine itself, the hydrogen production, the steam network and the CO_2 capture unit is studied and optimised here by applying the developed systematic thermo-environomic modelling and optimisation approach without including fluid simulation of the turbomachinery. Different process configurations are investigated in order to study the impact of FGR on the compressors, turbines, combustion, CO_2 capture and the steam network. Single stage and reheat combustion processes without and with CO_2 capture are evaluated to define with regard to the thermodynamic efficiency and the economic performance the best options for an integrated electricity generating process with efficient CO_2 capture and low CO_2 avoidance costs. The impact of H_2 injection to stabilise the combustion has been studied by considering the integration of syngas production. The results of the combustion studies from Fachhochschule Nordwestschweiz (FHNW) are integrated to define the amount of H_2 required in the burner for flame stability purposes.

5.2 Post-combustion CO_2 capture process description

Post-combustion CO_2 capture in power plants is studied by focusing on a natural gas combined cycle with flue gas recirculation and CO_2 capture (i.e. chemical absorption), illustrated in Figure 5.1 for a reheat combustion process and in Appendix Figure B.6 for the single stage combustion gas turbine.

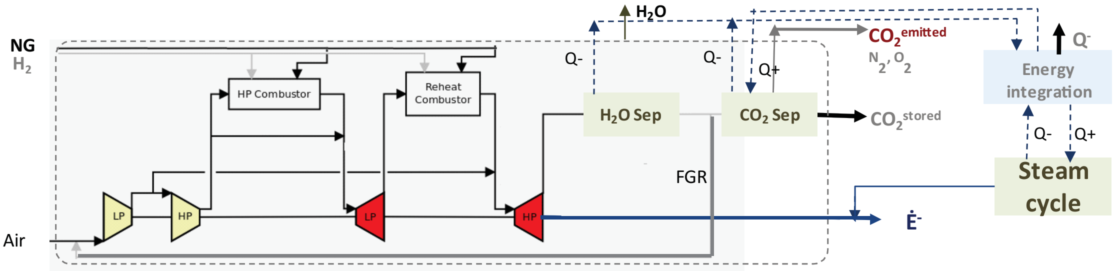

Figure 5.1: Process model of post-combustion CO_2 capture in an NGCC power plant with FGR.

5.3 Post-combustion CO_2 capture process modelling

The process models of the different process steps, being the gas turbine, the CO_2 capture and compression, and the steam network, are developed with different flowsheeting software. The connection between the different models is done by the material streams characteristics, namely composition, massflow, temperature and pressure as detailed in Figure 1.1. This application highlights again the usefulness of the special feature of the thermo-environomic modelling and optimisation framework which allows to set-up a process model by using parts developed with different flowsheeting software.

5.3.1 Power plant model

To study the combustion issues a modern, highly efficient, and low NOx emitting machine (similar to the Alstom GT26 (Alstom)) has been considered to develop a generic reheat gas turbine model with sequential combustion. For comparison purpose a generic single stage combustion gas turbine model has also been developed. The gas turbine models are developed with the *Belsim Vali* (Belsim S.A.) software and illustrated in Appendix Figures B.5&B.6. The details of the gas turbine modelling and the operating parameters are reported in Appendix B (Tables B.1-B.4). The main modelling assumption defining the plant capacity is that the volumetric flowrate at the compressor inlet is constant ($\dot{V}$=400m^3/s) to maintain the velocity triangle in the compressor. The turbine inlet temperature is limited by the capacity of the blade cooling system and controlled by the air excess in the combustor. The temperature is set to 1100^oC for the first turbine (LP) and to 1300^oC for the second one (HP). To model the recirculation, the recirculation itself, a heat recovery steam generator and the H_2 injection have been included. The flue gas recirculation (FGR) ratio is defined as the molar ratio of dry gas recycled to the total molar dry flow (after H_2O condensation). To address the flame stability concerns at high FGR, syngas can be injected. The syngas production is modelled by a high temperature oxygen separation membrane autothermal reforming reactor based on the same principles as in Section 3.3.1 (Appendix Figure B.7). The amount of H_2 to be added to the fuel is calculated based on measurements from FHNW that determined the amount of H_2 that is required as a function of the excess O_2 left after the combustion reported in Figure 5.2.

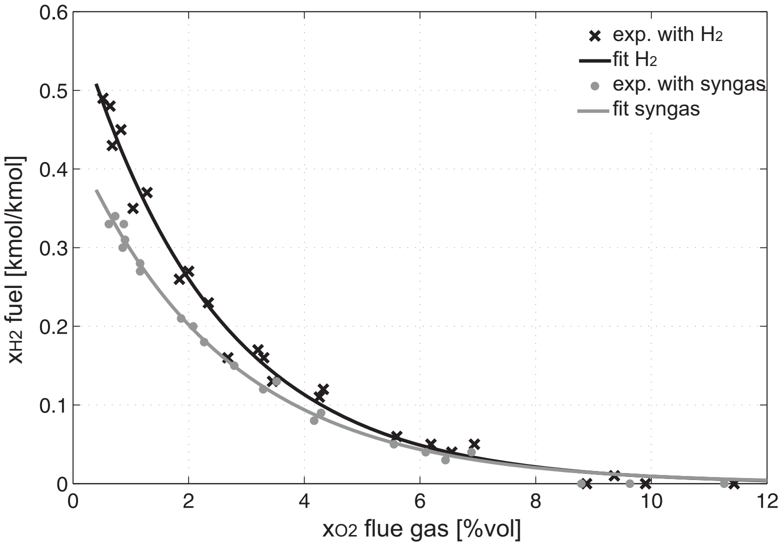

Figure 5.2: Fit of the FHNW data: amount of H_2 to be added for flame stability (Griffin and Mantzaras (2012)).

The results for pure H_2 and syngas injection have been fitted by Eqs.5.1 & 5.2, respectively.

$$x_{H2}(x_{O2}) = 0.6009 \cdot e^{(-0.4177 \cdot x_{O2})} \tag{5.1}$$

$$x_{H2}(x_{O2}) = 0.4356 \cdot e^{(-0.3839 \cdot x_{O2})} \tag{5.2}$$

where x_{O2} is the volume fraction of O_2 in the flue gas and x_{H2} the amount of H_2 required [kmol/kmol]. For the syngas case, this is the amount of H_2 after mixing of the syngas and the natural gas. The flowsheets of the gas turbine and the syngas production model are presented in Appendix Figures B.5-B.7. The main decision variables are given in Table 5.1.

Table 5.1: Decision variables and feasible range for optimisation for the NGCC plant.

Operating parameter	Range
FGR [-]	[0-0.56]
ATR temperature [K]	[1050-1300]
S/C [-]	[1.5-4]

5.3.2 CO_2 capture model

For separating the CO_2 generated in the combustion from the N_2 and excess O_2 contained in the exhaust gas, chemical absorption with monoethanolamine (MEA) is considered. The process model developed in *Aspen Plus* (AspenTech) is described in detail in Section 2.3.1. The captured CO_2 is compressed to 110 bar by a two stage compressor with intercooling modelled in *Belsim Vali* (Belsim S.A.).

5.3.3 Steam network model

The optimal steam network integration is defined in the energy integration model as explained in Girardin et al. (2009). Different headers are defined by the pressure, temperature, steam quality and the type being either production header (i.e. steam injection), usage header (i.e. steam distribution) or condensation header (i.e. steam is condensed and sent back to the HRSG). The steam network characteristics are detailed in Table 5.2 for both gas turbine configurations.

Table 5.2: Steam network characteristics for the NGCC plant (Li (2006)).

Steam cycle	GT simple		GT sequential	
	P [bar]	T [C]	P [bar]	T [C]
HP level	40	500.6	132	581.5
IP level			28.4	581.5
LP level	8	464.8	3	229.5
Condensation	0.06		0.05	

5.4 Performance evaluation of post-combustion CO_2 capture processes

The energy and economic costs of capturing CO_2 and the impact of CO_2 recirculation on the compressors, turbines, combustion, CO_2 capture and the steam network is assessed. The performance is expressed by the energy efficiency ϵ_{tot} (Eq.1.22), the electricity production costs COE, the CO_2 capture rate η_{CO2} and the CO_2 avoidance costs (Eq.1.26). The modelled gas turbine configuration with reheat combustion without FGR and without CO_2 capture is considered as a reference plant in the CO_2 avoidance costs assessment in order to compare performances calculated on a common basis. For the economic estimations a yearly operation of 8000h/y is considered together with the assumptions in Table 1.2. The plant capacity is defined by the volumetric flowrate at the compressor inlet. Assuming a flowrate of 400 m^3/s (Appendix Table B.2), this corresponds to a natural gas feed in the order of 560-580$MW_{th,NG}$. With regard to the gas turbine configuration, it is focused on the one with reheat combustion because it yields an around 7%-points higher efficiency and 10% lower electricity production costs then the single stage combustion gas turbine, as reported by the performance results in Table 5.3. The impact of post-combustion CO_2 capture and FGR is studied in detail hereafter for the gas turbine configuration with reheat combustion (Table 5.4).

Table 5.3: Performance of the different natural gas combined cycle configurations without FGR and without CO_2 capture (natural gas price 9.7\$/GJ_{NG}, operation 8000h/y)

	GT simp.	GT seq.
Feed [$MW_{th,NG}$]	481.4	563.2
	Power Balance	
Net Power [MW_e]	247	332
$\dot{E}^{-}_{SteamNetwork}$ [$MJ_e/GJ_{e,net}$]	312.3	340.2
$\dot{E}^{-}_{GasTurbine}$ [$MJ_e/GJ_{e,net}$]	687.7	659.8
	Performance (Assumptions Table 1.2)	
ϵ_{tot} [%]	51.3	58.9
ϵ_{ex} [%]	48.8	55.9
CO_2 emissions [kg_{CO2}/GJ_e]	123	105
Investment [\$/MW_e]	486	555
COE [\$/GJ_e]	21.1	19.02

5.4.1 CO_2 capture impact

The energy and cost penalty of the post-combustion CO_2 capture on the natural gas fuelled power plant performance is reported in Table 5.4. The comparison of the composite curves of the natural gas fuelled power plant without and with 85% CO_2 capture (no FGR) in Figure 5.3 clearly reveals the difference in the energy integration. The thermal energy demand for the solvent regeneration in the chemical absorption process leads to a reduction of the power cogeneration in the steam network of about 19$MJ_e/GJ_{e,net}$. The electricity consumption is increased due to the mechanical power requirement of the CO_2 capture unit (i.e. solvent pumping, blower) and of the CO_2 compressor. Consequently, the net electricity output with CO_2 capture is reduced by over 15%. This leads to a decrease of the overall energy efficiency from 58.8 to 49.9% without FGR. CO_2 compression to 110 bar accounts for 1.3%-points to the overall energy penalty of about 9%-points.

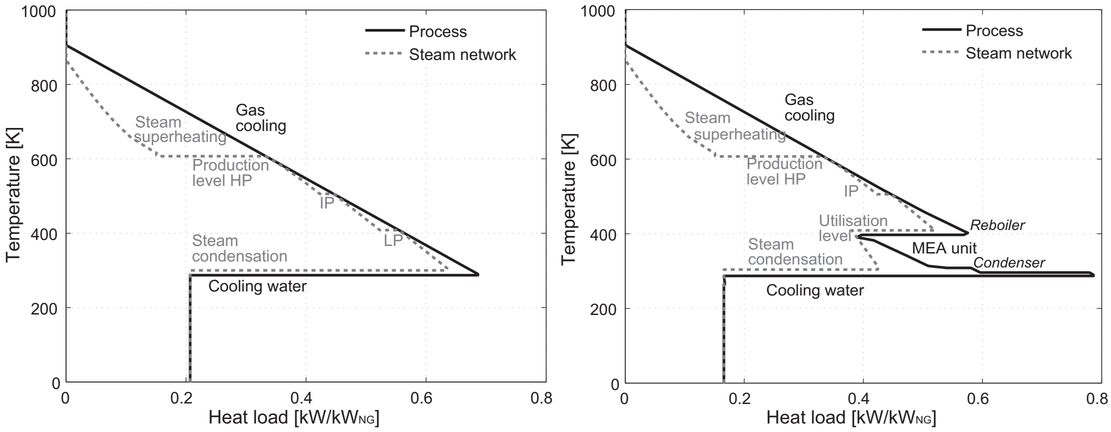

Figure 5.3: Integrated composite curve with steam network integration for the NGCC plant (no FGR) without (left) and with post-combustion CO_2 capture by chemical absorption (right).

The reduced productivity leads together with the additional investment costs for the CO_2 capture and compression equipment to around 25% higher electricity production costs as detailed in Figures 5.4&5.5. The reduction of the CO_2 emissions to $17.7\text{kg}_{CO2}/\text{GJ}_e$ (without FGR) leads to CO_2 avoidance costs around $55.8\$/\text{t}_{CO2,avoided}$. The dependence of the process competitiveness on the natural gas purchase price, which contributes to up to 80% of the COE (Figure 5.5), is investigated in detail in Chapter 8.

Table 5.4: Performance of the NGCC configurations without and with FGR and post-combustion CO_2 capture (natural gas price $9.7\$/\text{GJ}_{NG}$, operation 8000h/y).

	no CO_2 capture		85% CO_2 capture		Relative Impact	
FGR [%]	0	50	0	50	0	50
Feed [$\text{MW}_{th,NG}$]	563.2	592.2	563.2	592.2		
			Power Balance			
Net Power [MW_e]	331.6	343.8	280.9	296.3	-15.3%	-13.8%
$\dot{E}^+_{CO2,capture}$ [$\text{MJ}_e/\text{GJ}_{e,net}$]	0	0	64.2	48.3		
$\dot{E}^+_{CO2,compression}$ [$\text{MJ}_e/\text{GJ}_{e,net}$]	0	0	35.8	35.1		
$\dot{E}^+_{POX}$ [$\text{MJ}_e/\text{GJ}_{e,net}$]	0	13.8	0	16.1		
$\dot{E}^-_{SteamNetwork}$ [$\text{MJ}_e/\text{GJ}_{e,net}$]	340.2	358.8	321.3	339.4	-5.5%	-5.4%
$\dot{E}^-_{GasTurbine}$ [$\text{MJ}_e/\text{GJ}_{e,net}$]	659.8	655	778.7	760.1	+ 15.3%	+13.8%
			Performance (Assumptions Table 1.2)			
ϵ_{tot} [%]	58.88	58.07	49.89	50.04	-15.3%	-13.8%
$CO_{2,emitted}$ [kg/GJ_e]	105	99.7	17.7	13	-83.1%	-86.9%
Investment [$\$/\text{kW}_e$]	555	581	935	887	+68.5%	+52.7%
COE [$\$/\text{GJ}_e$]	19.02	19.37	23.9	23.6	+ 25.6%	+21.8%
Avoidance costs $\$/\text{t}_{CO2,avoided}$	-	-	55.8	48.7		

5.4.2 Flue gas recirculation impact

Sensitivity analyses have revealed that FGR does not considerably impact the process efficiency but improves the economics of CO_2 capture by increasing the CO_2 concentration in the flue gas illustrated in Figure 5.6 (left) and reducing therefore the CO_2 capture costs as reported in Table 5.4 and Figure 5.4.

The overall electricity production costs are however not significantly reduced with FGR since the natural gas purchase contributes to nearly 80% of the costs and the annual investment only to 10% as shown in Figure 5.5. The process efficiency is not affected considerably, since the higher natural gas consumption required for H_2 production to ensure combustion stability balances the slightly higher power output. Due to the emissions from the natural gas combustion satisfying the energy demands, the CO_2 capture rate decreases at very high FGR and the specific CO_2 emissions increase as reported in Figure 5.6 (left). This leads with regard to the CO_2 avoidance costs to an optimum FGR around 45%, illustrated in Figure 5.6 (right).

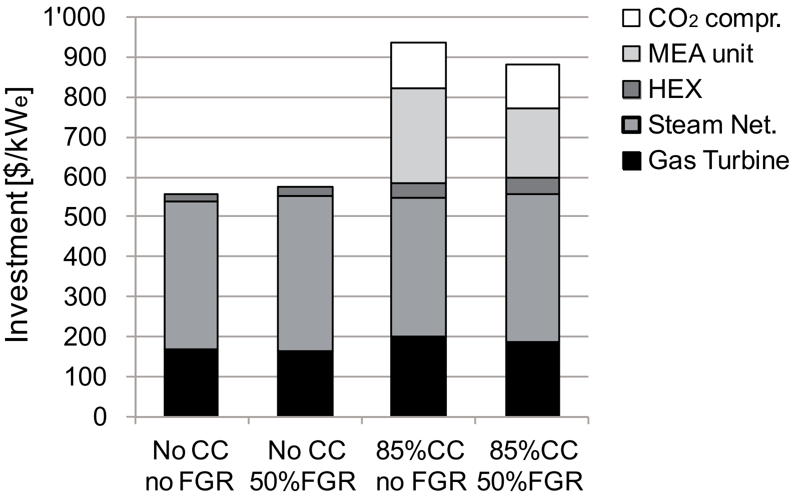

Figure 5.4: Specific investment costs buildup for the different NGCC configurations without and with FGR and post-combustion CO_2 capture reported in Table 5.4.

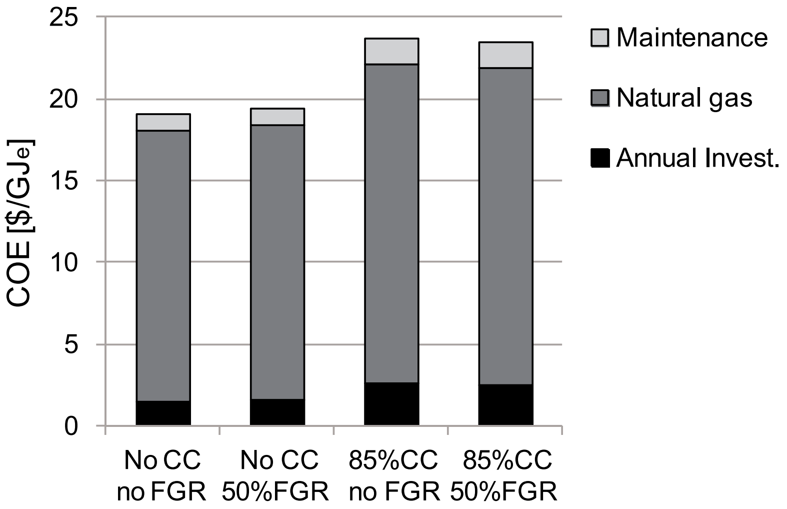

Figure 5.5: Production cost buildup for the different NGCC configurations without and with FGR and post-combustion CO_2 capture reported in Table 5.4.

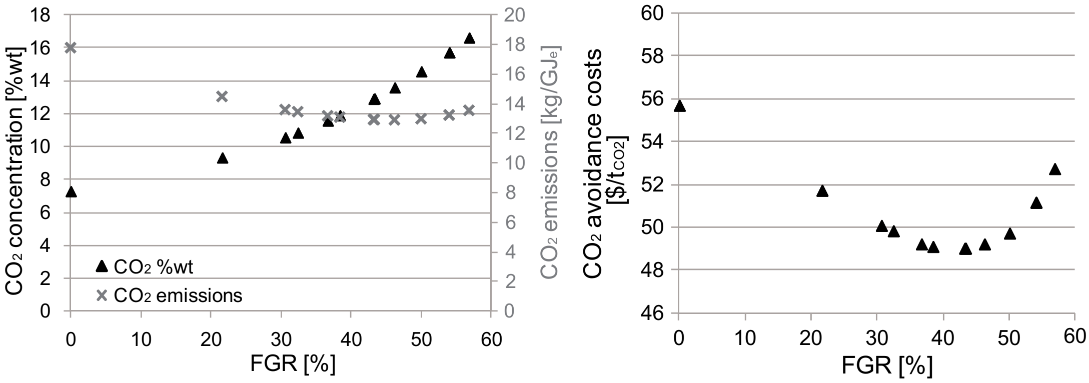

Figure 5.6: Influence of the FGR on the flue gas CO_2 concentration and the specific CO_2 emissions (left) and on the CO_2 avoidance costs (right) for the NGCC plant with 85% post-combustion CO_2 capture.

5.4.3 Multi-objective optimisation of post-combustion CO_2 capture processes

A multi-objective optimisation is performed in order to study the influence of the FGR together with the design of the CO_2 capture unit. Therefore, the electricity production costs COE are minimised and the CO_2 capture rate η_{CO2} is maximised with regard to the decision variables in Tables 5.1 and 2.2. The results represented by the optimal Pareto curve in Figure 5.7 reveal the trade-off between the CO_2 capture rate and the COE. This is explained by the reduced electricity output due to the energy demand for solvent regeneration and CO_2 compression, and the increased capital costs for the capture equipment. For an increase of the CO_2 capture rate, the specific CO_2 emissions decrease and reach a minimum at around 85% of CO_2 capture. This translates to an optimum in the CO_2 avoidance costs as already noted by sensitivity analysis. This can be explained by the fact that the FGR is a decision variable and that at high FGR more syngas has to be produced leading to higher emissions. In the optimisation high FGR are favoured. CO_2 capture in a process configuration with 50% FGR reduces the efficiency by around 8%-points and increases the electricity production costs up to 20% compared to a conventional NGCC plant. This leads to CO_2 avoidance costs in the range of $48\$/t_{CO2,avoided}$ with a natural gas price of $9.7\$/GJ_{NG}$.

A detailed analysis of the electricity production costs shows that nearly 80% of the costs are due to the purchase of natural gas. Consequently, the resource price evolution has a big influence on the process competitiveness. Sensitivity analysis on the natural gas price highlights the impact on the electricity production costs and on the CO_2 avoidance costs. To reach the target of $25\$/t_{CO2,avoided}$ ($20€/t_{CO2,avoided}$) set by the GTCO2 project (Griffin and Mantzaras (2012)) without a decrease of the investment costs, a natural gas price as low as $2.7\$/GJ_{NG}$ would be theoretically required which would lead to a decrease of the production of 2/3. However, the lowest realistic natural gas price that can be assumed according to the ZEP study (ZEP (2011)) is around $5.5\$/GJ_{NG}$. Assuming a natural gas price of $5.5\$/GJ_{NG}$, the target could also be reached by a decrease of the capital investment around 40%, respectively a 20%

investment decrease and gas price of $4\$/\mathrm{GJ}_{NG}$. The introduction of a carbon tax will also improve the competitiveness of post-combustion CO_2 capture processes. These economic aspects are discussed in detail in Chapter 8.

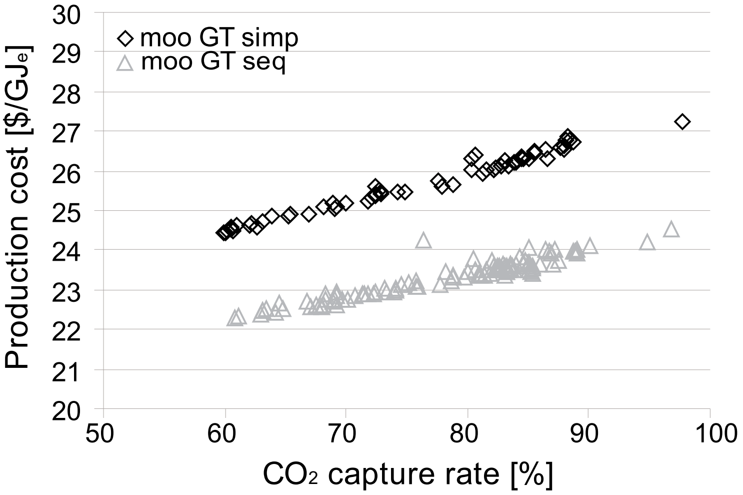

Figure 5.7: Pareto optimal frontiers for different NGCC configurations with post-combustion CO_2 capture.

5.4.4 Energy integration improvement: District heating

The detailed analysis of the composite curve of the NGCC plant with CO_2 capture in Figure 5.3 (right) reveals that part of the excess heat could not be valorised by the steam network. These heat losses at around 80^oC, removed by cooling water, have the right temperature to feed a district heating network and could consequently be valorised. Considering a district heating (DH) network with a supply temperature of 80^oC and a return temperature of 50^oC, Figure 5.8 illustrates the potential reduction of the energy losses. For this case, 46MW could be recovered for district heating. This allows to substitute the equivalent amount of natural gas, when one considers that a conventional boiler produces the same amount of heat from natural gas with an efficiency of $\eta_{boiler} = 85\%$. Taking into account this in the overall efficiency definition, expressed by Eq. 5.3, the district heating contribution would lead to an efficiency increase of 6%-points as reported in Table 5.5.

$$\begin{aligned}\epsilon_{tot,DH} &= \frac{\Delta \dot{E}^-}{\Delta h^0_{NG,in}\cdot \dot{m}_{NG,in} - \Delta h^0_{NG,subs}\cdot \dot{m}_{NG,subs}} \\ &= \frac{\Delta \dot{E}^-}{\Delta h^0_{feed,in}\cdot \dot{m}_{feed,in} - \frac{1}{\eta_{boiler}}\cdot \dot{Q}^-_{DH}} \end{aligned} \tag{5.3}$$

Considering that this heat could be sold at 120\$/MWh, the electricity production costs could be reduced by around 23%. For a yearly operation of 5000h/y the COE is increased by 7%. Around 81Mt_{CO2}/y could be avoided through the substitution of the emissions from conventional district heating. For CO_2 capture options, there is consequently a potential to recover excess heat for district heating. This analysis shows how the energy integration analysis allows to identify potential process improvements and optimal integrated process designs.

Table 5.5: Performance of the NGCC plant with 90% CO_2 capture with MEA without and with district heating DH (natural gas price 9.7\$/GJ_{NG}, operation 7500h/y).

	no CC	90% capture no DH	90% capture DH
$\dot{Q}_{DH}$ [MW]	0	0	46.5
Net Electricity [MW_e]	332	296	296
$\epsilon_{tot,DH}$ [%]	58.7	49.6	55.5
$CO_{2,emitted}$ [kg/GJ_e]	105.1	14.9	14.9 (10.3$kg_{CO2,substituted}$/GJ_e)
COE [\$/GJ_e]	18.8	23.7	18.4

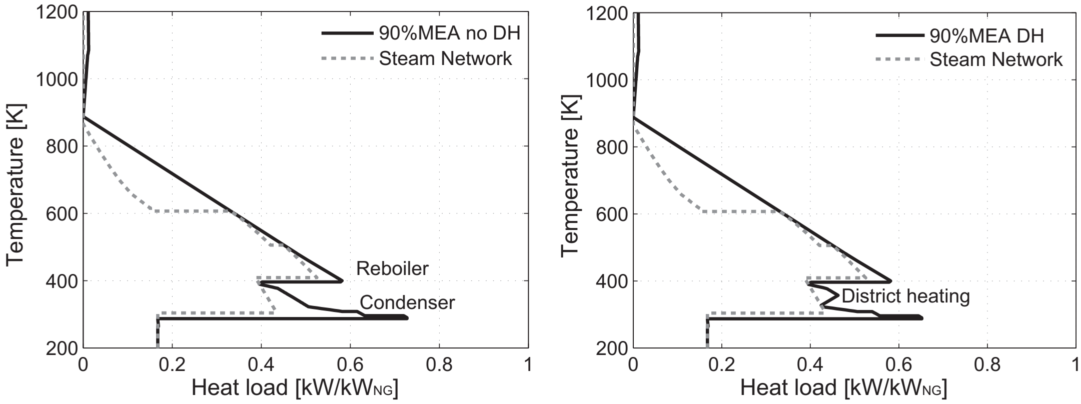

Figure 5.8: Integrated composite curves with steam network integration for the NGCC plant with 90% of post-combustion CO_2 capture without (left) and with district heating (right).

5.5 Conclusions

The systematic comparison and multi-objective optimisation of different NGCC process configurations with post-combustion CO_2 capture have shown that FGR does not impact considerably the process efficiency but improves the economics of CO_2 capture in gas turbine combined cycle power plants by increasing the CO_2 concentration in the flue gas and reducing the CO_2 capture cost and consequently the electricity production costs. Post-combustion CO_2 capture reduces the efficiency up to 9%-points and increases the production costs by around 25%. With 50% FGR, the CO_2 avoidance costs are decreased by more than 10% to around 47\$/$t_{CO2,avoided}$ considering a natural gas price of 9.7\$/GJ_{NG}. The competitiveness of these processes reveals to depend on the resource price and on the introduction of a carbon tax, which is assessed in detail in Chapter 8.

6 Thermo-economic comparison of post-combustion CO_2 capture by amines and chilled ammonia

The large energy penalty of post-combustion CO_2 capture by chemical absorption with amines has been revealed in Chapter 5. As a promising alternative having a lower regeneration energy demand, the chilled ammonia process (CAP) developed by Alstom is studied here in more detail. In addition, it is highlighted how process improvements reducing the exergy losses can be identified by the detailed analysis of the composite curves.

6.1 Introduction

The chilled ammonia process is proclaimed to be a high-potential technology for CO_2 capture. The core process operations are the low temperature (0-10^oC) absorption of CO_2 with an aqueous ammonia solution and the subsequent regeneration at higher temperature (Section 2.2.2). The main advantages are energy-efficient capture of CO_2, high purity CO_2, no degradation and low-cost globally available reagent (Alstom (2012)). Even if the chilled ammonia process benefits from a lower regeneration energy demand and from a higher pressure CO_2 product compared to amine processes, the process may become uncompetitive because of the large refrigeration loads required for the cooling down to the absorption temperature. According to Darde et al. (2010) a heat requirement lower than 2 GJ/t_{CO2} can be reached for the desorption at 90-110^oC for specific rich-CO_2 loadings and ammonia concentrations. Jilvero et al. (2011) report a reboiler duty in the range of 2.2-2.8 GJ/t_{CO2}, which leads to an efficiency decrease in the power plant between 8-10%-points depending on the available cooling water temperature. They conclude that the chilled ammonia process is beneficial in processes where low grade heat is already available. Only a few studies evaluate the efficiency of the total power plant system, most focus on the chilled ammonia process itself. In these studies, conclusions are drawn principally based on thermodynamic analysis and no detailed energy integration and economic evaluations are performed. By applying the developed systematic methodology, the objective of this study is to compare the performance of the post-combustion CO_2 capture by chilled ammonia and amines, and to assess the trade-offs between CO_2 capture, energy efficiency and economic penalty.

To compare the performance of the chemical absorption with MEA, studied in Section 5.4, with the chilled ammonia process for post-combustion CO_2 capture in an NGCC plant, the NGCC plant model previously described in Sections 5.3.1 (Figure 5.1) is combined with the chilled ammonia model that has been described in detail in Section 2.3. Typical operating conditions and design parameters of the chilled ammonia process illustrated in Appendix Figure B.2 are reported in Table 2.4. First a detailed comparison is made for a selected base case scenario with 50% FGR and 85% CO_2 capture and then a multi-objective optimisation is performed. The performance calculations are made for a plant capacity in the order of 580-590$MW_{th,NG}$ of natural gas (i.e. fixed volumetric flowrate at the compressor inlet (Table B.2)) and for the economic assumptions given in Table 1.2. The results presented in Section 5.4 have been updated for a yearly operation of 7500h/y.

6.2 Post-combustion CO_2 capture process performance comparison: Amines versus chilled ammonia

The performance results of the different NGCC power plants configurations without and with post-combustion CO_2 capture by MEA or ammonia, capturing 85% of the emissions, are summarised in Table 6.1 and discussed in the following sections. The key process design parameters are based on literature data and are reported in Appendix Table D.5.

Table 6.1: Performance of NGCC power plants configurations without CO_2 capture and with 85% post-combustion CO_2 capture with MEA and chilled ammonia. The corresponding operating conditions are reported in Appendix Table D.5.

System	NGCC	Post-comb. MEA	Post-comb. CAP
Feed [$MW_{th,NG}$]	588.7	585.6	586.4
η_{CO2} [%]	0	84.5	85.4
	Power Balance		
Net power [MW_e]	328	294	293
$\dot{E}^+_{Consumption}$ [$MJ_e/GJ_{e,net}$]	-	97	124
$\dot{E}^-_{SteamNetwork}$ [$MJ_e/GJ_{e,net}$]	340	339	365
$\dot{E}^-_{GasTurbine}$ [$MJ_e/GJ_{e,net}$]	660	758	759
	Performance (Assumptions Table 1.2)		
ϵ_{tot} [%]	58.7	50.2	50.02
CO_2 emissions [kg_{CO2}/GJ_e]	105	15	14
Investment [$/$kW_e$]	555	1028	1210
COE [$/$GJ_e$]	18.3	23.8	24.6
Avoidance costs [$/$t_{CO2,avoided}$]	-	61	69

6.2.1 Energy integration

The difference in the energy demand of both processes can be clearly seen by the energy integration, illustrated by the composite curves in Figure 6.1. The shift in the reboiler duty and hence in the steam consumption from the steam network is depicted by the length of the plateau around 400 K. For the chilled ammonia process, the integration of the refrigeration cycle, cooling the solvent down to the absorber temperature of 5^oC, is detailed in Figure 6.2.

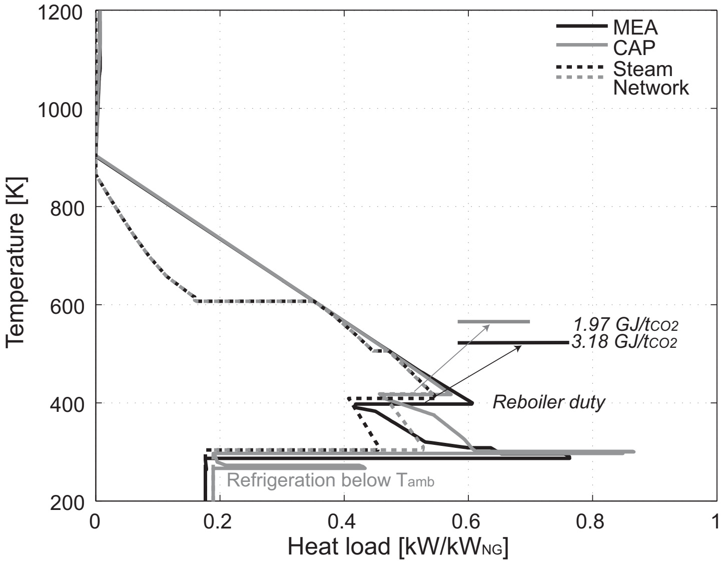

Figure 6.1: Composite curves with steam network integration for the NGCC plant with 85% of post-combustion CO_2 capture with MEA and CAP.

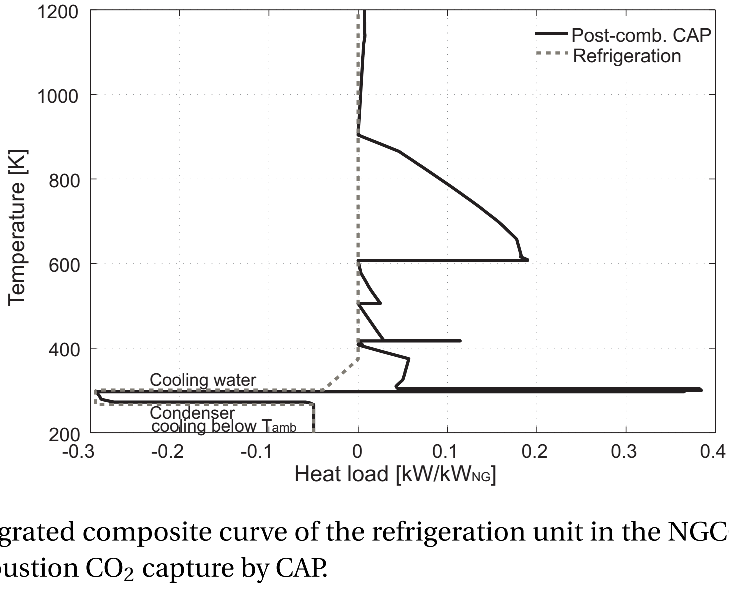

Figure 6.2: Integrated composite curve of the refrigeration unit in the NGCC configuration with post-combustion CO_2 capture by CAP.

The difference in the mechanical energy demands is reflected by the power balance reported in Figure 6.3. In the chilled ammonia process the steam network generates about $26MJ_e/GJ_{e,net}$

of electricity more, due to the lower steam consumption in the reboiler for the solvent regeneration. For the CO_2 compression to 110 bar, the power consumption is about 70% lower for the CAP process, since the reboiler operates already at 25 bar. However, the power consumption for the CO_2 capture is over 50% higher for the CAP process due to the electricity consumption in the refrigeration cycle, which translates into a $26 MJ_e/GJ_{e,net}$ higher overall electricity consumption. To assess the trade-off between the reboiler duty and the refrigeration duty, the energy demands are expressed in terms of exergy in Table 6.2 considering an ambient temperature of 20^oC.

Table 6.2: Specific exergy demands, expressed in GJ/t_{CO2}, of the CO_2 capture with MEA and chilled ammonia for the configurations reported in Table 6.1.

System	Post-comb. MEA	Post-comb. CAP
Reboiler duty [GJ/t_{CO2}]	0.823	0.579
Refrigeration duty [GJ/t_{CO2}]	0	0.408
CO_2 compression [GJ/t_{CO2}]	0.345	0.085

The net electricity generation and the efficiency are comparable for both processes, since the benefits from the reboiler duty and the CO_2 compression are balanced by the refrigeration penalty of the CAP process. There is hence a trade-off between the steam consumption for the solvent regeneration and the electricity consumption for the refrigeration to 5^oC in the present scenario. It is considered that cooling water is available at 20^oC. When the plant is operated in an Northern country, cooling water at 5^oC could be available (Jilvero et al. (2011)) and consequently the refrigeration penalty would be less important and the process competitiveness would be increased.

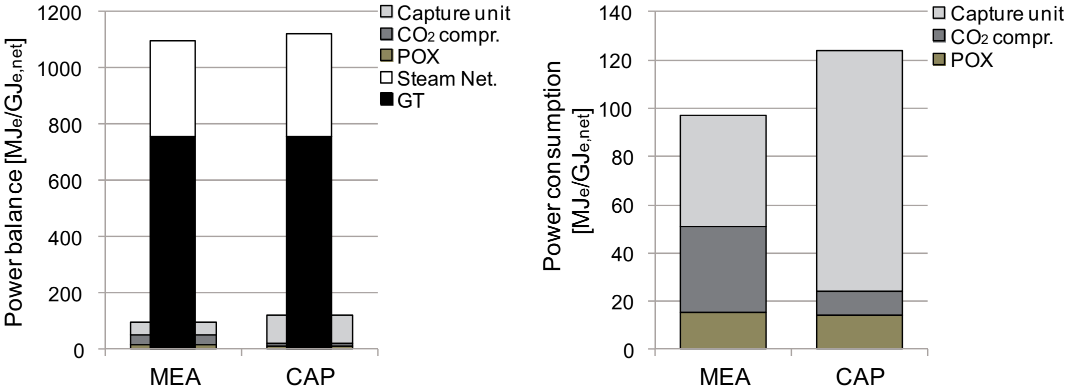

Figure 6.3: Comparison of the power balance for the NGCC plant with 85% post-combustion CO_2 capture by MEA and CAP (Table 6.1) (left). Zoom on the power consumption (right).

6.2.2 Economic performance

The economic performance of both processes is compared in Figure 6.4. The capital investment for the CAP process is about 18% higher due to the investment for the refrigeration unit (Figures 6.4 (left)). This translates into an electricity production costs increase of only 3%, since the resource purchase contributes to over 80% to the COE and the specific annual investment less than 10%, as detailed in Figure 6.4 (right). Consequently, these two post-combustion CO_2 capture process options yield similar performances and both technologies are competitive.

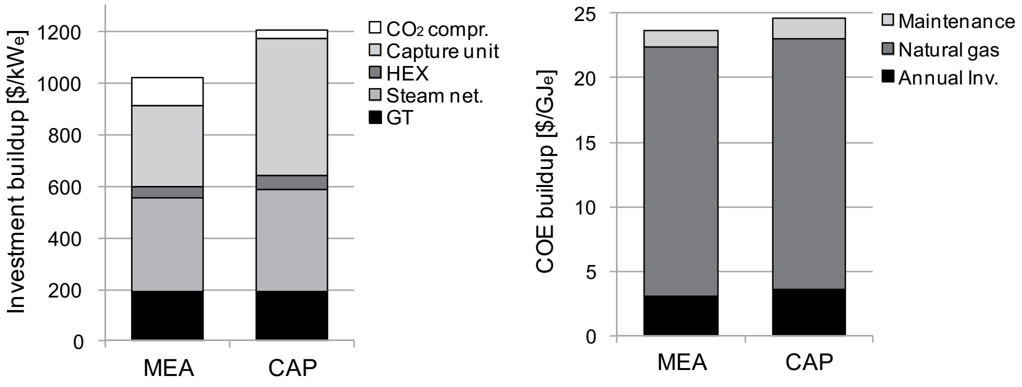

Figure 6.4: Comparison of the investment buildup (left) and of production cost buildup (right) for the NGCC plant with 85% post-combustion CO_2 capture by MEA and CAP (Table 6.1).

6.3 Multi-objective optimisation: Amines versus chilled ammonia

A multi-objective optimisation is performed to assess the performance and competition between post-combustion CO_2 capture with MEA and CAP in an NGCC plant. The CO_2 capture rate is maximised and the COE minimised with regard to the decision variables given in Tables 5.1 & 2.2 & 2.4. The results in Figure 6.5 reveal the trade-off between the CO_2 capture rate, the costs and the efficiency for the post-combustion with MEA and CAP.

For a CO_2 capture rate of 85%, both processes yield the same performance as discussed in the previous Section 6.2. At higher capture rates, post-combustion with MEA is more competitive than post-combustion with CAP. The MEA process yields higher efficiencies and lower costs than the CAP process, due to the trade-off between reboiler duty, refrigeration and CO_2 compression in the CAP process described in Figure 6.6. The reboiler duty of the CAP process increases with the CO_2 capture rate, which leads to a decrease of the electricity generation in the steam network. In addition, the benefit from the CO_2 compression is not sufficient to outweigh the increase of the refrigeration duty. Whereas for capture rates below 85%, the advantage from the CO_2 compression and the reboiler duty makes the CAP process more competitive than the MEA process for CO_2 capture in natural gas fed power plants. Consequently, the process competitiveness depends on the CO_2 capture rate and hence on the introduction of a carbon tax as discussed in Chapter 8.

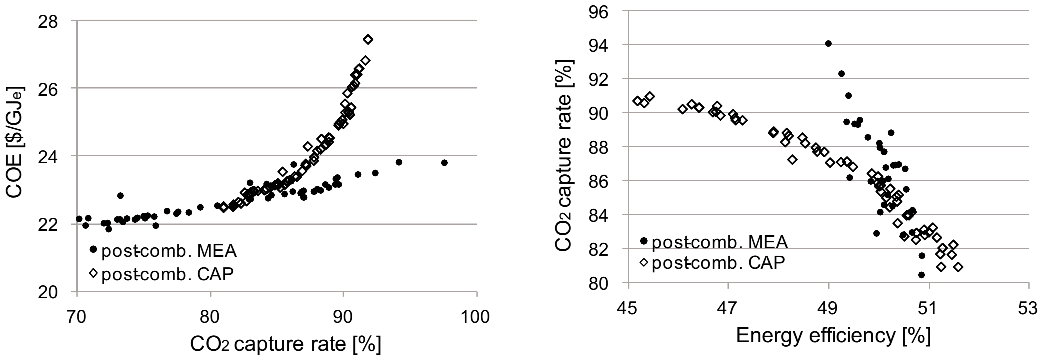

Figure 6.5: Pareto optimal frontiers (left) and CO_2 capture - efficiency trade-off (right) for post-combustion CO_2 capture with MEA and CAP in an NGCC plant.

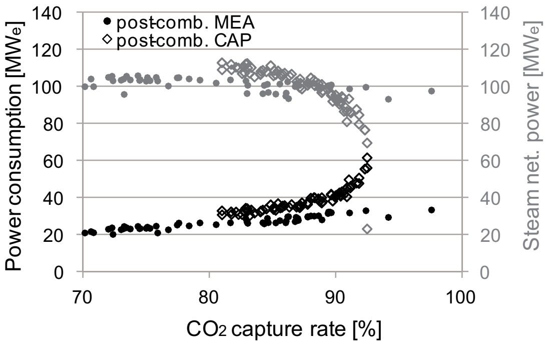

Figure 6.6: Trade-off along the Pareto optimal frontiers between the power consumption and the power generation by the steam network for the post-combustion CO_2 capture with MEA and CAP in an NGCC plant.

6.4 Chilled ammonia process improvement

The competitiveness of the CAP process reveals to depend on the refrigeration duty and consequently on the cooling utility for the absorption. The absorber and refrigeration unit integration and design are investigated here more in detail in order to assess the influence on the process performance and identify possible process improvements.

6.4.1 Energy integration improvement: Absorber design

In the previous studies, the absorber has been modelled as a single stage flash unit. The cooling down to the absorption temperature and the condensation heat load have been satisfied by a refrigeration cycle (compression heat pump) using ammonia as a refrigerant. Instead of removing all the heat at the lowest temperature (i.e. at the absorption temperature), it would be preferable from the energy integration point of view to cool down continuously and remove the condensation heat at different temperature levels, in such a way to reduce the exergy losses and increase the process performance. The detailed analysis of the energy integration and the absorber design, reveal that this could be achieved by considering an absorption column with several stages operating at different temperatures, instead of one single flash separation unit. The absorption reaction being exothermic, the temperature increases and consequently the column has to be cooled down in order to improve the absorption rate. To take advantage of the temperature profile in the column with regard to the refrigeration, side cooling at each stage has to be introduced. The absorption column is modelled as a series of four flash units with recycling and heat exchange at each separator. This model is preferred to the detailed column simulation by a RADFRAC column because of convergence matters. In fact, the initialisation of the stage cooling in a RADFRAC column is quite difficult, especially if the aim is to optimise the heat removal at each stage. Whereas in the series of flash units model, the tearings of the cyclic streams converge better, even when changing the temperature levels. In order to model the column accurately by the series of flash separators, the gas and lean solvent are cooled down to the absorption temperature (0-10^{o}C). The temperature of the top stage flash unit and the temperature increase of the subsequent flash separators are decision variables, which are optimised in the multi-objective optimisation of the global system. The objectives are the minimisation of the COE and the maximisation of the CO_2 capture rate. The Pareto results are illustrated in Figure 6.7 and compared to the one reported in Figure 6.5 (single flash stage model). It can be seen that by improving the quality of the process integration, post-combustion CO_2 capture with chilled ammonia becomes more competitive at high capture rates. This highlights the importance of the quality of the process integration and its influence on the process competitiveness and the decision-making.

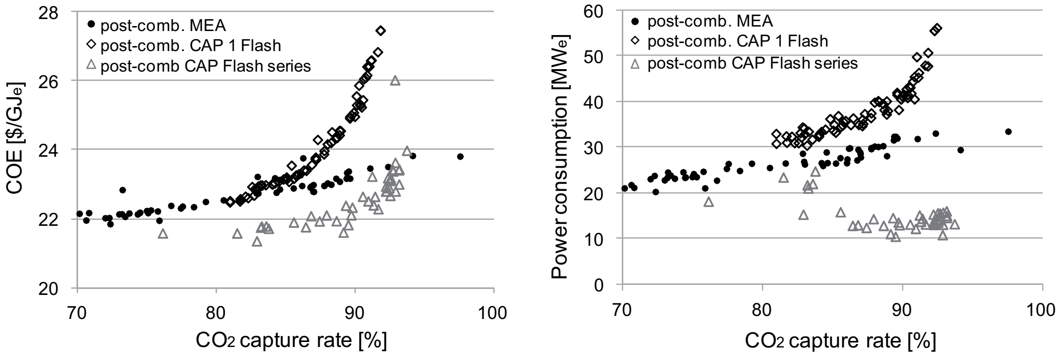

Figure 6.7: Pareto optimal frontiers (left) and power consumption (right) for the NGCC plant with post-combustion CO_2 capture by MEA and CAP modelled by a series of flash separators and a single stage flash.

Compared to the single flash modelling, the important difference is that the condenser duty has to be removed at higher temperature and could be satisfied completely or partially by conventional cooling water. Consequently, less cold utility has to be delivered by the refrigeration cycle and the electrical power demand is reduced and hence the efficiency increased and the COE reduced, as detailed in Figure 6.7. Since the flash units are optimised for each capture rate, the refrigeration power consumption is minimised for every point of the Pareto curve.

Compared to the single stage flash unit absorption model, the power consumption is reduced and does not increase considerably with the capture rate as shown in Figure 6.7 (right). For a capture rate of 90%, the improvement of the CAP process performance through process integration is reported in Table 6.3 and detailed by the composite curves in Figures 6.9-6.11.

Table 6.3: Performance comparison for NGCC power plants with 90% post-combustion CO_2 capture with MEA and chilled ammonia modelled by a single flash and a serie of flash units. The corresponding operating conditions are reported in Appendix Table D.6.

System	Post-comb. MEA	Post-comb. CAP 1 Flash unit	Post-comb. CAP Flash series
Feed [$MW_{th,NG}$]	588.4	586.6	588.6
η_{CO2} [%]	89.5	90.1	89.7
		Power Balance	
Net power [MW_e]	291.8	274.2	299.9
$\dot{E}^+_{CO2,capture}$ [$MJ_e/GJ_{e,net}$]	47.6	3.1	4
$\dot{E}^+_{Refrigeration}$ [$MJ_e/GJ_{e,net}$]	0	116.87	19.8
$\dot{E}^+_{CO2,compression}$ [$MJ_e/GJ_{e,net}$]	38.1	10.8	5.8
$\dot{E}^+_{POX}$ [$MJ_e/GJ_{e,net}$]	22.5	18.5	15.1
$\dot{E}^-_{SteamNetwork}$ [$MJ_e/GJ_{e,net}$]	341.3	335.2	301.7
$\dot{E}^-_{GasTurbine}$ [$MJ_e/GJ_{e,net}$]	766.9	814	743
		Performance (Assumptions Table 1.2)	
ϵ_{tot} [%]	49.6	46.7	50.9
CO_2 emissions [kg_{CO2}/GJ_e]	14.9	8.7	8.5
Investment [$\$/kW_e$]	909	1259	785
COE [$\$/GJ_e$]	23.7	26.2	22.5
Avoidance costs [$\$/t_{CO2,avoided}$]	60	82	44

The change of the CO_2 capture unit integration in the NGCC plant is highlighted in Figure 6.8. The advantage of satisfying the condenser duty with cooling water is revealed by the lower energy requirement below the ambient temperature. The integrated composite curve of the refrigeration cycle highlights this difference as well in Figure 6.9. The cogeneration potential is represented by the steam network integration in Figure 6.10. The decrease of the electricity consumption for the refrigeration by $97 MJ_e/GJ_{e,net}$ leads to an overall energy efficiency increase from 46.8 to 50.9% for a plant with 90% of post-combustion CO_2 capture.

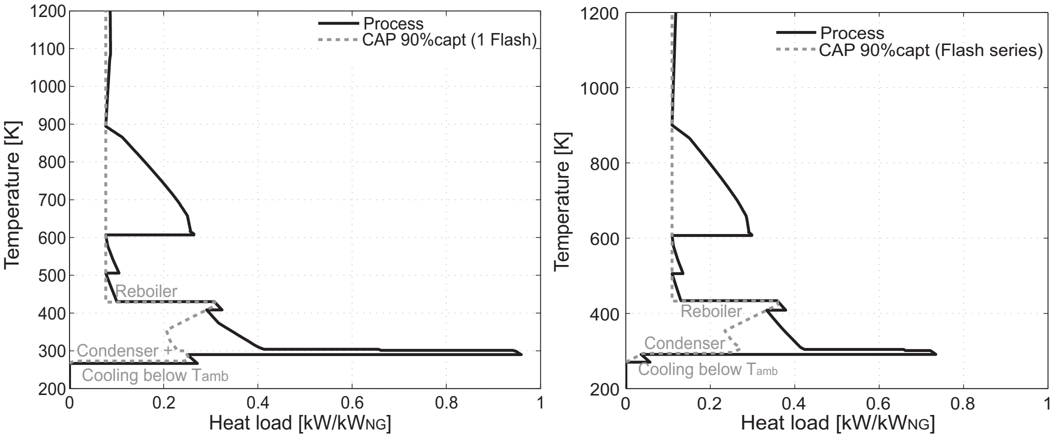

Figure 6.8: Comparison of the CO_2 capture unit integration for the NGCC plant with 90% of post-combustion CO_2 capture by CAP based on a single stage flash model (left) and on a series of flash units (right) (Table 6.3).

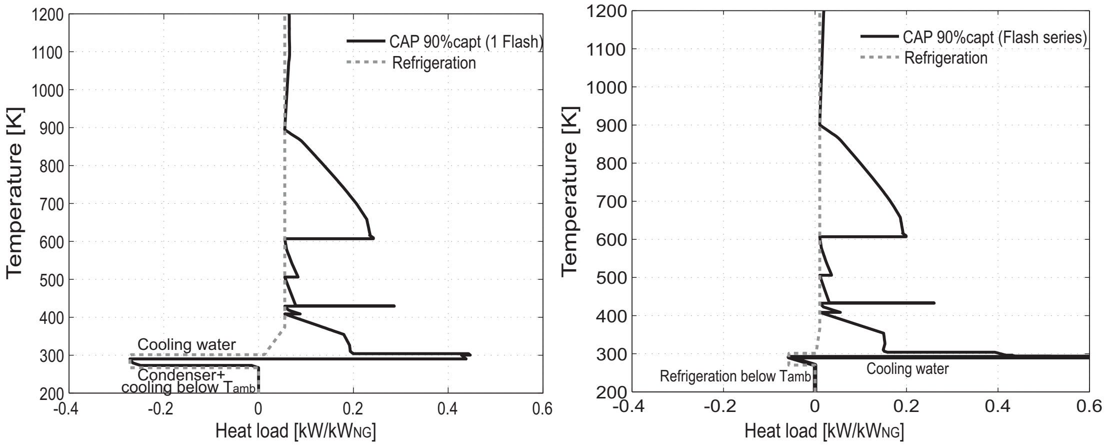

Figure 6.9: Comparison of the refrigeration integration for the NGCC plant with 90% of post-combustion CO_2 capture by CAP based on a single stage flash model (left) and on a series of flash units (right) (Table 6.3).

The detailed analysis of the power balance in Figure 6.11 highlights the decrease of the power consumption for the refrigeration, yielding a higher net electricity output and consequently a higher efficiency. Due to the decrease of the compression power, the capital investment and the electricity production costs are decreased from 26.2 to 22.5$\$/GJ_e$, as illustrated in Figure 6.12. Under these conditions the CAP process performs better in terms of energy efficiency and costs than the MEA process. For an NGCC plant with a capture rate of 90% the energy efficiency is increased by 1.3%-points for the CAP process compared to the MEA process and the COE is reduced by 1.2$\$/GJ_e$. This shows that the competitiveness of this process configuration highly depends on the process integration quality and on the available cooling utility for the chilled ammonia process. A sensitivity analysis on the cooling water temperature, reveals that the availability of low grade heat highly influences the performance of this CO_2

capture option. A decrease of $5^{o}C$ of the available cold utility, would reduce the refrigeration power consumption by 22%. Consequently, this option is especially competitive in Northern countries.

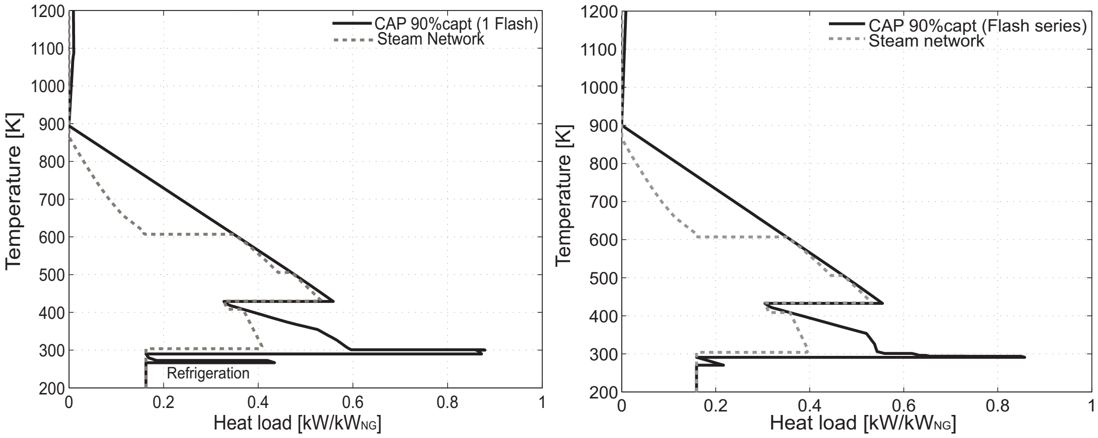

Figure 6.10: Comparison of the steam network integration for the NGCC plant with 90% of post-combustion CO_2 capture by CAP based on a single stage flash model (left) and on a series of flash units (right) (Table 6.3).

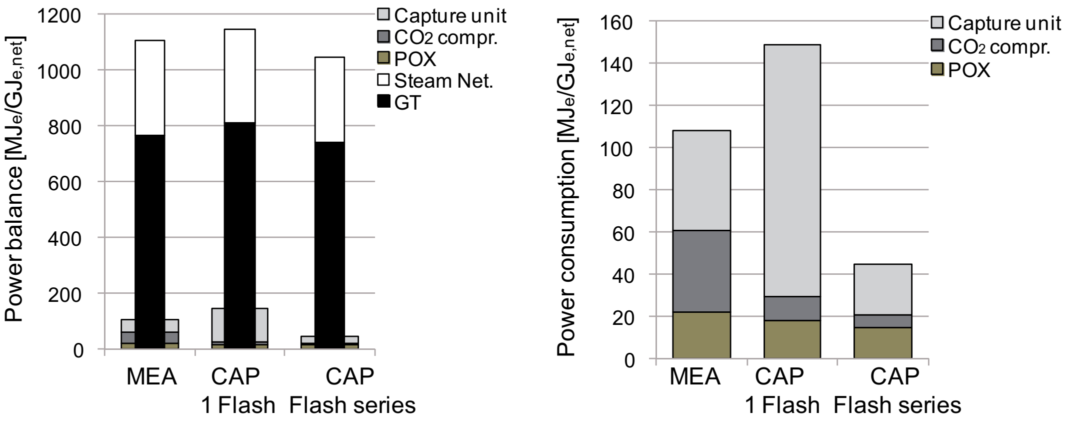

Figure 6.11: Comparison of the power balance for the NGCC plant wih 90% of post-combustion CO_2 capture by CAP modelled by a single stage flash or a series of flash units (left). Zoom on the power consumption buildup (right)(Table 6.3).

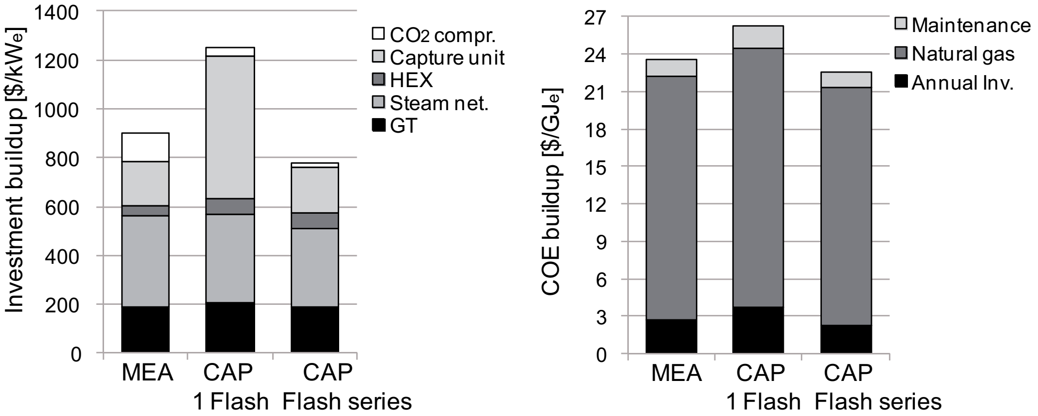

Figure 6.12: Comparison of the investment buildup (left) and production cost buildup (right) for the NGCC plant with 90% of post-combustion CO_2 capture by CAP modelled by a single stage flash or a series of flash units (Table 6.3).

6.4.2 Energy integration improvement: Refrigeration unit design

The preceding results have revealed that the refrigeration unit integration is a key element for the performance of the post-combustion CO_2 capture with chilled ammonia in an NGCC plant. Through a detailed analysis of the refrigeration unit integration, some additional improvements leading to a decrease of the exergy losses and an increase of the process performance, are identified. The analysis of the grand composite curve plotted in Carnot factor axis in Figure 6.13 (left) allows to identify the exergy losses by the area between the curve and the vertical axis. There are mainly three zones which can be depicted: at the level of the exhaust gas cooling at high temperature, of the CO_2 capture and of the refrigeration unit. At first the refrigeration unit integration is analysed in detail with the aim of identifying improvements that allow to reduce the exergy losses. The integrated composite curve of the refrigeration unit in Figure 6.13 (right), shows that these losses are due to the fact that the cooling utility is delivered by evaporation at constant temperature, while the streams have to be cooled down continuously from the ambient temperature to the absorption temperature.

In order to overcome this, it is proposed to insert a cooling cycle based on an ammonia-water mixture, illustrated in Figure 6.14. The major advantage of this cycle consists in the possibility of partially evaporating ammonia, due to the large boiling point difference between both compounds of the mixture. This leads in the H-T diagram to a slope for the evaporation, and not to a horizontal plateau at constant temperature as for the single compound evaporation. The main steps of this cycle are: expansion of the gas mixture, partial evaporation of ammonia, liquid-vapour separation, gas phase compression and liquid phase pumping, and mixing and condensation. The key decision variables are the ammonia concentration in the aqueous solution, the evaporation temperature and the cycle pressure.

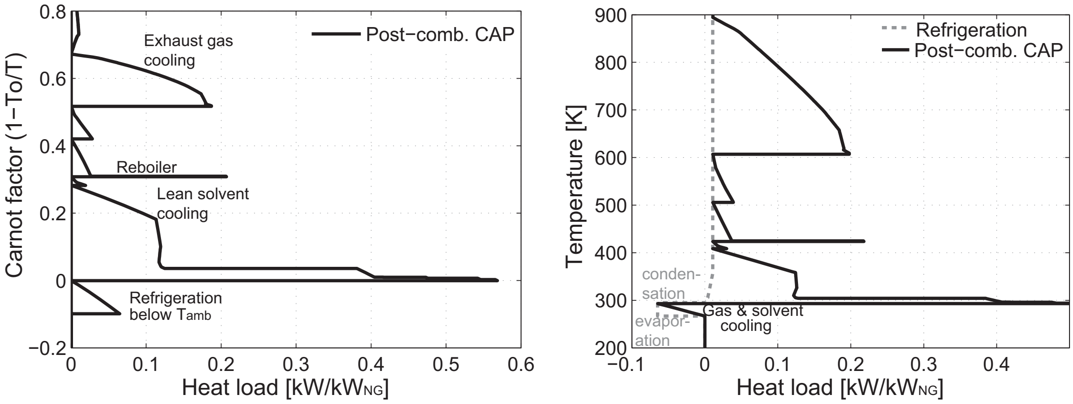

Figure 6.13: Energy integration results for the NGCC plant with 90% post-combustion CO_2 capture with CAP modelled by a series of flash unit and including a refrigeration cycle with ammonia: Grand composite curve in Carnot factor axis (left). Integrated composite curve of refrigeration unit (right).

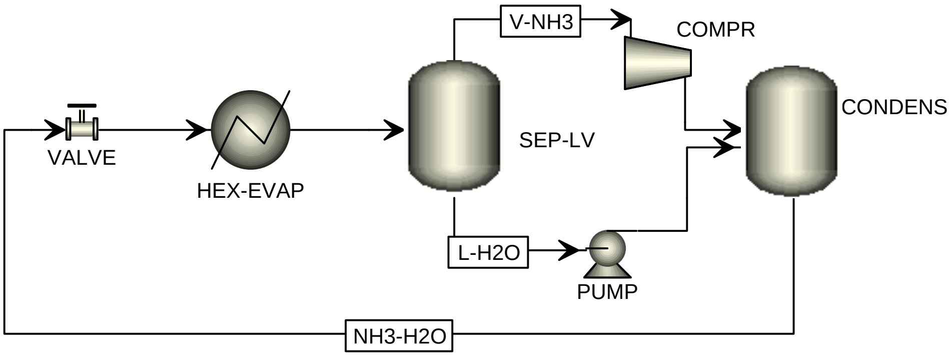

Figure 6.14: Refrigeration cycle using an ammonia-water mixture as refrigerant.

For the base case cycle, an aqueous solution with an NH_3 concentration of 62%mol, an evaporation temperature of 263.8 K and a condensation pressure of 7.8 bar have been considered. The performance results are summarised and compared in Table 6.4. The cycle performance is expressed by the coefficient of performance (COP) defined by the ratio of the cooling provided over the electrical energy consumption. As a comparison, the theoretical maximum thermal efficiency of a Carnot cycle operating between T_H=268 K and T_C=293 K is 8.5. In Figure 6.15 it is shown how this base case refrigeration cycle configuration affects the energy integration.

Table 6.4: Performance of the NGCC power plant with 90% post-combustion CO_2 capture with chilled ammonia (series of flash units) including different refrigeration options.

System	Refrig. NH_3	Refrig. NH_3-H_2O	Refrig. Opt. NH_3-H_2O
Feed [$MW_{th,NG}$]	588.6	586.8	586.8
		Power Balance	
Net power [MW_e]	299.9	301.5	306.7
$\dot{E}^+_{CO2,capture}$ [$MJ_e/GJ_{e,net}$]	4	2.5	2.4
$\dot{E}^+_{Refrigeration}$ [$MJ_e/GJ_{e,net}$]	19.8	27.8	13.8
$\dot{E}^+_{CO2,compression}$ [$MJ_e/GJ_{e,net}$]	5.8	9.2	9.0
$\dot{E}^+_{POX}$ [$MJ_e/GJ_{e,net}$]	15.1	16.9	16.6
$\dot{E}^-_{SteamNetwork}$ [$MJ_e/GJ_{e,net}$]	301.7	315.9	313.9
$\dot{E}^-_{GasTurbine}$ [$MJ_e/GJ_{e,net}$]	743	740.5	727.9
	Performance (Assumptions Table 1.2)		
ϵ_{tot} [%]	50.9	51.4	52.3
COP	5.68	4.62	7.18
CO_2 emissions [kg_{CO2}/GJ_e]	8.51	7.86	7.73
Investment [$/kW$_e$]	785	771	744
COE [$/GJ$_e$]	22.5	22.3	21.85
Avoidance costs [$/t$_{CO2,avoided}$]	44	41	36

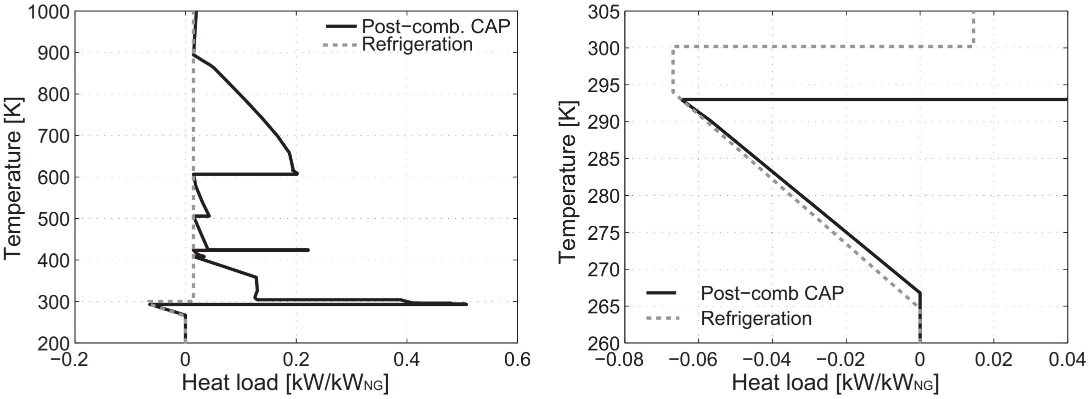

Figure 6.15: Integrated composite curve of the ammonia-water refrigeration cycle for the NGCC plant with 90% post-combustion CO_2 capture with chilled ammonia (left) (Table 6.4: Refrig. NH_3-H_2O). Zoom below ambient temperature (right).

Looking in detail at the refrigeration integration in Figure 6.15 (right), it is noticed that the performance could still be increased by reducing the exergy losses. In fact, the optimal process design depends on the NH_3/H_2O ratio of the refrigerant and on the ΔT_{min} in the heat exchangers. The sensitivity analysis results in Figure 6.16, show how the NH_3 concentration influences the thermodynamic and economic performance. When reducing, the NH_3 concentration, the slope representing the evaporation in the H-T diagram changes and consequently the exergy losses can be reduced.

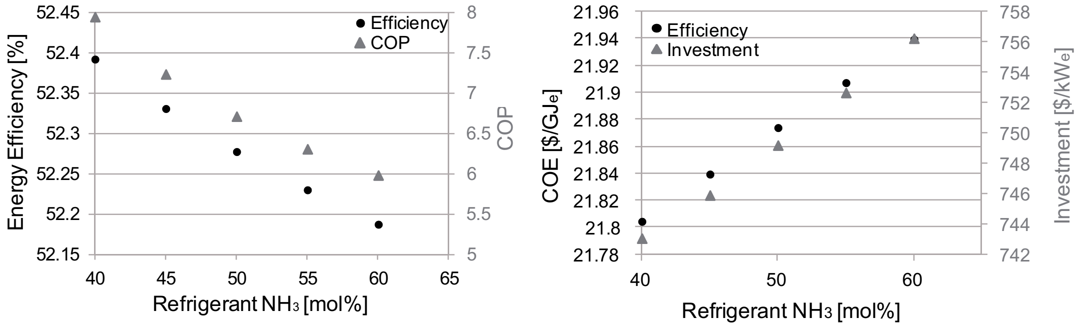

Figure 6.16: Influence of the ammonia concentration of the refrigerant on the performance of the NGCC plant with 90% post-combustion CO_2 capture with chilled ammonia including an ammonia-water refrigeration cycle.

The lowest exergy losses and consequently the highest thermodynamic efficiency can be reached with a low ΔT_{min} in the heat exchanger. The influence of the ΔT_{min} on the performance is illustrated in Figure 6.17. A low ΔT_{min} will lead to a large heat exchange area and consequently to high investment costs. There is a trade-off between the energy efficiency and the costs. With regard to the investment, the lowest cost is achieved for a $\Delta T_{min}/2$ of 2 yielding a good compromise between the heat exchanger and the compressor costs.

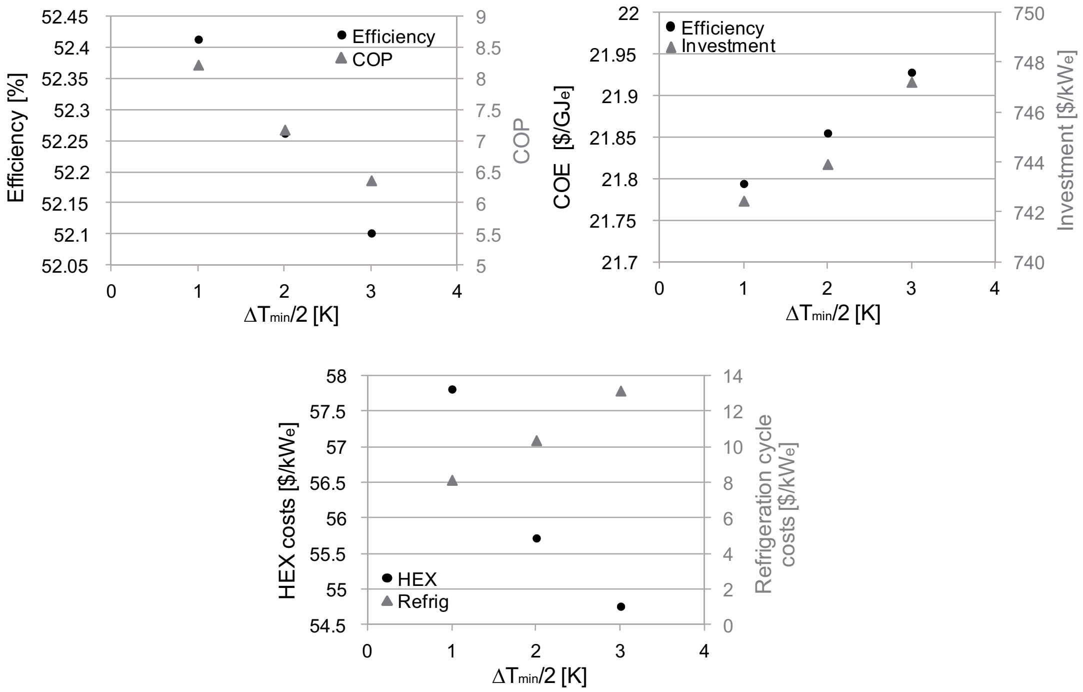

Figure 6.17: Influence of the ΔT_{min} in the refrigeration cycle heat exchangers on the performance of the NGCC plant with 90% post-combustion CO_2 capture with chilled ammonia including an ammonia-water refrigeration cycle.

Based on these results, the optimal process design for the refrigeration unit is identified. This design is characterised by a $DT_{min}/2$ of 2, a NH_3 concentration of 42.3%mol in the refrigerant, an evaporation temperature of 291 K and a condensation pressure of 5.1 bar. Compared to the configuration with the ammonia refrigeration, this option leads to an efficiency increase from 50.9 to 52.3% and to a cost decrease of 0.65$/GJ$_e$, as reported in Table 6.4 (Refrig. NH_3 vs Refrig. Opt. NH_3-H_2O). This performance increase is mainly related to the increase of the heat pumping coefficient of performance from 5.7 to 7.2. Figures 6.18 & 6.19 reveal the improvement in terms of energy integration and exergy losses reduction compared to the ammonia refrigeration cycle. Both refrigeration cycles have the advantage of using compounds that are used in the chilled ammonia process and so available in the plant.

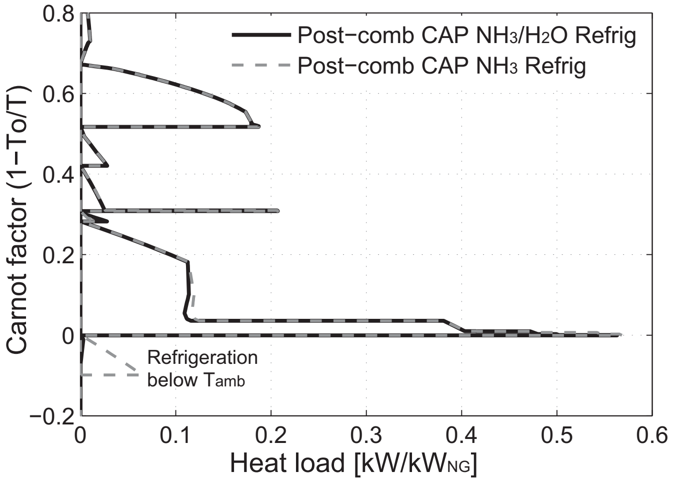

Figure 6.18: Comparison of the grand composite curve in Carnot factor axis of the NGCC plant with 90% post-combustion CO_2 capture with chilled ammonia including an ammonia or ammonia-water refrigeration cycle (Table 6.4: Refrig. NH_3 and Refrig. Opt. NH_3-H_2O).

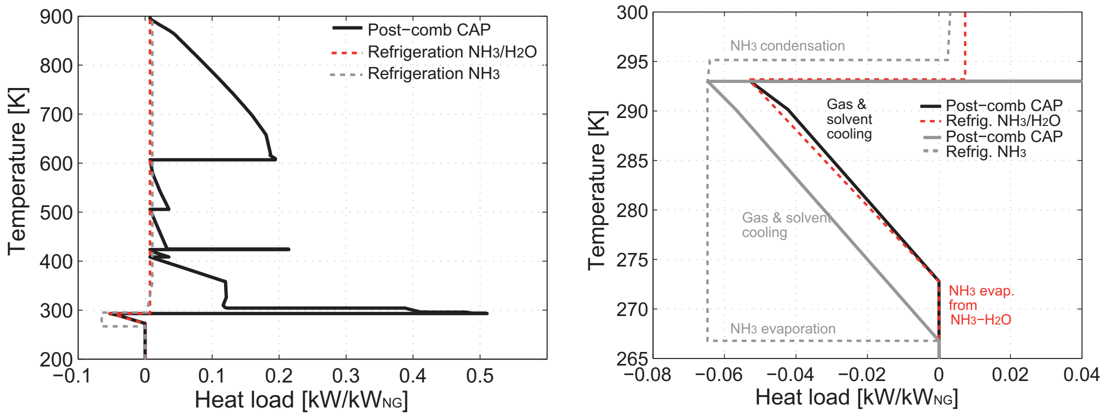

Figure 6.19: Comparison of the integrated composite curve of the ammonia and ammonia-water refrigeration cycle in the NGCC plant with 90% post-combustion CO_2 capture with chilled ammonia (left) (Table 6.4: Refrig. NH_3 and Refrig. Opt. NH_3-H_2O). Zoom below ambient temperature (right).

Pursuing the same strategy, additional improvements can be identified by the analysing Figure 6.18. The remaining exergy losses have already been depicted in Figure 6.13. In addition to these, the steam network integration can be improved by adjusting the steam condensation level to the cooling water temperature. This allows to slightly increase the electricity generation by the steam expansion and consequently the efficiency. By applying the same heat pumping principle, as for the refrigeration unit, the integration of the CO_2 capture unit can be improved by transferring heat from the lean solvent and the CO_2 cooling to the stripper to satisfy the reboiler duty. When introducing a compression heat pump using a NH_3/H_2O solution with an optimised NH_3 concentration of 87%mol and improving the steam network integration, the energy efficiency is increased by 0.38%-points to 52.64% and the COE is increased by $0.4\$/GJ_e$ as reported in Table 6.5 (EI Opt. NH_3/H_2O). The electricity generation by the steam network is increased by about $31.6MJ_e/GJ_{e,net}$ through the heat pumping consuming about $26MJ_e/GJ_{e,net}$. The additional investment of the heat pumping is around $126\$/kW_e$. The improvement of the energy integration is highlighted in Figure 6.20 by the reduction of the exergy losses.

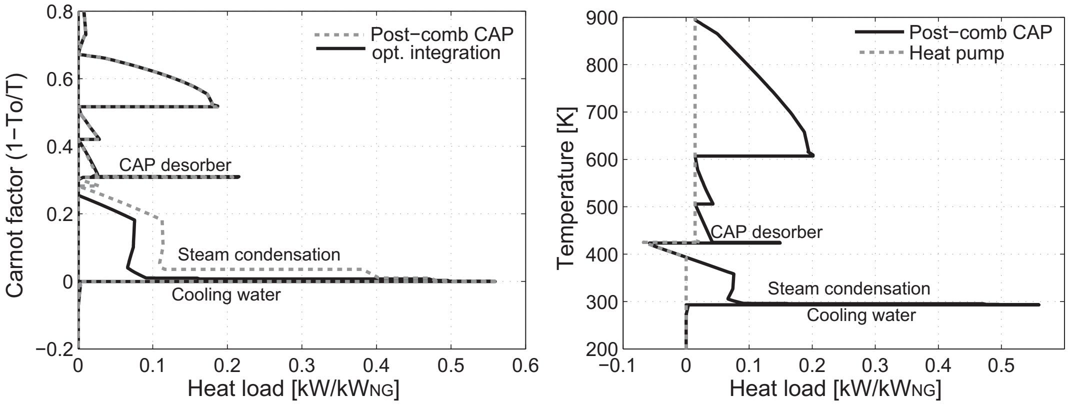

Figure 6.20: Comparison of the grand composite curve in Carnot factor axis of the NGCC plant with 90% post-combustion CO_2 capture with chilled ammonia including an ammonia-water refrigeration cycle and heat pumping (left). Integrated composite curve of the heat pumping using a ammonia-water mixture in the NGCC plant with 90% post-combustion CO_2 capture with chilled ammonia (right).

Table 6.5: Performance of NGCC power plants with 90% post-combustion CO_2 capture with chilled ammonia (series of flash units) for different energy integration (EI) improvements.

System	Refrig. Opt. NH_3-H_2O	EI Opt. NH_3-H_2O	EI Opt. MVR
Feed [$MW_{th,NG}$]	586.8	586.8	586.8
	Power Balance		
Net power [MW_e]	306.7	308.9	311.4
$\dot{E}^{+}_{CO2,capture}$ [$MJ_e/GJ_{e,net}$]	2.44	2.43	2.41
$\dot{E}^{+}_{HeatPumping}$ [$MJ_e/GJ_{e,net}$]	13.87	40.46	66.08
$\dot{E}^{+}_{CO2,compression}$ [$MJ_e/GJ_{e,net}$]	9.06	8.99	8.92
$\dot{E}^{+}_{POX}$ [$MJ_e/GJ_{e,net}$]	16.57	16.45	16.32
$\dot{E}^{-}_{SteamNetwork}$ [$MJ_e/GJ_{e,net}$]	313.97	345.60	376.77
$\dot{E}^{-}_{GasTurbine}$ [$MJ_e/GJ_{e,net}$]	727.98	722.73	716.96
	Performance (Assumptions Table 1.2)		
ϵ_{tot} [%]	52.26	52.64	53.06
Investment [$/$kW_e$]	744	870	968
COE [$/$GJ_e$]	21.85	22.26	22.53
Avoidance costs [$/$t_{CO2,avoided}$]	36	40	43

The alternative is to do a mechanical vapor recompression of sub-atmospheric pressure steam that is evaporated to recover the low temperature heat available, similar to the CO_2 capture integration improvement discussed in Section 3.4.2 for H_2 production plants. The heat pumping improves the overall energy efficiency to 53.1% and increases the COE by 2.3% compared to the configuration without heat pumping (Table 6.5:Refrig. NH_3/H_2O and EI Opt. MVR). The electricity generation by the steam network is increased by about 62.8$MJ_e/GJ_{e,net}$ through the heat pumping consuming about 52$MJ_e/GJ_{e,net}$. The additional investment of the heat pumping is around 224$/$kW_e$. Figure 6.21 shows the improvement of the energy integration. The exergy losses decrease is highlighted by the grand composite curve plotted in Carnot factor axis in Figure 6.21 (left). This alternative performs better since more heat can be transferred, which increases the electricity cogeneration by the steam network. For the heat pumping with NH_3/H_2O the lower temperature is limited by the process design and operating conditions. To improve the integration further one option which could be studied is a multiple stage heat pump system.

This step by step approach based on the results analysis shows how process improvements can be identified and optimal process configurations designed based on the optimisation results. This detailed analysis points out that the competitiveness of the chilled ammonia process highly depends on the quality of the process integration, especially of the absorber and the refrigeration utility. Compared to the chemical absorption with amines, this option reveals to be promising for post-combustion CO_2 capture concepts.

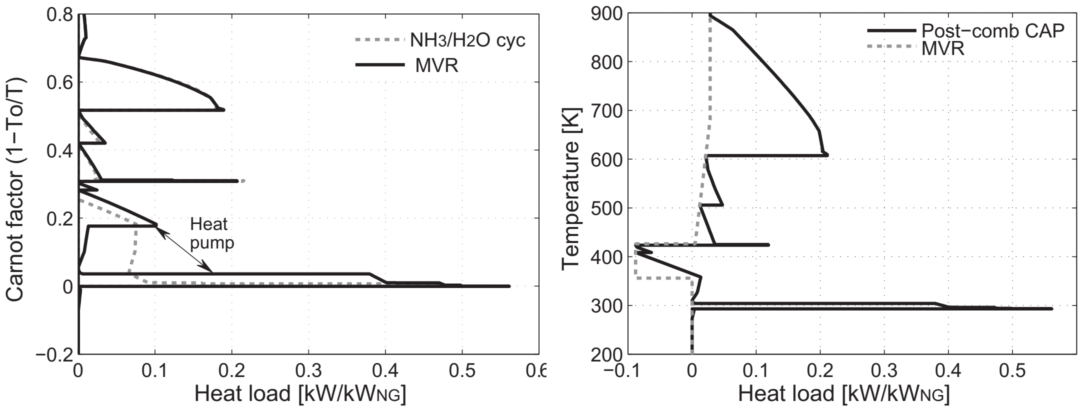

Figure 6.21: Comparison of the grand composite curve in Carnot factor axis of the NGCC plant with 90% post-combustion CO_2 capture with chilled ammonia including an ammonia-water refrigeration cycle and MVR (left). Integrated composite curve of the MVR in the NGCC plant with 90% post-combustion CO_2 capture with chilled ammonia (right).

6.5 Conclusions

The chilled ammonia process is proclaimed to be a promising alternative to post-combustion CO_2 capture with chemical absorption with amines in NGCC plants. The main advantage is the lower energy requirement for solvent regeneration in the CAP process. However, there is a trade-off between the energy benefit from the reboiler duty and the CO_2 compression, and the energy consumption for refrigeration to the absorption temperature (0-$10^{o}C$). The consistent comparison and multi-objective optimisation of both options with regard to the energy and cost penalty of post-combustion CO_2 capture reveals that the process integration quality and the ambient temperature and availability of low grade heat are major concerns for the competitiveness of the chilled ammonia process. When the refrigeration integration is not optimised, the MEA process performs better at capture rates above 85%, since the refrigeration penalty outweighs the benefits from the CAP process. However, when the integration of the absorption column and the refrigeration are improved the CAP process becomes more competitive than the MEA process for each capture rate because of the lower reboiler duty and the lower CO_2 compression work. The energy efficiency of 49.6% for an NGCC plant with 90% post-combustion CO_2 capture with MEA can be increased to around 52.3% with the chilled ammonia process and the COE decreased from 23.7 to $21.8\$/\mathrm{GJ}_e$. This increase of the efficiency results from the $29\mathrm{MJ}_e/\mathrm{GJ}_{e,net}$ lower CO_2 compression power and the lower energy demand for the CO_2 capture outbalancing the electricity consumption for the refrigeration being in the order of $13.8\mathrm{MJ}_e/\mathrm{GJ}_{e,net}$. By applying a systematic approach, it is shown how potential process improvements can be identified from the optimisation results by analysing in detail the energy integration results. For natural gas fired power plants applications, the competitiveness of these two technologies is consequently primarily defined by the technology availability and the economic scenario discussed in Chapter 8.

7 Process design optimisation strategy to develop energy and cost correlations of CO_2 capture processes

In the previous chapters the integration of CO_2 capture in power plants is studied and optimised. The optimisation of such complex integrated energy systems is quite time consuming, therefore the goal is here to develop a methodology to set-up simpler parameterised models of the CO_2 capture process. This approach presented in Tock and Maréchal (2012d) has been applied to study post-combustion CO_2 capture by chemical absorption with amines.

7.1 Introduction

To evaluate the impact of CO_2 capture on the power plant performance, thermodynamic, economic and environmental aspects have to be considered. When these analyses are performed by applying computer-aided tools as presented in the previous chapters, some challenges arise especially with regard to the computation time. Changing the design conditions of the ab- and desorption columns together with the flow of amines reveals to be sensitive to convergence and heavy in computation time, especially when the optimisation is to be done together with the variation of the CO_2 concentration and with the purpose of finding the best economical design from the CO_2 capture point of view. Recent studies have investigated the potential of replacing complex unit models of highly non-linear processes by compact yet accurate surrogate models reproducing the results of the rigorous model in a fraction of the simulation time without losing accuracy (Sipocz et al. (2011), Henao and Maravelias (2010, 2011), Biegler and Lang (2012)). In Biegler and Lang (2012) it is shown how reduced order models based on flowsheet optimisation can increase the efficiency of energy processes.

The idea is to develop an approach for setting-up a blackbox model of the CO_2 capture unit predicting the investment, as well as the heat demands and their temperature levels required for the combined heat and power integration model, by using correlations and neural networks that are set up from the optimisation results of the complex first-principle CO_2 capture unit model described in Section 2.3.1. The advantage of this approach with regard to the optimisation problem formulation is that the optimised CO_2 capture subproblem can be introduced in a larger process to perform optimisations of the global problem, and with regard to energy integration, that information about the heat demand and the temperature levels are conserved. This approach is applied to study flue gas recirculation (FGR) and CO_2 capture (CC) in NGCC power plants described and discussed in detail in Chapter 5.

7.2 Process design optimisation strategy

The approach to develop a simpler parameterised model of the CO_2 capture unit (i.e. subproblem) to be used in the overall process design optimisation (i.e. global problem) is implemented using process design techniques combining process modelling with established flowsheeting tools, and process integration in a multi-objective optimisation framework as illustrated in Figure 7.1. The thermo-economic modelling methodology follows the principles explained in Chapter 1.

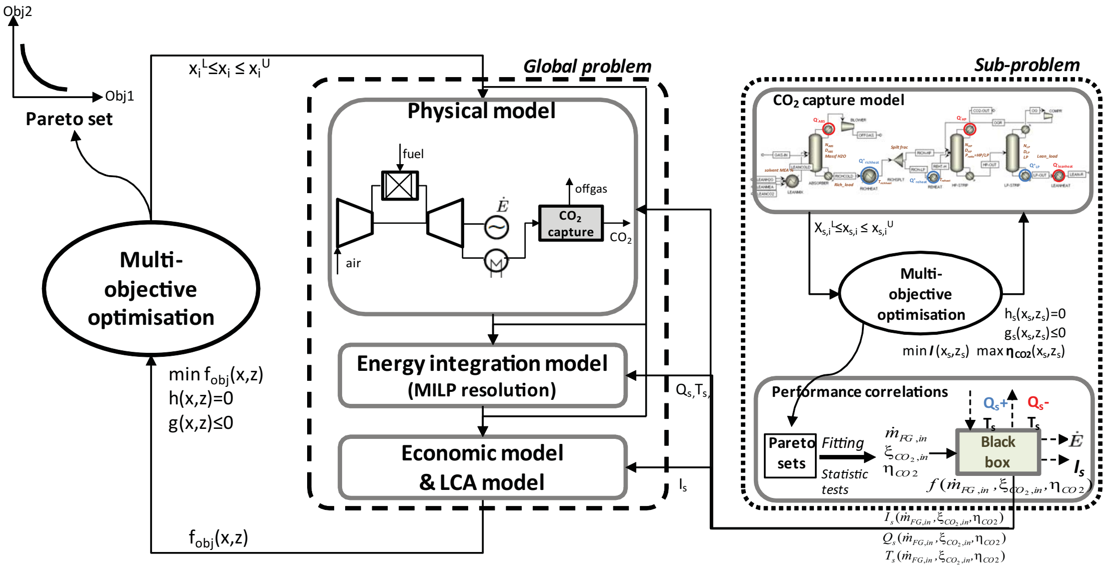
Obj2
Obj1
Pareto set
$x_i^L \le x_i \le x_i^U$
Global problem
Sub-problem
Physical model
fuel
offgas
$\dot{E}$
CO_2 capture
CO_2
air
Multi-objective optimisation
min $f_{obj}(x,z)$
$h(x,z)=0$
$g(x,z) \le 0$
Energy integration model
(MILP resolution)
Economic model & LCA model
Q_s, T_s
I_s
$f_{obj}(x,z)$
CO_2 capture model
$X_{s,i}^L \le x_{s,i} \le x_{s,i}^U$
Multi-objective optimisation
$h_s(x_s,z_s)=0$
$g_s(x_s,z_s) \le 0$
min $I(x_s,z_s)$ max $\eta_{CO2}(x_s,z_s)$
Performance correlations
Pareto sets
Fitting
Statistic tests
$\dot{m}_{FG,in}$
$\xi_{CO_2,in}$
η_{CO2}
Q_s+
Q_s-
T_s
T_s
Black box
$\dot{E}$
I_s
$f(\dot{m}_{FG,in}, \xi_{CO_2,in}, \eta_{CO2})$
$I_s(\dot{m}_{FG,in}, \xi_{CO_2,in}, \eta_{CO2})$
$Q_s(\dot{m}_{FG,in}, \xi_{CO_2,in}, \eta_{CO2})$
$T_s(\dot{m}_{FG,in}, \xi_{CO_2,in}, \eta_{CO2})$

Figure 7.1: Illustration of the process optimisation strategy to develop simpler parameterised CO_2 capture models.

The strategy is illustrated by the development of a simplified model for CO_2 capture by chemical absorption with amines. The developed first-principle CO_2 capture model corresponds to the one described in Section 2.3.1 (Figure 2.3). CO_2 compression to 110 bar is not included in the capture unit itself, but accounted in a separate model. A CO_2 purity of over 98%wt is targeted from a typical post-combustion flue gas consisting mainly of N_2, CO_2, excess O_2 and water. The CO_2 capture unit performance is expressed by the investment cost I, the CO_2 capture rate ($\eta_{CO2} = \frac{\dot{n}_{CO2captured}}{\dot{n}_{CO2,inFG}}$) and the energy demand (i.e. reboiler duty $\dot{Q}_{LP}$, electricity $\dot{W}$) and is mainly influenced by the design decision variables given in Table 2.2.

The selected input variables for the simpler parameterised blackbox model reflecting the process behaviour are the flue gas mass flow ($\dot{m}_{FG}$) and the CO_2 concentration in the flue gas (ξ_{CO2}) as illustrated in Figure 7.2. The absorber inlet temperature and pressure are kept constant by a blower and heat exchanger. The only decision variable is hence the CO_2 capture rate (η_{CO2}). Consequently, the number of decision variables of the overall process is smaller than the one for the subproblem since some parameters are internal to the blackbox system. The output parameters of the blackbox model are the investment, mechanical and thermal energy demand and the associated temperature levels.

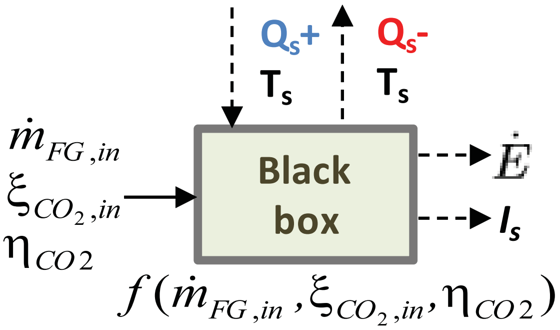

Figure 7.2: Blackbox model of the CO_2 capture process.

7.2.1 Subproblem optimisation

For different flue gas compositions (ξ_{CO2}: 0.065, 0.074, 0.081 and 0.09wt-) and flows ($\dot{m}_{FG}$: 655, 955, 1455, 1955, 2455 and 2955 t/h) an optimisation of the CO_2 capture subproblem is first performed. The multi-objective optimisation problem is solved by applying an evolutionary algorithm computing a set of optimal solutions in the form of a Pareto front. The objectives are to maximise the CO_2 capture rate η_{CO2} and to minimise the capital investment I with regard to the decision variables in Table 2.2. It is assumed that the objectives are not influenced by the pressure drop and the heat load. It has been demonstrated by sensitivity analyses that minimum pressure drops and heat loads are correlated with the maximum CO_2 capture rate. Consequently, the assumption is valid and the optimum of the subproblem is contained in the optimum of the global problem. The Pareto optimal frontiers computed for the different process configurations are illustrated in Figure 7.3. The influence of the flowrate on the equipment size and consequently on the investment is strongly reflected. Moreover, the investment is slightly affected by the CO_2 capture rate. Based on these optimisation results of the first-principle MEA unit model, the goal is to develop a simplified parameterised blackbox model described in Figure 7.2.

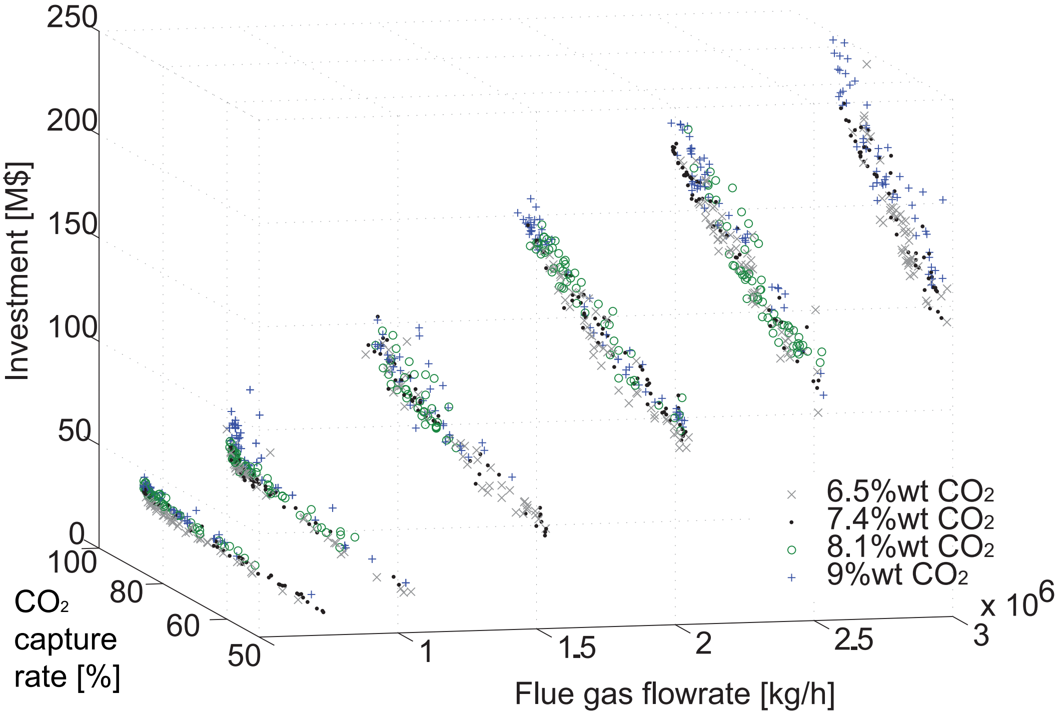

Figure 7.3: Pareto optimal frontiers showing the trade-off between investment and CO_2 capture rate for different $\dot{m}_{FG}$ and ξ_{CO2} in chemical absorption with MEA.

7.2.2 Surrogate model development

By fitting the generated Pareto fronts reported in Figure 7.3, regression correlations and neural networks are defined to predict the thermo-economic performance of the CO_2 capture unit with regard to the input variables η_{CO2} (x_1), $\dot{m}_{FG}$ (x_2) and ξ_{CO2} (x_3). Statistical tests are carried out to validate the proposed correlations. The F statistic is applied to test the model validity against the assumption that at least one coefficient of the correlation is significant. In addition, the validity of each coefficient is verified by the t-test following a Student's t distribution, if the null hypothesis is supported. The approach is illustrated here explicitly for setting up the investment cost correlations. The development of the correlations for the mechanical power, the heat load and the temperature levels follows the same approach (Appendix F).

CO_2 capture investment cost correlation

The goal is to develop a correlation of the investment I with regard to the input variables: I=$f(\eta_{CO2},\dot{m}_{FG},\xi_{CO2})=f(x_1,x_2,x_3)$. It is to note that the developed correlations for the investment cost do not follow the conventional cost estimation approach since they deal with the optimised investment computed from simulation with regard to certain decision variables. Three different approaches for fitting are discussed here and the detailed models are reported in Appendix F.

Polynomial fit. In a first attempt, multi-dimensional polynomial correlations are set up. Therefore, correlations are drawn for each data series with fixed ξ_{CO2} (I=$f_{\xi_{CO2}}(\eta_{CO2},\dot{m}_{FG})$) based on Eq.7.1 yielding for each one coefficient of determination values (R^2) around 0.98. According to the statistical tests, additional terms do not improve the goodness of fit. To include the variation with regard to ξ_{CO2}, a linear variation of the coefficients p_i in Eq.7.1 ($p_i = \kappa_{i,1} + \kappa_{i,2}\xi_{CO2}$) is first assumed. The statistical tests results reported in Table 7.1 show that some terms are not significant which leads to the final expression given by Eq.7.2.

$$f_{x3}(x_1,x_2) = p_{00} + p_{10}x_1 + p_{01}x_2 + p_{20}x_1^2 + p_{11}x_1x_2 \tag{7.1}$$

$$f(x_1,x_2,x_3) = k_0 + k_1x_1 + k_2x_2 + k_3x_1x_2 + k_4x_1x_3 + k_5x_2x_3 + k_6x_1x_2x_3 + k_7x_1^2x_3 \tag{7.2}$$

Table 7.1: Regression results for the investment cost correlation leading to Eq.7.2. ($t_{0.95}[1538]$=1.96, $F_{0.95}[7;1538]$=3.23)

	cst	x_1	x_2	$\mathbf{x_3}$	x_1x_2	x_1x_3	x_2x_3	$x_1x_2x_3$	$\mathbf{x_1^2}$	$x_1^2x_3$	R^2	F-value
Coefficient	33.663	-117.33	-1.93E-5	**0**	1.2E-4	-366.04	4.7E-4	-4.5E-4	**0**	796.38	0.977	9565
t-value	-	-12.18	-3.38	**1.64**	14.4	-2.87	7.53	-4.7	**0.45**	6.2		
pvalue	-	1.16E-32	7.4E-4	0.099	3.2E-44	0.004	8.3E-14	2.8E-6	0.65	6.6E-10		

Shortcut fit. In a second attempt, a correlation based on a shortcut model including the known physical relations in the absorption and desorption columns is set up. The number of stages is related to the absorbed fraction through the Kremser equation (Eq.7.3) assuming stage equilibrium instead of rate-based model, which allows together with the flue gas mass flowrate ($\dot{m}_{FG}$) to estimate the diameter (d) and height (h) through column design heuristics and consequently the investment costs I according to Eqs. 7.4-7.6. The constant parameters in these functions are defined by solving a minimisation problem in the least-square sense. A hybrid method combining mathematical programming and evolutionary algorithm for finding a good initial point has been used for this purpose.

$$N = a_1 \cdot log\left(\frac{a_2}{1-\eta_{CO2}} + a_3\right) + a_4 \tag{7.3}$$

$$d = f(\dot{m}_{FG},\xi_{CO2}) \tag{7.4}$$

$$h = f(N,d) \tag{7.5}$$

$$I = f(h,d) \tag{7.6}$$

Neural network. As a last approach, the neural network (NN) fitting tool from MATLAB (MathWorks Inc.) using the Levenberg-Marquardt backpropagation algorithm for network training is applied on the optimisation results dataset (i.e. training 55% of data, validation 25%, testing 20%). The two-layer feed-forward network with sigmoid hidden neurons and linear output neurons, illustrated in Figure 7.4, is well suited to fit such multi-dimensional mapping problems.

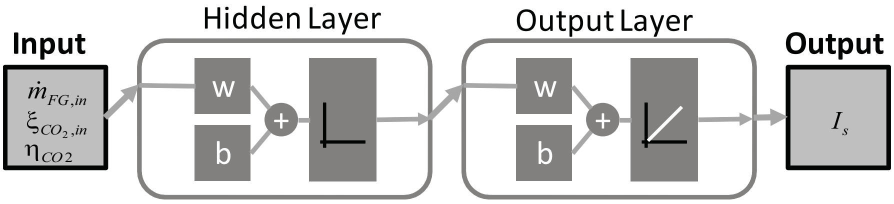

Figure 7.4: Scheme of the neural network.

Fitting results The goodness of fit of these approaches is compared in Figure 7.5 for the capital investment. The different fits give a good estimation of the capital investment costs.

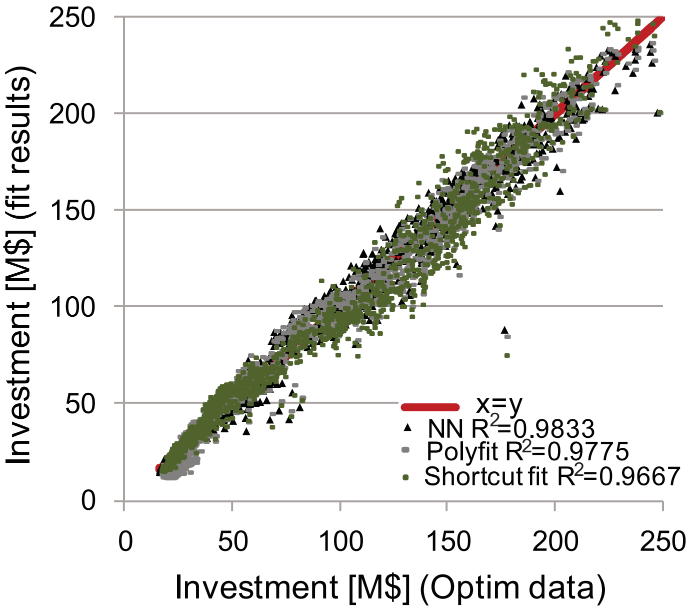

Figure 7.5: Fitted investment (Polynomial fit - polyfit Eq.7.2, fit based on shortcut model - shortcut fit, neural network - NN) versus calibration optimisation results.

Heat load and power consumption correlation

Following the same approach as for the investment cost estimation, correlations are developed for each heat load and for the overall energy consumption. For the polynomial fits the validity of each term is verified by statistic tests and for the neural networks the MATLAB (MathWorks Inc.) fitting tool is used. The details of these correlations are reported in Appendix F.

7.3 Application: NGCC with post-combustion CO_2 capture

To illustrate the approach, the integration of post-combustion CO_2 capture in power plants is studied. Therefore, the developed parameterised CO_2 capture blackbox models are integrated with a natural gas fired power plant model to optimise the process design with CO_2 capture as illustrated in Figure 7.1. The investigated process consists of a natural gas reheat gas turbine combined cycle with flue gas recirculation (FGR) and CO_2 capture studied in Chapter 5. The performance of the overall process comprising the integration of the parameterised CO_2 capture models is compared based on thermo-economic considerations assessing also the energy and economic costs of capturing CO_2 and the impact of CO_2 recirculation. For the economic performance evaluation the assumptions given in Table 1.2 are considered.

7.3.1 Base case comparison

The performance of the post-combustion CO_2 capture in the NGCC power plant is first assessed with the first-principle MEA model and then compared with the results obtained with the different blackbox models. For these base case configurations around 50% of FGR and 85% CO_2 capture are considered. The performance results are summarised in Table 7.2 and compared to a conventional NGCC plant without CO_2 capture. CO_2 capture decreases the efficiency by over 8%-points and increases the production costs by up to one third. These results are in the same range as the one given in Finkenrath (2011) reporting for a conventional NGCC an efficiency of 56.6%, CO_2 emissions of $102.8 kg_{CO2}/GJ_e$ and COE of $21.3\$/GJ_e$ and for a NGCC with post-combustion CO_2 capture an efficiency of 48.4%, CO_2 emissions of $15.3 kg_{CO2}/GJ_e$ and COE of $28.3\$/GJ_e$.

Table 7.2: Performance results of the base case NGCC plant configurations with 85% post-combustion CO_2 capture based on the first-principle MEA model and on different blackbox models.

Scenario	η_{CO2} [%]	ϵ_{tot} [%]	CO_2 emitted [kg/GJ_e]	COE [\$/GJ_e]	Avoidance costs [\$/$t_{CO2,avoided}$]
NGCC	0	58.75	105.08	18.32	-
MEA model	85.11	50.3	12.92	22.92	49.89
Polyfit	86.9	47.78	13.85	24.44	67.05
Shortcut fit	86.9	47.78	13.85	24.35	66.05
NN	86.9	46.70	14.17	24.97	73.11

The comparison of the results obtained with the first principle model with the one obtained with the blackbox model yields a difference in the production costs around 6% and in the efficiency of around 5%. This difference is essentially due to the overestimation of the reboiler duty in the blackbox models, as it can be seen on the composite curves in Figure 7.6.

The blackbox models overestimate the penalty of CO_2 capture on the power plant performance slightly. However, these simplified parameterised models reproduce the major trends and allow to reduce the computation time significantly as shown in Table 7.3. The shortcut fit including known physical relations performs slightly better than the other ones. Consequently, these simplified models allow to make a preliminary analysis of CO_2 capture process options.

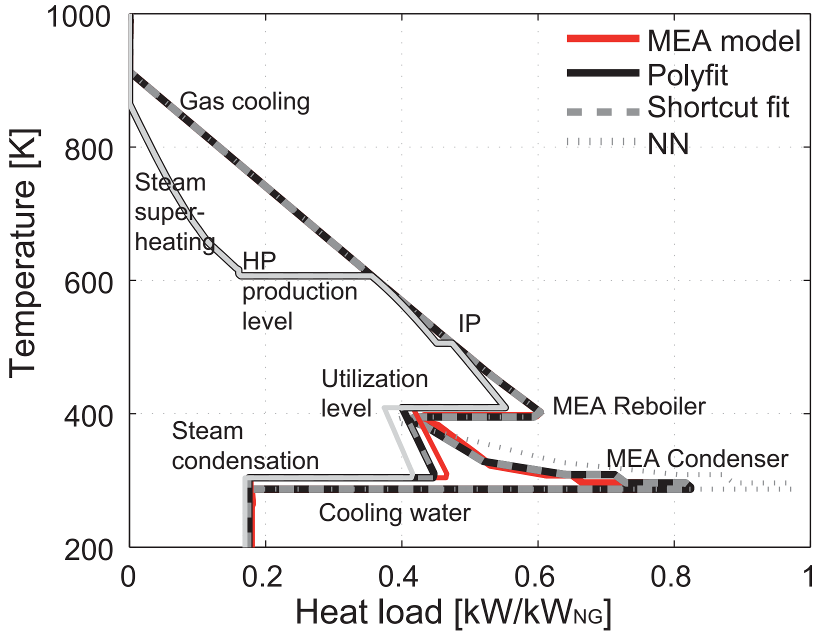

Figure 7.6: Comparison of the composite curves with steam network integration for the base case scenarios reported in Table 7.2.

Table 7.3: Computation time comparison for multi-objective optimisation of post-combustion CO_2 capture in the NGCC plant based on the first-principle MEA model and on different blackbox models (400 evaluations and initial population of 30).

Scenario	time 1 run [h:mm:ss]	time moo [h:mm:ss]
MEA model	0:01:57	10:08:33
BB Polyfit	0:01:05	4:54:32
BB Shortcut fit	0:01:03	4:56:17
BB NN	0:01:04	4:59:11

7.3.2 Global problem optimisation

To study the influence of CO_2 capture and flue gas recirculation on the power plant performance in more detail, a multi-objective optimisation of the global problem is performed. The objectives are the minimisation of the electricity production costs (COE) and the maximisation of the overall CO_2 capture rate (η_{CO2}). The decision variables for the power plant are the flue gas recirculation and in the case where syngas has to be injected the hydrogen production temperature and the steam to carbon ratio. Since the flue gas flowrate and the CO_2 concentration are defined by the power plant model, the number of decision variables for the parameterised CO_2 capture model is reduced to one, the CO_2 capture rate, compared to 15 for the first principle MEA model (Table 2.2). By using the blackbox models calibrated on the subproblem optimisation results for the optimisation of the global system, the hypothesis is made that for a given CO_2 capture rate the optimal solution corresponds to the minimal investment. The generated Pareto fronts in Figure 7.7 reveal the trade-off between the CO_2 capture rate and the electricity production costs. This trade-off is explained by the reduced electricity output due to the energy demand for solvent regeneration and CO_2 compression yielding a lower efficiency, and the increased capital investment costs for the capture equipment.

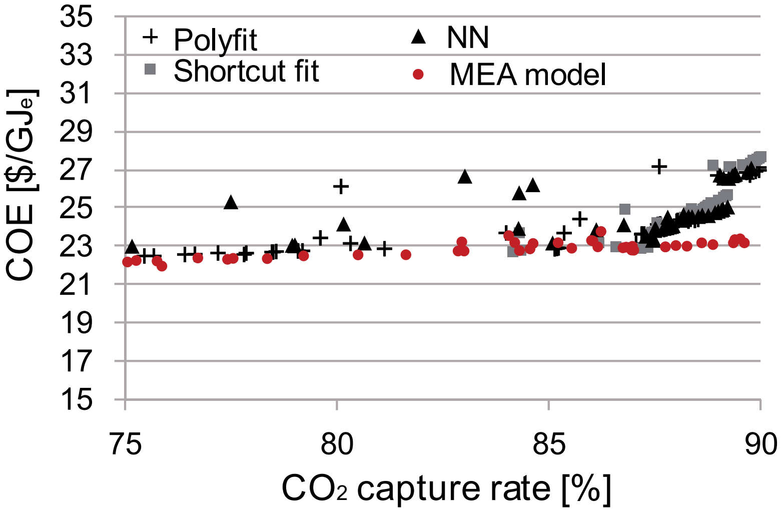

Figure 7.7: Pareto optimal frontiers of the global problem optimisation based on the first-principle MEA model and on different blackbox models.

Compared to the optimisation problem results including the first-principle MEA unit model (MEA model), the accuracy is nearly maintained for the problems including the different blackbox models up to 87% of CO_2 capture as illustrated by Figure 7.7. The comparison of the results in Table 7.4 for compromise Pareto solutions yielding a CO_2 capture rate of 87%, shows that the generated process configurations are similar. In fact, the optimised values of the FGR differ by less than 2%. For a chosen process configuration, the detailed CO_2 capture unit design can be recomputed subsequently based on the first principle CO_2 capture model. The values of the required input parameters defined in Table 2.2 can be approximated by interpolation from the data series used for the blackbox models calibration (Section 7.2.1) based on a griddata approach. The overall performance, design and operating conditions assessed in this way for the compromise configurations obtained through optimisation of the power plant with the parameterised CO_2 capture models are very close to the one resulting from the optimisation with the first principle CO_2 capture model. This high concordance is shown by the composite curves in Figure 7.8. This reveals that the subproblem optimum is included in the global problem optimum for solutions having a CO_2 capture rate below 87%.

Table 7.4: Performance of the compromise NGCC plant configurations with 87% post-combustion CO_2 capture based on the first-principle MEA model and on different blackbox models.

Scenario	η_{CO2} [%]	ϵ_{tot} [%]	CO_2 emit [kg/GJ$_e$]	COE [\$/GJ$_e$]	Avoidance costs [\$/t$_{CO2,avoided}$]	FGR [-]
NGCC	0	58.75	105.08	18.32	-	0
MEA model	86.94	50.28	16.16	22.80	50.35	0.539
Polyfit	87.02	50.29	12.93	23.20	52.93	0.528
Shortcut fit	87.16	50.6	13.23	22.90	49.90	0.543
NN	87.45	49.90	13.44	23.30	54.40	0.522

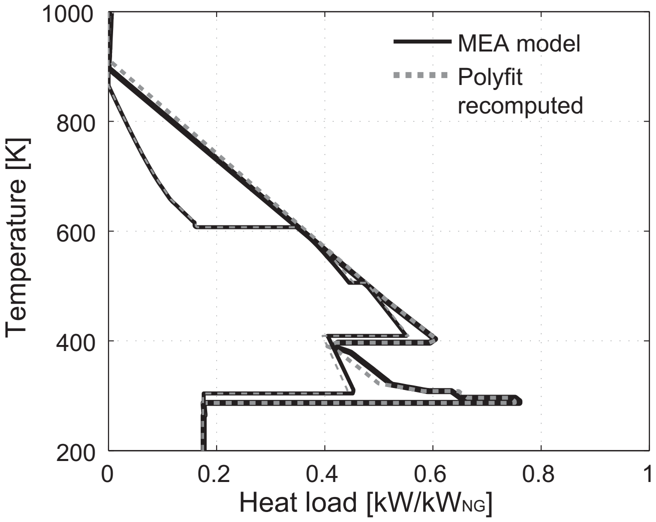

Figure 7.8: Composite curves for the compromise scenario generated by the first principle MEA model through optimisation and through recomputation of the parameterised polynomial model with the detailed MEA model.

At high CO_2 capture rates, there is however a divergence in the solutions. The optimisation of the power plant performance with the parameterised CO_2 capture models leads to process designs with low FGR (<12%), while the optimisation with the first-principle CO_2 capture model favours FGR above 50% at high CO_2 capture rates. This difference in the design of the power plant leads to a different design of the CO_2 capture unit due to the changes in the CO_2 concentration and the flue gas flow rate. Consequently, the assessed efficiencies and costs diverge. When recomputing the solution generated by the parameterised blackbox model with the first principle MEA model, a process design with a lower CO_2 capture rate (83% instead of 90%), higher efficiency and lower production costs is obtained. This indicates that the hypothesis that the subproblem optimum is included in the global problem optimum is not valid for high CO_2 capture rates. In fact, there is a compromise between the investment and the energy demands, which both affect the production costs. Consequently, it is possible to find for a given CO_2 capture rate a solution with a higher capital investment yielding a higher efficiency and lower COE. By recalculating the optimal solution found with the first-principle model with the parameterised model, the solution yields higher specific production costs per ton of CO_2 captured than the optimal solution found with the parameterised model. This explains why this solution has not been retained during the optimisation with the parameterised model. In fact the parameterised model cannot find this solution. In order to reflect this behaviour in the parameterised blackbox models, a solution would be to calibrate these models on the minimisation of the production costs accounting the heat demand at its exergy value, or on the minimisation of the exergy losses instead of the investment. Once the Pareto sets are generated with the modified objective function, the blackbox models of the CO_2 capture unit can be set up following the approach described here. The hypothesis of the optimality of the subproblem in the global problem has hence to be valid in order to take advantage from the reduction of the number of decision variables of the parameterised model in the global problem optimisation.

Using the simple blackbox models in the global problem optimisation, has the advantage of reducing the computation time considerably once the simplified model is set up. If the same number of evaluations is considered for each optimisation problem the computation time is reduced over 45%, as reported in Table 7.3. However, because of the changes in the number of decision variables, the number of evaluations for reaching a same level of convergence is different. It is noted that for the optimisation of the power plant with the first principle MEA model the convergence of the Pareto front is not considerably improved between 400 and 2000 evaluations. While for the optimisation of the power plant with the parameterised CO_2 capture model convergence is nearly reached around 180 evaluations for a same initial population. By taking into account the reduction of the number of evaluations in the optimisation, the use of the parameterised model leads to an additional computation time decrease which favours the use of this kind of simplified models in optimisation problems formulations. Consequently, such a quick first optimisation is appropriate for the preliminary design and evaluation of process options with CO_2 capture.

7.4 Conclusions

A strategy applying multi-objective optimisation for developing energy and cost correlations of CO_2 capture process units is presented. The advantage of this approach is that the simple parameterised models are developed based on optimisation results by applying polynomial fitting and neural networks. Consequently, the number of decision variables of the global problem is reduced compared to the subproblem optimisation. Using the parameterised blackbox models of the chemical absorption unit in the global optimisation of a power plant with CO_2 capture reduces the complexity and computation time without losing much accuracy for capture rates up to 87%. The inclusion of predictions of each heat load and the corresponding temperature level is advantageous with regard to the overall process integration. It is shown that the accuracy of the parameterised models highly depends on the model calibration. In fact, the hypothesis that the optimal solution of the global problem corresponds to the minimum investment for a given CO_2 capture rate reveals to be not valid at high capture rates because there is a compromise between capital investment and energy efficiency. A solution would be to calibrate the parameterised CO_2 capture models on the minimisation of the production costs accounting the heat demand at its exergy value instead of on the investment. The proposed approach to develop simplified models based on optimisation results is promising for the preliminary design and evaluation of process options with CO_2 capture, especially with regard to the computation time reduction and the reduction of the number of decision variables. However, in order to predict the process behaviour accurately in the whole space of the decision variables, the calibration data set has to be chosen in such a way that the hypothesis of the subproblem optimality is satisfied.

8 Systematic comparison of CO_2 capture options

In the previous chapters different pre- and post-combustion CO_2 capture process options have been described and optimised. It was highlighted that the competitiveness of CO_2 capture in electricity generating processes is highly influenced by the resource price and the introduction of a carbon tax. In this chapter it will be studied how the economic scenario affects the optimal process design and influences decision-making. In addition, the environmental benefit of capturing CO_2 will be investigated in detail by performing a LCA analysis for the different optimal process configurations that have been identified. Part of these results are summarised in Tock and Maréchal (2012f).

8.1 Introduction

The introduction of CO_2 capture in power plants, results in a performance penalty in terms of energy and cost, while it leads to an advantage with regard to the environmental impact. The process competitiveness on the energy market depends therefore on energetic, economic and environmental considerations simultaneously. As shown in the previous Chapters 3-6, different technologies and resources are in competition. A detailed comparison between the different process options, that are summarised in Figure 8.1, is made here in order to assess the impact of the CO_2 capture concept and technology, and of the resource type. To make a consistent comparison of the environmental impacts of fossil and renewable resources fed processes, the impacts of the whole life cycle from the resource extraction to the final product have to be taken into consideration. Therefore, life cycle impact assessment (LCIA) is performed here following the approach described in Gerber et al. (2011) and Gerber (2012).

The previous studies have shown that the prize competitiveness of CO_2 capture highly depends on the economic scenario, primarily on the resource purchase. The introduction of a carbon tax will favour CO_2 capture solutions in fossil resources fuelled power plants in the medium-term, before a switch to renewable resources in the long-term. In this chapter, these trade-offs are studied in detail and it is shown how the economic scenario influences the decision-making.

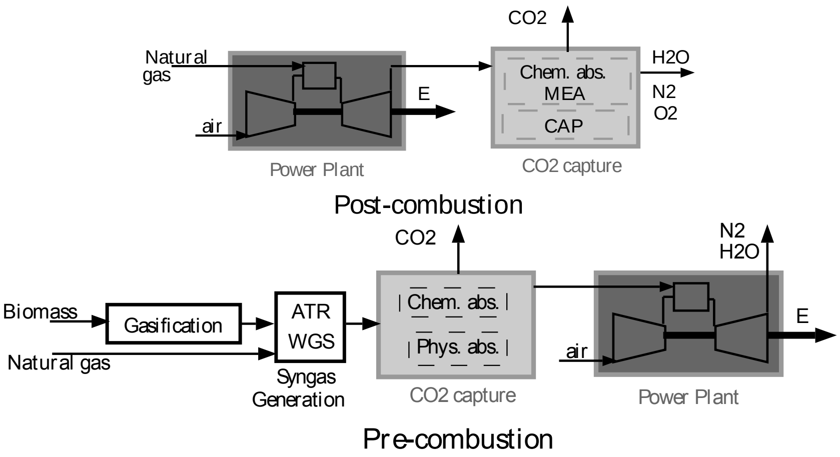

Figure 8.1: Investigated CO_2 capture options.

8.2 Performance comparison of CO_2 capture in power plants

The process performance of the compromise solutions identified from the optimisation results in the previous Chapters 3-6 is compared in detail in the following paragraphs.

8.2.1 Thermo-economic performance

The thermo-economic performance of the different compromise solutions capturing 90% of the CO_2 emissions for the natural gas based electricity generating processes and 60% for the biomass configurations is summarised in Figure 8.2 and Table 8.1. The details of the process design parameters are reported in Appendix Tables D.4 & D.7. Pre-combustion CO_2 capture processes reveals to perform slightly better in terms of energy efficiency than post-combustion CO_2 capture processes. In fact, in pre-combustion CO_2 capture processes the energy demand for CO_2 capture is lower, however the capital investment is larger because of the more complex installation. The electricity production costs are hence comparable for both concepts, since the higher productivity compensates the additional investment almost for the pre-combustion CO_2 capture processes. CO_2 capture in biomass fed processes leads to a lower electrical production efficiency and to higher costs due to the limited biomass conversion efficiency and to the high investment costs for the gasification process. However, these renewable processes have the advantage of capturing biogenic CO_2 and will thus become interesting if a carbon tax is introduced as shown in Section 8.3. It has to be noted that the considered biomass plant's capacity of 380$MW_{th,BM}$ is much lower than the one of the natural gas plants (580 and 725$MW_{th,NG}$). The biomass plant's scale is limited by the biomass availability and the logistics of wood transport, as explained in Gerber et al. (2011). The influence of the plant's capacity could be evaluated in a future economies of scale analysis based on the developed thermo-environomic models.

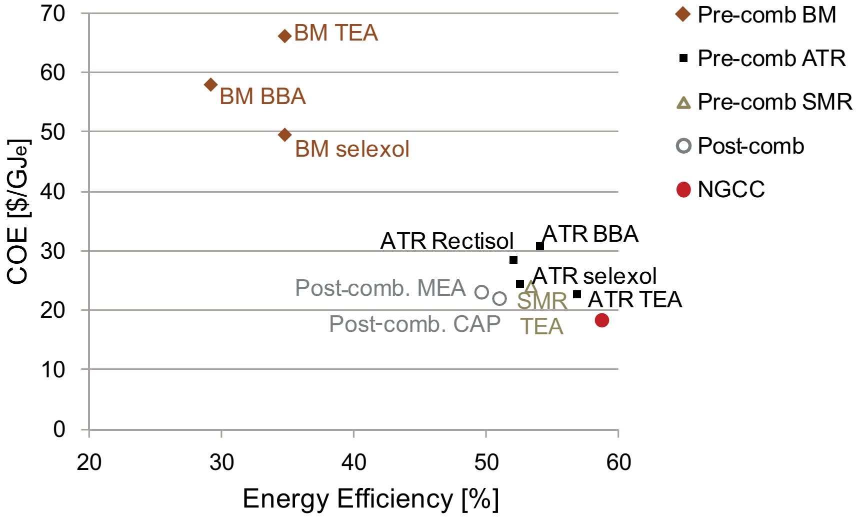

Figure 8.2: Performance results of the different power plant options with CO_2 capture reported in Table 8.1. For natural gas fed processes a capture rate of 90% is considered and 60% for biomass fed processes.

Table 8.1: Performance of the different power plant options with CO_2 capture. For natural gas fed processes a capture rate of 90% is considered and 60% for biomass fed processes. The corresponding operating conditions are reported in in Appendix Tables D.4 & D.7.

System Capture technology	NGCC no CC	Post-comb MEA	Post-comb CAP	ATR TEA	ATR Selexol	SMR TEA	BM TEA	BM Selexol
Feed [$MW_{th,NG/BM}$]	559	587	588	725	725	725	380	380
CO_2 capture [%]	0	89.5	89.7	89.7	89.1	89.3	59	59
ϵ_{tot} [%]	58.75	49.6	50.9	56.8	52.6	53.3	34.8	34.8
Power Balance								
Net electricity [MW_e]	328	291	299	408	375	381	132	132
$\dot{E}^+_{Consumption}$ [$MJ_e/GJ_{e,net}$]	-	108.3	44	91.9	146.6	48.1	342.4	342.4
$\dot{E}^-_{SteamNetwork}$ [$MJ_e/GJ_{e,net}$]	340.7	341.3	301	200	177.6	143.8	346.2	346.2
$\dot{E}^-_{GasTurbine}$ [$MJ_e/GJ_{e,net}$]	659.3	767	743	891.9	969	904.3	996.2	996.2
Economic Performance (Assumptions Table 1.2)								
Invest. [$/$kW_e$]	555	909	785	757	813	798.8	7380	3880
COE no CO_2 tax [$/$GJ_e$]	18.31	23.7	22.5	22.67	24.5	24.1	66.1	49.5
COE with CO_2 tax [$/$GJ_e$]	22	24.2	22.8	23.0	24.9	24.5	60.2	43.6
Avoidance costs [$/$t_{CO2,avoided}$]	-	60	43	46	66	62	173	113
Environmental Performance (FU=1GJ_e)								
CO_2 emissions [kg_{CO2}/GJ_e]	105	14.9	8.5	10.1	11.5	11.2	-170.4	-170.4
IPCC GWP [$kg_{CO2,eq}/GJ_e$]	120	34	27.7	30	31.9	36.1	-139.6	-134.2
EI99 [pts/GJ_e]	7.48	7.7	7.7	7.7	8.1	9.0	6.2	6.1
Impact 2002 [$10^{-3}pts/GJ_e$]	28.9	20.8	20.3	21.5	22.4	25	2.9	3.2
CML Acidification [$10^{-2}kg_{SO2,eq}/GJ_e$]	20.1	14.9	15.4	20.6	21.8	24.3	21.3	21.1
CML Eutrophication [10^{-3} $kg_{PO4,eq}/GJ_e$]	39	23.6	24.4	37.7	40.6	43.5	95.1	95

8.2.2 Environmental performance

In order to evaluate the environmental impacts of the whole process chain, life cycle assessment is performed. The major principles of LCA have been summarised in Section 1.3.4 and Gerber et al. (2011). The scope of this study being to evaluate power plants with CO_2 capture, 1 GJ_e of net electricity produced is chosen as a functional unit ($FU=1GJ_e$). In the life cycle inventory phase every flow, crossing the system boundaries as an extraction or an emission, which is necessary to one of the unit processes, is identified and quantified based on the process layouts described in Figures 3.2, 3.3 and 5.1. The major process steps are resource extraction, syngas production, gas treatment and CO_2 removal, and heat and power generation.

The data available from the Ecoinvent database (Ecoinvent) are used to compute the different contributions of the unit processes. For the life cycle impact assessment, different impact methods are considered: IPCC 07, Impact 2002+ (endpoint categories), Ecoindicator 99 (hierarchist perspective) and CML 2001. The IPCC 07 method calculates the global warming potential by using the characterisation factors of different gaseous emissions published by the International Panel on Climate Change in 2007 (IPCC). The global warming potential over 100 years is computed in terms of CO_2 equivalent emissions. In addition to the climate change impact, the impacts on the resources, the human health and the ecosystem quality are evaluated based on the damage-oriented Ecoindicator 99 method and the Impact 2002+ method. The CML method uses in opposition a problem-oriented approach. The considered impacts categories include the most currently used ones: acidification potential (European), climate change (GWP 100 years), eutrophication potential (generic) and stratospheric ozone depletion (ODP steady state). The results obtained with these impact methods are summarised in Table 8.1 for the different process options and discussed in detail hereafter.

With regard to the assessment of the global warming potential expressed in terms of CO_2 equivalent emissions, it has to be noted that fossil, biogenic and sequestrated CO_2 emissions from power plants are handled in a different manner. The GWP of fossil CO_2 emissions is standardised to 1, while for biogenic CO_2 emissions the GWP is considered as 0. When CO_2 is sequestrated, there is consequently a different effect on the GWP depending on the CO_2 origin. Storage of fossil CO_2 accounts as zero to GWP, while storage of biogenic CO_2 leads to a GWP of -1. The negative balance is due to the fact that the released CO_2 was previously fixed in the plant as hydrocarbon by photosynthesis.

The climate change impact of the different process options is detailed in Figure 8.3 for the IPCC 2007 method. Compared to a conventional NGCC plant without CO_2 capture, the benefit of capturing CO_2 can clearly been seen. For the natural gas fed processes, the major contributions to the greenhouse gas emissions are coming from the natural gas and from the uncaptured CO_2. With CO_2 capture, the contribution from the natural gas is slightly larger because of the lower power plant efficiency. For biomass fed processes, the advantage of capturing biogenic CO_2 is revealed by the negative overall CO_2 balance.

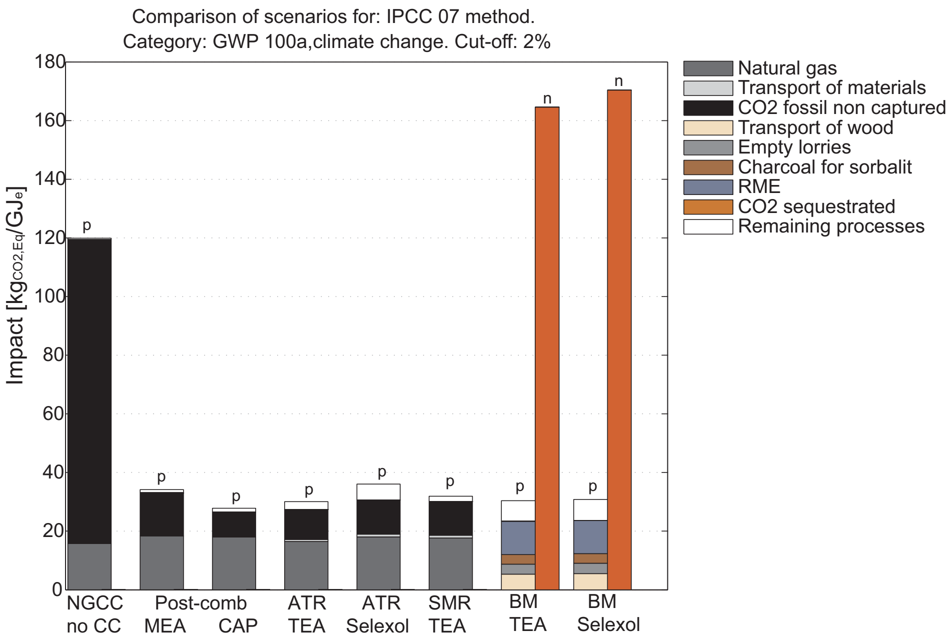

Figure 8.3: Comparison of the climate change impact of power plants without and with CO_2 capture based on the impact method IPCC 07 for $1GJ_e$. Contributions that are harmful are labelled with a p and beneficial ones with an n.

The damages on the other impact categories assessed with the Impact 2002+ and Ecoindicator 99 method are reported in Figure 8.4.

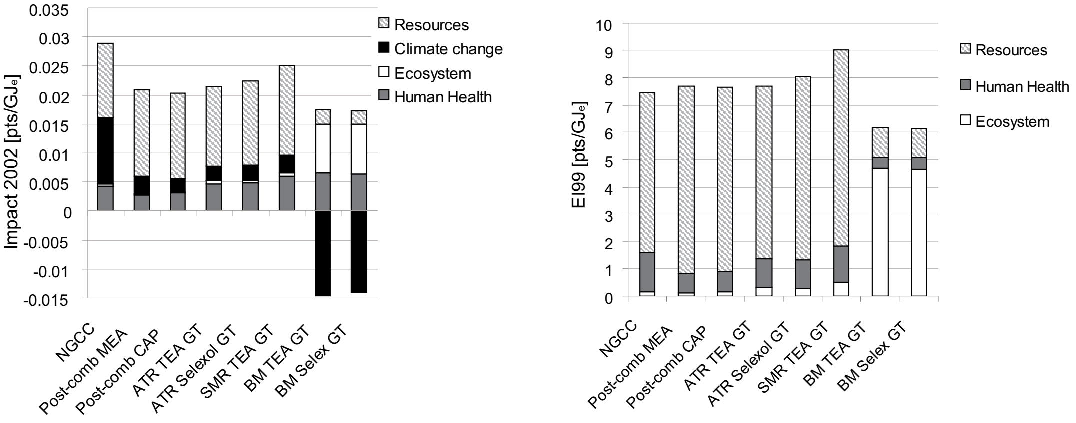

Figure 8.4: Comparison of the life cycle impacts of power plants without and with CO_2 capture based on the impact methods Impact 2002+ (left) and Ecoindicator 99-(h.a) (right) for $1GJ_e$. Contributions that are harmful are positive and beneficial ones negative.

It is to note that for the Impact 2002+ method the climate change impact is considered separately from the human health impact taking into account human toxicity, respiratory effects, ionising radiation, ozone layer depletion and photochemical oxidation. While for the Ecoindicator 99 method, climate change impacts are aggregated with carcinogenic, ionising radiation, ozone layer depletion and respiratory effects in the human health impact category. For natural gas fed processes, the largest impact is coming from the resources followed by the climate change, the human health and the ecosystem. While for biomass based processes, the impact on the ecosystem is much more important. The detailed contributions to these impact categories are presented for the Ecoindicator 99 method in Figures 8.5-8.7 and discussed hereafter.

For natural gas based processes with CO_2 capture, the impact on the resources reported in Figure 8.5 is large since fossil resources are depleted. Due to the energy demand for CO_2 capture and compression, the natural gas consumption is increased to produce 1 GJ of electricity compared to a conventional plant without CO_2 capture having a higher productivity. For processes using biomass, which is a renewable resource, the impact on the resources is not significant, however the impact on the ecosystem is important as shown in Figure 8.6. The usage of renewable resources, such as wood, influences of course the ecosystem. The largest contribution is however attributed to rape methyl ester (RME) consumed in the cold gas cleaning step. RME is produced from colza which is cultivated with insecticides. These insecticides have a large impact on the ecosystem. To reduce this impact alternative colza cultivation methods, the usage of other types of oils, and the development of alternative cleaning methods have to be investigated. When using palm biodiesel instead of RME, the ecosystem impact could be reduced by 35%. Based on the results from Section 3.4, analysing the production of H_2 production from biomass, one possible option would be to use this H_2 to produce ammonia for the fertiliser industry. Using renewable resources to produce ammonia will considerably reduce the environmental impact as reported in Tock et al. (2012g) and Perrenoud (2012), and consequently also the fertiliser impact.

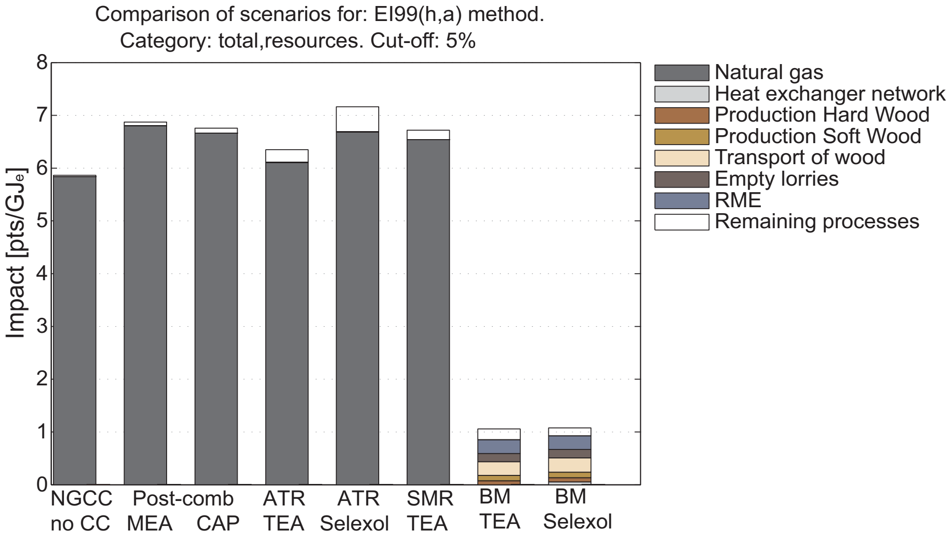

Figure 8.5: Contributions to the resources impact based on the impact method Ecoindicator 99-(h.a) for $1GJ_e$ of electricity produced by power plants without and with CO_2 capture.

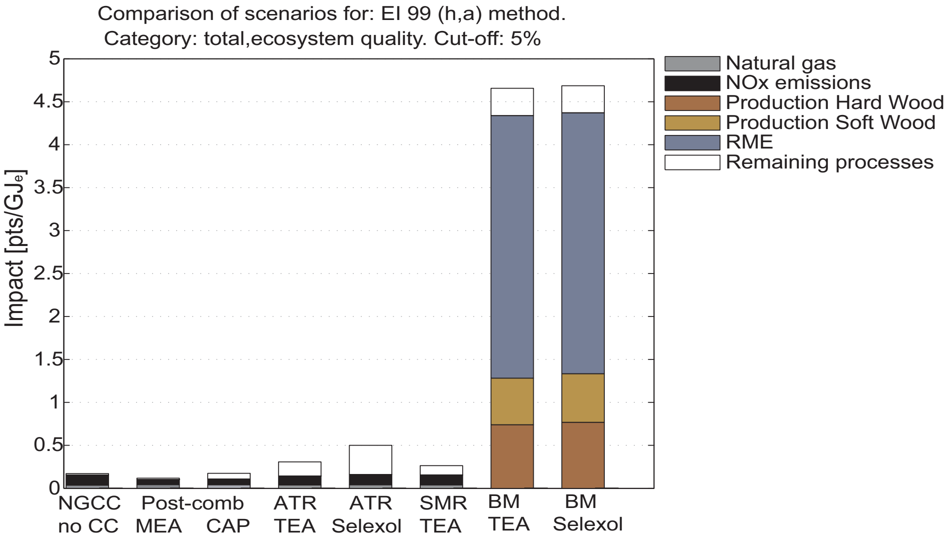

Figure 8.6: Contributions to the ecosystem impact based on the impact method Ecoindicator 99-(h.a) for $1GJ_e$ of electricity produced by power plants without and with CO_2 capture.

Regarding the impact on the human health illustrated in Figure 8.7, CO_2 capture in power plants is advantageous.

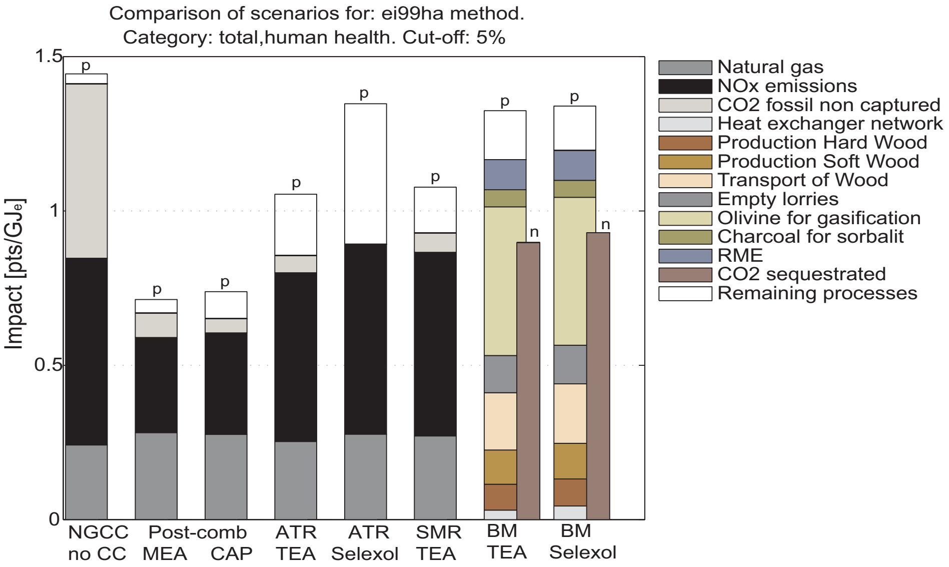

Figure 8.7: Contributions to the human health impact based on the impact method Ecoindicator 99-(h.a) for $1GJ_e$ of electricity produced by power plants without and with CO_2 capture. Contributions that are harmful are labelled with a p and beneficial ones with an n.

The reduction of the CO_2 emissions by CO_2 storage reduces the impact on the human health through the reduction of the climate change impact, accounted with the Ecoindicator 99 method in the human health impact. Pre-combustion CO_2 capture processes have a larger impact on the human health compared to post-combustion CO_2 capture processes due to the larger NOx emissions. For biomass based processes the olivine consumed in the gasification constitutes a large contribution. However, the negative impact from the capture of biogenic CO_2 leads to a low overall impact on the human health.

With regard to the acidification potential assessed with the CML method, the major contributions are the resources, the NO_x emissions and for biomass fed processes the RME, as reported in Figure 8.8. The comparison of the CO_2 capture options with the conventional NGCC plant shows that the impact is comparable. Only post-combustion CO_2 capture processes yielding slightly lower NO_x emissions have a lower impact. For the NO_x emissions estimation, power industry standards limiting the NO_x emissions to 25-45ppm have been considered. It has been assumed that the NO_x emissions do not exceed 30ppm. Consequently, technologies have to be available and implemented to abate the emissions to this level. This assumption explains the acidification potential trends. Similarly the eutrophication potential, mainly defined by the feedstock and the NO_x emissions, is comparable for pre-combustion CO_2 capture processes and slightly lower for post-combustion CO_2 capture processes as reported in Figure 8.9. Biomass based processes favoured with regard to the climate change impact, have a twice as high eutrophication impact. This is mainly due to the large contribution of the RME. As previously discussed this impact could be decreased by using alternative cultivation methods or gas cleaning technologies. The impact to the stratospheric ozone depletion is negligible for each CO_2 capture option.

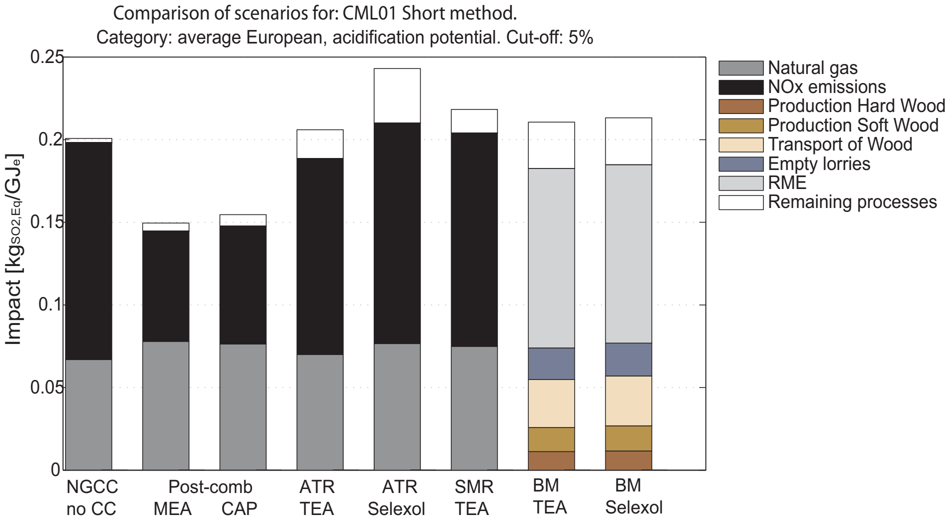

Figure 8.8: Contributions to the acidification potential based on the impact method CML01 for 1GJ$_e$ of electricity produced by power plants without and with CO_2 capture.

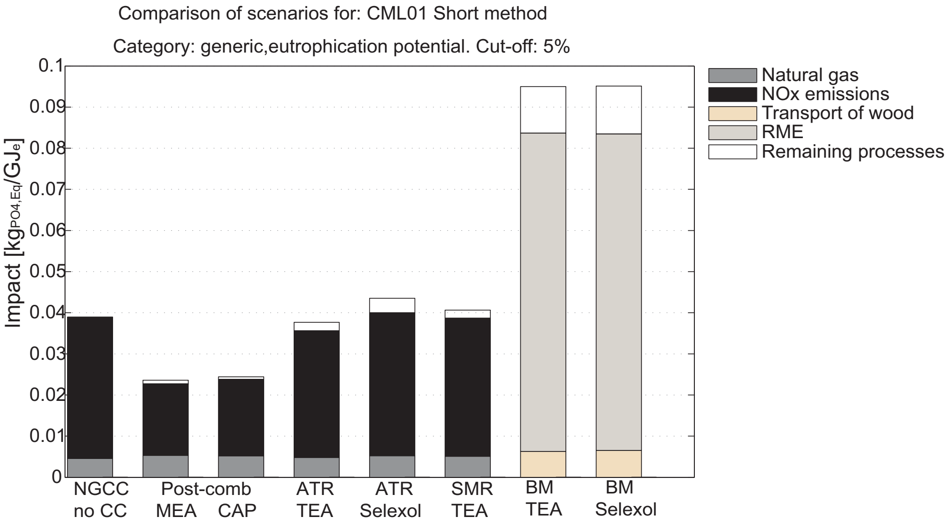

Figure 8.9: Contributions to the eutrophication potential based on the impact method CML01 for 1GJ$_e$ of electricity produced by power plants without and with CO_2 capture.

The comparison of the environmental impacts of CO_2 capture in power plants clearly reveals the benefit of reducing greenhouse gas emissions on the climate change. Taking into account also other environmental impacts, no clear decision in favour of one specific capture concept can be made. With regard to the resources depletion and the climate change, the most promising solution is obviously CO_2 capture in power plants using renewable resources which leads to a negative CO_2 balance. Similar conclusions can also been drawn for CO_2 capture in H_2 plants as reported in Appendix E.

In order to evaluate the environmental competitiveness of these power plants options with CO_2 capture, a comparison with other power plants options using fossil or renewable resources, like coal fired power plants, hydro power, nuclear or solar is made. The environmental impacts of these processes are taken from Ecoinvent (Ecoinvent) for the IPCC 2007 and the Ecoindicator 99 method. The results reported in Figures 8.10&8.11 show that compared to conventional fossil power plants, CO_2 capture is advantageous especially in terms of the climate change impact. Renewable alternatives, such as hydroelectricity and photovoltaic (PV) being in competition with the biomass based processes, are promising solutions for the future because of the low environmental impacts. Compared to these processes, the renewable biomass fed processes have the advantage of capturing biogenic CO_2 and yielding a negative CO_2 balance. However, the impacts of gas cleaning and treatment have to be improved by future developments, as discussed previously, to improve the overall environmental performance. Nuclear power plants remain to be heavily discussed due to the risks and impacts of the radioactive waste and are at the time being abandoned by many European politicians.

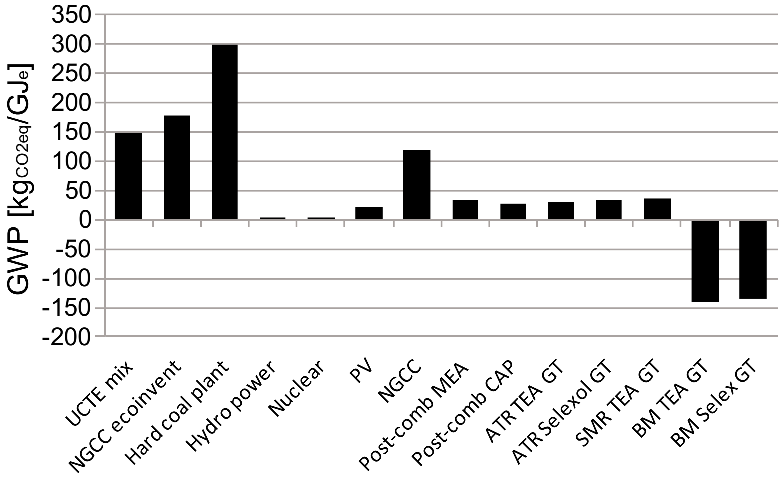

Figure 8.10: Comparison of the environmental performance of electricity generating processes from Ecoinvent (Ecoinvent) and this study (Table 8.1) based on the IPCC impact method.

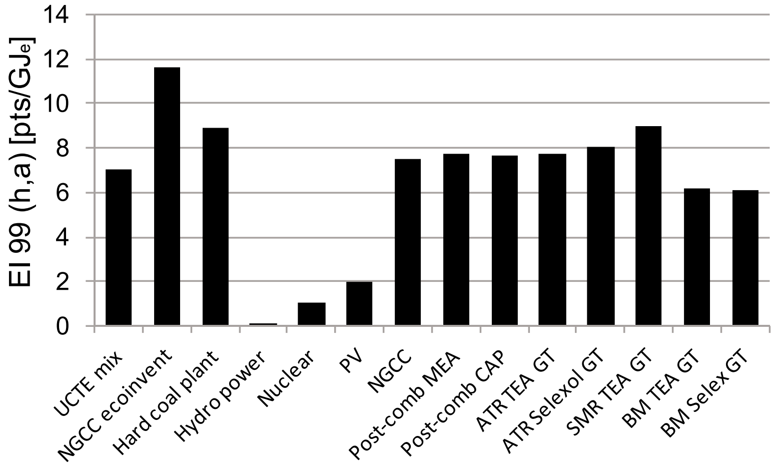

Figure 8.11: Comparison of the environmental performance of electricity generating processes from Ecoinvent (Ecoinvent) and this study (Table 8.1) based on the Ecoindicator impact method.

8.3 Influence of the economic scenarios on the competitiveness of the configurations

The analysis of the economic performance in Chapters 3-6 has revealed that the resource price highly influences the electricity production costs. In order to evaluate the competitiveness of the different CO_2 capture options in power plants applications, sensitivity analysis is first performed on the resource price and the influence of the introduction of a carbon tax is investigated. Then the influence of the economic scenario on the optimal process design and the decision-making is studied.

The analysis of the fossil fuel market over the last years, reveals diverse patterns over time and with regard to the geographic location (i.e. Europe, the United States and Japan) (IEA (2012, 2011b), European Commission (2011, 2010) and Eurostat), as reported in Appendix G. The large fluctuations result from multiple factors affecting the trading. The natural gas price evolution goes in pair with the oil price, while the coal price does not follow the oil price and is predicted to stabilise around 5\$/GJ_{coal} in 2030 (European Commission (2011)). Consequently, the gas to coal price ratio is projected to increase steadily and will together with the carbon price influence investment decisions in the power sector. European gas prices are about twice as high as US gas prices and are projected to be 10\$/GJ_{NG} in 2020, 12\$/GJ_{NG} in 2030 and 16\$/GJ_{NG} in 2050 for the *EU 'Reference'* energy scenario (European Commission (2011)). Future natural gas prices highly depend on the future impact of shale gas which is controversy. Consequently, it is very difficult to project future gas prices.

In a similar way, the carbon tax price is influenced by multiple factors. The emission trading system (ETS) directive has been established in the European Union to promote greenhouse gas emissions reductions in a cost effective and economically efficient manner (European Commission (2012)). The carbon price drop from around 25€/t_{CO2} in 2008 to below 10€/t_{CO2} in the second half of 2011. This evolution coincides with the buildup in surplus of allowances and international credits, and with the financial crisis. According to the predictions from the Energy Roadmap 2050 (European Commission (2011)), carbon tax prices will rise moderately until 2030 and significantly in the last two decades providing support to low carbon technologies and energy efficiency. For the current policy initiatives (CPI) scenario, taking into account the latest policies on energy efficiency, taxation and infrastructure, the carbon tax is predicted to increase to 15€/t_{CO2} in 2020, to 32€/t_{CO2} in 2030 and to 51€/t_{CO2} in 2050. In Switzerland, the situation is different since the carbon tax price is not affected continuously by trading. A tax of 12CHF/t_{CO2} was introduced in 2008 and increased to 36 CHF/t_{CO2} in 2010 in order to reach the target of 33% of emissions reductions in 2020 compared to 1990 (BAFU 2012). With the actual evolution this target might still not be reached, therefore an increase to 60CHF/t_{CO2} could be foreseen for 2014 and to 72CHF/t_{CO2} (or 84CHF/t_{CO2}) in 2016 and 96CHF/t_{CO2} (or 120CHF/t_{CO2}) in 2020 (Schweizerische Bundesrat (2012)). The maximal tax is however limited to 120CHF/t_{CO2}.

Due to this large uncertainty in costs projections, several scenarios are investigated here in order to assess the influence on the competitiveness of the different CO_2 capture options in power plants applications. More details about the price fluctuations and predictions, and the distribution functions of the economic assumptions are reported in Appendix G.

8.3.1 Sensitivity analysis

For some compromise electricity generating process solutions with CO_2 capture, reported in Table 8.1, a sensitivity analysis is performed on the resource purchase price to see the impact on the electricity production costs. The results in Figure 8.12 clearly reveal a linear dependence between the COE and the gas price. Since the specific annual investment is comparable for these process configurations, the process competitiveness is determined primarily by the resource purchase. Without the introduction of a carbon tax, the conventional NGCC plant without CO_2 capture is the most competitive option. However, when a carbon tax of $35\$/t_{CO2}$ is introduced, its benefit is reduced and the scenarios with 90% of CO_2 capture become competitive. The break even natural gas price for which the post-combustion CO_2 capture process becomes competitive is around $6\$/GJ_{NG}$ for a carbon tax of $35\$/t_{CO2}$. Consequently, there is a trade-off between the natural gas price and the carbon tax.

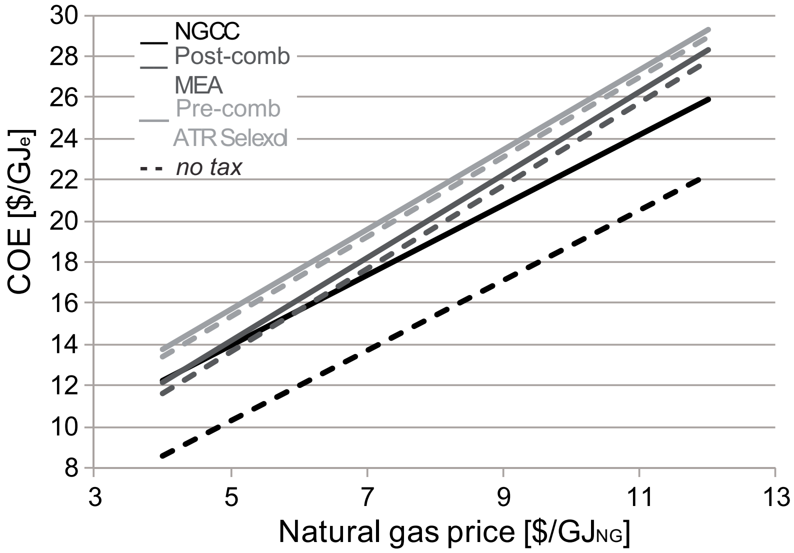

Figure 8.12: Influence of the natural gas purchase price on the electricity production costs without (- -) and with (–) the inclusion of a carbon tax of $35\$/t_{CO2}$ for the process configurations reported in Table 8.1.

The influence of the carbon tax on the electricity production costs considering a natural gas price of $9.7\$/GJ_{NG}$ and a biomass price of $5\$/GJ_{BM}$ respectively is illustrated in Figure 8.13. Under these conditions, the break even carbon tax is around $50\$/t_{CO2}$ for post-combustion CO_2 capture with MEA and around $62\$/t_{CO2}$ for pre-combustion CO_2 capture with Selexol. Due to the benefit of capturing biogenic CO_2, CO_2 capture in biomass fed power plants becomes competitive with natural gas fed processes for a carbon tax of $62\$/t_{CO2}$. The inclusion of a carbon tax will hence promote biomass based processes. In these analyses, the CO_2 capture rate and thus the process design are fixed. However, it is evident that there is a trade-off between the economic performance and assumptions, and the process design, in particular the CO_2 capture rate. This issue is addressed in detail in the following Section 8.3.2.

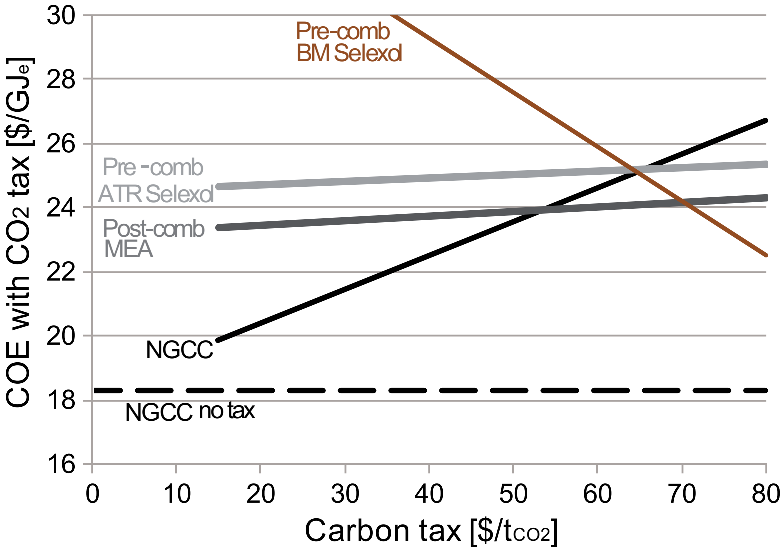

Figure 8.13: Influence of the carbon tax on the electricity production costs without and with CO_2 capture for a natural gas price of 9.7\$/GJ$_{NG}$ and a biomass price of 5\$/GJ$_{BM}$ for the process configurations reported in Table 8.1.

8.3.2 Economic scenarios influence

In order to study the influence of the economic scenario on the process design, it is focused on three different capture options, namely post-combustion CO_2 capture with MEA applied to the NGCC plant and pre-combustion CO_2 capture with Selexol in natural gas fuelled power plants (i.e. ATR) and in biomass based power plants. The analyses are based on the Pareto optimal frontiers that are resulting from the multi-objective optimisations made in Sections 4.4 & 6.3 (Figures 4.5 & 6.5). These optimisations maximising the energy efficiency and/or the CO_2 capture rate and/or minimising the production costs have revealed the trade-off between energy efficiency, costs and CO_2 capture. For each scenario the process configurations yielding the lowest COE are identified on the following graphs by a red circle.

The influence of the inclusion of a carbon tax on the economic performance is illustrated in Figure 8.14. It can be seen that with a low carbon tax (20\$/t$_{CO2}$), the CO_2 capture rate does not significantly impact the electricity production costs. While, the inclusion of a high carbon tax (65\$/t$_{CO2}$) favours process configurations with a high CO_2 capture rate leading to lower electricity production costs. In addition, the renewable biomass fed process becomes competitive under these conditions. With a carbon tax of 20\$/t$_{CO2}$, the COE of the reference plant without CO_2 capture becomes 20.4$/GJ$_e$, respectively 25.2$/GJ$_e$ with a tax of 65$/t$_{CO2}$. With high CO_2 taxes, pre- and post-combustion CO_2 capture is advantageous with regard to an NGCC plant without CO_2 capture.

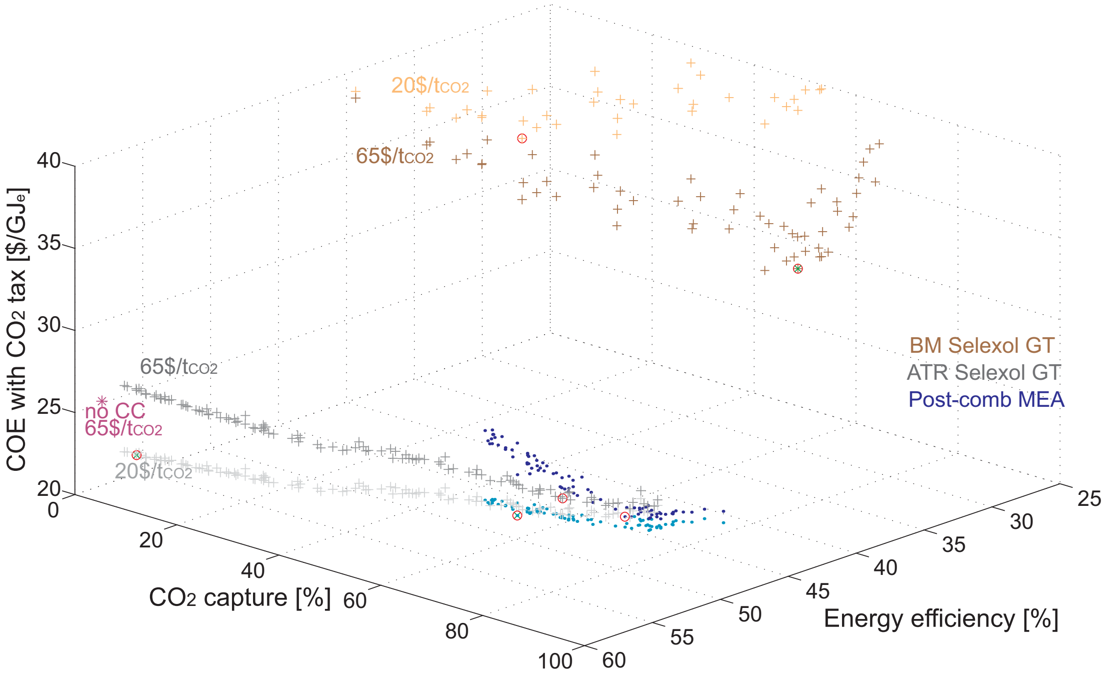

Figure 8.14: Influence of the carbon tax on the electricity production costs for different CO_2 capture process options.

The optimal CO_2 capture rate is consequently defined by the economic considerations. The trade-off between the resource price and the carbon tax is illustrated in Figure 8.15. It can be seen that a low resource price (5.5$/GJ$_{NG}$) and a high carbon tax (65$/t$_{CO2}$) favour process configurations with a high CO_2 capture rate. While process configurations with lower capture rates are more competitive for the other economic conditions.

In order to study the influence of the economic scenario on the competitiveness of the process configurations more in detail two different economic scenarios are compared with the base case assumptions reported in Table 1.2. For each economic scenario the major assumptions are summarised in Table 8.2.

Table 8.2: Definition of the economic scenarios.

Scenario	Base	Low	High
Resource price [$/GJ$_{res}$]	9.7	14.2	5.5
Carbon tax [$/t$_{CO2}$]	35	20	55
Yearly operation [h/y]	7500	4500	8200
Expected lifetime [y]	25	15	30
Interest rate [%]	6	4	8

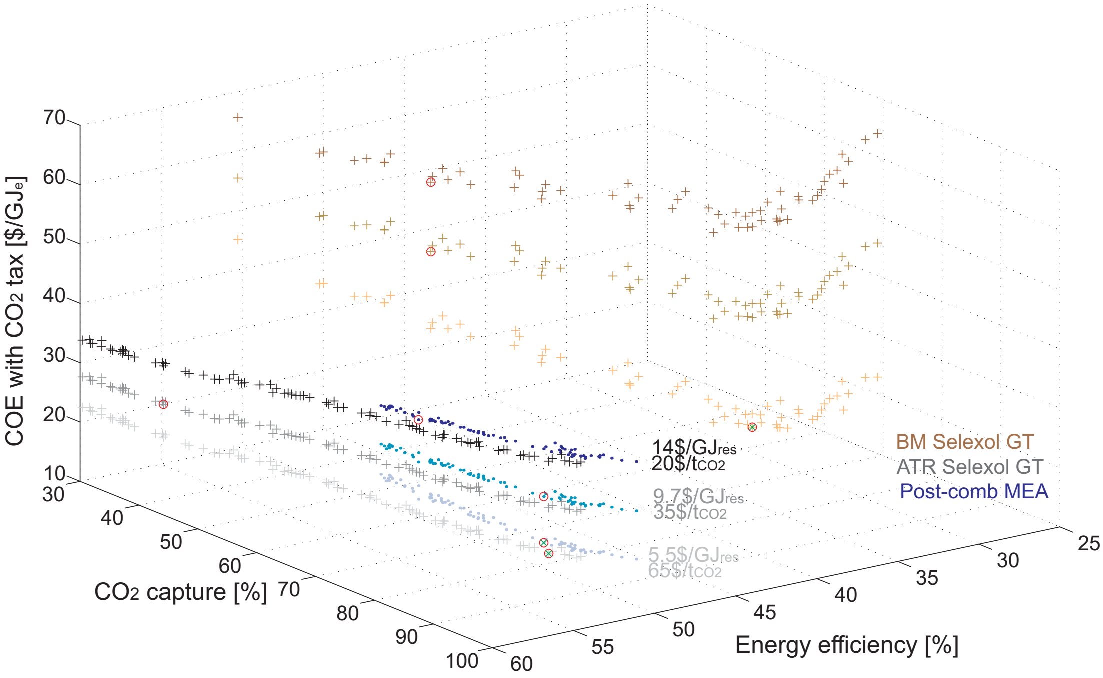

Figure 8.15: Influence of the carbon tax and of the resource price on the electricity production costs for different CO_2 capture process options.

For power plants with pre-combustion CO_2 capture with Selexol, it is highlighted in Figure 8.16 how the optimal process design is influenced by the economic scenario. For part load operation, high resource prices and a low carbon tax (*low*), CO_2 capture is not beneficial. While for medium load operation, low resource price and high carbon tax (*high*), process configurations with high CO_2 capture rates are favoured. For the economic scenario *high*, the electricity production costs (incl. CO_2 tax) decrease with increasing CO_2 capture rates (Figure 8.16 (left)) can be explained by the profit from the carbon tax. Compared to a conventional NGCC plant without CO_2 capture, the process competitiveness can be expressed by the CO_2 avoidance costs calculated based on the COE including the carbon tax. It is considered that the reference plant is also submitted to the different economic scenarios. When including the carbon tax, the COE of the NGCC plant becomes $27.5\$/GJ_e$ for the *low*, $21.99\$/GJ_e$ for the *base* and $17\$/GJ_e$ for the *high* economic scenario, respectively. Figure 8.16 (right) reveals that with the base case assumptions CO_2 avoidance costs below $50\$/t_{CO2,avoided}$ can be reached for capture rates above 40%, while for the economic scenario *low*, negative CO_2 avoidance costs can be reached for capture rates above only 30%. Above 40% CO_2 capture, the decrease of the CO_2 avoidance costs with the CO_2 capture rate increase is less distinct. For power plants with post-combustion CO_2 capture similar trends are revealed in Figure 8.17.

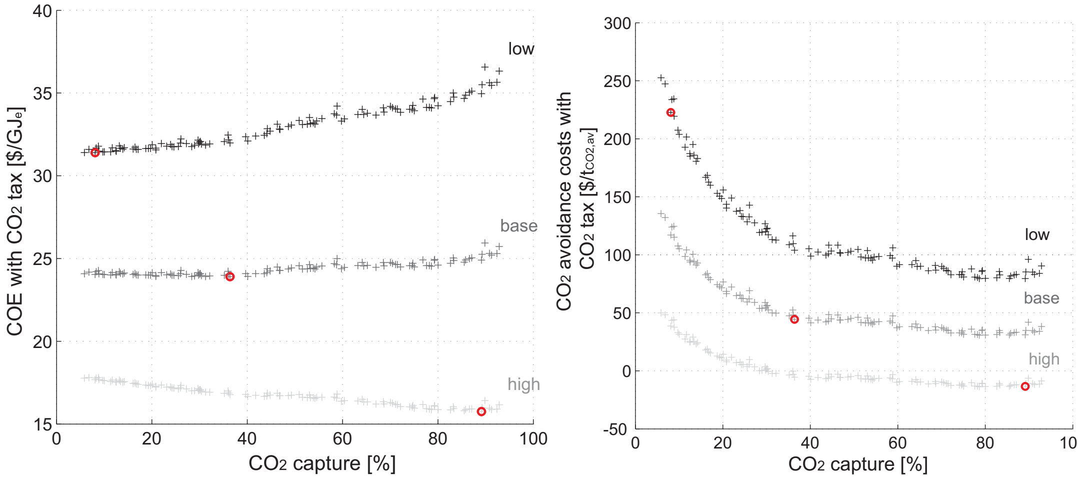

Figure 8.16: Influence of the economic scenarios defined in Table 8.2 on the performance of pre-combustion CO_2 capture with Selexol in a natural gas fired power plant using ATR.

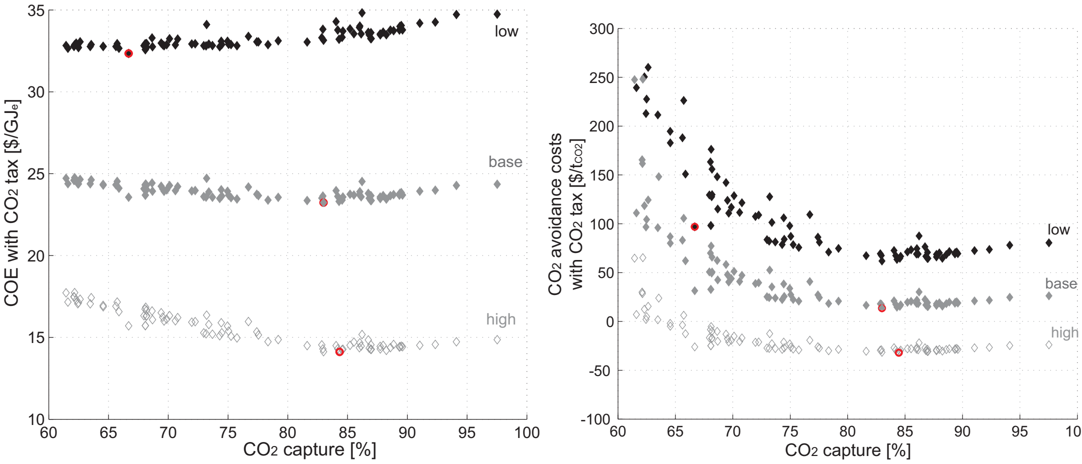

Figure 8.17: Influence of the economic scenarios defined in Table 8.2 on the performance of post-combustion CO_2 capture with MEA in a natural gas fired power plant.

For biomass based power plants an optimum with regard to the CO_2 capture rate can clearly be identified in Figure 8.18. At capture rates above 70%, the production costs increase due to the increase in capital costs and the decrease in efficiency, which are not compensated by the benefit of the carbon tax (Figure 8.18 (left)). Below 70% of CO_2 capture, the capture of an additional unit of CO_2 does not impact significantly the COE. The CO_2 avoidance costs variation in Figure 8.18 (right) translates these trends and shows the advantage of capturing biogenic CO_2. Even if, the biomass conversion is lower and the capital investment larger than for natural gas based processes, biomass conversion processes become hence competitive under specific economic conditions due to the benefit from the carbon tax.

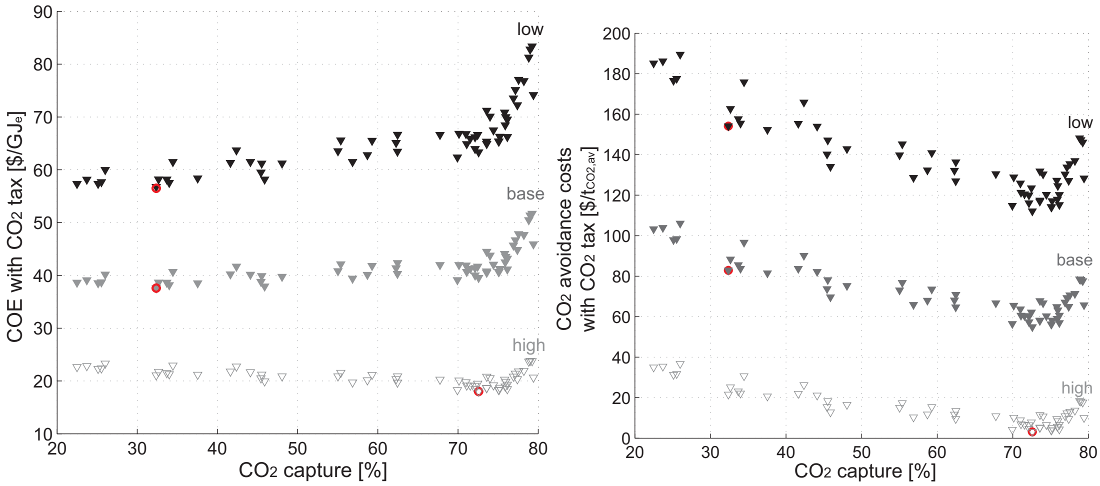

Figure 8.18: Influence of the economic scenarios defined in Table 8.2 on the performance of pre-combustion CO_2 capture with Selexol in a biomass fed power plant.

These results clearly reveal the dependence of the CO_2 capture competitiveness on the economic scenario and consequently on the decision-making with regard to the CO_2 capture rate and the process configuration.

The comparison in Figure 8.19 of the results for these three electricity generating processes with CO_2 capture shows again how the choice of the optimal process configuration is affected by the economic scenario. The 2D representation in Figure 8.20, highlights the competition between different configurations. For the economic scenario *low*, post-combustion CO_2 capture processes perform best in terms of the electricity production costs for each capture rate. For the base case assumptions, pre- and post-combustion CO_2 capture in natural gas fuelled power plants perform equally in terms of COE for capture rates between 60 and 75%, whereas biomass based processes are more expensive. While for the economic scenario *high*, CO_2 capture in biomass fed processes generating green electricity becomes much more competitive. For natural gas fed power plants, pre-combustion CO_2 capture is advantageous with regard to the COE for capture rates below 75% and post-combustion CO_2 capture for higher capture rates. For high capture rates post-combustion CO_2 capture in NGCC plants seems to perform best with regard to the electricity production costs, while pre-combustion CO_2 in natural gas fed power plants is advantageous in terms of energy efficiency and CO_2 capture in biomass based power plants is beneficial with regard to the environmental performance. Consequently, there is a competition between the different processes. The production priority and scope define the decision that has to be taken. In Section 8.3.2, an approach to support decision-making from these Pareto results under different economic scenarios will be presented.

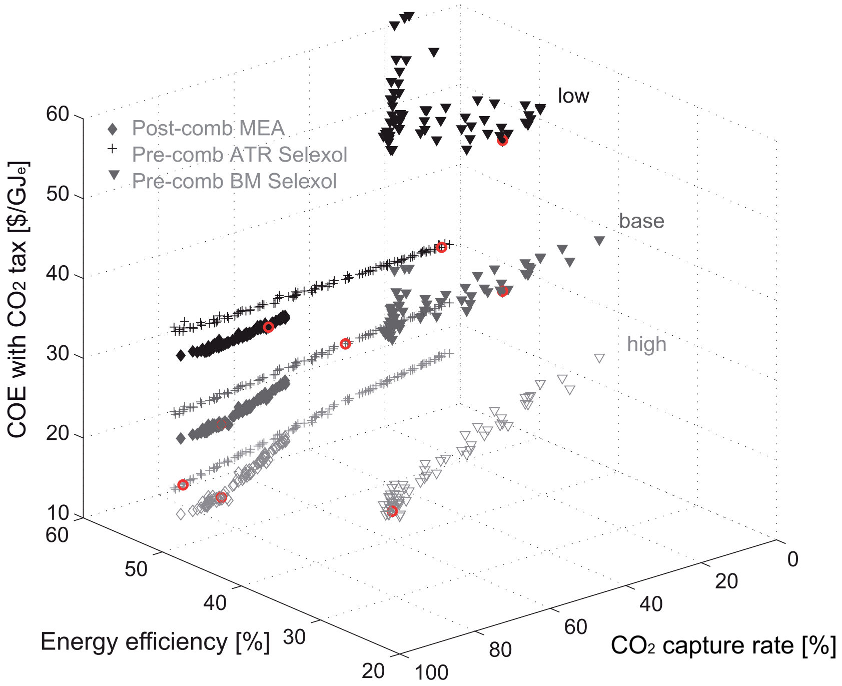

Figure 8.19: Influence of the economic scenarios defined in Table 8.2 on the performance of electricity generating processes with CO_2 capture.

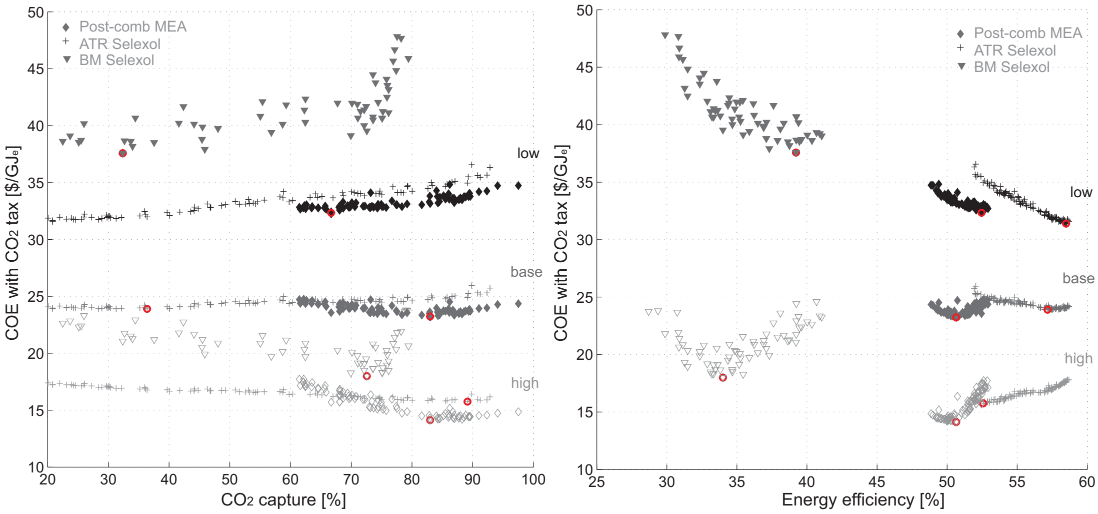

Figure 8.20: Influence of the economic scenarios defined in Table 8.2 on the performance of electricity generating processes with CO_2 capture - 2D representation.

Monte Carlo simulation

Considering the uncertainty of the economic assumptions, a Monte Carlo simulation can be performed in order to evaluate the impact on the economic performance. For this purpose, the input economic parameters presented in Table 8.2 are described by distribution functions presented in detail in Appendix G.2. In addition, an uncertainty of ±30% (Turton (2009)) is included for the capital investment estimation. The characteristics of the distribution functions (i.e. uniform, normal or beta distribution) describing the different variables are defined in Table 8.3.

Table 8.3: Parameters of the distribution functions for the economic assumptions (illustrated in Appendix Figures G.4 & G.5).

	Distribution	Parameter A	Parameter B	Parameter C
Resource price [$/GJ$_{Res}$]	Normal	μ=9.7	σ=2.5	-
Carbon tax [$/t$_{CO2}$]	Beta	a=2	b=1.5	cst=100
Yearly operation [h/y]	Beta	a=3.9	b=1.2	cst=8600
Interest rate [-]	Normal	μ=0.06	σ=0.01	-
Economic lifetime [y]	Beta	a=5.8	b=4	cst=40
Investment [-]	Uniform	a=-0.3	b=0.3	-

The objective functions for the Monte Carlo simulation are the minimisation of the electricity production costs including the carbon tax and the minimisation of the CO_2 avoidance costs. In the CO_2 avoidance costs calculation, it is assumed that the COE includes the carbon tax and that the reference NGCC plant's COE is also subject to the economic scenario variation. A Monte Carlo simulation is performed to evaluate the competitiveness of the different compromise process configurations reported in Table 8.1. Figure 8.21 summarises the results for the conventional NGCC plant without CO_2 capture and for the different electricity generating process configurations with CO_2 capture (i.e. 90% of CO_2 capture for natural gas fed processes and 60% for biomass ones). For each scenario, the performance reported in Table 8.1 for the base case economic assumptions (Table 1.2) is highlighted by a characteristic marker. The performance variation with the economic scenario is illustrated by the area with the corresponding colour. The area represents the boundary of the objective functions variation, when changing the economic assumptions according to the distribution functions. For the NGCC reference plant, the COE variation is pointed out for two extreme economic scenarios. These results reveal that by taking into account the uncertainty of the economic assumptions, the different CO_2 capture processes compete with conventional NGCC plants if a carbon tax is introduced. For certain economic scenarios, negative CO_2 avoidance costs are achieved, which underline that CCS can become a competitive alternative compared to NGCC plants without CO_2 capture.

Here the Monte Carlo approach has been applied to the results in order to study the influence of the economic assumptions. Following the stochastic methodology presented in Dubuis (2012), uncertainty could in addition be included in the design and multi-objective optimisation of the energy systems.

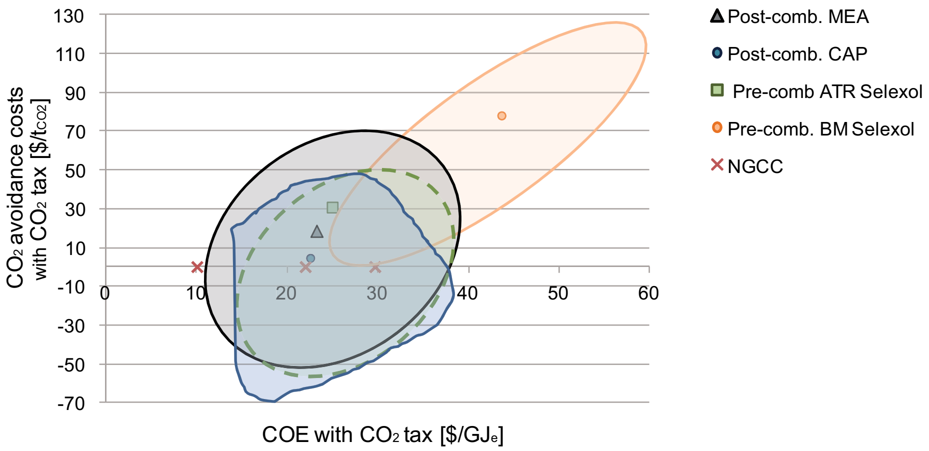

Figure 8.21: Assessment of the influence of the economic assumptions uncertainty on the COE and CO_2 avoidance costs accounting for a CO_2 tax, for the configurations presented in Table 8.1. The markers represent the performance for the base case economic scenario, and the corresponding coloured area the variation of the COE with the economic conditions.

Decision-making

The previous results have shown that the various process options are in competition and that the competitiveness of the process configurations highly depends on the economic scenario. In order to support decision-making based on the Pareto results obtained for different economic scenarios, a selection approach is proposed here. To illustrate this approach, it is focused again on the three representative capture options, namely post-combustion CO_2 capture with MEA applied to the NGCC plants and pre-combustion CO_2 capture with Selexol in natural gas fuelled power plants based on ATR and in biomass fired power plants. The analyses are based on the optimisation results, revealing the trade-off between energy efficiency and CO_2 capture (Sections 4.4 & 6.3, Figures 4.5 & 6.5). The economic scenarios are defined by the distribution functions given in Table 8.3.

Looking at results such as in Figure 8.19, it is not obvious which configuration has to be chosen from the Pareto results. The aim is here to propose an approach which allows to identify the optimal process design from the Pareto-optimal solutions taking into account the economic conditions sensitivity. First a series of 1000 economic scenarios is randomly generated by applying the distribution functions given in Table 8.3. For every single economic scenario the economic performance (i.e. COE including carbon tax) of the Pareto-optimal solutions is then recomputed. From the Pareto-optimal solutions the five best configurations that yield the lowest COE (including CO_2 tax) are then identified. After having identified the five most economically competitive configurations for all the economic scenarios, it is possible to see if some configurations are dominating or if some are never part of the five best performing ones. In order to evaluate this quantitatively, the probability to be part of the five best performing configurations is then assessed for each point of the Pareto front. This allows finally to identify the most economically competitive process configurations in the wide range of economic scenarios.

For the NGCC plant with post-combustion CO_2 capture, Figures 8.22&8.23 reveal how the choice of the optimal process configurations is influenced by the economic scenario. Process configurations with CO_2 capture rates between 80 and 85% appear to be the best choice for a large range of economic scenarios. Configurations with lower capture rates are mainly selected for economic scenarios with a carbon tax below 35\$/t_{CO2}, as previously discussed.

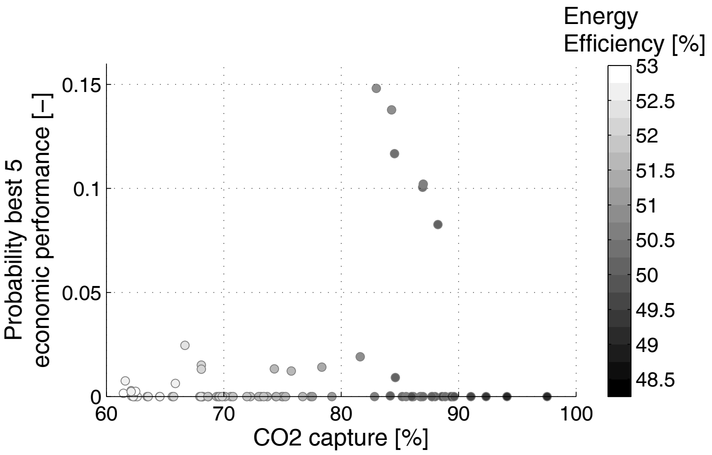

Figure 8.22: Natural gas fired power plant performance with post-combustion CO_2 capture with MEA: Probability of each point to be part of the top 5 configurations yielding the best economic performance under different economic scenarios.

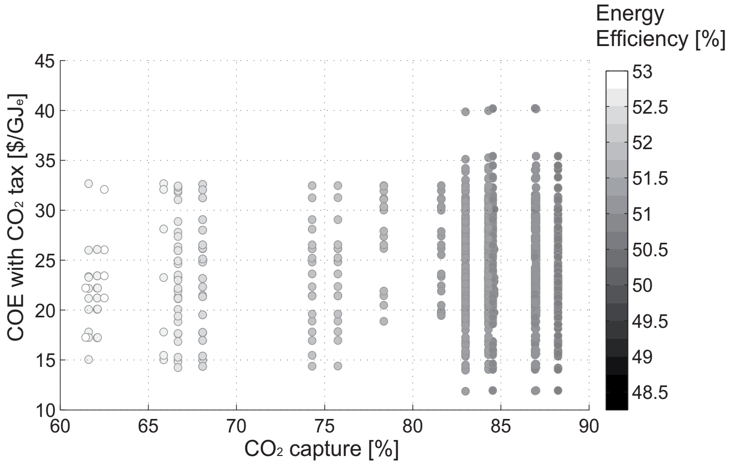

Figure 8.23: Natural gas fired power plant performance with post-combustion CO_2 capture with MEA: Influence of the economic scenario on the electricity production costs (incl. a carbon tax) of the best 5 economic performance configurations.

The results for natural gas or biomass fired power plants with pre-combustion CO$_2$ capture with Selexol represented in Figures 8.24& 8.25 respectively, reveal that process configurations with intermediate CO$_2$ capture rates are the best choice for a large range of economic conditions. For natural gas fuelled power plants, over 80% of pre-combustion CO$_2$ capture becomes competitive with high carbon taxes (>45$/t$_{CO2}$) and low resource prices.

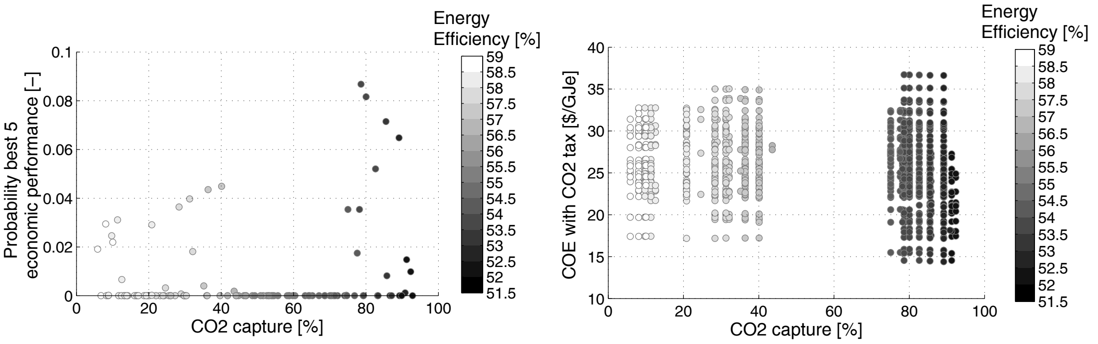

Figure 8.24: Natural gas fired power plant performance with pre-combustion CO$_2$ capture with Selexol: Probability of each point to be part of the top 5 configurations yielding the best economic performance under different economic scenarios (left) and respective influence on the electricity production costs including a carbon tax (right).

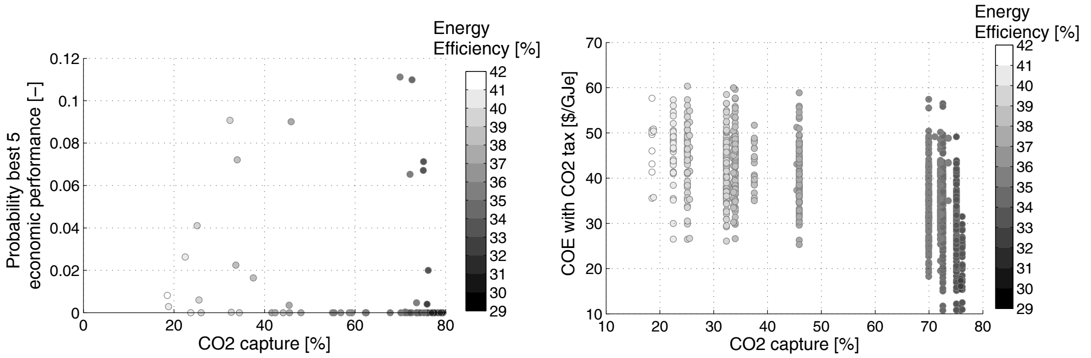

Figure 8.25: Biomass fired power plant performance with pre-combustion CO$_2$ capture with Selexol: Probability of each point to be part of the top 5 configurations yielding the best economic performance under different economic scenarios (left) and respective influence on the electricity production costs including a carbon tax (right).

Instead of choosing the best configuration for a given power plant and CO$_2$ capture scenario, the same approach could be used to identify the best configuration with regard to the different process options. When considering the three investigated CO$_2$ capture options together for the decision-making, the configurations yielding the best economic performance for different economic conditions are identified in Figure 8.26. These results reveal that post-combustion CO$_2$ capture is the best economic choice for capture rates between 70 and 85%. Pre-combustion CO$_2$ capture configurations, being slightly more expensive for similar capture rates, yield however slightly better efficiencies. Depending on the production scope, this could affect decision-making for the more expensive solution. For some marginal economic scenarios (i.e.

high CO_2 tax, low biomass purchase price, low gasifier investment), CO_2 capture in biomass fed power plants becomes a competitive alternative. This is also illustrated in Figure 8.27 showing the variation of the COE of the most economically competitive configurations and the upper and lower borderline performance of all the Pareto-optimal solutions. The economic conditions corresponding to the lower and upper boundary are respectively: 5042//7260h/y, 7.29//62.3\$/GJ$_{res}$, 89//55.8\$/t$_{CO2}$, 6.3//4.1% interest, 25.5//20y lifetime and -23//+25% investment costs estimation.

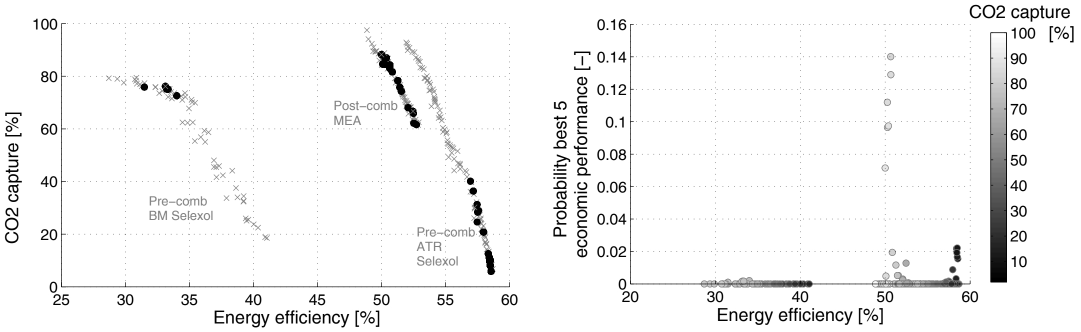

Figure 8.26: Power plants performance with CO_2 capture: Influence of the economic scenario on the top 5 configurations yielding the best economic performance. Decision-making based on the Pareto front (black points) (left) and corresponding probability of each point to be part of the top 5 configurations yielding the best economic performance under different economic scenarios (right).

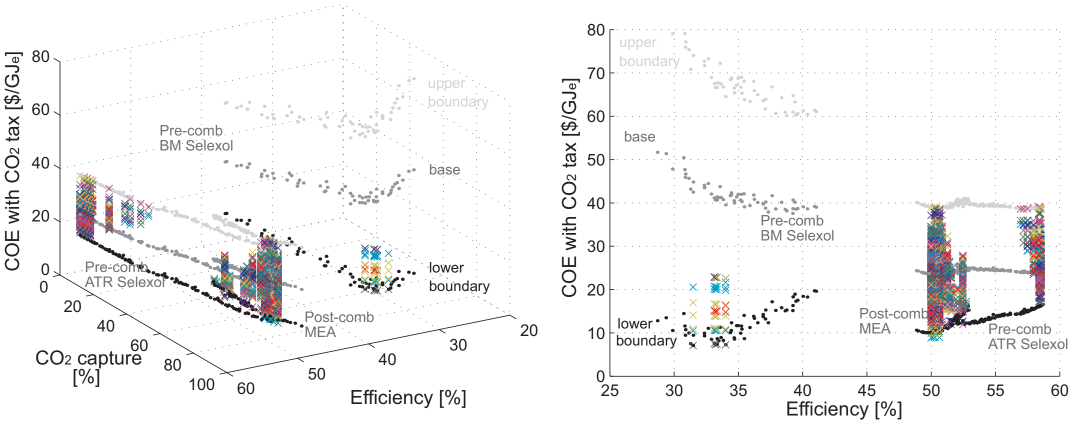

Figure 8.27: Power plants performance with CO_2 capture: Influence of the economic scenario on the decision-making based on the top 5 configurations yielding the best economic performance (left) 2D representation showing the trade-off between COE and energy efficiency (right).

As shown in Figure 8.27 and already discussed previously, biomass fed processes are not competitive for the base case economic scenario and post-combustion CO_2 capture performs best for capture rates around 70-85%. However, when gas prices increase (i.e. moving toward upper boundary) the natural gas based processes become uncompetitive compared to base case biomass configurations. These results point out the competition between the different processes and the influence of the economic scenario on the decision-making. This competition is also highlighted in Figure 8.28 evaluating the overall competitiveness of each Pareto-optimal solution compared to the most-economically competitive solution for the considered economic scenarios. These results clearly show the close competition between post- and pre-combustion CO_2 capture and reveal again the influence of the CO_2 capture rate.

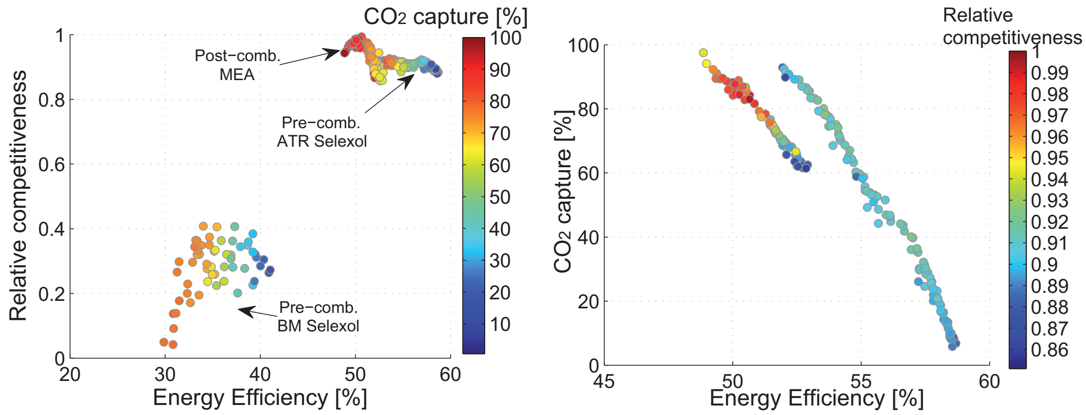

Figure 8.28: Relative competitiveness of each Pareto optimal solution with regard to the most economically competitive solution for the considered economic scenarios (right). Zoom on the relative competitiveness of CO_2 capture in natural gas fired power plants (left).

The performance results of the most economically competitive process designs for each CO_2 capture scenario are summarised in Table 8.4 and the process design parameters are reported in Appendix Tables D.8 & D.9.

From these results, it can be concluded that CO_2 capture becomes economically competitive for captures rates between 70 and 85% when a carbon tax is applied. The various natural gas fed power plants designs with CO_2 capture lead to an average efficiency decrease of 8% (2.3-13.7%). The energy integration of the natural gas fuelled power plant configurations with post-combustion with MEA and pre-combustion with Selexol is compared by the composite curves in Figure 8.29. For the other configurations the process design and energy integration is reported in Appendix D (Figures D.1-D.3). Taking into account the uncertainty of the economic projections the variation in the electricity production costs including a CO_2 tax are illustrated in Figure 8.30 and compared with a conventional NGCC plant without CO_2 capture. These results show that CCS can become an energy, cost and environmental-efficient alternative on the future energy market.

Table 8.4: Performance of the most economically competitive power plant options with CO_2 capture. The corresponding process design parameters are reported in Appendix Tables D.8 & D.9.

System	NGCC no CC	Post-comb MEA	Post-comb CAP	ATR TEA	ATR Selexol	SMR TEA	BM TEA	BM Selexol
Feed [$MW_{th,NG/BM}$]	559	582	587	725	725	725	380	380
CO_2 capture [%]	0	82.98	89.47	83.04	78.63	70.14	33.37	69.93
CO_2 emissions [kg_{CO2}/GJ_e]	105	13.9	8.6	16.5	22.2	29.7	-79.2	-198.1
ϵ_{tot} [%]	58.75	50.65	51.54	57.38	53.59	56.0.6	42.28	35.45
Power Balance								
Net electricity [MW_e]	328	295	302	410	383	400	161	135
$\dot{E}^+_{Consumption}$ [$MJ_e/GJ_{e,net}$]	0	88	34.3	78.6	131.2	6.7	198.2	260.1
$\dot{E}^-_{SteamNetwork}$ [$MJ_e/GJ_{e,net}$]	341	337	299	198	172.8	140.9	341.1	692.2
$\dot{E}^-_{GasTurbine}$ [$MJ_e/GJ_{e,net}$]	659	751	735.3	880.6	958.4	865.8	857.1	567.9
Base case economic scenario (Table 1.2)								
COE no CO_2 tax [$\$/GJ_e$]	18.31	22.7	21.8	22.0	23.7	21.9	38.1	46.1
COE incl. CO_2 tax [$\$/GJ_e$]	22	23.2	22.1	22.6	24.5	22.9	28.1	21.1
Annual Invest. [$\$/GJ_e$]	1.1	2.1	1.8	1.9	2.2	1.6	7.6	9.5
Avoidance costs [$\$/t_{CO2,avoided}$]	-	48.6	36.4	41.5	65.7	47.3	107	91
Avoid. cost incl. CO_2 tax [$\$/t_{CO2,avoided}$]	-	13.6	1.4	6.5	30.7	12.3	72	56
Economic scenario variation (Table 8.3)								
COE incl. CO_2 tax [$\$/GJ_e$] (min)	18.3	9	6.6	7.8	12.8	9	10.8	15
COE incl. CO_2 tax [$\$/GJ_e$] (max)	28.8	40	45	37.8	42	41	81.9	69
Avoid. cost incl. CO_2 tax [$\$/t_{CO2,avoided}$] (min)	-	-63	-72	-62	-49	-63	-22	0
Avoid. cost incl. CO_2 tax [$\$/t_{CO2,avoided}$] (max)	-	121	127	151	127	152	185	253

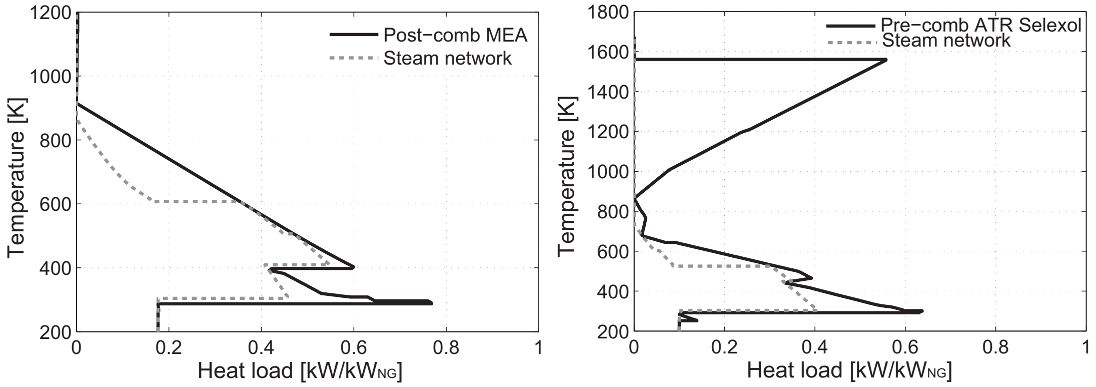

Figure 8.29: Integrated composite curves of the most economically competitive natural gas fired power plant options with post-combustion CO_2 capture with MEA (left) and with pre-combustion CO_2 capture with Selexol (right) reported in Table 8.4.

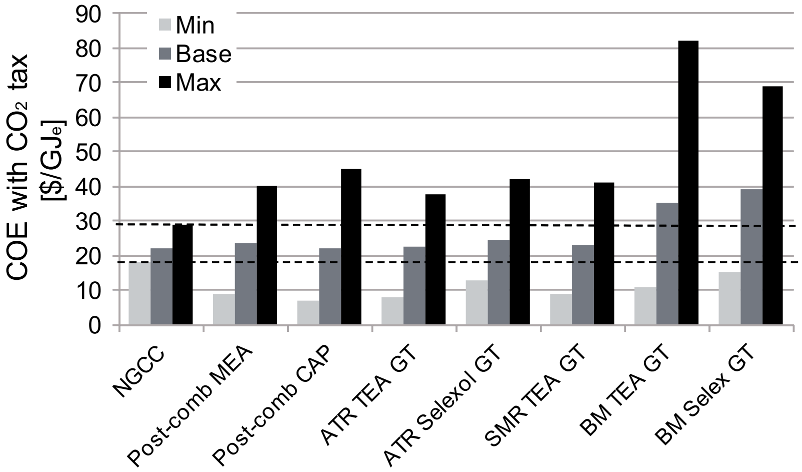

Figure 8.30: Comparison of the most economically competitive power plant options with CO_2 capture based on the economic performance variation, with regard to the different economic scenarios, expressed by the COE including CO_2 tax (Table 8.4).

After this comparative study applying first a systematic methodology for generating process configurations by multi-objective and then a selection tool for supporting decision-making based on the Pareto-optimal solution, one could ask about how the objective function choice influences the optimal process design. From the discussion in Appendix C, it turns out that ideally three objectives, including a thermodynamic, economic and environmental dimension, have to be considered, respectively two objectives whereof one combines two of these dimensions. By changing the objective function different optimal process configurations could emerge, because of the close competition between the different process options. In order to reveal the optimal process design with regard to different objectives the same analysis could be repeated for several objective functions in a future study.

8.4 Market competition of CO_2 capture in power plants

When evaluating the market competition of CO_2 capture in power plants applications, it is inevitable to compare the thermo-environomic performance with the other competitors on the electricity market. In this study, it was focused on pre- and post-combustion CO_2 capture in natural gas or biomass fuelled power plants. Beside other alternative renewable solutions, one major competitor using a fossil resource has not been addressed here, namely coal fired power plants. By applying the same concepts and technologies, CO_2 could be captured in coal fired power plants to reduce the global CO_2 emissions. In addition, the oxy-fuel and chemical looping combustion options for CO_2 capture have not been evaluated. As mentioned in the introductory chapter several research studies have investigated CO_2 capture in coal fired power plants and oxy-fuel combustion options over the last years. However, no holistic approach including simultaneously energetic, economic and environmental considerations has been applied. By applying the systematic thermo-environomic modelling and optimisation approach developed in this thesis, coal fired power plants capturing CO_2 by post-, pre- or oxy-fuel combustion could be included in the superstructure and compared with the other options in a future study. Following this approach, the energy integration of several pre-combustion CO_2 capture options in coal fired power plants has already been optimised in Urech et al. (2012). However, no economic and LCA aspects have been included yet.

In order to assess the competitiveness of the different processes, the performance results of this study are compared with literature data for CO_2 capture in power plants, including pre-, post- and oxy-fuel combustion concepts. The results published by IEA (Finkenrath (2011)) for electricity generation in OECD countries and by ZEP (ZEP (2011)) for European countries are considered. Tables 8.5 & 8.6 summarise the results for different power plant systems with and without CO_2 capture.

Table 8.5: Performance results reported by IEA (Finkenrath (2011)) for OECD countries. The costs range takes into account the variation of the resource price with regard to the countries. For the efficiency the OECD average value is given.

System CO_2 capture	NGCC no CC	NGCC post-comb.	IGCC no CC	IGCC pre-comb.	PC no CC	PC post-comb
ϵ_{tot} [%]	56.6	48.4	41.4	30.9	41.4	30.9
COE [$\$/GJ_e$]	17.8-23.9	23.3-35	13.6-19.1	23.3-32.5	13.9-21.7	22.2-33.6
Avoid. cost [$\$/t_{CO2,avoided}$]	-	62-128	-	40-69	-	40-74

Table 8.6: Performance results reported by ZEP (ZEP (2011)) for European countries. The conservative, high-cost plant designs representing today's technology choices (Base) and the optimised cost estimations considering advanced future technology (Optim) are reported here. The costs ranges take into account the low and high resource price scenario. For the currency exchange 1.25$/€ is used.

System CO_2 capture	NGCC no CC	NGCC post-comb.	Hard coal no CC	Hard coal post-comb.	Hard coal pre-comb.	Hard coal oxy-comb.
Base						
ϵ_{tot} [%]	58	48	46	38	38	35.4
COE [$\$/GJ_e$]	16.4-32.3	24.5-44.8	15.4-18.3	22.9-26.3	24.4-27.8	28.4-32.1
Avoid. cost [$\$/t_{CO2,avoided}$]	-	115-156	-	40-43	48-51.5	71-75
Optim						
ϵ_{tot} [%]	60	52				36.3
COE [$\$/GJ_e$]	15.8-31.1	22.2-40	-	21.8-25.2	23-26.3	20.3-23.8
Avoid. cost [$\$/t_{CO2,avoided}$]	-	82.4-113	-	34-35.6	40.6-43	35.6-39.5

The results reported in this study for the optimal configurations with 90% of CO_2 capture (Table 8.1) and for the configurations yielding the best economic performance under various economic scenarios (Table 8.4) are in agreement with these literature data for CO_2 capture in NGCC power plants. This confirms that the applied systematic methodology computes reliable results. The energy efficiency results of this study are slightly better than reported ones, because of the performance improvement by optimal process integration. This is also highlighted in Urech et al. (2012) for CO_2 capture in coal fired power plants. Compared to natural gas fuelled power plants, CO_2 capture in coal fired power plants results in slightly lower cost penalty due to the larger CO_2 concentration in the flue gas. However, the energy penalty for CO_2 capture and compression leads to an energy efficiency drop to 30% for the electricity generation.

Looking at the thermodynamic performance, CO_2 capture in biomass based plants can consequently compete with coal fired power plants. But coal fired power plants keep a big advantage with regard to the economic performance due to the low coal price. The specific CO_2 emissions of coal fired power plants being more than twice as high as for natural power plants, $227\text{kg}_{CO2}/\text{GJ}_e$ compared to $103\text{kg}_{CO2}/\text{GJ}_e$, the introduction of a carbon tax will greatly penalise conventional coal fired power plants without CO_2 capture. Consequently, the introduction of a carbon tax will favour CCS and renewable biomass based processes. The environmental benefit of CO_2 capture has already been revealed in Figure 8.11. These results show that CO_2 capture has to be regarded as a competitive option for future sustainable energy systems.

8.5 Conclusions

The study of the process performance under different economic scenarios has revealed the influence on the competitiveness of the process configurations. The choice of the optimal process design is highly influenced by the resource price and the introduction of a carbon tax. When a high carbon tax is introduced, high CO_2 capture rates become attractive and negative CO_2 avoidance costs can be reached. Due to the advantage of capturing biogenic CO_2, biomass fed power plants become also competitive. With regard the economic performance post-combustion CO_2 capture in NGCC plants seems to perform best at capture rates around 70-85%, while pre-combustion CO_2 in natural gas fired power plants is advantageous in terms of energy efficiency and CO_2 capture in biomass based power plants is beneficial from an environmental point of view. Consequently, there is a competition between the different processes and the different objectives. The choice of the optimal process configuration is hence defined by the production scope and the priorities given to the different thermo-environomic criteria.

Conclusions

To meet the targets of sustainable development and greenhouse gas emissions reduction, the deployment of cost-competitive innovative low-carbon energy conversion systems is decisive. The design of such complex integrated energy conversion systems represents an important challenge for the engineers and requires the development of process design tools taking into account energetic, economic and environmental aspects simultaneously. In this thesis, a systematic framework for studying, designing and optimising complex integrated energy systems is developed. The proposed thermo-environomic optimisation strategy is applied for the comprehensive and consistent analysis, comparison and optimisation of fuel decarbonisation process options. The environmental benefit, and the energy and cost penalty of CO_2 capture in H_2 and power generation plants, fuelled with either fossil or renewable resources, is assessed in a uniform manner for different carbon capture technologies. The process competitiveness is systematically evaluated by taking into account several aspects, such as the process configuration and design, the energy price fluctuation and the introduction of a carbon tax. Based on the optimisation results, trade-offs are assessed to support decision-making and identify optimal process configurations with regard to the polygeneration of H_2, electricity, heat and captured CO_2. The approach turns out to be well suited to target the best possible performance and eliminate solutions that are not worth to be investigated further. This developed tool can consequently support decision-making and serve process engineers in the research and development of optimal plant designs taking into account economic, energetic and environmental considerations simultaneously.

The proposed methodology combines flowsheeting models, energy integration techniques, economic evaluation and life cycle assessment in a multi-objective optimisation platform. Such an integrated, holistic approach is rarely applied in conventional studies. The dissociation of the system models from the system design methods turns out to be valuable for assembling process unit models developed with different software. Candidate process technologies for fuel decarbonisation processes producing H_2 and/or electricity are identified and assessed in a superstructure, and thermo-environomic models are developed. Due to the uniform structure of the models, the superstructure can be easily extended and updated with additional options in the future. These models, taking into account different resources and technology options, are flexible and robust to reflect accurately the influence of the operating conditions on the chemical conversion and on the energy demand. There is consequently a trade-off between the level of detail of the models and their robustness. When experimental data are available, a systematic parameter validation of the developed models can be performed, which could then be applied for the design of experiments.

The analyses of the fuel decarbonisation processes have pointed out that process integration is a major concern. The competitiveness of the different process configurations is highly influenced by the rational energy recovery through cogeneration valorising the heat losses by electricity generation. When capturing CO_2 by chemical absorption with amines, the introduction of mechanical vapour recompression turns out to improve the quality of the process integration by making more heat available for cogeneration and consequently reducing the overall energy efficiency penalty between 5 and 20% depending on the process configuration. Moreover it appears that, by improving the quality of the refrigeration integration, the chilled ammonia process outperforms the chemical absorption with MEA for post-combustion CO_2 capture in NGCC plants. The energy efficiency of the chilled ammonia process capturing 90% of the emissions of an NGCC plant can be increased from 46.7% to about 53% by improving the quality of the process integration. This emphasises the need for a detailed analysis of the process integration results before the final process design and decision-making. The inclusion of the process integration in the design process has the advantage of reflecting the influence of the design and operation on the thermo-environomic performance of an energy balanced system.

The economic performance evaluation has highlighted that the energy price sensitivity and the environmental policy highly influence the market competitiveness of the process configurations. The resource purchase contributes to more than two thirds of the electricity production costs, while the annualised capital investment only amounts for around 10% and the maintenance for the remaining part. In this study, the investment costs are estimated based on equipment sizing and costing heuristics, which allows to easily re-evaluate the performance for different plant sizes. This consistent, uniform approach, estimating the costs with an error of ±30%, allows to compare process options and to rank systems. However, for making investment decisions the availability of reliable commercial cost data is crucial. When real market data are available, the cost estimations used in this thesis can be validated and the results from the comparative study verified and updated.

The comparison of the whole life cycle environmental impacts of H_2 and power generation plants has revealed the benefit of CO_2 capture with regard to the global warming impact. The capture of biogenic CO_2 emissions from biomass fired power plants leads to a negative CO_2 balance and is consequently promising. However, to improve the overall environmental impact the harmful contributions from gas cleaning and treatment have to be decreased.

A multi-objective optimisation of the thermo-environomic performance was performed in order to assess the trade-offs with respect to the process configuration and operating conditions, and to support decision-making. The energy and cost penalty of different CO_2 capture concepts and technologies, applied in H_2 and power generation plants, was consistently evaluated and compared based on the optimisation results. Within the goal of assessing the impact of CO_2 capture, the chosen objectives were to maximise the CO_2 capture rate and the energy efficiency. The generated Pareto optimal frontiers provide knowledge about promising configurations and offer the choice among several alternatives. By introducing the fluctuation of the resource purchase price, the carbon tax and the economic assumptions, the costs are evaluated for different economic scenarios. An approach for supporting decision-making based on the Pareto-optimal solutions is proposed.

CO_2 capture decreases the electrical generation efficiency by 9%-points and increases the production costs by around 25%. This penalty is related on the one hand to the capture cost and on the other hand to the compression cost. The compression penalty corresponds to about 2%-points of the efficiency decrease and is hardly avoidable when one wants to transport and store the CO_2. The CO_2 compression cost could be partly avoided when the CO_2 is reused for other purposes. The comparison between pre-combustion and post-combustion CO_2 capture in natural gas fed power plants reveals that pre-combustion CO_2 capture by physical absorption with Selexol capturing 90% of the emissions yields a 3%-points higher efficiency (52.6%) than post-combustion CO_2 capture by chemical absorption with MEA yielding an efficiency of 49.6%. This can be explained by the lower energy consumption for solvent regeneration in physical absorption processes. However, the economic performance is comparable with 24.5 and $23.7\$/GJ_e$ respectively for a natural gas price of $9.7\$/GJ_{NG}$. With regard to a conventional NGCC plant, having an efficiency of 58.7% and yielding electricity production costs of $18.3\$/GJ_e$, the economic competitiveness of these options highly depends on the introduction of a carbon tax and on the natural gas price. Without a carbon tax, the CO_2 avoidance costs are $60\$/t_{CO2,avoided}$ and $66\$/t_{CO2,avoided}$ for post-combustion and pre-combustion CO_2 capture in natural gas fuelled power plants, respectively. When a carbon tax is introduced, CO_2 capture processes become economically attractive. For a natural gas price of $9.7\$/GJ_{NG}$, the break even carbon tax is around $50\$/t_{CO2}$ for post-combustion with MEA and around $62\$/t_{CO2}$ for pre-combustion CO_2 capture with Selexol. Due to the advantage of capturing biogenic CO_2, biomass fed power plants yielding an efficiency of around 35% become also competitive from an environmental and economic point of view. Compared to CO_2 capture in coal fired power plants, yielding an efficiency around 33%, biomass based processes are competitive from a thermodynamic point of view. The economic performance turns out to be highly dependent on the resource price and on the imposed carbon tax. Post-combustion CO_2 capture in NGCC plants seems to perform best with regard to the economic performance, while pre-combustion CO_2 capture in natural gas fired power plants appears to be the most attractive from the energy efficiency point of view. The gain in efficiency is however not compensated by the increase of the investment. It could be mentioned here that the fuel options have not been evaluated here. These could make the pre-combustion more advantageous by increasing the efficiency of the hydrogen conversion. CO_2 capture in biomass based power plants is beneficial from an environmental point of view, but these plants require more investment and are highly penalised by the efficiency of the biomass conversion. Biomass conversion processes become however competitive when CO_2

taxes are high (>65\$/t_{CO2}) and when cheap biomass is available, for example waste biomass. Consequently, there is a competition between the various process options and the different objectives. The choice of the optimal process configuration is hence defined by the production scope, the priorities given to the different criteria and the market conditions. To support decision-making an approach is proposed to identify the most economically competitive configuration for a wide range of economic scenarios.

When including the fluctuation of the resource price, the carbon tax and the other economic assumptions, through distribution functions, it is pointed out that CO_2 capture becomes economically competitive for capture rates between 70 and 85% and not for rates up to 95% as commonly supposed. Taking into account the different economic scenarios, the electricity production costs and CO_2 avoidance costs are in the range of 9-41\$/GJ_e and -62-135\$/$t_{CO2,avoided}$, respectively. Negative avoidance cost meaning that the CO_2 capture becomes more economical than the conventional process for the given economic conditions. An NGCC plant configuration with post-combustion CO_2 capture capturing 83% of the emissions turns out to be the best compromise solution. However, pre-combustion CO_2 capture processes are in close competition. From an environmental point of view, CO_2 capture in biomass fuelled power plants is also a promising alternative which might become economically viable; if technology development and deployment proceeds and/or if high CO_2 taxes are imposed.

It can be concluded that CO_2 capture in power plants fuelled with fossil or renewable resources, is a promising solution which can become competitive in a medium term on the energy market. To reliably establish the technology on a large scale, R&D efforts should continue to address the technology availability issues and focus on the reduction of the energy and cost penalty of CCS.

Perspectives

The proposed process engineering method turns out to be a powerful tool to compare systematically different process options, assess trade-offs and support decision-making under different economic scenarios. The framework has the potential to be applied for studying all kinds of energy conversion systems. By expanding the superstructure with additional options, the energy market competitiveness can be accurately simulated with the aim of supporting decision-making. The constant upgrade, expansion and validation of the thermo-environomic models is one of the major future tasks. For making investment decisions, the availability of market equipment cost data would be an asset. Further optimisations based on three objectives (i.e. energetic, economic and environmental) could be performed in order to assess the trade-offs with regard to multiple objectives. However, increasing the number of objectives induces a larger computation time and difficulties for results visualisation and interpretation. Regarding the prospects of CO_2 capture options, several additional issues concerning power plants and H_2 applications have to be considered, as discussed here below.

CO_2 capture in coal fired power plants

With respect to CO_2 emissions mitigation in the electricity production, CO_2 capture in coal fired power plants, inducing most of the emissions, has to be investigated in addition to the natural gas and biomass options studied here. Compared to NGCC plants, coal fired power plants, yielding a 25% lower efficiency and around 50% higher CO_2 emissions, are actually competitive due to the low coal price. The introduction of a carbon tax and CO_2 capture would consequently penalise the performance of these plants. In Urech et al. (2012), a detailed energy integration analysis and optimisation of three different pre-combustion CO_2 options in an IGCC plant is performed using the methodology presented here. Compared to the conventional IGCC plant, CO_2 capture introduces an energy penalty of 7.6-8.6%-points for the different systems. For a consistent competitiveness evaluation, this study has to be completed with an economic and environmental evaluation by applying the proposed systematic thermo-environomic optimisation methodology. The developed superstructure of fuel decarbonisation options has hence to be extended by including the coal fired power plants options and oxy-fuel combustion processes in order to assess the potential of CO_2 capture in the different power plant systems.

H_2 as an energy vector

In the pre-combustion CO_2 capture processes, the H_2 intermediate generated from fossil or renewable resources could, instead of being burnt in gas turbine to generate electricity, be used as a fuel in fuel cell systems or as a product for many other applications, such as ammonia production for example.

Fuel cell applications. Fuel cell applications are regarded as promising alternatives on the future energy market. In Maréchal et al. (2005) and Autissier et al. (2007), a thermo-economic optimisation of two different types of fuel cells systems; PEMFC (Proton Exchange Membrane Fuel Cell) and SOFC (Solid Oxide Fuel Cell), using natural gas as a resource, was performed and revealed the potential of this technology. With such systems an efficiency around 50-60% could be reached, however to be competitive the equipment cost has to be reduced through technology developments increasing the reliability. An innovative hybrid SOFC-gas turbine system has been presented in Facchinetti et al. (2011). This system can reach an energy efficiency up to 80% with CO_2 separation through oxy-fuel combustion. Instead of using natural gas as a resource, renewable resources could also be used in fuel cell applications. The systematic process integration and optimisation of a SOFC-gas turbine hybrid cycle fuelled with hydrothermally gasified waste biomass made in Facchinetti et al. (2012) demonstrates the considerable potential of the system that allows for converting wet waste biomass into electricity at an energy efficiency of up to 63%, while simultaneously enabling the separation of biogenic carbon dioxide for further use or sequestration. Through optimal process integration the first law efficiency is improved by around 4% with respect to a non-integrated system. These studies emphasise that fuel cell applications have to be considered as promising options on the future energy market, even when including CO_2 capture.

Ammonia production from biomass. Alternatively, the H_2-rich fuel generated from biomass gasification could be used to produce ammonia instead of generating electricity. This process studied in detail in Tock et al. (2012g) and Perrenoud (2012), reveals again the importance of process integration and highlights the benefit with regard to the environmental impact. When using a renewable resource, such as wood, and capturing the CO_2 emissions, the environmental impact of the fertiliser industry, which is mainly based on ammonia, could be reduced considerably. Consequently, the H_2 production from renewable resources has to be investigated not only for applications in the power sector but also as chemical.

Table 8.7: Performance comparison of H_2 applications.

Reference	this study	this study	this study	this study
Product	H_2	H_2	$\dot{E}$	$\dot{E}$
System	ATR	FICFB	ATR	FICFB
CO_2 capture	90	55-63	90	60
Resource	NG	BM	NG	BM
ϵ [%]	78-82	48-61	49-53.3	34.8
Production costs	15.3-19\$/GJ$_{H2}$	28-46\$/GJ$_{H2}$	22-24\$/GJ$_e$	49-66\$/GJ$_e$

Reference	Maréchal et al. (2005)	Autissier et al. (2007)	Facchinetti et al. (2011)	Facchinetti et al. (2012)	Tock et al. (2012g)	Tock et al. (2012g)
Product	$\dot{E}$	$\dot{E}$	$\dot{E}$	$\dot{E}$	NH_3	NH_3
System	SMR/POX-PEM	SOFC-GT	SOFC-GT	SOFC-GT	SMR	FICFB
CO_2 capture	no	no	yes	88-95%	90%	70%
Resource	NG	NG	NG	BM	NG	BM
ϵ [%]	48-54	44-70	80	56-63	65.6	50.6
Specific Invest.	450-2000\$/kW$_e$	2400-6700\$/kW$_e$	-	-	-	-

The comparison of some performance results in Table 8.7, reveals the interest of studying in detail the different applications of H_2-rich fuel produced from fossil and renewable resources with regard to the future energy market. A consistent thermo-environomic comparison and optimisation of the different options could be made in a future study by following the systematic approach presented in this thesis.

In the perspective of a sustainable energy future driven by greenhouse gas constraints, CO_2 emissions have to be decreased, energy conversion efficiency has to be increased and fossil resources have to be progressively replaced by renewable resources. For the purpose of designing such complex integrated energy conversion systems and guiding decision-making and development, the systematic framework developed in this thesis proves to be beneficial. It turns out that process integration is a key point on which future developments have to focus. In the way towards a renewable future, CO_2 capture and storage applied to H_2 and power generation plants fuelled with fossil resources appears to be a competitive transitional solution for mitigating climate change. CO_2 capture in thermo-chemical conversion biomass based processes reveals also to be a promising alternative for the polygeneration of H_2 heat, electricity and captured CO_2 on the future energy market.

Bibliography

Adhikari, S., Fernando, S., 2006. Hydrogen membrane separation techniques. Industrial & Engineering Chemistry Research 45 (3), 875–881.

Alstom, 2012. Alstom Power. http://www.alstom.com.

Andersen, T., Kvamsdal, H. M., Bolland, O., 2000. Gas turbine combined cycle with CO2 capture using auto-thermal reforming of natural gas. ASME paper 2000-GT-0162.

AspenTech, Aspen Technologies Inc., last visited 12/2012. http://www.aspentech.com.

Autissier, N., Palazzi, F., Maréchal, F., van Herle, J., Favrat, D., 2007. Thermo-Economic optimization of a solid oxide fuel cell, gas turbine hybrid system. Journal of Fuel Cell Science and Technology 4 (2), 123–129.

Ball, M., Wietschel, M., 2009. The Hydrogen Economy: Opportunities and Challenges. Cambridge University Press, Cambridge.

Barg, C., Ferreira, J., Trierweiler, J., Secchi, A., 2000. Simulation and optimization of an industrial PSA unit. Brazilian Journal of Chemical Engineering 17, 695–704.

Bart, H., von Gemmingen, U., 2005. Adsorption. In: Ullmann's Encyclopedia of Industrial Chemistry. Wiley InterScience.

Bartels, J. R., Pate, M. B., Olson, N. K., 2010. An economic survey of hydrogen production from conventional and alternative energy sources. International Journal of Hydrogen Energy 35 (16), 8371–8384.

Belsim S.A., last visited 12/2012. http://www.belsim.com.

Bernier, E., Maréchal, F., Samson, R., 2010. Multi-objective design optimization of a natural gas-combined cycle with carbon dioxide capture in a life cycle perspective. Energy 35 (2), 1121–1128.

Biegler, L., Lang, Y.-D., 2012. Multi-scale optimization for advanced energy processes. In: Karimi, I., Srinivasan, R. (Eds.), Proceedings of the 11th International Symposium on Process Systems Engineering - PSE 2012. Computer-aided Chemical Engineering. Elsevier, pp. 51–60.

Bolland, O., Mathieu, P., 1998. Comparison of two CO2 removal options in combined cycle power plants. Energy Conversion and Management 39 (16-18), 1653–1663.

Bolland, O., Undrum, H., 2003. A novel methodology for comparing CO2 capture options for natural gas-fired combined cycle plants. Advances in Environmental Research 7 (4), 901–911.

Bolliger, R., 2010. Méthodologie de la synthèse des systèmes énergètiques industriels. Ph.D. thesis, EPFL, Lausanne.

Bolliger, R., Becker, H., Maréchal, F., 2009. New generic approach for the analysis of energy conversion system models. In: Process Systems Engineering, PSE09. Computer Aided Chemical Engineering. Elsevier.

Bredesen, R., Jordal, K., Bolland, O., 2004. High-temperature membranes in power generation with CO2 capture. Chemical Engineering and Processing 43 (9), 1129–1158.

Brunetti, A., Scura, F., Barbieri, G., Drioli, E., 2010. Membrane technologies for CO2 separation. Journal of Membrane Science 359 (1-2), 115–125.

Bundesamt für Umwelt BAFU, last visited 12/2012. http://www.bafu.admin.ch/.

Burr, B., Lyddon, L., 2008. A comparison of physical solvents for acid gas removal. Tech. rep., Bryan Research & Engineering, Bryan, Texas, USA.

Carpentieri, M., Corti, A., Lombardi, L., 2005. Life cycle assessment LCA of an integrated biomass gasification combined cycle IBGCC with CO2 removal. Energy Conversion and Management 46, 1790–1808.

Casas, N., Schell, J., Pini, R., Mazzotti, M., 2012. Fixed bed adsorption of CO2/H2 mixtures on activated carbon: experiments and modeling. Adsorption 18, 143–161.

Chauvel, A., Fourrier, G., Raimbault, C., 2001. Manuel d'évaluation économique des procédés, 2nd Edition. Edition TECHNIP.

Chen, W., Chiu, T., Hung, C., 2010a. Enhancement effect of heat recovery on hydrogen production from catalytic partial oxidation of methane. International Journal of Hydrogen Energy 35 (14), 7427–7440.

Chen, W., Lin, M., Lu, J., Chao, Y., Leu, T., 2010b. Thermodynamic analysis of hydrogen production from methane via autothermal reforming and partial oxidation followed by water gas shift reaction. International Journal of Hydrogen Energy 35 (21), 11787–11797.

Chevalier, G., Diamond, L., Leu, W., 2010. Potential for deep geological sequestration of CO2 in Switzerland: a first appraisal. Swiss Journal of Geosciences 103, 427–455.

Chiesa, P., Consonni, S., 2000. Natural gas fired combined cycles with low CO2 emissions. Journal of Engineering for Gas Turbines and Power 122 (3), 429–436.

Chiesa, P., Consonni, S., Kreutz, T., Williams, R., 2005a. Co-production of hydrogen, electricity and CO2 from coal with commercially ready technology. Part A: Performance and emissions. International Journal of Hydrogen Energy 30 (7), 747–767.

Chiesa, P., Lozza, G., Malandrino, A., Romano, M., Piccolo, V., 2008. Three-reactors chemical looping process for hydrogen production. International Journal of Hydrogen Energy 33 (9), 2233–2245.

Chiesa, P., Lozza, G., Mazzocchi, L., 2005b. Using hydrogen as a gas turbine fuel. Journal of Engineering for Gas Turbines and Power 127, 73–80.

Cohce, M., Dincer, I., Rosen, M., 2010. Thermodynamic analysis of hydrogen production from biomass gasification. International Journal of Hydrogen Energy 35 (10), 4970–4980.

Consonni, S., Viganò, F., 2005. Decarbonized hydrogen and electricity from natural gas. International Journal of Hydrogen Energy 30 (7), 701–718.

Cormos, C., 2010. Evaluation of energy integration aspects for IGCC-based hydrogen and electricity co-production with carbon capture and storage. International Journal of Hydrogen Energy 35 (14), 7485–7497.

Corradetti, A., Desideri, U., 2005. Analysis of Gas-Steam combined cycles with natural gas reforming and CO2 capture. Journal of Engineering for Gas Turbines and Power 127 (3), 545–552.

Corti, A., Lombardi, L., 2004. Biomass integrated gasification combined cycle with reduced CO2 emissions: Performance analysis and life cycle assessment (LCA). Energy 29 (12-15), 2109 – 2124.

Damen, K., van Troost, M., Faaij, A., Turkenburg, W., 2006. A comparison of electricity and hydrogen production systems with CO2 capture and storage. Part A: Review and selection of promising conversion and capture technologies. Progress in Energy and Combustion Science 32 (2), 215–246.

Damen, K., van Troost, M., Faaij, A., Turkenburg, W., 2007. A comparison of electricity and hydrogen production systems with CO2 capture and storage–Part B: Chain analysis of promising CCS options. Progress in Energy and Combustion Science 33 (6), 580–609.

Darde, V., Maribo-Mogensen, B., van Well, W. J., Stenby, E. H., Thomsen, K., 2012. Process simulation of CO2 capture with aqueous ammonia using the extended UNIQUAC model. International Journal of Greenhouse Gas Control 10 (0), 74–87.

Darde, V., Thomsen, K., van Well, W. J., Stenby, E. H., 2010. Chilled ammonia process for CO2 capture. International Journal of Greenhouse Gas Control 4 (2), 131–136.

Dave, N., Do, T., Puxty, G., Rowland, R., Feron, P., Attalla, M., 2009. CO2 capture by aqueous amines and aqueous ammonia-A Comparison. Energy Procedia 1 (1), 949–954.

Davison, J., Arienti, S., Cotone, P., Mancuso, L., 2009. Co-production of hydrogen and electricity with CO2 capture. Energy Procedia 1 (1), 4063–4070.

Davison, J., Arienti, S., Cotone, P., Mancuso, L., 2010. Co-production of hydrogen and electricity with CO2 capture. International Journal of Greenhouse Gas Control 4 (2), 125 – 130.

Dickinson, R., 2008. Expanding Process Modelling Capability through software interoperability standards: Application, extension and maintenance of CAPE OPEN standards. Computer Aided Chemical Engineering 25, 537–538.

Dubuis, M., 2012. Energy system design under uncertainty. Ph.D. thesis, EPFL, Lausanne.

Dufour, J., Serrano, D. P., Gálvez, J. L., González, A., Soria, E., Fierro, J. L., 2012. Life cycle assessment of alternatives for hydrogen production from renewable and fossil sources. International Journal of Hydrogen Energy 37 (2), 1173 – 1183.

Ecoinvent, last visited 12/2012. http://www.ecoinvent.ch/.

Ertesvåg, I. S., Kvamsdal, H. M., Bolland, O., 2005. Exergy analysis of a gas-turbine combined-cycle power plant with precombustion CO2 capture. Energy 30 (1), 5–39.

European Commission, 2010. EU energy trends to 2030 - Update 2009. Report, European Commission.

European Commission, 2011. Energy roadmap 2050. Communication from the Commission to the Council, the European Parliament, the European Economic and Social Committee and the Committee of Regions. SEC(2011) 1565/2, European Commission.

European Commission, 2012. The state of the european carbon market in 2012. Report from the Commission to the European Parliament and the council COM(2012) 652, European Commission.

Eurostat, last visited 12/2012. European Commission. http://epp.eurostat.ec.europa.eu/portal/page/portal/eurostat/home.

Facchinetti, E., Favrat, D., Maréchal, F., 2011. Innovative hybrid cycle solid oxide fuel cell - inverted gas turbine with CO2 separation. Fuel Cells 11 (4), 565–572.

Facchinetti, E., Gassner, M., D'Amelio, M., Maréchal, F., Favrat, D., 2012. Process integration and optimization of a solid oxide fuel cell - gas turbine hybrid cycle fueled with hydrothermally gasified waste biomass. Energy 41 (1), 408 – 419.

Figueroa, J. D., Fout, T., Plasynski, S., McIlvried, H., Srivastava, R. D., 2008. Advances in CO2 capture technology–The U.S. Department of Energy's Carbon Sequestration Program. International Journal of Greenhouse Gas Control 2 (1), 9–20.

Finkenrath, M., 2011. Cost and performance of carbon dioxide capture from power generation. Report, International Energy Agency.

Franz, J., Scherer, V., 2010. An evaluation of CO2 and H2 selective polymeric membranes for CO2 separation in IGCC processes. Journal of Membrane Science 359 (1-2), 173–183.

Gal, E., 2006. Ultra cleaning of combustion gas including the removal of CO2. Patent WO/2006/022885.

Gassner, M., Baciocchi, R., Maréchal, F., Mazzotti, M., 2009. Integrated design of a gas separation system for the upgrade of crude SNG with membranes. Chemical Engineering and Processing: Process Intensification 48 (9), 1391–1404.

Gassner, M., Maréchal, F., 2009a. Methodology for the optimal thermo-economic, multi-objective design of thermochemical fuel production from biomass. Computers & Chemical Engineering 33 (3), 769–781.

Gassner, M., Maréchal, F., 2009b. Thermo-economic process model for the thermochemical production of Synthetic Natural Gas (SNG) from lignocellulosic biomass. Biomass & Bioenergy 33 (11), 1587–1604.

Gassner, M., Maréchal, F., 2009. Thermodynamic comparison of the FICFB and Viking gasification concepts. Energy 34 (10), 1744–1753.

Gerber, L., 2012. Integration of life cycle assessment in the conceptual design of renewable energy conversion systems. Ph.D. thesis, EPFL, Lausanne.

Gerber, L., Gassner, M., Maréchal, F., 2011. Systematic integration of LCA in process systems design: Application to combined fuel and electricity production from lignocellulosic biomass. Computers & Chemical Engineering 35 (7), 1265 – 1280.

Girardin, L., Bolliger, R., Marechal, F., 2009. On the use of process integration techniques to generate optimal steam cycle configurations for the power plant industry. In: Pres'09. Vol. 18 of Chemical Engineering Transactions. Aidic Servizi Srl, Milano, Italy, pp. 171–176.

Göppert, U., Maurer, G., 1988. Vapor-liquid equilibria in aqueous solutions of ammonia and carbon dioxide at temperatures between 333 and 393K and pressures up to 7 MPa. Fluid Phase Equilibria 41 (1-2), 153–185.

Göttlicher, G., 1999. Energetik der Kohlendioxidrückhaltung in Kraftwerken. Fortschritt-Berichte VDI 421.

Gouedard, C., Picq, D., Launay, F., Carrette, P.-L., 2012. Amine degradation in CO2 capture. I. A review. International Journal of Greenhouse Gas Control 10 (0), 244 – 270.

Griffin, T., Mantzaras, I., 2012. Technologies for Gas Turbine Power Generation with CO2 Mitigation. Final report.

Griffin, T., Sundkvist, S. G., Asen, K., Bruun, T., 2005. Advanced Zero Emissions Gas Turbine Power Plant. Journal of Engineering for Gas Turbines and Power 127 (1), 81–85.

Hamelinck, C. N., Faaij, A. P. C., 2002. Future prospects for production of methanol and hydrogen from biomass. Journal of Power Sources 111 (1), 1–22.

Häussinger, P., Lohmüller, R., Watson, A. M., 2000. Hydrogen. In: Ullmann's Encyclopedia of Industrial Chemistry. Wiley-VCH.

Heldebrant, D. J., Yonker, C. R., Jessop, P. G., Phan, L., 2009. CO2 -binding organic liquids (CO2 BOLs) for post-combustion CO2 capture. Energy Procedia 1 (1), 1187–1195.

Henao, C. A., Maravelias, C. T., 2010. Surrogate-based process synthesis. In: 20th European Symposium on Computer Aided Process Engineering - ESCAPE20.

Henao, C. A., Maravelias, C. T., 2011. Surrogate-based superstructure optimization framework. AIChE Journal 57 (5), 1216–1232.

Hetland, J., 2009. Assessment of pre-combustion decarbonisation schemes for polygeneration from fossil fuels. Clean Technologies and Environmental Policy 11 (1), 37–48.

Hiller, H., Reimert, R., Marschner, F., Renner, H., Boll, W., 2006. Gas production. In: Ullmann's Encyclopedia of Industrial Chemistry. Wiley-VCH.

IEA, 2011a. CO2 emissions from fuel combustion - Highlights. IEA Statistics, International Energy Agency.

IEA, 2011b. Medium-term Oil & Gas Markets. Report, International Energy Agency.

IEA, 2012. Key World Energy Statistics. Report, International Energy Agency.

ISO, 2006a. Environmental management - Life Cycle Assessment - Principles and framework. International standard, ISO 14040.

ISO, 2006b. Environmental management - Life Cycle Assessment - Requirements and guidelines. International standard, ISO 14044.

Jee, J., Kim, M., Lee, C., 2001. Adsorption characteristics of hydrogen mixtures in a layered bed: Binary, ternary, and Five-Component mixtures. Industrial & Engineering Chemistry Research 40 (3), 868–878.

Jericha, H., Gottlich, E., Sanz, W., Heitmeir, F., 2004. Design Optimization of the Graz Cycle Prototype Plant. Journal of Engineering for Gas Turbines and Power 126 (4), 733–740.

Jilvero, H., Normann, F., Andersson, K., Johnsson, F., 2011. Thermal integration and modelling of the chilled ammonia process. Energy Procedia 4, 1713–1720.

Jilvero, H., Normann, F., Andersson, K., Johnsson, F., 2012. Heat requirement for regeneration of aqueous ammonia in post-combustion carbon dioxide capture. International Journal of Greenhouse Gas Control 11 (0), 181 – 187.

Kanniche, M., Gros-Bonnivard, R., Jaud, P., Valle-Marcos, J., Amann, J., Bouallou, C., 2010. Pre-combustion, post-combustion and oxy-combustion in thermal power plant for CO2 capture. Applied Thermal Engineering 30 (1), 53–62.

Klemeš, J., Bulatov, I., Cockerill, T., 2007. Techno-economic modelling and cost functions of CO2 capture processes. Computers & Chemical Engineering 31 (5-6), 445–455.

Klimantos, P., Koukouzas, N., Katsiadakis, A., Kakaras, E., 2009. Air-blown biomass gasification combined cycles (BGCC): System analysis and economic assessment. Energy 34 (5), 708 – 714.

Koroneos, C., Dompros, A., Roumbas, G., 2008. Hydrogen production via biomass gasification–A life cycle assessment approach. Chemical Engineering and Processing: Process Intensification 47 (8), 1261–1268.

Koroneos, C., Dompros, A., Roumbas, G., Moussiopoulos, N., 2004. Life cycle assessment of hydrogen fuel production processes. International Journal of Hydrogen Energy 29 (14), 1443–1450.

Kreutz, T., Williams, R., Consonni, S., Chiesa, P., 2005. Co-production of hydrogen, electricity and CO2 from coal with commercially ready technology. Part B: Economic analysis. International Journal of Hydrogen Energy 30 (7), 769–784.

Kurz, F., Rumpf, B., Maurer, G., 1995. Vapor-liquid-solid equilibria in the system NH3—CO2—H2O from around 310 to 470K: New experimental data and modeling. Fluid Phase Equilibria 104, 261–275.

Kvamsdal, H. M., Jordal, K., Bolland, O., 2007. A quantitative comparison of gas turbine cycles with CO2 capture. Energy 32 (1), 10–24.

Li, H., 2006. Environomic modeling and multi-objective optimisation of integrated energy systems for power and cogeneration. Ph.D. thesis, EPFL, Lausanne.

Li, H., Maréchal, F., Burer, M., Favrat, D., 2006. Multi-objective optimization of an advanced combined cycle power plant including CO2 separation options. Energy 31 (15), 3117–3134.

Longanbach, J., Rutkowski, M., Klett, M., White, J., Schoff, R., Buchanan, T., 2002. Hydrogen production facilities plant performance and cost comparisons. Report prepared for the USDOE National Energy Technology Laboratory (NETL) by Parsons Infrastructure and Technology Group, Inc.

Lozza, G., Chiesa, P., 2002a. Natural Gas Decarbonization to Reduce CO2 Emission From Combined Cycles—Part I: Partial Oxidation. Journal of Engineering for Gas Turbines and Power 124 (1), 82–88.

Lozza, G., Chiesa, P., 2002b. Natural Gas Decarbonization to Reduce CO2 Emission From Combined Cycles—Part II: Steam-Methane Reforming. Journal of Engineering for Gas Turbines and Power 124 (1), 89–95.

Lutz, A. E., Bradshaw, R. W., Bromberg, L., Rabinovich, A., 2004. Thermodynamic analysis of hydrogen production by partial oxidation reforming. International Journal of Hydrogen Energy 29 (8), 809–816.

Lutz, A. E., Bradshaw, R. W., Keller, J. O., Witmer, D. E., 2003. Thermodynamic analysis of hydrogen production by steam reforming. International Journal of Hydrogen Energy 28 (2), 159–167.

MacDowell, N., Florin, N., Buchard, A., Hallett, J., Galindo, A., Jackson, G., Adjiman, C. S., Williams, C. K., Shah, N., Fennell, P., 2010. An overview of CO2 capture technologies. Energy & Environmental Science 3 (11), 1645.

Malek, A., Farooq, S., 1998. Hydrogen purification from refinery fuel gas by pressure swing adsorption. AIChE Journal 44 (9), 1985–1992.

Mann, M., Spath, P., 1997. Life cycle assessment of a biomass gasification combined-cycle system. Technical report, National Renewable Energy Laboratory.

Maréchal, F., Kalitventzeff, B., 1998. Process integration: Selection of the optimal utility system. Computers & Chemical Engineering 22, 149–156.

Maréchal, F., Palazzi, F., Godat, J., Favrat, D., 2005. Thermo-Economic modelling and optimisation of fuel cell systems. Fuel Cells 5 (1), 5–24.

Mathias, P. M., Reddy, S., O'Connell, J. P., 2010. Quantitative evaluation of the chilled-ammonia process for CO2 capture using thermodynamic analysis and process simulation. International Journal of Greenhouse Gas Control 4 (2), 174–179.

Mathieu, P., Nihart, R., 1999. Zero-Emission MATIANT cycle. Journal of Engineering for Gas Turbines and Power 121 (1), 116–120.

MathWorks Inc., MATLAB, last visited 12/2012. http://www.mathworks.ch/.

McDonell, V. G., 2006. Key combustion issues associated with syngas and high-hydrogen fuels. Tech. rep., National Energy Technology Laboratory.

Meerman, J., Hamborg, E., van Keulen, T., Ramirez, A., Turkenburg, W., Faaij, A., 2012. Techno-economic assessment of CO2 capture at steam methane reforming facilities using commercially available technology. International Journal of Greenhouse Gas Control 9 (0), 160 – 171.

Metz, B., Davidson, O., de Coninck, H., Loos, M., Meyer, L., 2005. IPCC special report on carbon dioxide capture and storage. Report, Cambridge University Press.

Molyneaux, A., Leyland, G., Favrat, D., 2010. Environomic multi-objective optimisation of a district heating network considering centralized and decentralized heat pumps. Energy 35 (2), 751–758.

Morandin, M., Dubuis, M., Diethelm, S., Maréchal, F., 2009. Thermodynamic analysis and heat integration of wood gasifier - SOFC systems. In: Proceedings of the 3rd European Fuel Cell Technology & Applications 'Piero Lunghi Conference' EFC09.

Mueller-Langer, F., Tzimas, E., Kaltschmitt, M., Peteves, S., 2007. Techno-economic assessment of hydrogen production processes for the hydrogen economy for the short and medium term. International Journal of Hydrogen Energy 32 (16), 3797–3810.

Mussatti, D. C., 2002. EPA air pollution control cost manual. Report EPA/452/B-02-001, United States Environmental Protection Agency Office of Air Quality Planning and Standards.

Nord, L. O., Anantharaman, R., Bolland, O., 2009. Design and off-design analyses of a pre-combustion CO2 capture process in a natural gas combined cycle power plant. International Journal of Greenhouse Gas Control 3 (4), 385–392.

Ockwig, N. W., Nenoff, T. M., 2007. Membranes for hydrogen separation. Chemical Reviews 107 (10), 4078–4110.

Oh, P., Ray, A. K., Rangaiah, G., 2001. Triple-objective optimization of an industrial hydrogen plant. Journal of chemical engineering of Japan 34 (11), 1341–1355.

Oh, P. P., Rangaiah, G. P., Ray, A. K., 2002. Simulation and multiobjective optimization of an industrial hydrogen plant based on refinery Off-Gas. Industrial & Engineering Chemistry Research 41 (9), 2248–2261.

Olajire, A. A., 2010. CO2 capture and separation technologies for end-of-pipe applications - A review. Energy 35 (6), 2610 – 2628.

Olofsson, I., Nordin, A., Söderlind, U., 2005. Initial review and evaluation of process technologies and systems suitable for Cost-Efficient Medium-Scale gasification for biomass to liquid fuels. Report 05-02 ISSN 1653-0551 ETPC, Energy Technology & Thermal Process Chemistry, University of Umea.

Pahng, F., Senin, N., Wallace, D., 1998. Distribution modeling and evaluation of product design problems. Computer-Aided Design 30 (6), 411 – 423.

Parsons, E. L., Shelton, W. W., Lyons, J. L., 2002. Advanced fossil power systems comparison study. Final report, National Energy Technology Laboratory.

Pathare, R., Agrawal, R., 2010. Design of membrane cascades for gas separation. Journal of membrane science 364 (1-2), 263–277.

Perrenoud, M., 2012. Thermo-environomic evaluation of ammonia production. Master Project, EPFL, Lausanne.

Petrakopoulou, F., Tsatsaronis, G., 2012. Production of hydrogen-rich fuels for pre-combustion carbon capture in power plants: A thermodynamic assessment. International Journal of Hydrogen Energy 37 (9), 7554 – 7564.

Pilavachi, P. A., Stephanidis, S. D., Pappas, V. A., Afgan, N. H., 2009. Multi-criteria evaluation of hydrogen and natural gas fuelled power plant technologies. Applied Thermal Engineering 29 (11-12), 2228–2234.

Pinsent, B. R. W., Pearson, L., Roughton, F. J. W., 1956. The kinetics of combination of carbon dioxide with ammonia. Transactions of the Faraday Society 52, 1594.

Radgen, P., Cremer, C., Warkentin, S., Gerling, P., May, F., Knopf, S., 2005. Verfahren zur CO2-Abscheidung und -Speicherung. Abschlussbericht Forschungsbericht 20341110 UBA-FB 000938, Frauenhofer-Institut für Systemtechnik und Innovationsforschung, Bundesanstalt für Geowissenschaften und Rohstoffe.

Rajesh, J. K., Gupta, S. K., Rangaiah, G. P., Ray, A. K., 2001. Multi-objective optimization of industrial hydrogen plants. Chemical Engineering Science 56 (3), 999–1010.

Ramage, M. P., 2004. The hydrogen economy: Opportunities, costs, barriers and R&D needs. National academics press, National Research council, Committee on Alternatives and Strategies for Future Hydrogen Production and Use, National Research Council, National Academy of Engineering.

Rao, A. B., Rubin, E. S., 2002. A technical, economic, and environmental assessment of Amine-Based CO2 capture technology for power plant greenhouse gas control. Environmental Science & Technology 36 (20), 4467–4475.

Ridolfi, R., Sciubba, E., Tiezzi, E., 2009. A multi-criteria assessment of six energy conversion processes for H2 production. International Journal of Hydrogen Energy 34 (12), 5080–5090.

Ritter, J. A., Ebner, A. D., 2007. State-of-the-Art adsorption and membrane separation processes for hydrogen production in the chemical and petrochemical industries. Separation Science and Technology 42 (6), 1123.

Romano, M. C., Chiesa, P., Lozza, G., 2010. Pre-combustion CO2 capture from natural gas power plants, with ATR and MDEA processes. International Journal of Greenhouse Gas Control 4 (5), 785–797.

Romeo, L. M., Bolea, I., Escosa, J. M., 2008. Integration of power plant and amine scrubbing to reduce CO2 capture costs. Applied Thermal Engineering 28 (8-9), 1039–1046.

Rosen, M. A., 1996. Thermodynamic comparison of hydrogen production processes. International Journal of Hydrogen Energy 21 (5), 349–365.

Rosen, M. A., Scott, D. S., 1998. Comparative efficiency assessments for a range of hydrogen production processes. International Journal of Hydrogen Energy 23 (8), 653–659.

Rubin, E. S., Chen, C., Rao, A. B., 2007. Cost and performance of fossil fuel power plants with CO2 capture and storage. Energy Policy 35 (9), 4444–4454.

Schell, J., Casas, N., Blom, R., Spjelkavik, A. I., Andersen, A., Cavka, J. H., Mazzotti, M., 2012. MCM-41, MOF and UiO-67/MCM-41 adsorbents for pre-combustion CO2 capture by PSA: adsorption equilibria. Adsorption 18, 213–227.

Schlauer, J., 2008. Absorption, 1. Fundamentals. In: Ullmann's Encyclopedia of Industrial Chemistry. Wiley InterScience.

Schweizerische Bundesrat, 2012. Verordnung über die Reduktion der CO2-Emissionen (CO2-Verordnung). http://www.news.admin.ch/NSBSubscriber/message/attachments/26845.pdf.

Seo, Y. S., Shirley, A., Kolaczkowski, S. T., 2002. Evaluation of thermodynamically favourable operating conditions for production of hydrogen in three different reforming technologies. Journal of Power Sources 108 (1-2), 213–225.

Simbeck, D., Chang, E., 2002. Hydrogen supply: Cost estimate for hydrogen Pathways-Scoping analysis. Tech. Rep. NREL/SR-540-32525, National Renewable Energy Laboratory.

Sipocz, N., Tobiesen, F. A., Assadi, M., 2011. The use of artificial neural network models for CO2 capture plants. Applied Energy 88 (7), 2368–2376.

Sircar, S., Golden, T., 2000. Purification of hydrogen by pressure swing adsorption. Separation Science and Technology 35 (5), 667–687.

Spath, P., Aden, A., Eggeman, T., Ringer, M., Wallace, B., Jechura, J., 2005. Biomass to hydrogen production detailed design and economics utilizing the battelle columbus laboratory indirectly heated gasifier. Tech. Rep. NREL/TP-510-37408, National Renewable Energy Laboratory.

Spath, P., Dayton, D., 2003. Preliminary Screening-Technical and economic assessment of synthesis gas to fuels and chemicals with emphasis on the potential for Biomass-Derived syngas. Tech. Rep. NREL/TP-510-34929, National Renewable Energy Laboratory, Colorado.

Spath, P. L., Mann, M. K., 2001. Life cycle assessment of hydrogen production via natural gas steam reforming. Tech. Rep. NREL/TP-570-27637, National Renewable Energy Laboratory.

Stolten, D., 2010. Hydrogen and fuel cells: Fundamentals, Technologies and Applications. Wiley-VCH, Weinheim.

Tarun, C. B., Croiset, E., Douglas, P. L., Gupta, M., Chowdhury, M. H., 2007. Techno-economic study of CO2 capture from natural gas based hydrogen plants. International Journal of Greenhouse Gas Control 1 (1), 55–61.

Thomsen, K., Rasmussen, P., 1999. Modeling of vapor-liquid-solid equilibrium in gas-aqueous electrolyte systems. Chemical Engineering Science 54 (12), 1787–1802.

Tock, L., Gassner, M., Maréchal, F., 2010. Thermochemical production of liquid fuels from biomass: Thermo-economic modeling, process design and process integration analysis. Biomass and Bioenergy 34 (12), 1838 – 1854.

Tock, L., Maréchal, F., 2012a. Co-production of hydrogen and electricity from lignocellulosic biomass: Process design and thermo-economic optimization. Energy 45 (1), 339 – 349.

Tock, L., Maréchal, F., 2012b. H2 processes with CO2 mitigation: Thermo-economic modeling and process integration. International Journal of Hydrogen Energy 37 (16), 11785 – 11795.

Tock, L., Maréchal, F., 2012c. CO2 mitigation in thermo-chemical hydrogen processes: Thermo-environomic comparison and optimization. Energy Procedia 29 (0), 624 – 632.

Tock, L., Maréchal, F., 2012d. Process design optimization strategy to develop energy and cost correlations of CO2 capture processes. In: Bogle, I. D. L., Fairweather, M. (Eds.), 22nd European Symposium on Computer Aided Process Engineering. Vol. 30 of Computer Aided Chemical Engineering. Elsevier, pp. 562 – 566.

Tock, L., Maréchal, F., 2012e. Platform development for studying integrated energy conversion processes: Application to a power plant process with CO2 capture. In: Karimi, I., Srinivasan, R. (Eds.), Proceedings of the 11th International Symposium on Process Systems Engineering - PSE 2012. Computer-aided Chemical Engineering. Elsevier, pp. 1015–1019.

Tock, L., Maréchal, F., 2012f. Process engineering method for systematically comparing CO2 capture options. Submitted to 23rd European Symposium on Computer Aided Process Engineering - ESCAPE 2013, Lappeenranta.

Tock, L., Maréchal, F., Perrenoud, M., 2012g. Evaluation thermo-environomique de la production d’ ammoniac. Submitted to XIVe congrès de la Société Française de Génie des Procédés, October 2013, Lyon, France.

Toonssen, R., Woudstra, N., Verkooijen, A., 2008. Exergy analysis of hydrogen production plants based on biomass gasification. International Journal of Hydrogen Energy 33 (15), 4074–4082.

Turton, R., 2009. Analysis, Synthesis, and Design of Chemical Processes, 3rd Edition. Prentice Hall, Upper Saddle River, N.J.

Ulrich, G., Vasudevan, P., 2003. A Guide to Chemical Engineering Process Design and Economics a Practical Guide, 2nd Edition. CRC, Boca Raton, Fla.

Urech, J., Tock, L., Harkin, T., Hoadley, A., Maréchal, F., 2012. An Assessment of different solvent-based capture technologies within an IGCC-CCS power plant. Submitted to Energy.

Valenti, G., Bonalumi, D., Macchi, E., 2009. Energy and exergy analyses for the carbon capture with the chilled ammonia process (CAP). Energy Procedia 1 (1), 1059–1066.

van Herle, J., Maréchal, F., Leuenberger, S., Favrat, D., 2003. Energy balance model of a sofc cogenerator operated with biogas. Journal of Power Sources 118 (1-2), 375 – 383.

van Weenen, W. F., Tielrooy, J., 1983. How to optimize hydrogen plant designs. International Journal of Hydrogen Energy 8 (9), 689–700.

Wallquist, L., Werner, M., 2008. Carbon dioxide Capture and Storage - CCS Studie zum Entwicklungsstand von CCS in der Schweiz. IED working paper 4, IED- Institute for Environmental Decisions, ETHZ.

Wappel, D., Gronald, G., Kalb, R., Draxler, J., 2010. Ionic liquids for post-combustion co2 absorption. International Journal of Greenhouse Gas Control 4 (3), 486 – 494.

Winter, C., 2009. Hydrogen energy – abundant, efficient, clean: A debate over the energy-system-of-change. International Journal of Hydrogen Energy 34 (14, Supplement 1), S1–S52.

Yang, H., Xu, Z., Fan, M., Gupta, R., Slimane, R. B., Bland, A. E., Wright, I., 2008. Progress in carbon dioxide separation and capture: A review. Journal of Environmental Sciences 20 (1), 14–27.

Yuan, W., Sammons, N. E., McGlocklin, K. H., Eden, M. R., 2008. Economic analysis and process integration of hydrogen production strategies. In: Braunschweig, B., Joulia, X. (Eds.), 18th European Symposium on Computer Aided Process Engineering. Vol. 25 of Computer Aided Chemical Engineering. Elsevier, pp. 1083 – 1088.

ZEP, 2011. The costs of CO2 capture, transport and storage - Post-demonstration CCS in the EU. Report, European Technology Platform.
URL http://www.zeroemissionsplatform.eu/library.html

ZEP, 2012. European Technology Platform for Zero Emission Fossil Fuel Power Plants. http://www.zeroemissionsplatform.eu/library.html.

Zhang, N., Lior, N., 2008. Comparative study of two low CO2 emission power generation system options with natural gas reforming. Journal of Engineering for Gas Turbines and Power 130 (5), 051701–11.

A Cost correlations comparison

This appendix reveals the difficulty of estimating accurately the equipment costs when taking into account the influence of the plant size and of the operating conditions. Several design heuristics for process sizing and cost correlations are compared by evaluating the costs of CO_2 capture by chemical absorption.

To estimate the investment costs for chemical absorption, different approaches are found in literature in addition to the one from Turton (2009) and Ulrich and Vasudevan (2003) described in Section 1.3.4. After a brief description of the various approaches, the results of these estimations are compared here.

In Klemeš et al. (2007) a techno-economic model is established to evaluate the capital cost and the on-going costs associated with each component and with the net CO_2 release with regard to the design parameters (i.e. plant size, flue gas characteristics, capture technology, efficiency,...). The facilities that are accounted for are: the flue gas blower, absorber, regenerator, solvent processing area, MEA reclaimer, steam extractor, heat exchanger, pumps and CO_2 compressor. Parametric cost estimation relationships are defined for different CO_2 capture rates (90%, 85% and 80%) for plant sizes in the range of 300-2000MW_e. The cost estimations are defined as a function of the plant size [MW_e] or as a function of the amount of CO_2 avoided [Mt_{CO2}] according to relations Eq.A.1 and Eq.A.2 respectively. The parameters of these cost functions are defined for: the process facilities cost PFC [M$], total capital requirement TCR [M$], annual TCR [M$/y] , operating and maintenance cost O&M (variable, fixed, total) [M$/y], sorbent [M$/y], steam [M$/y], electricity [M$/y], waste disposal [M$/y] and the total annual cost [M$/y].

$$Cost = A + B * (plant\ size\ [MW]) \tag{A.1}$$

$$Cost = A' + B' * (amount\ CO_2\ avoided[MtCO_2]) \tag{A.2}$$

In Chauvel et al. (2001) the equation Eq.A.3 is reported to estimate the base cost (P_B) in french francs ($1FF_{1998}$= $0.17\$_{1998}$) of a distillation unit and material and installation factors are given to calculate the capital cost.

$$P_B[FF_{1985}] = e^{(4.3588+0.5848ln(\dot{m}_{dist})-0.7540ln(ln(vr))-0.3477ln(x_l)-0.1138ln(P))} \tag{A.3}$$

with $\dot{m}_{dist}$ the molar flow of the distillate [kmol/h], vr the relative volatility, x_l the molar fraction [%] of light component in the feed and P the pressure at the top of the column.

A detailed method for columns sizing and cost estimation based on the diameter, number of stages and pressure is also outlined in Chauvel et al. (2001). Based on the size, the weight of the material is defined and the costs are estimated for the different components of the column.

Another procedure for estimating the capital costs for vertical packed bed gas absorbers using counter-current flow to remove gaseous pollutants is described in Mussatti (2002). Cost estimates from gas absorber vendors for a range of tower dimensions (height, diameter) are used to fit a linear relation between the total tower cost (TTC [$\$_{1991}$]) and the absorber surface area S $[ft^2]$ expressed by Eq.A.4. To take into account the construction material a material factor is introduced. The total installation costs including tower cost, packings, auxiliaries, instrumentation and installation are also defined.

$$TTC[\$_{1991}] = 115 * S[ft^2] \tag{A.4}$$

The results of the described cost correlations are compared for one base case scenario with the flue gas characteristics given in Table A.1 and the base case chemical absorption process parameters given in Table 2.2. The number of stages and the column diameter are fixed, while the HETP is calculated by HETP=(diameter)$^{0.3}$. For the columns a maximal diameter of 5m is considered. If the diameter value calculated by Eq.1.11 is higher, several units operating in parallel are considered.

Table A.1: Flue gas characteristics for the comparison of the investment cost estimates of a chemical absorption installation.

Flue Gas	Mass flow [t/h]	CO_2 [%wt]	H_2O [%wt]	O_2 [%wt]	N_2 [%wt]
FG_1	600	6	5	3	86
FG_2	900	5	15	0	80
FG_3	1700	14.5	2	5	78.5

The results in Table A.2 clearly reveal a large range of variation in the estimations. In addition, the correlations behave differently with regard to the changing composition and the size increase. This reveals the difficulty of estimating accurately the equipment costs when taking into account the influence of the plant size and of the operating conditions.

Table A.2: Influence of the cost correlations on the capital investment estimation [M$] of a chemical absorption unit for CO_2 capture from the flue gas (Table A.1).

Flue gas composition	FG_1	FG_2	FG_3
Klemeš et al. (2007)	21	25.6	141
Turton (2009), Ulrich and Vasudevan (2003)	12	15.5	112
Mussatti (2002)	42.5	45.8	132
Chauvel et al. (2001) (Short)	36.5	44.8	159
Chauvel et al. (2001) (Detail)	7.9	11.3	98

B Process units flowsheets

This appendix reports the conceptual flowsheets of different process units involved in the studied fuel decarbonisation processes.

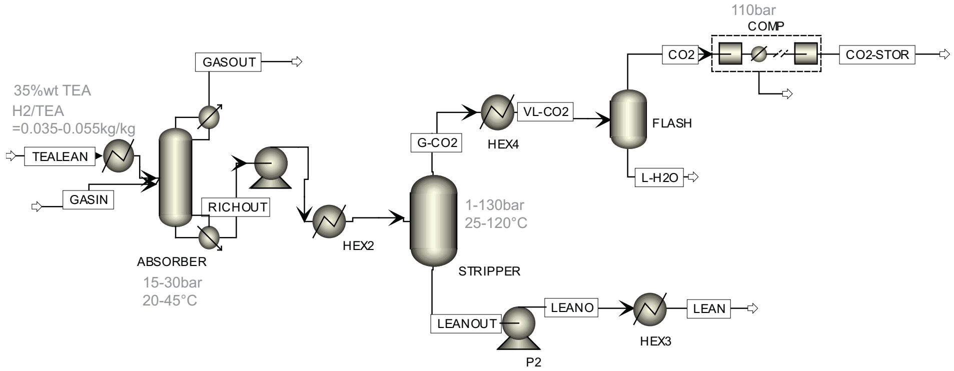
110bar
COMP
CO2
CO2-STOR
GASOUT
35%wt TEA
H2/TEA
=0.035-0.055kg/kg
TEALEAN
GASIN
RICHOUT
ABSORBER
15-30bar
20-45°C
HEX2
G-CO2
HEX4
VL-CO2
FLASH
L-H2O
1-130bar
25-120°C
STRIPPER
LEANOUT
P2
LEANO
HEX3
LEAN

Figure B.1: Flowsheet of the chemical absorption process using an aqueous TEA solution.

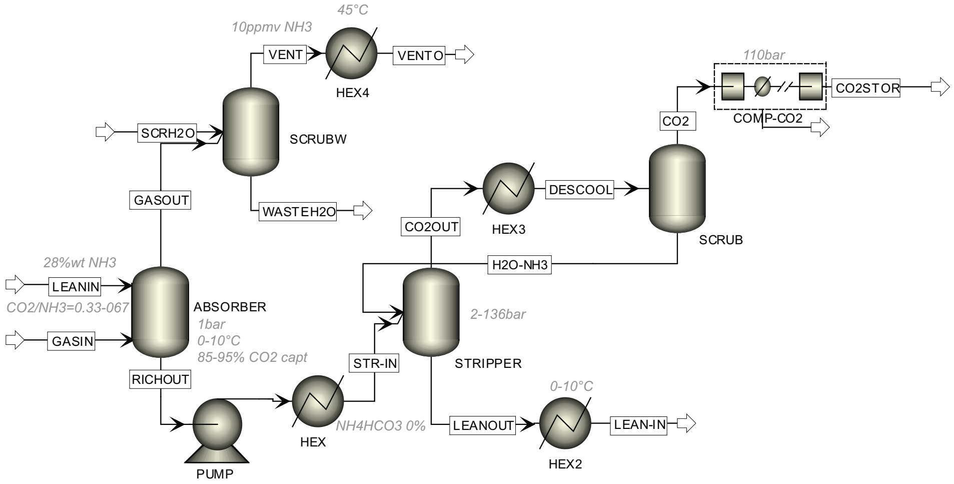
45°C
10ppmv NH3
VENT
HEX4
VENTO
110bar
CO2STOR
COMP-CO2
CO2
SCRH2O
SCRUBW
GASOUT
WASTEH2O
DESCOOL
CO2OUT
HEX3
SCRUB
28%wt NH3
LEANIN
CO2/NH3=0.33-067
GASIN
ABSORBER
1bar
0-10°C
85-95% CO2 capt
H2O-NH3
2-136bar
STRIPPER
STR-IN
RICHOUT
PUMP
HEX
NH4HCO3 0%
LEANOUT
0-10°C
HEX2
LEAN-IN

Figure B.2: Flowsheet of the chilled ammonia process.

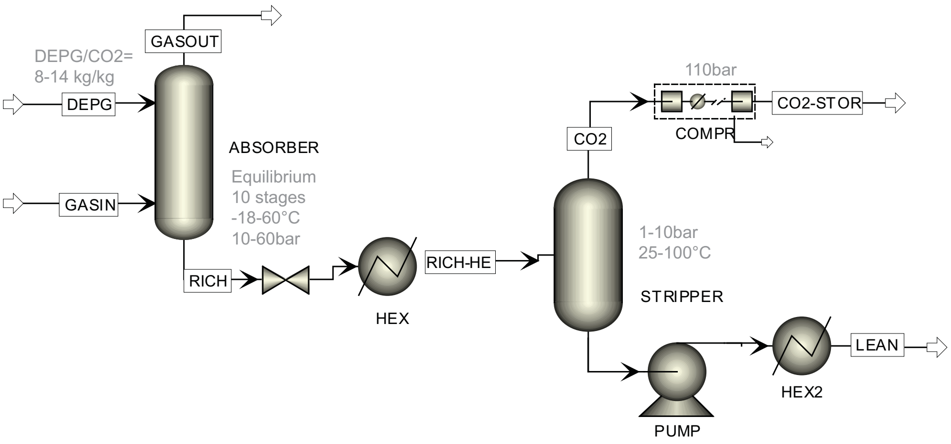
GASOUT
DEPG/CO2=
8-14 kg/kg
DEPG
GASIN
ABSORBER
Equilibrium
10 stages
-18-60°C
10-60bar
RICH
HEX
RICH-HE
110bar
COMPR
CO2
CO2-STOR
1-10bar
25-100°C
STRIPPER
LEAN
HEX2
PUMP

Figure B.3: Flowsheet of the physical absorption process using the Selexol solvent.

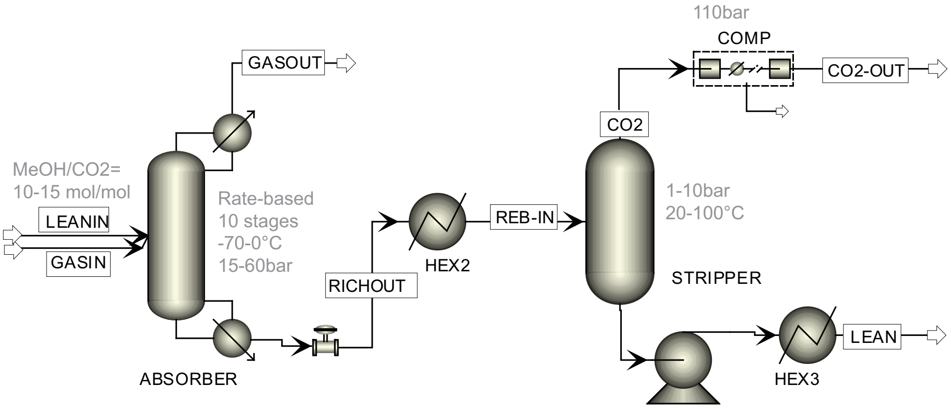
110bar
COMP
GASOUT
CO2-OUT
CO2
MeOH/CO2=
10-15 mol/mol
LEANIN
GASIN
Rate-based
10 stages
-70-0°C
15-60bar
HEX2
REB-IN
RICHOUT
1-10bar
20-100°C
STRIPPER
LEAN
HEX3
ABSORBER

Figure B.4: Flowsheet of the physical absorption process using the Rectisol solvent.

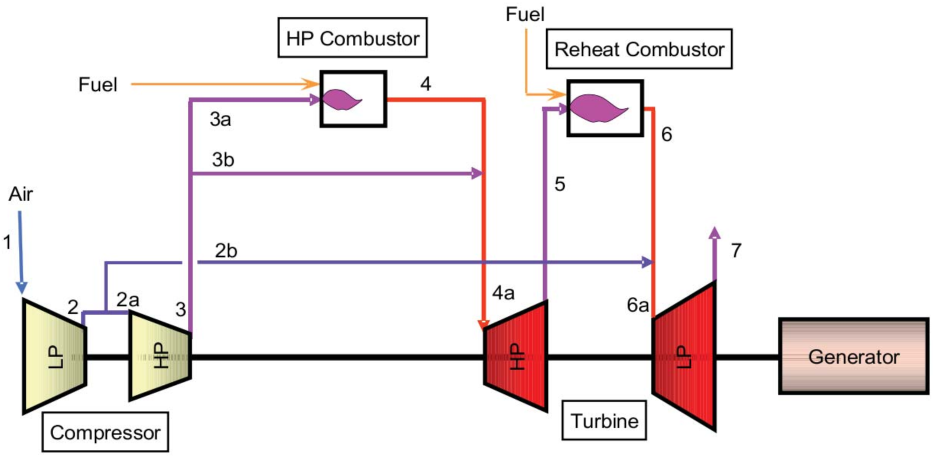
HP Combustor
Fuel
Reheat Combustor
Fuel
4
3a
3b
6
5
Air
1
2b
7
2
2a
3
4a
6a
LP
HP
HP
LP
Generator
Compressor
Turbine

Figure B.5: Generic gas turbine model with reheat combustion.

In collaboration with the FHNW the generic gas turbine model with reheat combustion (without FGR) illustrated in Figure B.5 has been developed based on the characteristics given in Table B.1. In order to model the recirculation the assumptions reported in Table B.2 are made. The air composition (%mol) is 77 N_2, 20.74 O_2, 1.009 H_2O, 0.9271 Ar and 0.0316 CO_2.

Table B.1: Characteristics of the generic gas turbine model with reheat combustion illustrated in Figure B.5.

Stream	Mass Flow [kg/s]	Temperature [^oC]	Remarks
11	500.0	15.0	Standard, wet Air p=1atm
2	500.0	466.6	p2/p1=20, $\epsilon_{isentropic}$=83%
2a	390.0	466.6	x.2a=78 %vol
2b	110.0	466.6	
3	390.0	560.6	p3/p2=1.5; $\epsilon_{isentropic}$=88%
3a	226.2	560.6	x.3a=58 %vol
3b	163.8	560.6	
4	231.9	1447.1	$\epsilon_{combustion}$=100%
4a	395.7	1106	
5	395.7	942.0	p4/p5=1.875, $\epsilon_{isentropic}$=87%
6	402.2	1477.0	$\epsilon_{combustion}$=100%
6a	512.2	1283.6	
7	512.2	631.7	p6/p7=16, $\epsilon_{isentropic}$=88%

Table B.2: Modelling assumptions of the generic gas turbine model with reheat combustion and FGR illustrated in Figure B.5.

Constants	Remarks
V_1=400m^3/s	Constant volumetric flow rate to maintain velocity triangle in compressor
X_{2a}=77%	With FGR, the split fractions of these flows are given by the
X_{3a}=61%	geometry and the type of fluid. It is assumed that they are constant.
T_{4a}=1100^oC	The inlet flow temperature of the turbines is limited by the capacity of the
T_{6a}=1300^oC	blade cooling system and is controlled by the air excess in the combustor.

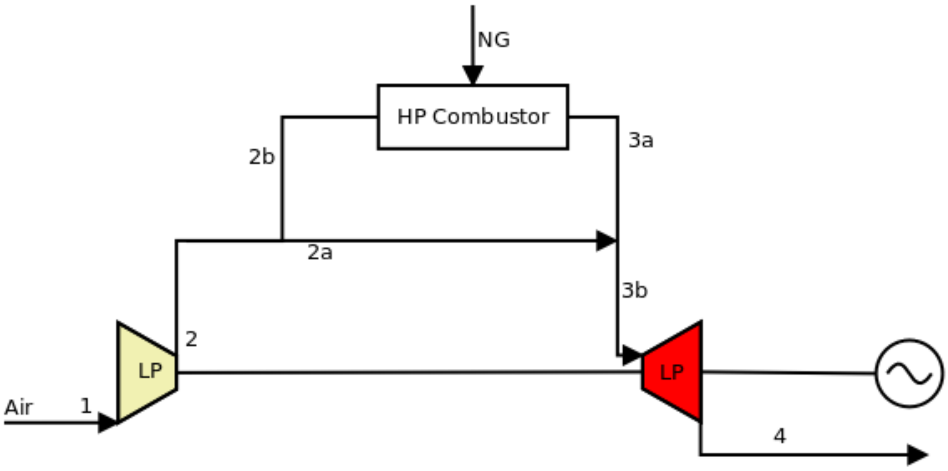

Figure B.6: Generic gas turbine model with a single combustion stage.

The characteristics of the generic gas turbine model with a single combustion stage (without FGR) reported in Figure B.6 are given in Table B.3. In order to model the recirculation the assumptions reported in Table B.4 are made.

Table B.3: Characteristics of the generic gas turbine model with a single combustion stage illustrated in Figure B.6.

Stream	Mass Flow [kg/s]	Temperature [^oC]	Remarks
1	540	25	P_1=1 bar
2	540	428	$P_2/P_1=16, \epsilon_{isentropic}=85\%$
2a	216	428	
2b	324	428	$\dot{m}_{2a}/\dot{m}_{2b}= 0.6$
3a	333.2	1479.5	
3b	549.2	1100	
4	549.2	516.6	$P_{3b}/P_4=16, \epsilon_{isentropic}=87\%$

Table B.4: Modelling assumptions of the generic gas turbine model with a single stage combustion and FGR illustrated in Figure B.6.

Constants	Remarks
$V_1=400m^3/s$	Constant volumetric flow rate to maintain velocity triangle in compressor.
$X_{2a}=60\%$	With FGR, the split fractions of these flows are given by the geometry and the type of fluid. It is assumed that they are constant.
$T_{3b}=1100^oC$	The inlet flow temperature of the turbines is limited by the capacity of the blade cooling system and is controlled by the air excess in the combustor.

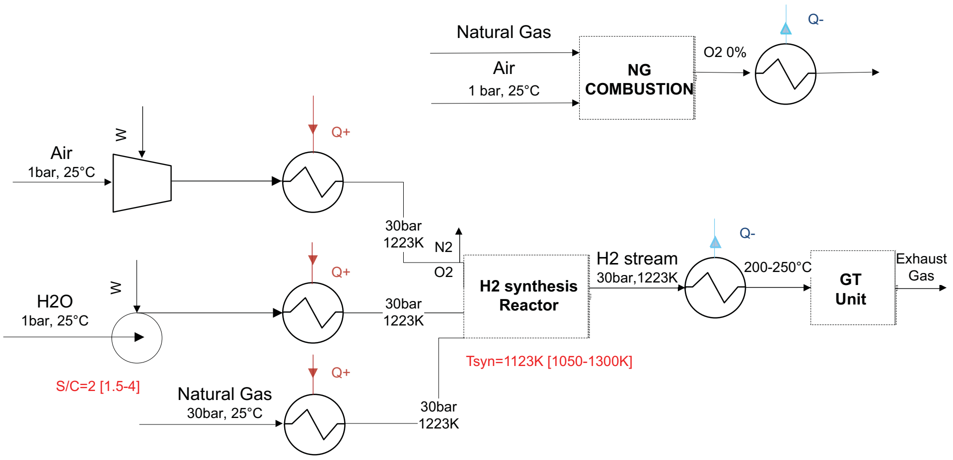
Natural Gas
Air
1 bar, 25°C
NG COMBUSTION
O2 0%
Q-
Air
1bar, 25°C
W
Q+
30bar
1223K
N2
O2
H2 synthesis Reactor
H2 stream
30bar,1223K
Q-
200-250°C
GT Unit
Exhaust Gas
H2O
1bar, 25°C
W
Q+
30bar
1223K
Tsyn=1123K [1050-1300K]
S/C=2 [1.5-4]
Q+
Natural Gas
30bar, 25°C
30bar
1223K

Figure B.7: Syngas production by the ATR membrane reactor for injection in the combustion chamber of the NGCC plant with FGR.

C Objective function choice

In this appendix the influence of the objective function choice on the Pareto-optimal solutions is discussed. For studying CO_2 capture options in power plants, energetic, economic and environmental aspects are of concern. Consequently, appropriate performance indicators that can be considered as objective function for the optimisation are the energy efficiency, the CO_2 capture rate, the specific CO_2 emissions per GJ of electricity produced, the capital investment costs and the production costs.

The influence of the objective function choice on the generated Pareto-optimal solutions is discussed here for the multi-objective optimisation of the pre-combustion CO_2 capture with Selexol and the post-combustion CO_2 capture with MEA in a natural gas fired power plant.

The following objective function choices are first analysed for the electricity production process from natural gas with pre-combustion CO_2 capture with Selexol:

· maximising the efficiency ϵ_{tot} and maximising the CO_2 capture rate (CC) η_{CO2}
· minimising the specific CO_2 emissions kg_{CO2}/GJ_e and minimising the investment
· minimising the specific CO_2 emissions kg_{CO2}/GJ_e and minimising the production costs COE
· maximising ϵ_{tot}, maximising η_{CO2} and minimising COE

The variation in terms of thermodynamic, environmental and economic performance of the Pareto-optimal solutions obtained with the various objective functions is reported in Figures C.1&C.2. These results show that:

· The optimisation of the CO_2 capture rate and of the efficiency leads to the optimisation of the CO_2 capture integration. The solutions that emerge have a higher efficiency and lower environmental impact but are more expensive than the solutions from the optimisation including an economic objective.

· When the COE is considered as objective, slightly lower production costs can be reached compared to the optimisation with regard to the efficiency and the CO_2 capture rate. This decrease of the COE results from lower capital investment costs and not from a higher efficiency. In fact, for a given efficiency the decrease of the production costs is linked to the lower CO_2

capture rate (i.e. higher environmental impact). An increase of the CO_2 capture level would go in pair with an additional investment and lead to suboptimal solutions with regard to the COE. In the same way, the efficiency is deceased for a given CO_2 capture level. This illustrates the trade-off between CO_2 capture, cost and efficiency.

· When the investment and the specific emissions are optimised, solutions with a low capture rate and a high efficiency emerge, since the CO_2 capture is penalised by the costs.

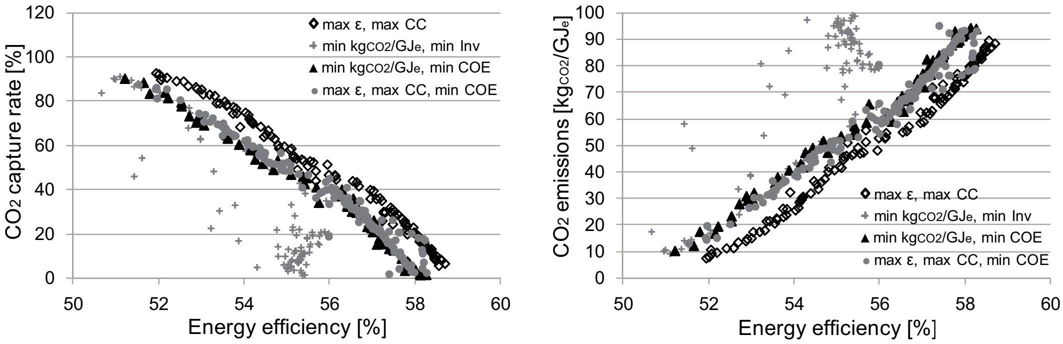

Figure C.1: Trade-off between thermodynamic and environmental performance of the pre-combustion CO_2 capture in a natural gas fired power plant assessed for different objective functions choices.

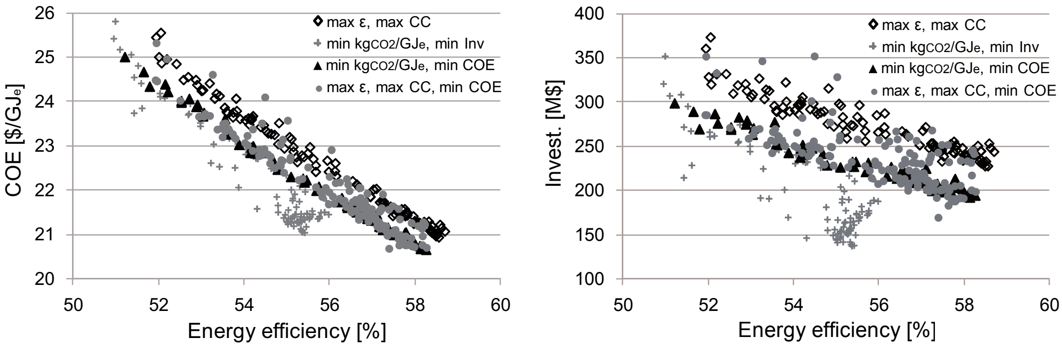

Figure C.2: Trade-off between thermodynamic and economic performance of the pre-combustion CO_2 capture in a natural gas fired power plant assessed for different objective functions choices.

The comparison between the solutions generated by the COE and the investment optimisation points out the low contribution of the investment to the COE which is mainly defined by the resource price and consequently correlated to the efficiency. For the post-combustion CO_2 capture in an NGCC plant this trend is highlighted by studying the optimisation results of:

· maximising the efficiency ϵ_{tot} and maximising the CO_2 capture rate (CC) η_{CO2}
· minimising the specific CO_2 emissions kg_{CO2}/GJ_e and minimising the COE
  (including a carbon tax)
· maximising η_{CO2} and minimising COE

The results reported in Figure C.3 reveal that the Pareto-optimal solutions are almost not influenced by the choice of the objective function. This characteristic underlines the strong correlation between the efficiency and the COE and supports the choice of the two objective functions; energy efficiency and CO_2 capture rate.

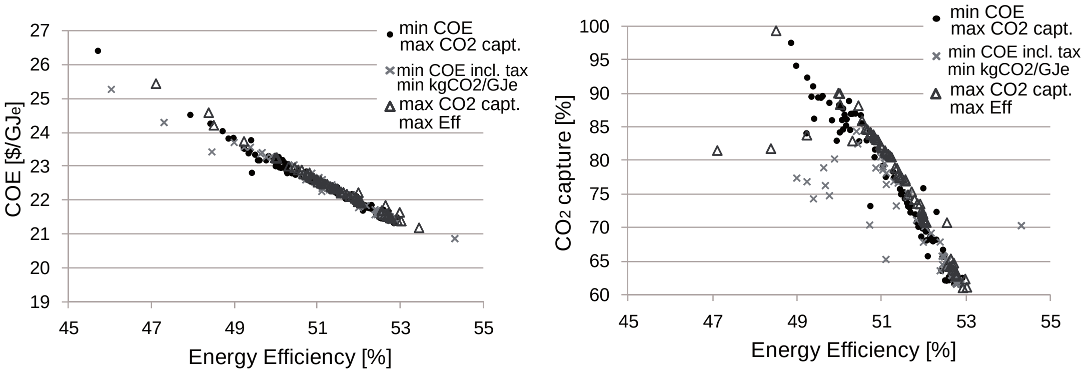

Figure C.3: Trade-off between thermodynamic, environmental and economic performance of post-combustion CO_2 capture in a natural gas fired power plant assessed for different objective functions choices.

A multi-objective optimisation with regard to three objectives (i.e. thermodynamic, economic and environmental) would probably be the best choice, but much more time consuming. In this study, the energy efficiency and the CO_2 capture rate were chosen as objective function for the pre-combustion processes. The economic dimension was included to support decision-making, by studying the influence of the economic scenario on the economic competitiveness of the Pareto-optimal solutions reflecting the trade-off between the energy penalty and the CO_2 capture (Chapter 8). This choice was made with the aim of optimising the CO_2 capture unit integration. As the electricity production costs are mainly defined by the resource price, the COE and the efficiency are highly correlated and the multi-objective optimisations with regard to two objectives, including no economic dimension were considered to be appropriate. In addition, it was assumed that minimising the CO_2 capture rate goes in pair with the investment minimisation. However, this a posteriori analysis shows that for the pre-combustion scenario there is a bias in the results, whereas for post-combustion scenarios the assumptions are confirmed.

As shown in Figures C.1&C.2, the Pareto solutions for the pre-combustion CO_2 capture by Selexol in a natural gas fuelled power plant are influenced in a greater extent by the choice of the objective function. This could be explained by the higher capital investment costs induced by the complex installation, including a reforming and shift reactor. The different compromise configurations that are identified from these results for a given energy efficiency are compared in Table C.1.

When no economic indicator is included in the objective function, the optimal solution yielding an efficiency around 52% captures between 10 and 15% more CO_2, but leads to around 2% higher production costs. The detailed analysis of the process designs reveals that in this solution the reforming is operated at a higher temperature and that the S/C ratio is lower.

Table C.1: Performance comparison of compromise solutions, assessed from different multi-objective optimisations of pre-combustion CO_2 capture in a natural gas fuelled power plants.

Objectives	max ϵ_{tot} max η_{CO2}	min $kg_{CO2,emitted}/GJ_e$ min Invest.	min $kg_{CO2,emitted}/GJ_e$ max COE	max ϵ_{tot} max η_{CO2} max COE
		Process Performance		
ϵ_{tot} [%]	52.58	52.73	52.53	52.50
η_{CO2} [%]	89.14	74.90	79.64	80.71
$kg_{CO2,emitted}/GJ_e$	14.99	26.55	21.62	20.49
COE [$/GJ$_e$]	24.50	23.96	24.02	24.03
Invest [M$]	309.9	274.8	271.8	271.4
		Process design		
Reforming T [K]	1287	1192	1179	1175
Reforming P [bar]	27.8	29	20	23
S/C [-]	3.9	4.1	4.9	5.6
WGS T_{HTS} [K]	650	653	627	666
WGS T_{LTS} [K]	428	467	503	518
Flue gas T [^oC]	40	43	38	39
Flue gas P [^oC]	13	38	28	22
Absorber T [^oC]	-18	-14	-18	- 6
DEPG/CO_2 ratio [kg/kg]	12.3	10.7	11.7	13.5
Regeneration T [^oC]	32	50	75	29
Regeneration P [bar]	4.3	3.7	8.3	4.5

In order to assess the influence on the competitiveness analysis made in Chapter 8.3, the specific CO_2 emissions and the COE should be chosen as objective functions in a future study or an optimisation with regard to three objectives has to be performed.

D Compromise process configurations

This appendix reports the process design parameters and operating conditions for the different compromise process configurations identified from the multi-objective optimisation.

Table D.1: Operating conditions for the different compromise H_2 process options with pre-combustion CO_2 capture, whose performance results are reported in Table 3.3.

Process	ATR self	ATR self no MVR	SMR self	BM self	ATR E_{imp}	SMR E_{imp}	BM E_{imp}	BM E_{imp} no CC	BM E_{imp} no MVR
Installation [$MWth_{NG/BM}$]	725	725	725	380	725	725	380	380	380
CO_2 capture [%]	89.9	89.9	88.5	64.3	89.6	89.3	65	0	47
$\theta_{wood,drying\_out}$ [%wt]	-	-	-	19.7	-	-	33	33	33
Gasification T [K]	-	-	-	1148.5	-	-	1015.2	1015.2	1015.2
Gasification P [bar]	-	-	-	1.78	-	-	1.82	1.82	1.82
Reforming T [K]	1338.2	1338.2	1199.6	1012.5	1297.5	1179.6	1000.7	1000.7	1000.7
Reforming P [bar]	25.31	25.31	12.02	-	29.95	2.03	-	-	-
S/C [-]	1.6	1.6	2.3	0.9	1.8	2.2	1.6	1.6	1.6
WGS T_{HTS} [K]	586.8	586.8	636.9	587.2	587.8	694.4	665.2	665.2	665.2
WGS T_{LTS} [K]	508	508	432.4	497.6	522.8	459	473	473	473
WGS P [bar]	-	-	-	23.6	-	-	13.6	13.6	13.6
Combustion inlet T [K]	773.15	773.15	773.15	867.7	773.15	773.15	8004	8004	8004
Turbine inlet T [K]	1680	1680	1680	1646.9	1680	1680	1500	1500	1500
HP level [bar]	125	125	125	120.8	125	125	99	99	99
MP level [bar]	90	90	90	67.4	90	90	70	70	70
LP level [bar]	28	28	28	-	28	28	-	-	-
Steam superheating [K]	823	823	823	820	823	550	700.8	700.8	700.8
Utilisation level [K]	550	550	550	473	550	550	504	504	504
Utilisation level [K]	450	450	450	300	450	450	300	300	300
Condensation level [K]	293	293	293	292	293	293	292	292	292

Table D.2: Operating conditions for the different compromise power plants options with pre-combustion CO_2 capture, whose performance results are reported in Table 3.4.

Process	ATR GT	SMR GT	BM GT
Installation [MWth$_{NG/BM}$]	725	725	380
CO_2 capture [%]	89.2	90	65.6
$\theta_{wood,drying\_out}$ [%wt]	-	-	13.6
Gasification T [K]	-	-	1090.8
Gasification P [bar]	-	-	2.65
Reforming T [K]	1079.6	1055.5	1051
Reforming P [bar]	4.86	2.7	-
S/C [-]	3.05	5.8	-
WGS T$_{HTS}$ [K]	594.9	590.2	613.2
WGS T$_{LTS}$ [K]	434.6	468.3	474.4
WGS P [bar]	-	-	7.1
Combustion inlet T [K]	773.15	773.15	878
Turbine inlet T [K]	1680	1680	1650
HP level [bar]	125	125	114
MP level [bar]	90	93	66
LP level [bar]	28	3	-
Steam superheating [K]	823	823	823
Utilisation level [K]	550	513	454
Utilisation level [K]	450	300	300
Condensation level [K]	293	293	292

Table D.3: Operating conditions for the different compromise H_2 plant options with pre-combustion CO_2 capture, whose performance results are reported in Table 4.1.

Resource	NG	NG	BM	NG	NG	BM
Process	ATR self	ATR self	FICFB self	ATR E$_{imp}$	ATR E$_{imp}$	FICFB E$_{imp}$
Capture technology	TEA	Selexol	Selexol	TEA	Selexol	Selexol
$\theta_{wood,drying\_out}$ [%wt]	-	-	17.7	-	-	19.7
Gasification T [K]	-	-	1067	-	-	1141
Gasification P [bar]	-	-	5.8	-	-	3.1
Reforming T [K]	1157	1327.3	1097.9	1386	1275.3	1150
Reforming P [bar]	19.1	25.83	-	23.9	16.6	-
WGS T$_{HTS}$ [K]	608.6	656.2	631.8	677.1	591.9	639.5
WGS T$_{LTS}$ [K]	470.9	470.6	513.8	440.8	513.6	551.1
WGS P [bar]	-	-	9.96	-	-	1.7
S/C [-]	4.3	2.1	2.56	3.74	3.1	3.6
Flue gas T [^oC]	32.74	31.1	27.2	35.7	35.1	27.5
Flue gas P [^oC]	24.3	19.3	30.9	28.2	41.8	34.2
Absorber T [^oC]	26.6	-11.2	14.5	26.9	-18	2.2
TEA concentration [%wt]	37.6	-	-	30.2	-	-
H_2/TEA ratio [kg/kg]	0.039	-	-	0.037	-	-
DEPG/CO_2 ratio [kg/kg]	-	13.4	10.5	-	13.99	10.9
Regeneration T [^oC]	111.8	42.5	70.3	117.1	51.5	75.3
Regeneration P [bar]	2.85	2.17	7.1	5.0	4.4	1.9
Turbine inlet T [K]	1678	1680	1680	1596	1680	1680

Table D.4: Operating conditions for the different compromise power plant options with pre-combustion CO_2 capture, whose performance results are reported in Tables 4.2 & 8.1.

System	ATR TEA	ATR Selexol	ATR Rectisol	SMR TEA	BM TEA	BM Selexol
$\theta_{wood,drying\_out}$ [%wt]	-	-	-	-	15	29
Gasification T [K]	-	-	-	-	1123.1	1071.6
Gasification P [bar]	-	-	-	-	3.5	1.58
Reforming T [K]	1289.3	1287.8	1318	1339	1145	1196.5
Reforming P [bar]	23.83	27.86	26.54	18.9	-	-
WGS T_{HTS} [K]	636.35	650.29	646.37	631.97	637.04	683
WGS T_{LTS} [K]	423	428.39	439.55	515.33	534.03	567.99
WGS P [bar]	-	-	-	-	6.61	6.7
S/C [-]	2.9	3.9	3.4	3.5	3.03	3.59
Flue gas T [^oC]	41.34	40.2	30.5	31.2	29.77	20.97
Flue gas P [^oC]	20.77	13.45	15.48	22.14	26.88	15
Absorber T [^oC]	29.5	-18	-43.9	41.2	23.5	22.9
TEA concentration [%wt]	33.5	-	-	30.1	27.5	-
H_2/TEA ratio [kg/kg]	0.035	-	-	0.037	0.038	-
DEPG/CO_2 ratio [kg/kg]	-	12.3	-	-	-	11.34
MeOH/ CO_2 ratio [kmol/kmol]	-	-	12.1	-	-	-
Regeneration T [^oC]	120	32	61.15	115.6	114.29	69.9
Regeneration P [bar]	6.4	13.45	4.4	3.0	1.67	6.43
Turbine inlet T [K]	1537	1680	1680	1500	1656	1648

Table D.5: Operating conditions for the base case power plant options with post-combustion CO_2 capture, whose performance results are reported in Table 6.1.

System	Post-comb MEA	Post-comb CAP
FRG [%]	51.7	50.6
$T_{reforming,H2}$ [K]	1072.6	1126.8
S/C [-]	2.7	3.4
Lean solvent CO_2 loading [kmol/kmol]	0.206	0.398
Rich solvent CO_2 loading [kmol/kmol]	0.49	-
Rich solvent pre-heat T [^oC]	105.7	-
Rich solvent re-heat T [^oC]	122.8	-
LP stripper pressure [bar]	2.03	-
HP / LP pressure ratio [-]	1.35	-
MEA % in solvent [-]	0.318	-
Absorber steam out [kg_{H2O}/t_{FG}]	308.63	-
Split fraction [-]	0.67	-
Nb stages absorber	15.5	-
Nb stages HP stripper	11.4	-
Nb stages LP stripper	8.8	-
Absorber diameter [m]	14.4	-
HP stripper diameter [m]	6	-
LP stripper diameter [m]	2	-
Absorber T_{in} [K]	-	274.6
Stripper P [bar]	-	25.9

Table D.6: Operating conditions for the power plant options with 90% post-combustion CO_2 capture, whose performance results are reported in Table 6.3.

System	Post-comb MEA	Post-comb CAP 1 Flash unit	Post-comb CAP Flash series
FRG [%]	55.5	53	51
$T_{reforming,H2}$ [K]	1076.6	1078.4	1203
S/C [-]	3.5	3.7	4
Lean solvent CO_2 loading [kmol/kmol]	0.198	0.355	0.468
Rich solvent CO_2 loading [kmol/kmol]	0.45	-	-
Rich solvent pre-heat T [^oC]	100.12	-	-
Rich solvent re-heat T [^oC]	122.7	-	-
LP stripper pressure [bar]	1.92	-	-
HP / LP pressure ratio [-]	1.35	-	-
MEA % in solvent [-]	0.337	-	-
Absorber steam out [kg_{H2O}/t_{FG}]	307.8	-	-
Split fraction [-]	0.53	-	-
Nb stages absorber	15.5	-	-
Nb stages HP stripper	10.7	-	-
Nb stages LP stripper	6.8	-	-
HP stripper diameter [m]	5.6	-	-
LP stripper diameter [m]	2.8	-	-
Absorber T_{in} [K]	-	274.8	278.3
Absorber Flash T [K]	-	274.8	295.6/295.9/296
Stripper P [bar]	-	28.2	39.07

Table D.7: Operating conditions for the different compromise power plant options with post-combustion CO_2 capture, whose performance results are reported in Table 8.1.

System	Post-comb MEA	Post-comb CAP
Lean solvent CO_2 loading [kmol/kmol]	0.198	0.468
Rich solvent CO_2 loading [kmol/kmol]	0.455	-
Rich solvent pre-heat T [^oC]	100.12	-
Rich solvent re-heat T [^oC]	122.71	-
LP stripper pressure [bar]	1.926	-
HP / LP pressure ratio [-]	1.357	-
MEA % in solvent [-]	0.337	-
Absorber steam out [kg_{H2O}/t_{FG}]	307.78	-
Split fraction [-]	0.534	-
Nb stages absorber	15.5	-
Nb stages HP stripper	10.6	-
Nb stages LP stripper	6.8	-
Absorber diameter [m]	16.1	-
HP stripper diameter [m]	5.6	-
LP stripper diameter [m]	2.8	-
Absorber T_{in} [K]	-	278.27
Absorber Flash T [K]	-	295.6
Stripper P [bar]	-	39.07

Table D.8: Operating conditions for the most economically competitive power plant options with post-combustion CO_2 capture, whose performance results are reported in Table 8.4.

System	Post-comb MEA	Post-comb CAP
FGR [%]	44.5	49.3
$T_{Reforming,H2}$ [K]	1135	1286
S/C ratio$_{Reforming,H2}$ [-]	2.1	2.5
Lean solvent CO_2 loading [kmol/kmol]	0.206	0.366
Rich solvent CO_2 loading [kmol/kmol]	0.499	-
Rich solvent pre-heat T [^oC]	105.11	-
Rich solvent re-heat T [^oC]	125.21	-
LP stripper pressure [bar]	2.041	-
HP / LP pressure ratio [-]	1.376	-
MEA % in solvent [-]	0.34	-
Absorber steam out [kg_{H2O}/t_{FG}]	307.78	-
Split fraction [-]	0.554	-
Nb stages absorber	13.9	-
Nb stages HP stripper	9.5	-
Nb stages LP stripper	7	-
Absorber diameter [m]	15.5	-
HP stripper diameter [m]	6	-
LP stripper diameter [m]	4.6	-
Absorber T_{in} [K]	-	278.27
Absorber Flash T [K]	-	293.1 / 296.8
Stripper P [bar]	-	42.2

Table D.9: Operating conditions for the most economically competitive power plant options with pre-combustion CO_2 capture, whose performance results are reported in Table 8.4.

System	ATR Selexol	ATR TEA	SMR TEA	BM Selexol	BM TEA
$\theta_{wood,drying\_out}$ [%wt]	-	-	-	31	14
Gasification T [K]	-	-	-	1182.2	1157.3
Gasification P [bar]	-	-	-	1.04	2.02
Reforming T [K]	1202.6	1273.2	1349.1	1200	1111
Reforming P [bar]	28.1	22.4	23.7	-	-
WGS T_{HTS} [K]	652.3	594.4	612.6	675.8	678.7
WGS T_{LTS} [K]	425.7	489.8	478.1	565.3	502.5
WGS P [bar]	-	-	-	5.14	3.57
S/C [-]	4.2	2.5	3.2	3.7	3.8
Flue gas T [^oC]	41.5	29.3	33.8	23	31.6
Flue gas P [^oC]	14.3	17.4	17.1	15.6	15.7
Absorber T [^oC]	-16.1	28.9	25.5	10.7	44.3
TEA concentration [%wt]	-	32	36	-	39
H_2/TEA ratio [kg/kg]	-	0.035	0.048	-	0.038
DEPG/CO_2 ratio [kg/kg]	11.5	-	-	11.3	-
Regeneration T [^oC]	45.3	118	120	69.4	109.66
Regeneration P [bar]	6.9	9.5	16.9	6.6	16.8
Turbine inlet T [K]	1500	1684	1680	1696	1659

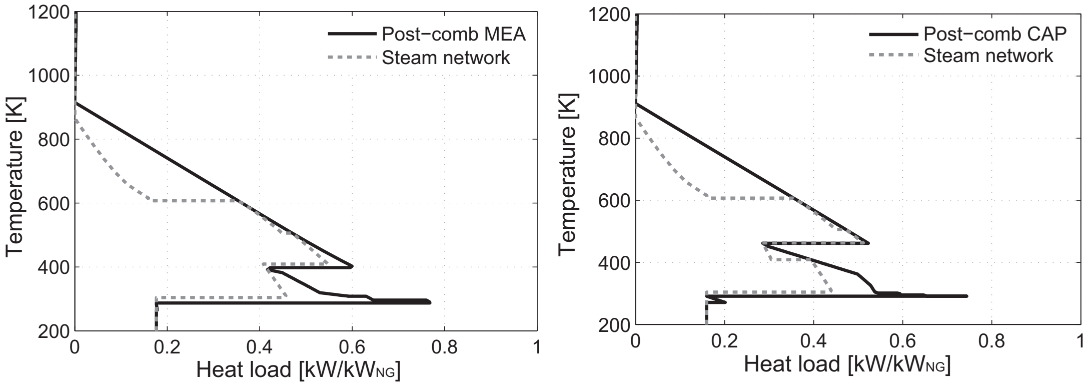

Figure D.1: Integrated composite curves of the most economically competitive natural gas fuelled power plant configuration with post-combustion CO_2 capture with MEA (left) and chilled ammonia (right) reported in Table 8.4.

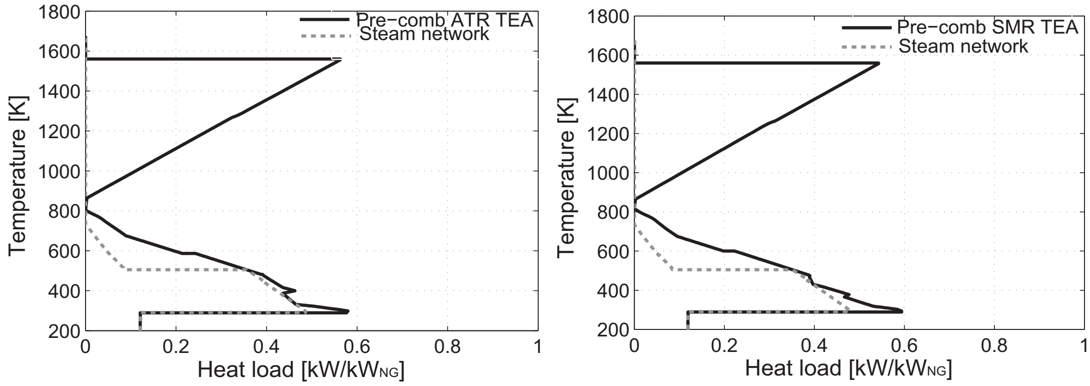

Figure D.2: Integrated composite curves of the most economically competitive natural gas fuelled power plant configuration with pre-combustion CO_2 capture by chemical absorption with TEA; ATR (left) and SMR (right) reported in Table 8.4.

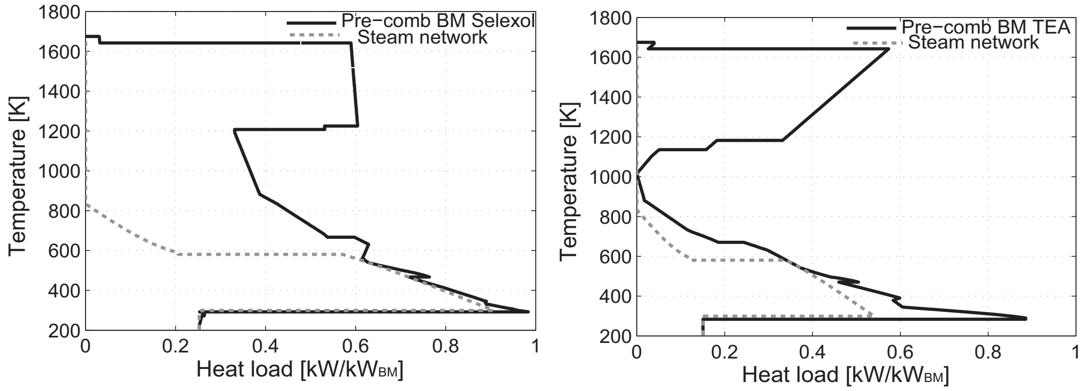

Figure D.3: Integrated composite curves of the most economically competitive biomass based power plant configuration with pre-combustion CO_2 capture by Selexol (left) and TEA (right) reported in Table 8.4.

E H_2 processes: Environmental impacts

Table E.1: Performance of different H_2 plant options with CO_2 capture. For natural gas fed processes a capture rate of 90% is considered and 55% for biomass fed processes.

System	ATR self TEA	ATR Eimp TEA	ATR self Selexol	ATR Eimp Selexol	BM self TEA
Feed [MW_{th}]	725	725	725	725	380
ϵ_{tot} [%]	78.9	83.6	80.1	82.9	48
Net electricity [MW_e]	0	66.9	0	54.8	0
Prod. costs [$\$/GJ_{H2}$]	15.6	19.6	15.3	19	46
Annual Invest. [$\$/GJ_{H2}$]	1.27	0.92	1.18	1.07	9.2
CO_2 emissions [kg_{CO2}/GJ_{H2}]	11	6.2	7	6.3	- 115
IPCC GWP [$kg_{CO2,eq}/GJ_{H2}$]	26.5	19.0	20.6	18.8	-93.8
EI99 [pts/GJ_{H2}]	5.3	4.3	4.9	4.3	4.4
Impact 2002 [$10^{-3} pts/GJ_{H2}$]	14.3	12.8	12.9	12.5	2.4
CML Acidification [$10^{-2} kg_{SO2,eq}/GJ_{H2}$]	79.3	55.8	69.7	53.7	15.1
CML Eutrophication [$10^{-3}\ kg_{PO4,eq}/GJ_{H2}$]	8.2	4.5	7.1	4.2	6.7

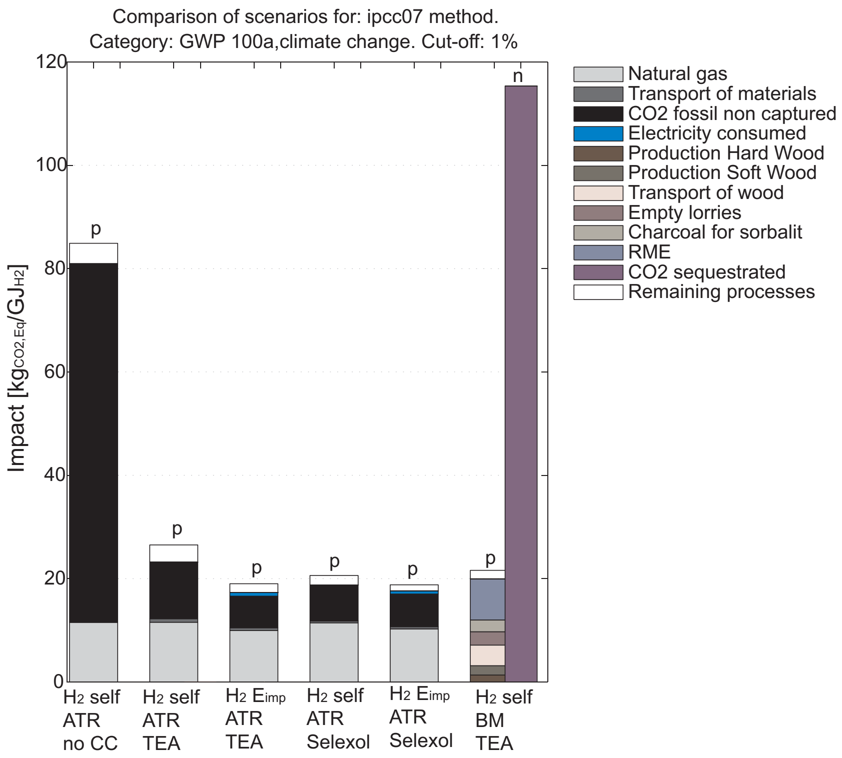

Figure E.1: Comparison of the climate change impact of H_2 processes without and with CO_2 capture (Table E.1) based on the impact method IPCC07 for $1GJ_{H2}$. Contributions that are harmful are labelled with a p and beneficial ones with an n.

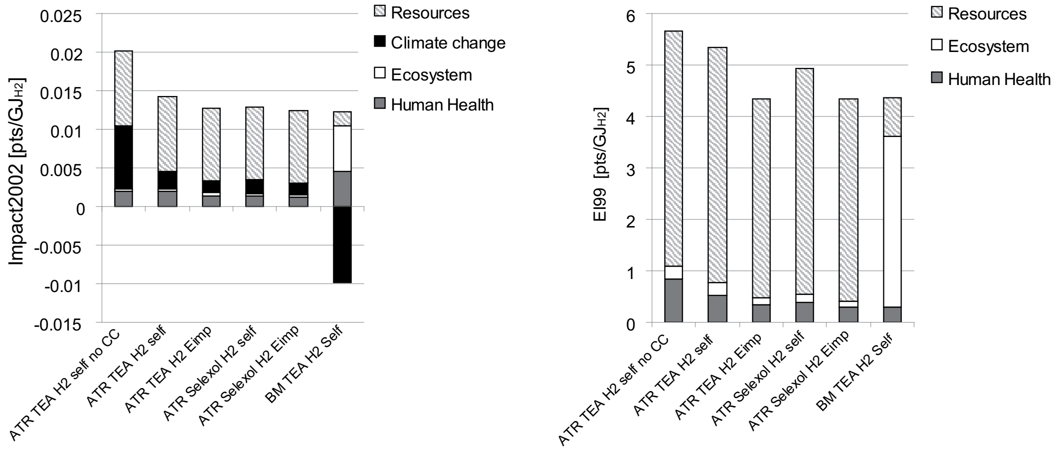

Figure E.2: Comparison of the life cycle impacts of H_2 processes without and with CO_2 capture (Table E.1) based on the impact method Impact 2002 (left) and Ecoindicator99-(h.a) (right) for $1GJ_{H2}$. Contributions that are harmful are positive and beneficial ones negative.

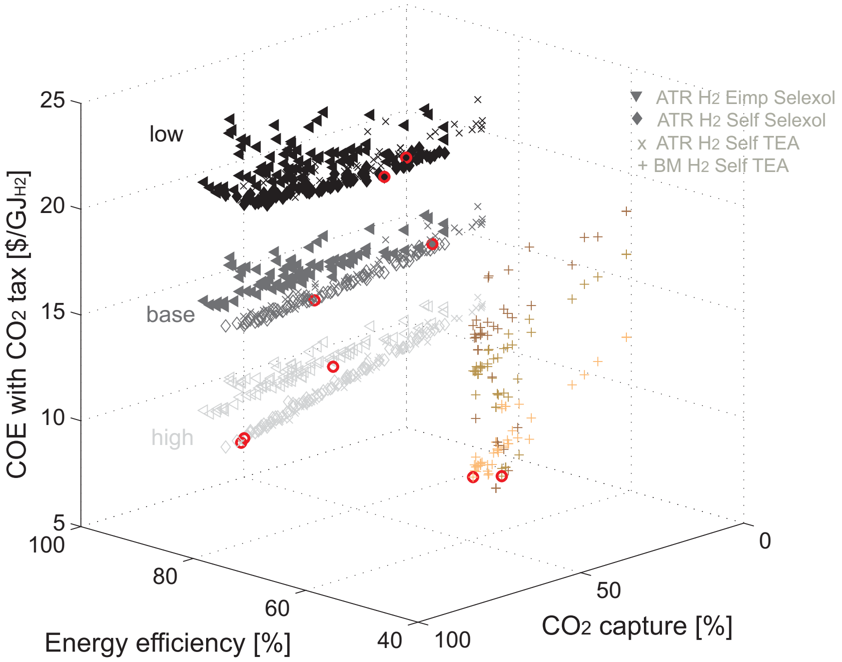

Figure E.3: Influence of the economic scenarios defined in Table 8.2 on the performance of H_2 processes with CO_2 capture.

F Parameterised CO_2 capture models

The details of the parameterised CO_2 capture models presented in Chapter 7 are given here. By applying different approaches, correlations have been developed based on the flowsheet illustrated in Figure 2.3 for estimating the investment costs, the power consumption, the heat loads and the corresponding temperature levels.

F.1 Polynomial fit

Table F.1: Parameterised CO_2 capture model: Polynomial fit.

Term	cst	η_{CO2}	$\dot{m}_{FG}$	$\eta_{CO2}\dot{m}_{FG}$	$\eta_{CO2}\xi_{CO2}$	$\dot{m}_{FG}\xi_{CO2}$	$\eta_{CO2}\dot{m}_{FG}\xi_{CO2}$	${\eta_{CO2}}^2$	${\eta_{CO2}}^2\xi_{CO2}$
$\dot{Q}_{leanheat}$ [W]	$6.251\cdot10^7$	$-1.097\cdot10^8$	0	-23.99	0	$-1.314\cdot10^3$	-540.4	$5.9\cdot10^7$	0
$\dot{Q}_{richheat}$ [W]	$-8.954\cdot10^6$	0	-39.17	89.102	0	$1.615\cdot10^3$	-709.93	0	0
$\dot{Q}_{Absorber}$ [W]	$6.412\cdot10^7$	$-1.836\cdot10^8$	-23.7435	-33.839	0	0	-47.279	$1.229\cdot10^8$	0
$\dot{Q}_{HP}$ [W]	$1.353\cdot10^7$	0	0	-24.499	0	0	-295.44	0	0
Pre_Richheat T [^oC]	26.759	2.8955	$1.563\cdot10^{-6}$	$-1.092\cdot10^{-6}$	120.825	0	0	0	28.918
$\dot{E}$ [kW_e]	$7.568\cdot10^7$	$-3.779\cdot10^4$	$-6.2\cdot10^{-3}$	0.0416	$-9.441\cdot10^4$	0.148	-0.148	0	$2.382\cdot10^5$
I [M$]	33.7	-117.41	$-1.933\cdot10^{-5}$	$1.26\cdot10^{-4}$	-366.8	$4.8\cdot10^{-4}$	$-4.577\cdot10^{-4}$	0	797.6

Table F.2: Parameterised CO_2 capture model: Polynomial fit $\dot{Q}$_reheat.

Term	cst	$\dot{m}_{FG}$	$\dot{m}_{FG}\xi_{CO2}$	$\eta_{CO2}\dot{m}_{FG}\xi_{CO2}$	${\eta_{CO2}}^2\dot{m}_{FG}\xi_{CO2}$	$\eta_{CO2}{\dot{m}_{FG}}^2\xi_{CO2}$	$\eta_{CO2}\dot{m}_{FG}{\xi_{CO2}}^2$	$\eta_{CO2}{\dot{m}_{FG}}^2{\xi_{CO2}}^2$	${\dot{m}_{FG}}^2{\xi_{CO2}}^2$
$\dot{Q}_{Reheat,specific}$ [$W/^oC$]	$4.029\cdot10^4$	-0.3035	19.848	9.120	0.7325	$2.848\cdot10^{-6}$	-25.018	$-2.56\cdot10^{-5}$	$1.602\cdot10^{-6}$

With the aim of performing energy integration, the heat loads and the corresponding temperature levels have to be estimated for the parameterised CO_2 capture model. Several temperature levels that are not varying considerably with the input variables are considered as constant. The absorber offgas temperature (GAS_OUT) is fixed to 39.65^oC, the preheating of the lean solvent (preleanheat T) to 120^oC, the richheat temperature to 105^oC and the reheat temperature to 125^oC. The heat load of the *reheat* heat exchanger is highly influenced by the split fraction and the temperatures which are decision variables in the first principle model. Consequently, the heat load is predicted based on the specific heat load normalised by the factor (1-split)$\cdot\Delta T$. This factor is approximated with regard to the input variables (η_{CO2}, $\dot{m}_{FG}$,

ξ_{CO2}) by interpolation from the dataset that is used to set up the blackbox model. The same approach is applied to estimate the heat load of the low pressure desorber $\dot{Q}_{LP}$.

The goodness of fit is illustrated in Figure F.1 for the total power consumption.

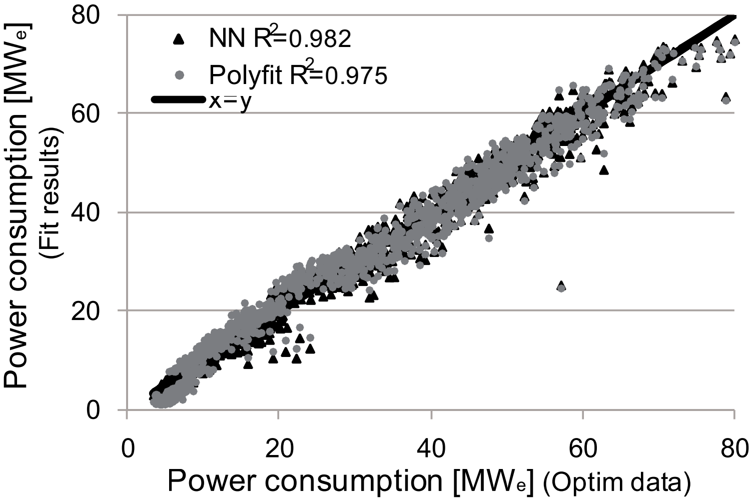

Figure F.1: Fitted total power consumption (Polynomial fit - polyfit, neural network - NN) versus calibration optimisation results.

F.2 Shortcut fit

By applying the shortcut fit approach, the investment costs I are estimated based on the columns height and diameter according to equations Eqs.F.2 -F.6.

$$d = 0.0284 \cdot \dot{m}_{FG}^{0.5} \cdot \xi_{CO2}^{0.1254} \tag{F.1}$$

$$N = 4 + 15 \cdot ln(1/(1-\eta_{CO2})) \tag{F.2}$$

$$HETP = 3.258 \cdot d^{7.5568} \tag{F.3}$$

$$h = N \cdot HETP \tag{F.4}$$

$$F = 10^{3.0532+0.3273 \cdot log(h)+0.0305 \cdot log(h^2)}/10^6 \tag{F.5}$$

$$I = -2.7409 + 1.0208 \cdot F \tag{F.6}$$

G Economic Scenarios

This appendix summarises data for the projections of the gas and carbon tax evolution in the European Union and in Switzerland. Based on this information different economic scenarios are set up to assess the competitiveness of the process configurations. The distribution functions for the different economic assumptions are described and illustrated.

G.1 Market price evolution

The natural gas price fluctuation and projection for different time horizons and geographical locations are reported in Figures G.1-G.3.

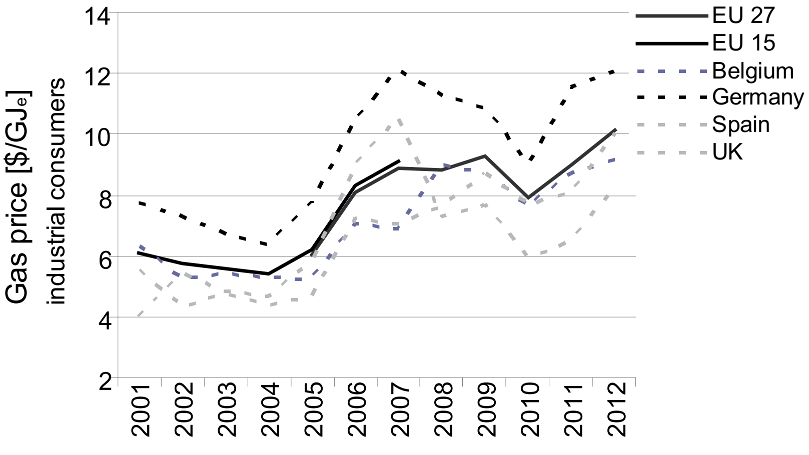

Figure G.1: Fluctuation of the natural gas price (industrial consumers) from 2001 to 2012 for some European Union states (Eurostat).

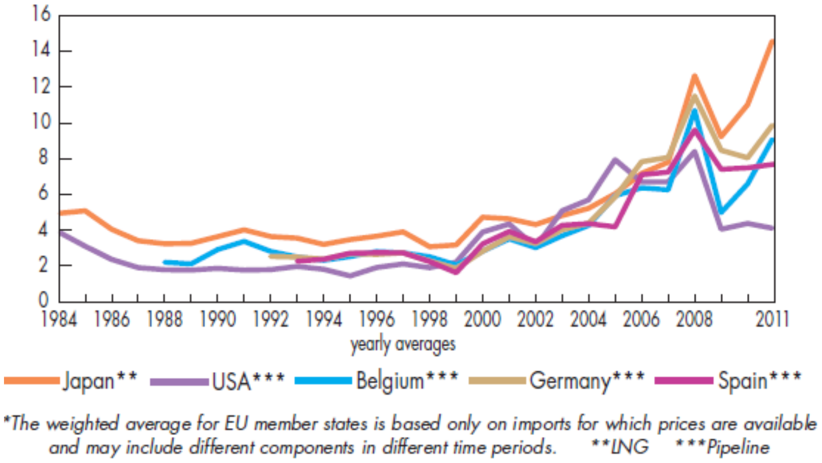

Figure G.2: Fluctuation of the natural gas import price [$/MBtu] from 1984 to 2011 in different countries (IEA (2012)).

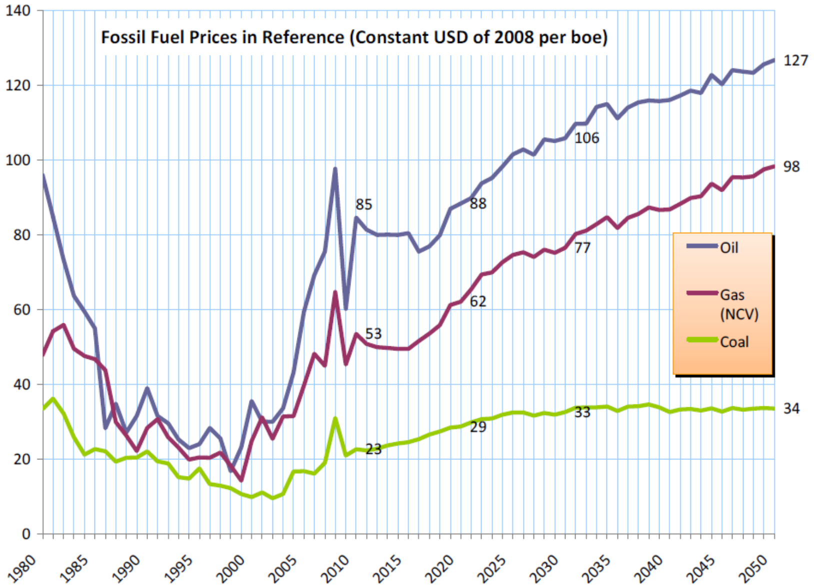

Figure G.3: Fossil fuel price fluctuation and projection to 2050 for the EU '*Reference*' energy scenario (European Commission (2011)).

With regard to the future carbon tax, the European Commission has published different predictions based on various energy scenarios represented in Table G.1.

Table G.1: ETS prices in $€_{08}/t_{CO2}$ (European Commission (2011)).

Scenario	2020	2030	2040	2050
Reference	18	40	52	50
CPI	15	32	49	51
High Energy Efficiency	15	25	87	234
Diversified supply technologies	25	52	95	265
High RES	25	35	92	285
Delayed CCS	25	55	190	270
Low nuclear	20	63	100	310

G.2 Distribution functions

The price variation presented in Section G.1 is described by a probability distribution function. Based on the available data, the appropriate distribution is selected and the parameters are identified. For the different economic assumptions the parameters of the probability density functions are reported in Table 8.3 and the distributions are represented in Figures G.4&G.5.

The normal or Gaussian distribution is a continuous probability distribution that has a bell-shape probability density function (Eq.G.1). The parameter μ is the mean and σ^2 is the variance and σ the standard deviation.

The continuous uniform distribution is characterised by the lower a and upper b endpoint defining the distribution support. Each point in this interval is equally probable. The probability density function for x$\in[a,b]$ is given by Eq.G.2.

The beta distribution is a continuous probability distribution that is defined in the interval [0,1] and is parameterised by two positive shape parameters a and b. This distribution characterised by the probability density function Eq.G.3 is frequently applied to model the behaviour of random variables limited to a finite interval.

$$f(x;\mu,\sigma^2) = \frac{1}{\sigma\sqrt{2\Pi}}e^{-\frac{1}{2}\left(\frac{x-\mu}{\sigma}\right)^2} \tag{G.1}$$

$$f(x) = \frac{1}{a-b} \tag{G.2}$$

$$f(x;a,b) = cst\cdot x^{a-1}\cdot(1-x)^{b-1} \tag{G.3}$$

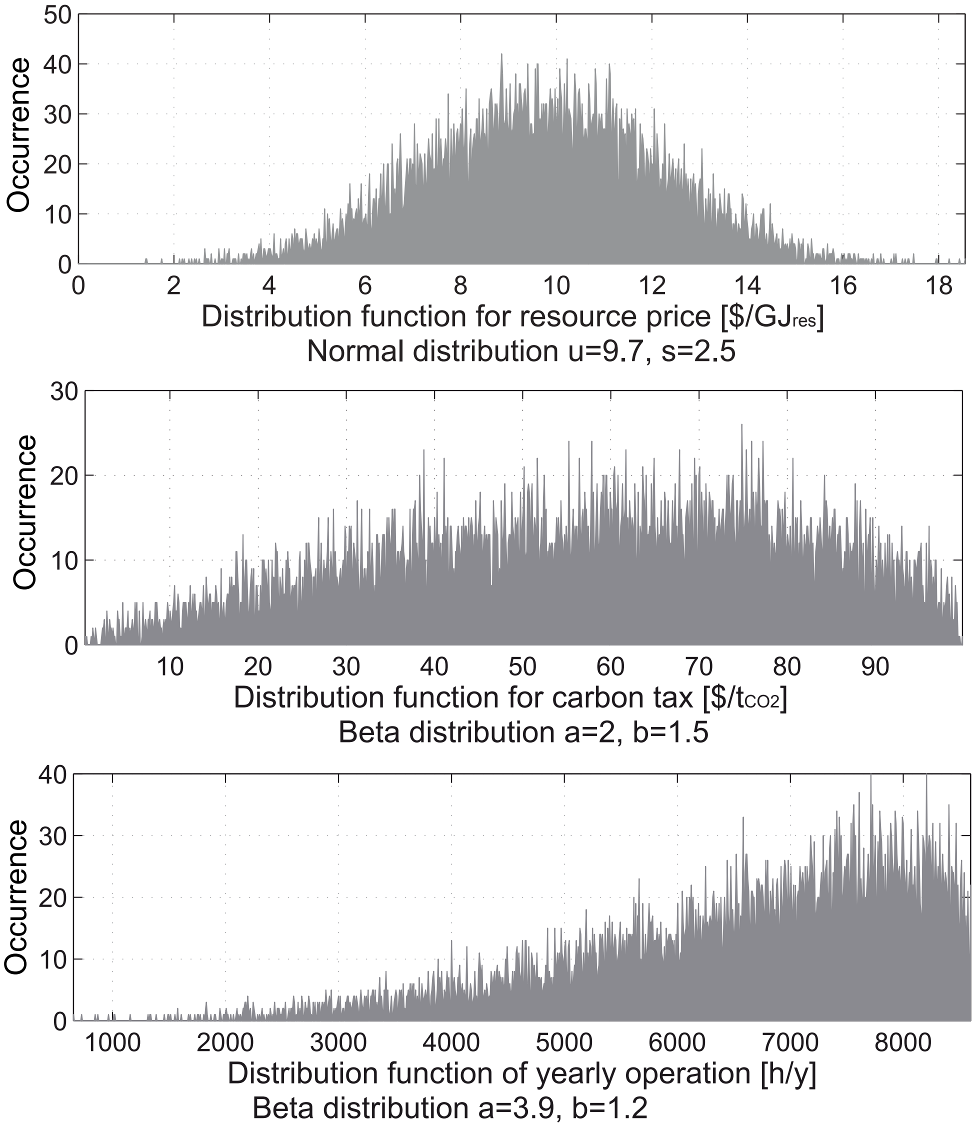

Figure G.4: Distribution functions of the resource price, the carbon tax and the yearly operation.

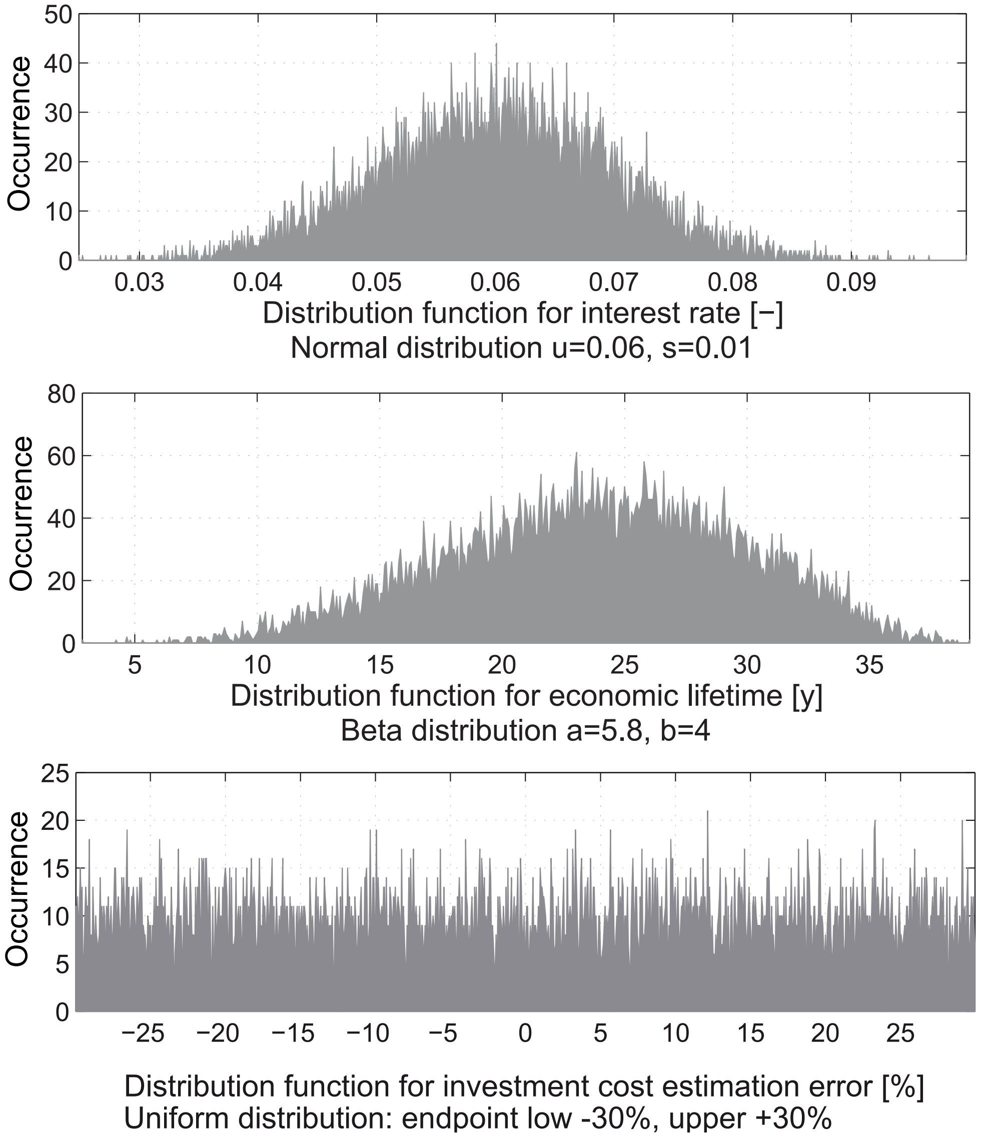

Figure G.5: Distribution functions of the interest rate, the lifetime and the investment cost estimation error.

Nomenclature

Abbreviations

ATR	Autothermal Reforming
AZEP	Advanced Zero Emissions Power Plant
BBA	Chemical absorption blackbox model
BM	Biomass
BtL	Biomass to Liquid
CAP	Chilled Ammonia Process
CC	Carbon Capture
CCS	Carbon Capture and Storage
CGC	Cold Gas Cleaning
CLC	Chemical Looping Combustion
COE	Cost Of Electricity
COM	Operation and Maintenance Cost
COP	Coefficient Of Performance
CPI	Current Policy Initiatives Scenario
CPO	Catalytic Partial Oxidation
DEA	Diethanolamine
DH	District Heating
E_{imp}	Electricity Import
EI 99	Ecoindicator 99
EOR	Enhanced Oil Recovery
ETS	Emission Trading System
FG	Flue Gas
FGR	Flue Gas Recirculation
FHNW	Fachhochschule Nordwestschweiz
FICFB	Fast Internally Circulating Fluidised Bed
FU	Functional Unit
GT	Gas Turbine
GWP	Global Warming Potential
HETP	Height Equivalent to a Theoretical Plate
HEX	Heat Exchanger
HHV	Higher Heating Value

HP	High Pressure steam level
HTS	High Temperature Shift
IECM	Integrated Environmental Control Model
IBGCC	Integrated Biomass Gasification Combined Cycle
IGCC	Integrated Gasification Combined Cycle
IP	Intermediate Pressure steam level
IPCC	Intergovernmental Panel on Climate Change
LCA	Life Cycle Assessment
LCI	Life Cycle Inventory
LCIA	Life Cycle Impact Assessment
LHV	Lower Heating Value
LP	Low Pressure steam level
LTS	Low Temperature Shift
MDEA	Methyldiethanolamine
MEA	Monoethanolamine
MILP	Mixed Integer Linear Programming
MOO	Multi-Objective Optimisation
MVR	Mechanical Vapour Recompression
NG	Natural Gas
NGCC	Natural Gas Combined Cycle
NN	Neural Network
NSGA	Non-dominated Sorting Genetic Algorithm
OECD	Organisation for Economic Co-operation and Development
PC	Pulverised Coal Plant
PEMFC	Proton Exchange Membrane Fuel Cell
PG	Producer Gas
PV	Photovoltaic
POX	Partial Oxidation
PSA	Pressure Swing Adsorption
RME	Rape Methyl Ester
Self	Self-sufficient (in terms of energy)
SMR	Steam Methane Reforming
SNG	Synthetic Natural Gas
SOFC	Solid Oxide Fuel Cell
TEA	Triethanolamine
TTC	Total Tower Cost
VLE	Vapour Liquid Equilibrium
WGS	Water-Gas Shift
ZEP	Zero Emissions Platform

Greek letters

Δh^o	Lower heating value, kJ/kg
ΔT_{min}	Minimum approach temperature, K
$\Delta \tilde{h}_r{}^0$	Standard heat of reaction at $25^o C$, kJ/mol
ϵ	Tray efficiency, -
ϵ_{eq}	Natural gas equivalent efficiency, %
ϵ_{tot}	Energy efficiency, %
γ	Scale exponent, -
η_{CO2}	CO_2 capture rate, %
π	Volume cost, $\$/m^3$
ρ	Density, kg/m^3
θ_{wood}	Wood humidity, %wt

Roman letters

A	Characteristic size parameter,
C	Cost, $
C_{BM}	Bare module cost, $
c_{el}	Electricity purchase cost, $/GJ$_e$
C_{GR}	Grass roots cost, $
C_I	Initial investment cost, $
C$_{I,d}$	Annual investment cost, $/GJ
C_M	Maintenance cost, $/GJ
C_{OL}	Operating labour cost, $/GJ
C_P	Production cost, $/GJ
C_{pc}	Purchase cost, $
C_{RM}	Raw material cost, $/GJ
c_{RM}	Raw material purchase cost, $/GJ$_{RM}$
C_{UT}	Utilities cost, $/GJ
COE	Electricity production cost, $/GJ$_e$
d	Diameter, m
$\dot{E}$	Mechanical/electrical power, kW$_e$
F_M	Material factor, -
F_p	Pressure factor, -
h	Height, m
I	Actualisation factor,
I	Investment, $
i_r	Interest rate, %
K_i	Constant,
K_{SB}	Souders-Brown constant,
$\dot{m}$	Mass flow, kg/s
$\dot{n}$	Molar flow, kmol/s
n	Technical and economic lifetime, years
Nb$_{stages}$	Number of stages, -

P	Pressure, bar
P_a	Annual production, GJ/y
$\dot{Q}$	Heat, kW
T	Temperature, K
T_o	Ambient Temperature, K
T_{amb}	Ambient Temperature, K
u_g	Gas velocity, m/s
u_{mean}	Mean gas velocity, m/s
$\dot{V}$	Volumetric flowrate, m^3/s
V	Volume, m^3

Subscripts

BM	Biomass
cc	Plant with carbon capture
NG	Natural gas
ref	Reference plant without carbon capture
res	Resource: Natural gas (NG) or wood (BM)
RM	Raw material

Superscripts

$^+$	Material/energy stream entering the system
$^-$	Material/energy stream leaving the system

List of Figures

1 World CO_2 emissions from fuel combustion by sector in 2010 (IEA (2011a)). . . 1

2 World total primary energy supply by fuel in 2010 (IEA (2012)). Others: 2.3% Hydro. 1

3 CO_2 capture and storage principle. 3

4 CO_2 capture concepts: (a) Post-combustion CO_2 capture. (b) Oxy-fuel combustion. (c) Pre-combustion CO_2 capture. 3

1.1 Illustration of the developed platform for studying energy conversion systems. 16

1.2 Typical system's boundary for the life cycle inventory. 26

1.3 (a) Schematic process description. (b) Avoided CO_2 definition illustration. . . . 26

1.4 Schematic illustration of the thermo-environomic optimisation strategy. 29

2.1 CO_2 separation technologies. 31

2.2 Schematic flowsheet of the chemical absorption process (omitting pressure change devices). 33

2.3 Process model of the CO_2 capture by chemical absorption with amines. Decision variables reported in Table 2.2 and heat exchanges (i.e. hot stream: red, cold stream: blue) are depicted. 38

3.1 Process superstructure of the pre-combustion CO_2 capture process options. . . 46

3.2 Process layout of the natural gas reforming processes with pre-combustion CO_2 capture. The products are defined by the decisions made at the cross points A and B. 50

3.3 Process layout of the biomass conversion processes with pre-combustion CO_2 capture. The products are defined by the decisions made at the cross points A and B. 51

3.4 Pareto optimal frontiers for CO_2 capture in H_2 production processes maximising the energy efficiency and the CO_2 capture rate. Dashed lines represent the CO_2 capture level of configurations yielding a compromise with regard to both objectives. 55

3.5 Multi-objective optimisation results of CO_2 capture in H_2 production processes: Trade-off between CO_2 capture rate and power consumption. 56

3.6 Multi-objective optimisation results of CO_2 capture in natural gas fed H_2 production processes: Trade-off between efficiency, CO_2 capture rate and production costs. 56

3.7 Power generation by the steam network and by the H_2-rich fuel gas turbine along the Pareto optimal frontiers of the H_2 production by ATR (self and Eimp) with CO_2 capture. 57

3.8 Integrated composite curves of self-sufficient H_2 production processes with CO_2 capture using different resources reported in Table 3.3 (ATR self, SMR self, BM self). The steam network integration is omitted on the figure for clarity. 59

3.9 Integrated composite curves of the self-sufficient natural gas fed H_2 production process with CO_2 capture without (left) and with MVR integration (right) reported in Table 3.3 (ATR self and ATR self no MVR). 60

3.10 MVR integration for the self-sufficient natural gas fed H_2 production process with CO_2 capture (Table 3.3 ATR self). 60

3.11 Integrated composite curves for the biomass fed H_2 production process (with electricity import) without and with CO_2 capture (left) and with MVR (right) reported in Table 3.3 (BM Eimp, no CC and no MVR). 61

3.12 Power balance of the different H_2 process configurations with CO_2 capture reported in Table 3.3. 62

3.13 Production costs buildup for the different H_2 process configurations with CO_2 capture reported in Table 3.3 based on the base case economic assumptions given in Table 1.2. 63

3.14 Capital investment buildup for the different H_2 process configurations with CO_2 capture reported in Table 3.3. 63

3.15 Multi-objective optimisation results of power plant's configurations with precombustion CO_2 capture (left). Net electricity generation and power consumption variation with the CO_2 capture rate along the Pareto optimal frontiers (right). 65

3.16 Integrated composite curves of power plant's configurations with pre-combustion CO_2 capture using different resources (Table 3.4). The steam network integration is omitted on the figure for clarity. 66

4.1 Trade-off between CO_2 mitigation, energy efficiency and production cost for H_2 production process configurations including different CO_2 capture technologies. 71

4.2 Comparison of the composite curves for self-sufficient H_2 production processes capturing 90% of the CO_2 by chemical or physical absorption (Table 4.1: ATR self TEA & Selexol). The steam network integration is omitted on the figure for clarity. 72

4.3 Power balance for the different H_2 production process configurations with CO_2 capture reported in Table 4.1. 73

4.4 Production cost buildup for the different H_2 production process configurations with CO_2 capture reported in Table 4.1. 73

4.5 Trade-off between CO_2 mitigation, energy efficiency and production cost for power plant configurations including different pre-combustion CO_2 capture technologies. 74

4.6 Power balance for the different electricity generating configurations with pre-combustion CO_2 capture, reported in Table 4.2. 76

4.7 Production cost buildup for the different electricity generating configurations with pre-combustion CO_2 capture, reported in Table 4.2. 76

4.8 Integrated composite curves comparison for electricity generation from natural gas by SMR and ATR with 90% of CO_2 capture by chemical absorption with TEA (Table 4.2). 77

4.9 Integrated composite curves comparison for electricity generation from natural with 90% of CO_2 capture by chemical absorption with TEA with and without H_2 purification by PSA (Table 4.2). 78

5.1 Process model of post-combustion CO_2 capture in an NGCC power plant with FGR. 82

5.2 Fit of the FHNW data: amount of H_2 to be added for flame stability (Griffin and Mantzaras (2012)). 83

5.3 Integrated composite curve with steam network integration for the NGCC plant (no FGR) without (left) and with post-combustion CO_2 capture by chemical absorption (right). 85

5.4 Specific investment costs buildup for the different NGCC configurations without and with FGR and post-combustion CO_2 capture reported in Table 5.4. 87

5.5 Production cost buildup for the different NGCC configurations without and with FGR and post-combustion CO_2 capture reported in Table 5.4. 87

5.6 Influence of the FGR on the flue gas CO_2 concentration and the specific CO_2 emissions (left) and on the CO_2 avoidance costs (right) for the NGCC plant with 85% post-combustion CO_2 capture. 88

5.7 Pareto optimal frontiers for different NGCC configurations with post-combustion CO_2 capture. 89

5.8 Integrated composite curves with steam network integration for the NGCC plant with 90% of post-combustion CO_2 capture without (left) and with district heating (right). 90

6.1 Composite curves with steam network integration for the NGCC plant with 85% of post-combustion CO_2 capture with MEA and CAP. 93

6.2 Integrated composite curve of the refrigeration unit in the NGCC configuration with post-combustion CO_2 capture by CAP. 93

6.3 Comparison of the power balance for the NGCC plant with 85% post-combustion CO_2 capture by MEA and CAP (Table 6.1) (left). Zoom on the power consumption (right). 94

6.4 Comparison of the investment buildup (left) and of production cost buildup (right) for the NGCC plant with 85% post-combustion CO_2 capture by MEA and CAP (Table 6.1). 95

6.5 Pareto optimal frontiers (left) and CO_2 capture - efficiency trade-off (right) for post-combustion CO_2 capture with MEA and CAP in an NGCC plant. 96

6.6 Trade-off along the Pareto optimal frontiers between the power consumption and the power generation by the steam network for the post-combustion CO_2 capture with MEA and CAP in an NGCC plant. 96

6.7 Pareto optimal frontiers (left) and power consumption (right) for the NGCC plant with post-combustion CO_2 capture by MEA and CAP modelled by a series of flash separators and a single stage flash. 97

6.8 Comparison of the CO_2 capture unit integration for the NGCC plant with 90% of post-combustion CO_2 capture by CAP based on a single stage flash model (left) and on a series of flash units (right) (Table 6.3). 99

6.9 Comparison of the refrigeration integration for the NGCC plant with 90% of post-combustion CO_2 capture by CAP based on a single stage flash model (left) and on a series of flash units (right) (Table 6.3). 99

6.10 Comparison of the steam network integration for the NGCC plant with 90% of post-combustion CO_2 capture by CAP based on a single stage flash model (left) and on a series of flash units (right) (Table 6.3). 100

6.11 Comparison of the power balance for the NGCC plant wih 90% of post-combustion CO_2 capture by CAP modelled by a single stage flash or a series of flash units (left). Zoom on the power consumption buildup (right)(Table 6.3). 100

6.12 Comparison of the investment buildup (left) and production cost buildup (right) for the NGCC plant with 90% of post-combustion CO_2 capture by CAP modelled by a single stage flash or a series of flash units (Table 6.3). 101

6.13 Energy integration results for the NGCC plant with 90% post-combustion CO_2 capture with CAP modelled by a series of flash unit and including a refrigeration cycle with ammonia: Grand composite curve in Carnot factor axis (left). Integrated composite curve of refrigeration unit (right). 102

6.14 Refrigeration cycle using an ammonia-water mixture as refrigerant. 102

6.15 Integrated composite curve of the ammonia-water refrigeration cycle for the NGCC plant with 90% post-combustion CO_2 capture with chilled ammonia (left) (Table 6.4: Refrig. NH_3-H_2O). Zoom below ambient temperature (right). 103

6.16 Influence of the ammonia concentration of the refrigerant on the performance of the NGCC plant with 90% post-combustion CO_2 capture with chilled ammonia including an ammonia-water refrigeration cycle. 104

6.17 Influence of the ΔT_{min} in the refrigeration cycle heat exchangers on the performance of the NGCC plant with 90% post-combustion CO_2 capture with chilled ammonia including an ammonia-water refrigeration cycle. 104

6.18 Comparison of the grand composite curve in Carnot factor axis of the NGCC plant with 90% post-combustion CO_2 capture with chilled ammonia including an ammonia or ammonia-water refrigeration cycle (Table 6.4: Refrig. NH_3 and Refrig. Opt. NH_3-H_2O). 105

6.19 Comparison of the integrated composite curve of the ammonia and ammonia-water refrigeration cycle in the NGCC plant with 90% post-combustion CO_2 capture with chilled ammonia (left) (Table 6.4: Refrig. NH_3 and Refrig. Opt. NH_3-H_2O). Zoom below ambient temperature (right). 105

6.20 Comparison of the grand composite curve in Carnot factor axis of the NGCC plant with 90% post-combustion CO_2 capture with chilled ammonia including an ammonia-water refrigeration cycle and heat pumping (left). Integrated composite curve of the heat pumping using a ammonia-water mixture in the NGCC plant with 90% post-combustion CO_2 capture with chilled ammonia (right). . 106

6.21 Comparison of the grand composite curve in Carnot factor axis of the NGCC plant with 90% post-combustion CO_2 capture with chilled ammonia including an ammonia-water refrigeration cycle and MVR (left). Integrated composite curve of the MVR in the NGCC plant with 90% post-combustion CO_2 capture with chilled ammonia (right). 108

7.1 Illustration of the process optimisation strategy to develop simpler parameterised CO_2 capture models. 110

7.2 Blackbox model of the CO_2 capture process. 111

7.3 Pareto optimal frontiers showing the trade-off between investment and CO_2 capture rate for different $\dot{m}_{FG}$ and ξ_{CO2} in chemical absorption with MEA. . . . 112

7.4 Scheme of the neural network. 114

7.5 Fitted investment (Polynomial fit - polyfit Eq.7.2, fit based on shortcut model - shortcut fit, neural network - NN) versus calibration optimisation results. . . . 114

7.6 Comparison of the composite curves with steam network integration for the base case scenarios reported in Table 7.2. 116

7.7 Pareto optimal frontiers of the global problem optimisation based on the first-principle MEA model and on different blackbox models. 117

7.8 Composite curves for the compromise scenario generated by the first principle MEA model through optimisation and through recomputation of the parameterised polynomial model with the detailed MEA model. 118

8.1 Investigated CO_2 capture options. 122

8.2 Performance results of the different power plant options with CO_2 capture reported in Table 8.1. For natural gas fed processes a capture rate of 90% is considered and 60% for biomass fed processes. 123

8.3 Comparison of the climate change impact of power plants without and with CO_2 capture based on the impact method IPCC 07 for $1GJ_e$. Contributions that are harmful are labelled with a p and beneficial ones with an n. 125

8.4 Comparison of the life cycle impacts of power plants without and with CO_2 capture based on the impact methods Impact 2002+ (left) and Ecoindicator 99-(h.a) (right) for $1GJ_e$. Contributions that are harmful are positive and beneficial ones negative. 125

8.5 Contributions to the resources impact based on the impact method Ecoindicator 99-(h.a) for $1GJ_e$ of electricity produced by power plants without and with CO_2 capture. 126

8.6 Contributions to the ecosystem impact based on the impact method Ecoindicator 99-(h.a) for $1GJ_e$ of electricity produced by power plants without and with CO_2 capture. 127

8.7 Contributions to the human health impact based on the impact method Ecoindicator 99-(h.a) for $1GJ_e$ of electricity produced by power plants without and with CO_2 capture. Contributions that are harmful are labelled with a p and beneficial ones with an n. 127

8.8 Contributions to the acidification potential based on the impact method CML01 for $1GJ_e$ of electricity produced by power plants without and with CO_2 capture. 128

8.9 Contributions to the eutrophication potential based on the impact method CML01 for $1GJ_e$ of electricity produced by power plants without and with CO_2 capture. 129

8.10 Comparison of the environmental performance of electricity generating processes from Ecoinvent (Ecoinvent) and this study (Table 8.1) based on the IPCC impact method. 130

8.11 Comparison of the environmental performance of electricity generating processes from Ecoinvent (Ecoinvent) and this study (Table 8.1) based on the Ecoindicator impact method. 130

8.12 Influence of the natural gas purchase price on the electricity production costs without (- -) and with (–) the inclusion of a carbon tax of $35\$/t_{CO2}$ for the process configurations reported in Table 8.1. 132

8.13 Influence of the carbon tax on the electricity production costs without and with CO_2 capture for a natural gas price of $9.7\$/GJ_{NG}$ and a biomass price of $5\$/GJ_{BM}$ for the process configurations reported in Table 8.1. 133

8.14 Influence of the carbon tax on the electricity production costs for different CO_2 capture process options. 134

8.15 Influence of the carbon tax and of the resource price on the electricity production costs for different CO_2 capture process options. 135

8.16 Influence of the economic scenarios defined in Table 8.2 on the performance of pre-combustion CO_2 capture with Selexol in a natural gas fired power plant using ATR. 136

8.17 Influence of the economic scenarios defined in Table 8.2 on the performance of post-combustion CO_2 capture with MEA in a natural gas fired power plant. . . 136

8.18 Influence of the economic scenarios defined in Table 8.2 on the performance of pre-combustion CO_2 capture with Selexol in a biomass fed power plant. 137

8.19 Influence of the economic scenarios defined in Table 8.2 on the performance of electricity generating processes with CO_2 capture. 138

8.20 Influence of the economic scenarios defined in Table 8.2 on the performance of electricity generating processes with CO_2 capture - 2D representation. 138

8.21 Assessment of the influence of the economic assumptions uncertainty on the COE and CO_2 avoidance costs accounting for a CO_2 tax, for the configurations presented in Table 8.1. The markers represent the performance for the base case economic scenario, and the corresponding coloured area the variation of the COE with the economic conditions. 140

8.22 Natural gas fired power plant performance with post-combustion CO_2 capture with MEA: Probability of each point to be part of the top 5 configurations yielding the best economic performance under different economic scenarios. 141

8.23 Natural gas fired power plant performance with post-combustion CO_2 capture with MEA: Influence of the economic scenario on the electricity production costs (incl. a carbon tax) of the best 5 economic performance configurations. 141

8.24 Natural gas fired power plant performance with pre-combustion CO_2 capture with Selexol: Probability of each point to be part of the top 5 configurations yielding the best economic performance under different economic scenarios (left) and respective influence on the electricity production costs including a carbon tax (right). 142

8.25 Biomass fired power plant performance with pre-combustion CO_2 capture with Selexol: Probability of each point to be part of the top 5 configurations yielding the best economic performance under different economic scenarios (left) and respective influence on the electricity production costs including a carbon tax (right). 142

8.26 Power plants performance with CO_2 capture: Influence of the economic scenario on the top 5 configurations yielding the best economic performance. Decision-making based on the Pareto front (black points) (left) and corresponding probability of each point to be part of the top 5 configurations yielding the best economic performance under different economic scenarios (right). 143

8.27 Power plants performance with CO_2 capture: Influence of the economic scenario on the decision-making based on the top 5 configurations yielding the best economic performance (left) 2D representation showing the trade-off between COE and energy efficiency (right). 143

8.28 Relative competitiveness of each Pareto optimal solution with regard to the most economically competitive solution for the considered economic scenarios (right). Zoom on the relative competitiveness of CO_2 capture in natural gas fired power plants (left). 144

8.29 Integrated composite curves of the most economically competitive natural gas fired power plant options with post-combustion CO_2 capture with MEA (left) and with pre-combustion CO_2 capture with Selexol (right) reported in Table 8.4. 145

8.30 Comparison of the most economically competitive power plant options with CO_2 capture based on the economic performance variation, with regard to the different economic scenarios, expressed by the COE including CO_2 tax (Table 8.4).146

B.1 Flowsheet of the chemical absorption process using an aqueous TEA solution. 173

B.2 Flowsheet of the chilled ammonia process. 173

B.3 Flowsheet of the physical absorption process using the Selexol solvent. 174

B.4 Flowsheet of the physical absorption process using the Rectisol solvent. 174

B.5 Generic gas turbine model with reheat combustion. 174

B.6 Generic gas turbine model with a single combustion stage. 175

B.7 Syngas production by the ATR membrane reactor for injection in the combustion chamber of the NGCC plant with FGR. 176

C.1 Trade-off between thermodynamic and environmental performance of the pre-combustion CO_2 capture in a natural gas fired power plant assessed for different objective functions choices. 178

C.2 Trade-off between thermodynamic and economic performance of the pre-combustion CO_2 capture in a natural gas fired power plant assessed for different objective functions choices. 178

C.3 Trade-off between thermodynamic, environmental and economic performance of post-combustion CO_2 capture in a natural gas fired power plant assessed for different objective functions choices. 179

D.1 Integrated composite curves of the most economically competitive natural gas fuelled power plant configuration with post-combustion CO_2 capture with MEA (left) and chilled ammonia (right) reported in Table 8.4. 186

D.2 Integrated composite curves of the most economically competitive natural gas fuelled power plant configuration with pre-combustion CO_2 capture by chemical absorption with TEA; ATR (left) and SMR (right) reported in Table 8.4. 186

D.3 Integrated composite curves of the most economically competitive biomass based power plant configuration with pre-combustion CO_2 capture by Selexol (left) and TEA (right) reported in Table 8.4. 186

E.1 Comparison of the climate change impact of H_2 processes without and with CO_2 capture (Table E.1) based on the impact method IPCC07 for $1GJ_{H2}$. Contributions that are harmful are labelled with a p and beneficial ones with an n. 188

E.2 Comparison of the life cycle impacts of H_2 processes without and with CO_2 capture (Table E.1) based on the impact method Impact 2002 (left) and Ecoindicator99-(h.a) (right) for $1GJ_{H2}$. Contributions that are harmful are positive and beneficial ones negative. 188

E.3 Influence of the economic scenarios defined in Table 8.2 on the performance of H_2 processes with CO_2 capture. 189

F.1 Fitted total power consumption (Polynomial fit - polyfit, neural network - NN) versus calibration optimisation results. 192

G.1 Fluctuation of the natural gas price (industrial consumers) from 2001 to 2012 for some European Union states (Eurostat). 193

G.2 Fluctuation of the natural gas import price [$/MBtu] from 1984 to 2011 in different countries (IEA (2012)). 194

G.3 Fossil fuel price fluctuation and projection to 2050 for the EU '*Reference*' energy scenario (European Commission (2011)). 194

G.4 Distribution functions of the resource price, the carbon tax and the yearly operation. 196

G.5 Distribution functions of the interest rate, the lifetime and the investment cost estimation error. 197

List of Tables

1 Comparison of CO_2 capture processes (Figueroa et al. (2008), Kanniche et al. (2010), Radgen et al. (2005), Olajire (2010)). 6

2 Performance of state-of-the-art power plants configurations with and without CO_2 capture based on references: Kanniche et al. (2010), Parsons et al. (2002), Rubin et al. (2007), Damen et al. (2006), Kvamsdal et al. (2007), Bolland and Undrum (2003), Chiesa and Consonni (2000), Zhang and Lior (2008), Lozza and Chiesa (2002b,a), Mann and Spath (1997), Carpentieri et al. (2005). 10

3 Performance of state-of-the-art H_2 plants configurations with and without CO_2 capture based on references: Longanbach et al. (2002), Bartels et al. (2010), Toonssen et al. (2008) and Hamelinck and Faaij (2002). 10

1.1 Assumptions for the sizing of the SMR and WGS reactors (Maréchal et al. (2005)). 22

1.2 Assumptions for the economic analysis. 24

1.3 Reference plants performance considered for the CO_2 avoidance costs assessment. 27

2.1 Comparison of the physical and chemical ab- and adsorption processes for CO_2 separation (Göttlicher (1999)). 37

2.2 Decision variables and feasible range for optimisation for the chemical absorption process using an aqueous MEA solution. 39

2.3 Decision variables and feasible range for optimisation for the chemical absorption process using an aqueous TEA solution. 39

2.4 Decision variables and feasible range for optimisation for the chilled ammonia process. 41

2.5 Decision variables and feasible range for optimisation for the physical absorption process using the Rectisol solvent. 41

2.6 Decision variables and feasible range for optimisation for the physical absorption process using the Selexol solvent. 42

3.1 Parameters for the energy-flow models of the pre-combustion CO_2 capture processes using natural gas or biomass as a feedstock. 51

3.2 Operating conditions and feasible range for optimisation for the pre-combustion CO_2 capture processes using natural gas or biomass as a feedstock. 52

3.3 Performance of H_2 process configurations with pre-combustion CO_2 capture. The net electricity output expressed in MJ of electricity per GJ of hydrogen is negative when the integrated process requires electricity importation and positive when it generates electricity. The corresponding operating conditions are reported in Appendix Table D.1. 58

3.4 Performance of the compromise power plants configurations with pre-combustion CO_2 capture. The electricity balance is expressed in MJ of electricity per GJ of net electricity produced. The corresponding operating conditions are summarised in Appendix Table D.2. 65

4.1 Performance of the compromise H_2 production process configurations with CO_2 capture. The specific performances are expressed per GJ of H_2 produced. The corresponding operating conditions are reported in Appendix Table D.3. 71

4.2 Performance of the compromise electricity generation configurations with pre-combustion CO_2 capture. The specific performances are expressed per GJ of electricity produced. The corresponding operating conditions are reported in Appendix Table D.4. 75

5.1 Decision variables and feasible range for optimisation for the NGCC plant. . . . 83

5.2 Steam network characteristics for the NGCC plant (Li (2006)). 84

5.3 Performance of the different natural gas combined cycle configurations without FGR and without CO_2 capture (natural gas price 9.7\$/GJ$_{NG}$, operation 8000h/y) 85

5.4 Performance of the NGCC configurations without and with FGR and post-combustion CO_2 capture (natural gas price 9.7\$/GJ$_{NG}$, operation 8000h/y). . . 86

5.5 Performance of the NGCC plant with 90% CO_2 capture with MEA without and with district heating DH (natural gas price 9.7\$/GJ$_{NG}$, operation 7500h/y). . . 90

6.1 Performance of NGCC power plants configurations without CO_2 capture and with 85% post-combustion CO_2 capture with MEA and chilled ammonia. The corresponding operating conditions are reported in Appendix Table D.5. 92

6.2 Specific exergy demands, expressed in GJ/t_{CO2}, of the CO_2 capture with MEA and chilled ammonia for the configurations reported in Table 6.1. 94

6.3 Performance comparison for NGCC power plants with 90% post-combustion CO_2 capture with MEA and chilled ammonia modelled by a single flash and a serie of flash units. The corresponding operating conditions are reported in Appendix Table D.6. 98

6.4 Performance of the NGCC power plant with 90% post-combustion CO_2 capture with chilled ammonia (series of flash units) including different refrigeration options. 103

6.5 Performance of NGCC power plants with 90% post-combustion CO_2 capture with chilled ammonia (series of flash units) for different energy integration (EI) improvements. 107

7.1 Regression results for the investment cost correlation leading to Eq.7.2. ($t_{0.95}[1538]=1.96$, $F_{0.95}[7;1538]=3.23$) 113

7.2 Performance results of the base case NGCC plant configurations with 85% post-combustion CO_2 capture based on the first-principle MEA model and on different blackbox models. 115

7.3 Computation time comparison for multi-objective optimisation of post-combustion CO_2 capture in the NGCC plant based on the first-principle MEA model and on different blackbox models (400 evaluations and initial population of 30). 116

7.4 Performance of the compromise NGCC plant configurations with 87% post-combustion CO_2 capture based on the first-principle MEA model and on different blackbox models. 118

8.1 Performance of the different power plant options with CO_2 capture. For natural gas fed processes a capture rate of 90% is considered and 60% for biomass fed processes. The corresponding operating conditions are reported in in Appendix Tables D.4 & D.7. 123

8.2 Definition of the economic scenarios. 134

8.3 Parameters of the distribution functions for the economic assumptions (illustrated in Appendix Figures G.4 & G.5). 139

8.4 Performance of the most economically competitive power plant options with CO_2 capture. The corresponding process design parameters are reported in Appendix Tables D.8 & D.9. 145

8.5 Performance results reported by IEA (Finkenrath (2011)) for OECD countries. The costs range takes into account the variation of the resource price with regard to the countries. For the efficiency the OECD average value is given. 147

8.6 Performance results reported by ZEP (ZEP (2011)) for European countries. The conservative, high-cost plant designs representing today's technology choices (Base) and the optimised cost estimations considering advanced future technology (Optim) are reported here. The costs ranges take into account the low and high resource price scenario. For the currency exchange 1.25$/€ is used. 147

8.7 Performance comparison of H_2 applications. 154

A.1 Flue gas characteristics for the comparison of the investment cost estimates of a chemical absorption installation. 170

A.2 Influence of the cost correlations on the capital investment estimation [M$] of a chemical absorption unit for CO_2 capture from the flue gas (Table A.1). 171

B.1 Characteristics of the generic gas turbine model with reheat combustion illustrated in Figure B.5. 175

B.2 Modelling assumptions of the generic gas turbine model with reheat combustion and FGR illustrated in Figure B.5. 175

B.3 Characteristics of the generic gas turbine model with a single combustion stage illustrated in Figure B.6. 176

B.4 Modelling assumptions of the generic gas turbine model with a single stage combustion and FGR illustrated in Figure B.6. 176

C.1 Performance comparison of compromise solutions, assessed from different multi-objective optimisations of pre-combustion CO_2 capture in a natural gas fuelled power plants. 180

D.1 Operating conditions for the different compromise H_2 process options with pre-combustion CO_2 capture, whose performance results are reported in Table 3.3. 181

D.2 Operating conditions for the different compromise power plants options with pre-combustion CO_2 capture, whose performance results are reported in Table 3.4. 182

D.3 Operating conditions for the different compromise H_2 plant options with pre-combustion CO_2 capture, whose performance results are reported in Table 4.1. 182

D.4 Operating conditions for the different compromise power plant options with pre-combustion CO_2 capture, whose performance results are reported in Tables 4.2 & 8.1. 183

D.5 Operating conditions for the base case power plant options with post-combustion CO_2 capture, whose performance results are reported in Table 6.1. 183

D.6 Operating conditions for the power plant options with 90% post-combustion CO_2 capture, whose performance results are reported in Table 6.3. 184

D.7 Operating conditions for the different compromise power plant options with post-combustion CO_2 capture, whose performance results are reported in Table 8.1. 184

D.8 Operating conditions for the most economically competitive power plant options with post-combustion CO_2 capture, whose performance results are reported in Table 8.4. 185

D.9 Operating conditions for the most economically competitive power plant options with pre-combustion CO_2 capture, whose performance results are reported in Table 8.4. 185

E.1 Performance of different H_2 plant options with CO_2 capture. For natural gas fed processes a capture rate of 90% is considered and 55% for biomass fed processes.187

F.1 Parameterised CO_2 capture model: Polynomial fit. 191

F.2 Parameterised CO_2 capture model: Polynomial fit $\dot{Q}$_reheat. 191

G.1 ETS prices in $€_{08}/t_{CO2}$ (European Commission (2011)). 195

Curriculum Vitae

Personal details

Name	Laurence TOCK
Date of birth	25.04.1985
Nationality	Luxembourgish
Contact	laurence.tock@gmail.com

Education

2009	–	2013	École Polytechnique Fédérale de Lausanne, Switzerland *PhD thesis at the Industrial Energy Systems Laboratory*
2004	–	2009	École Polytechnique Fédérale de Lausanne, Switzerland *MSc in Chemical engineering and biotechnology*
1997	–	2004	Lycée Classique de Diekirch, Luxembourg *Diplôme de fin d'études secondaires* *orientation sciences et mathématiques*

Scientific experience and internships

2009	–	2013	Industrial energy systems laboratory, EPFL, Switzerland *Teaching assistant and project supervision* *Course: Modelling and optimisation of energy systems*
		2007	Goodyear Innovation Centre Luxembourg, "Analytical Test Laboratory" Internship 6 weeks *Analysis and synthesis of new rubber mixtures* *to develop a more robust and sustainable product*
		2006	Goodyear Wire Plant Luxembourg, "QTECH Laboratory" Internship 6 weeks *Active participation in the chemical analysis and tests* *allowing to control rigorously under time constraints the product quality*